UNIVERSITY
MAR 10 1962
LIBRARY

JOURNAL

OF THE

FISHERIES RESEARCH BOARD OF CANADA

Volume 18, No. 6

CONTENTS

(*Concluded overleaf*)

OTTAWA
DECEMBER
1961

NOTES

Editor:

W. E. Ricker
Fisheries Research Board of Canada
P.O. Drawer 100
Nanaimo, B.C., Canada

Associate Editor:

N. M. Carter
Fisheries Research Board of Canada
Sir Charles Tupper Building
Ottawa, Ont., Canada

Manuscripts for publication should be addressed to the Editor

ROGER DUHAMEL, F.R.S.C.
QUEEN'S PRINTER AND CONTROLLER OF STATIONERY
OTTAWA, 1961

Proximate Composition of Canadian Atlantic Fish. III. Sectional Differences in the Flesh of a Species of Chondrostei, one of Chimaerae, and of Some Miscellaneous Teleosts[1]

By D. I. Fraser, A. Mannan[2] and W. J. Dyer

Fisheries Research Board of Canada
Technological Station, Halifax, N.S.

ABSTRACT

Proximate analyses of sections of the flesh of several teleosts and also of a sturgeon and a chimaera are reported. Among the teleosts the proximate composition of the white meat is very similar, with the exception of the fat, which varies from 0.7% in the lean species such as haddock to 12% in the spiny eel. Protein (protein N × 6.25) ranges from 14.8 to 16.2% for most species, but is lower in the sturgeon and chimaera, while the previously reported values for mackerel, tuna and halibut are higher. The belly flap tissue is only slightly more fatty than the white meat in haddock and the white sucker, in contrast to the high values for halibut and mackerel. The brown lateral layer contains about 2% lipid in haddock and wolffish with much higher values in other species; its non-protein N content is similar to that of the white meat for the most part. Although present only in traces in some species, the brown lateral layer makes up about 8% of the flesh of the tail section of the haddock, but only 1% of the middle section.

INTRODUCTION

Previous papers in this series (Mannan *et al.*, 1961a,b) have dealt with the variation in composition of the different sections of the edible portion of halibut, mackerel, tuna and swordfish. In order to gain a picture of the variation over a range of fish species, further work on several species of teleosts, including haddock, cod, rosefish, spiny eel, shad, and the white sucker is now reported. Because of their taxonomic position between the elasmobranchs and teleosts, a sea sturgeon and a chimaera are also included.

A few studies on the Pacific salmon have been reported. Thurston (1958) studied the variation in moisture, fat, protein and ash in various sections of Alaska pink salmon (*Oncorhynchus gorbuscha*), and similar results were obtained by Thurston and Groninger (1959) in Puget Sound pink salmon. The steak section of the Alaska samples, including the dark meat, averaged higher in fat content at the nape, 4.8%, than in the caudal section, 2.6%, with intermediate values in the centre, 3.5%. The fat content of the fatty tissue around the dorsal fin, of the brown lateral layer and of the belly flap was much higher and more variable, averaging 15.7, 12.5 and 9.5% respectively; light meat averaged 2.1%. Thurston also concluded that variation with sex and size was small in comparison with that due to sexual maturity, agreeing with the much earlier work of Dill

[1]Received for publication March 17, 1961.
[2]Present address: Fishery Technology Laboratory, Rajgonj, Comilla, East Pakistan.

(1921). Some of these changes have also been studied recently in sockeye salmon (*Oncorhynchus nerka*) by Idler and Bitners (1958).

A thorough study of the fat and water distribution in the musculature of Atlantic herring (*Clupea harengus*) was carried out in Germany by Brandes and Dietrich (1953). The belly-flap muscle gave very high lipid values, about 47% as compared to values of 23 to 27% for the muscle at the anterior end of the fillet, 27 to 31% at the thickest part, and 14 to 18% at the caudal end of the fillet. Fat and moisture were found to be closely related.

EXPERIMENTAL

Sources of Specimens and Sampling

The species are classified according to the American Fisheries Society (1960) and Jordan and Evermann (1896) as follows:

Class CHONDRICHTHYES	
Order CHIMAERIFORMES (CHIMAERAE)	*Hydrolagus affinis*—chimaera
Class OSTEICHTHYES	
Order ACIPENSERIFORMES (CHONDROSTEI)	*Acipenser oxyrhynchus*—Atlantic (sea) sturgeon
Order CLUPEIFORMES (ISOSPONDYLI)	*Alosa sapidissima*—American shad
	Clupea harengus harengus—Atlantic herring
Order CYPRINIFORMES (OSTARIOPHYSI)	*Catostomus commersoni*—white sucker
Order NOTACANTHIFORMES (HETEROMI)	*Notacanthus nasus*—spiny eel
Order GADIFORMES (ANACANTHINI)	*Gadus morhua*—cod
	Melanogrammus aeglefinus—haddock
Order PERCIFORMES (PERCOMORPHI)	*Sebastes marinus*—rosefish
	Anarhichas lupus—wolffish (Atlantic)

Two specimens of *spiny eel* were obtained through the courtesy of Mr George Sullivan of this Board's office in Halifax. They were caught at 120 fathoms near Green Bank; one was 51 cm long (December 1960), and the other 112 cm (January 19, 1961). Samples of the white dorsal meat at the thick part of the fish (A) were taken. Only a trace of brown lateral-line tissue was present, but in the larger fish there was a layer of white fat (blubber, FL) about 1.3 cm thick at the dorsal line. This extended around the belly as a thin layer under the skin, comprising one-fifth of the weight of the flesh of a cross-sectional steak at the thick portion of the fish.

The minced mixed fillets (M) of a *shad* 32 cm long, caught by net near Halifax on November 2, 1960, were analyzed.

Several specimens of *white sucker*, all 43 cm long, were netted in a river (Halifax County) on May 28, 1959. Samples of the flesh from sections A, B (tail section, white meat), and C (belly flap) (Mannan *et al.*, 1961a) from two fish were minced and mixed for analysis. Similar samples were taken from two fish stored for 3 months at –23°C. No trace of brown lateral-line flesh was observed.

The *sturgeon*, measuring 80 cm long, was caught in salt water in St. Margaret's Bay on April 30, 1954, and was alive prior to sampling (Dingle and Dyer, 1955).

The *chimaera*, 118 cm long, was a ripe female caught on November 19, 1960, off St. Pierre Bank at 300 fathoms. The thick white dorsal muscle was analyzed in both these specimens.

The *haddock*, market size, were caught in Terence Bay, near Halifax, on April 20, June 6 and July 24, 1959. The first lot was frozen (in polyethylene bags) and stored for 2 months at –23°C, while the other two lots were sampled while still in the pre-rigor state (iced). Samples of the white meat were taken between myotomes 7 and 14 at the thick part of the fish (A); sample B included the fillet portion from the tail almost to the vent, while sample C was the belly flap, which was not included in A. In the June 6 lot, a section L, midway between the nape and the tail was also taken.

The May 28, 1959, sample of *cod* (lot I, Table III) was taken live from the fish-holding tank at the laboratory.

A *wolffish*, 74 cm long, was caught on February 6, 1960, and brought in alive from the Banks by the Board's research vessel *A. T. Cameron*.

For comparison purposes, the average composition of cod and rosefish fillets from previously reported frozen storage experiments are included in Table V.

The *cod* samples were of minced, mixed lots of fillets (M) from commercial market-size fish. Lot II samples were from cod caught off Sable Island on July 12, 1955, iced 2 days on a trawler (Dyer, Fraser, Ellis and MacCallum, 1957); lot III from a July 26, 1956, catch also off Sable Island, landed after 2 days in ice (Dyer, Fraser and MacCallum, 1957); lot IV from Western Bank, October 25, 1956, landed after 1 day in ice on a trawler; lot V from Quero Bank, October 18, 1957, landed after 8 days in ice (Dyer and Fraser, 1959); lot VI from off Sable Island, September 13, 1957, landed after 4 days in ice. The fillets had been frozen in commercial 1-lb blocks with machine-sealed, waxed paper overwrap, and were stored at either –18°C or at –23°C. Samples were periodically removed, cut into small pieces with a knife and well mixed, while the flesh was still hard frozen, to avoid loss of any drip that might be formed on thawing. There was no change in any of the values reported during storage of these frozen lots.

The *rosefish*, lot VII, was from a lot landed by trawler on November 13, 1952.

TABLE I. Composition of edible portions of miscellaneous teleosts, Chondrostei, Chimaerae. All values are on wet-weight basis. Crude protein calculated from total N × 6.25; protein from protein N × 6.25. Total S_1 is sum of water, lipid, ash and crude protein; total S_2 is sum of water, lipid, ash and protein. (A—thick section, white meat; B—tail section, white meat; C—belly flap; M—minced mixed fillets; FL—white fatty blubber.)

Miscellaneous teleosts	Section	Water	Lipid	Ash	TN	Crude protein	Total S_1	NPN	PN	Protein	Total S_2	TMA	TMAO	SPN	AM	Alb	FFA	NPN
		%	%	%	%	%	%	%	%	%	%	*mg N/100 g*		—	*% TPN*	—	*% lipid*	*%TN*
HETEROMI																		
Spiny eel																		
Dec. 1960	A	73.5	5.4	...	2.99	18.7	...	0.40	2.59	16.2	...	2.2	78	...	...	...	...	13.4
Jan. 1961	A	67.5	12.2	1.07	2.65	16.6	97.4	0.40	2.25	14.1	94.9	0.3	98	...	...	...	...	15.1
	FL	31.1	56.0	0.52	1.21	7.6	95.2	0.20	1.01	6.2	93.9	0.3	41	...	...	...	...	16.5
ISOSPONDYLI																		
Shad																		
Nov. 1960	M	72.9	17.2	...	2.92	18.3	...	0.37	2.56	16.0	...	1.8	30	...	...	...	...	12.7
OSTARIOPHYSI																		
White sucker																		
May 1959,	A	80.6	1.1	1.30	2.80	17.5	100.5	0.40	2.40	15.0	98.0	0.1	0.1	98	74	24	2.0	14.3
(Av. of 2 fish)	B	80.8	2.0	1.20	2.92	18.3	102.2	0.40	2.51	15.7	99.7	...	...	...	...	...	2.6	13.7
	C	80.0	0.9	1.50	2.78	17.4	99.8	0.40	2.38	14.9	97.3	...	...	...	...	...	3.2	14.4
Frozen 3 mo. at −23°C	A	81.9	1.4	1.30	2.65	16.6	101.1	0.34	2.31	14.4	99.0	...	...	91	67	24	10	12.8
	B	81.5	1.1	1.30	2.65	16.6	100.4	0.36	2.29	14.3	98.2	...	...	89	69	20	11	13.6
	C	81.3	1.3	1.50	2.53	15.8	99.9	0.34	2.19	13.7	97.8	...	...	...	...	...	10	13.4
CHONDROSTEI																		
Sea sturgeon																		
Apr. 1954	A	77.8	6.2	...	2.27	14.2	...	0.34	1.93	12.1	...	0	0	...	...	...	...	15.0
CHIMAERAE																		
Chimaera																		
Nov. 1960	A	83.4	0.7	...	2.90	18.1	...	1.36	1.54	9.6	...	0.4	234	...	...	...	...	46.9

Analytical Procedures

The analytical procedures are given in Part I of this series (Mannan *et al.*, 1961a). Values in Tables I and III of the present paper for total nitrogen (TN), non-protein nitrogen (NPN), trimethylamine oxide (TMAO), trimethylamine (TMA), salt-peptizable protein (SPN) and actomyosin (AM), are the average of duplicate determinations.

RESULTS AND DISCUSSION

Spiny Eel

The spiny eel was a fatty fish, 5.4 to 12.2% lipid in the white flesh (Table I), with the other constituents having values similar to those in the other teleost fishes analyzed. The fatty "blubber" tissue in the larger specimen contained 56% lipid, but only 6.2% protein (protein N $\times$ 6.25) in agreement with the reduced moisture content of 31%. NPN, ash, and TMAO were also correspondingly lower.

Shad

The shad, having 17.2% lipid but a normal protein content of 16%, was a fall specimen in good condition. Clark and Almy (1918) also reported high lipid values for shad prior to the spawning migration in April, whereas in the spawning or spent fish in May and June the fat was reduced to 3 to 6%, with a slight lowering of protein as well. Herring belong to this family, and Leim (1958) found fat values as low as 1.2% in April and June, with values as high as 27.5% in August to November in the Bay of Fundy. Here, spawning occurs mainly in the late fall (Tibbo and Legaré, 1960).

White Sucker

The white sucker was a non-fatty fish, with no dark muscle, and showed almost no variation between the thick muscle A, the tail portion B, or the belly flap C. Other values were almost identical with those of haddock and cod, except for the absence of TMAO. There is a possibility that the fat may have been depleted by spawn formation and samples taken earlier in the season should be examined. Protein extractability was only slightly less after frozen storage for 3 months at –23°C.

Sturgeon and Chimaera

The sturgeon was medium-fatty, containing about 6% lipid. The moisture content was rather high and protein was rather low, being only 12.1%. The chimaera, on the other hand, being more closely allied to the elasmobranchs, was quite different; its lipid and protein contents were very low, 0.7 and 9.6% respectively, while the moisture content was high, 83.4%. In this respect, it would be interesting to determine whether this was related to the spawning

condition or was characteristic of this species. According to Vinogradov (1953), no analytical data have been reported for this Order. About 47% of the total nitrogen was NPN, and the TMAO was also very high, 234 mg N per 100 g. The latter compares with the value of 180 found in the Pacific species (*Hydrolagus colliei*) (Norris and Benoit, 1945), and with the high TMAO and urea contents in the elasmobranchs (Dyer, 1952; Groninger, 1959).

Haddock

In haddock, a thin layer of dark fatty tissue, much less pronounced than in mackerel, is present under the skin along the sides of the fish and thickens towards the tail. Dissection showed that it comprised 8% of the edible tissue in the tail section, but only 0.8% in the cross-section at the thick part of the fish (Table II).

Table II. Proportion of skin, bone and edible meat in steaks from a haddock 64 cm long, landed very fresh, probably no more than 1 to 2 days on ice, on Feb. 1, 1961.

	Steak A (thick section; total weight 396 g)	Steak B (tail section; total weight 166 g)
	%	%
Proportion of total weight:		
Skin	5.8	6.0
Bone	10.4	9.0
Fins	4.0	9.6
Edible portion	79.8	75.4
Proportion of edible portion:		
White meat	82	92
Dark layer	0.8	8
Belly flap	17	0

The belly flap comprised about 17% of the edible portion of the latter. The lipid content of the brown lateral line tissue was 2% (Table III) and thus the B section (including dark meat) should have been slightly higher in lipid, but the differences were much smaller than in halibut and the fatty species. The belly flap of the various samples was somewhat higher in lipid, 0.89%, as compared to averages of 0.71 and 0.77 in the A and B sections. Little difference appeared in protein, moisture or in NPN between the various sections. Comparable data for average values reported by various authors (Table IV) agree closely, except for fat content, which depends on the method used (Mannan *et al.*, 1961a). The proportion of the total nitrogen contributed by NPN, 16%, was slightly higher than in the halibut, but lower than in the mackerel family. Komarov (1932) found an NPN content of 0.38% which is slightly less than that found here, 0.45% (wet weight).

An increase in moisture content during June to July was not found in the present samples, although Crooks and Ritchie (1939) noted an increase from the

TABLE III. Composition of edible portions of haddock, cod, and wolffish. All values are on wet-weight basis. DB—reddish brown lateral line tissue. L—central section. (Other details as in heading of Table I.)

	Section	Water	Lipid	Ash	TN	Crude protein	Total S_1	NPN	PN	Protein	Total S_2	TMA	TMAO	SPN	Alb	FFA	NPN
		%	%	%	%	%	%	%	%	%	%	mg N/100 g		% TPN		% lipid	% TN
Haddock:																	
June 1959, Pre-rigor	A	81.3	0.68	1.25	2.95	18.4	101.6	0.47	2.49	15.5	98.6	1.2	51	93	21	5.3	15.7
	L	81.2	0.70	1.15	2.94	18.4	101.4	0.46	2.49	15.5	98.6	0.7	58	97	25	4.6	15.5
	B	81.1	0.70	1.20	2.86	17.9	100.9	0.46	2.40	15.0	98.0	0.7	57	92	25	4.2	16.1
July 1959, Pre-rigor	A	81.3	0.74	1.30	2.78	17.4	100.7	0.46	2.32	14.5	97.8	0.4	55	99	24	1.8	16.5
	B	81.0	0.82	1.26	2.72	17.0	100.1	0.52	2.20	13.8	96.9	0.5	53	97	22	3.6	19.1
	C	82.2	0.99	1.10	2.70	16.9	101.2	0.45	2.25	14.0	98.3	0.7	42	88	24	5.1	16.6
Apr. 1959, Frozen 2 months at −23°C	A	79.7	0.69	1.10	2.89	18.1	99.6	0.43	2.46	15.4	96.9	0.5	47	78	28	32	14.9
	B	79.4	0.80	1.20	3.16	19.8	101.2	0.44	2.71	16.9	98.3	0.5	43	82	27	27	14.0
	C	80.1	0.83	1.13	2.84	17.8	99.9	0.43	2.41	15.1	97.1	0.5	44	67	25	31	15.1
Feb. 1961	A	79.8	0.72	1.13	3.10	19.4	101.0	0.37	2.73	17.1	98.7	0.3	61	...	...	...	11.9
	B	80.4	0.75	1.15	3.03	18.9	101.3	0.39	2.64	16.5	99.9	0.4	62	...	...	...	12.9
	C	80.5	0.86	1.09	2.99	18.7	101.2	0.35	2.64	16.5	100.0	1.8	39	...	...	...	11.7
	DB	81.1	2.0	1.15	2.96	18.5	102.8	(0.31)	2.65	16.6	100.9	...	...	...	...	...	(10.5)
Average	A	80.5	0.71	1.20	2.93	18.3	100.7	0.43	2.50	15.6	98.0	...	53	...	...	...	14.8
Average	B	80.5	0.77	1.20	2.94	18.4	100.9	0.45	2.49	15.6	98.3	...	54	...	...	...	15.5
Average	C	80.9	0.89	1.11	2.84	17.8	100.8	0.41	2.43	15.3	98.5	...	42	...	...	...	14.5
Cod:																	
May 1959, Pre-rigor	A	80.3	0.71	1.36	2.80	17.5	99.9	0.47	2.33	14.6	97.0	...	...	...	...	3	16.7
	B	79.8	0.70	1.21	2.87	17.9	99.6	0.47	2.40	15.0	96.7	...	...	...	...	4	16.3
	M	80.6	0.77	1.29	2.92	18.2	100,9	0.47	2.45	15.3	98.0	0.3	90	92	22	2	16.3
Wolffish:																	
Feb. 1960	A	79.7	2.1	1.16	2.96	18.5	101.5	0.40	2.56	16.0	99.0	0.2	52	...	...	2	13.5
	B	...	1.0	...	...	...	...	...	...	...	...	...	...	...	...	5	...

yearly average of 81.0% to values of 84.1% in May and 82.7% in July. This corresponds to the spawning period, which, according to Homans and Vladykov (1954), is mainly in April and May in the Canadian Atlantic area. These authors also state that haddock do not feed during the period just prior to or during spawning. In starving cod held 78 days in a tank at about 14°C, the

TABLE IV. Proximate composition of edible flesh of haddock (wet-weight basis; crude protein calculated from total N × 6.25).

Source of data	Water	Lipid	Ash	Crude protein
	%	%	%	%
Crooks and Ritchie (1939)	79.3–84.1	0.09–0.27	Av. 1.24	. . .
	Av. 81.0	Av. 0.13	–	. . .
McCance and Widdowson (1940)	81.3	0.6	. . .	15.9
Reay *et al.* (1943)	79.1–84.1	0.1–0.6	. . .	14.6–20.3
Watt and Merrill (1950)	80.7	0.1	1.4	18.2
Braekkan (1958)	78.6	0.25	1.1	19.7
Average A and B (Table III)	80.5	0.74	1.20	18.3

moisture increased from about 80 to between 84 and 88% (Love, 1958). Thus, the utilization of protein and its replacement by water in the final stages of the maturation period, when the fish are fasting as well, may be greater in these species than in those with fat reserves. Even in salmon, a considerable proportion of the energy requirements for maturation is supplied by the body protein in addition to that derived from the fat reserves (Idler and Bitners, 1958). These authors also show that the protein and fat lost are only partially replaced by a gain of water in the flesh. A few analyses of cod showed protein, fat and water percentages almost identical to those in haddock, and no gross difference was found between the various sections.

Wolffish

The sample of wolffish flesh gave values almost identical to those of haddock, except that the white flesh had 2.1% fat. Only a very thin yellowish fatty layer along the lateral line was present in this species, and an excised sample contained only 2.6% lipid. The 0.40% NPN value was higher than that (0.26%) reported by Shewan (1951).

Cod

Some analyses for minced, mixed fillets (M) from commercial market-size cod are summarized in Table V. Moisture, lipid, protein, and soluble protein nitrogen values are almost identical to those of haddock, with NPN being a bit lower and TMAO higher. It is interesting to note that the average protein found in cod, 15.6%, agreed well with the value of 15.2% obtained by Dambergs (1959) by an extraction procedure not involving nitrogen estimations.

TABLE V. Summary of composition of cod and rosefish fillets from frozen storage experiments. Average values (wet-weight basis) are given, together with the standard deviation in parentheses, followed by the number of samples analyzed.

Sample		Water	Lipid	TN	Crude protein	NPN	PN	Protein	TMA	TMAO	SPN	Alb	NPN
		%	%	%	%	%	%	%	mg N/100 g		% TPN		% TN
Cod:													
Jul. 12/55, iced 2 days	M	80.6 (±0.55) 56	... –	2.83 (±0.056) 47	17.7 –	0.35 (±0.02) 49	2.48 (±0.06) 47	15.5 –	0.97 (±0.34) 43	59.8 (±8.2) 24	92 –	23 –	12.3 –
Jul. 26/56, iced 2 days	M	81.7 (±0.63) 125	... –	2.80 (±0.045) 16	17.5 –	0.31 (±0.018) 16	2.49 –	15.6 –	1.1 (±0.42) 16	61.7 (±9.3) 8	83 (±2.5) 8	20 (±2.0) 8	11.1 –
Oct. 25/56, iced 1 day	M	81.6 (±0.76) 24	... –	... –	... –	... –	... –	... –	0.5 –	75 –	86 –	23 –	... –
Oct. 18/56, iced 8 days	M	81.3 (±0.45) 26	... –	... –	... –	... –	... –	... –	6.0 –	78 –	86 –	22 –	... –
Sept. 13/57, iced 4 days	M	81.4 (±0.44) 69	0.59 (±0.074) 81	... –	... –	... –	... –	... –	0.70 (±0.21) 12	... –	91 –	23 –	... –
Rosefish:													
Nov. 13/52	M	79.6 (±0.63) 11	3.3* (±0.92) 14	2.80 (±0.077) 11	17.5 –	0.31 (±0.055) 12	2.49 –	15.6 –	4.0 –	... –	83 –	20 –	11.1 –

*Crude fat by acid hydrolysis (A.O.A.C., 1955). Fat by $CHCl_3$–Na_2SO_4 (Dyer and Morton, 1956) is 2.0 (±0.63) 18.

Rosefish

Previous analyses of rosefish (Dyer *et al.*, 1956) showed a fat content averaging about 3.3% (Table V), but otherwise the composition was identical to haddock.

Table VI. Proximate composition (on wet-weight basis) of various members of the cod family. Percentages of crude protein calculated from total N × 6.25. (Data from Braekkan, 1958.)

	Water	Lipid	Ash	Crude protein
	%	%	%	%
Cod—*Gadus morhua*	80.4	0.34	1.1	18.1
Coalfish—*Gadus virens* (=American pollock—*Pollachius virens*)	78.4	0.7	1.2	19.4
Pollack—*Gadus pollachius*	77.7	0.6	1.6	19.1
Haddock—*Gadus aeglefinus*	78.6	0.25	1.1	19.7
Ling—*Molva molva*	78.5	0.32	1.5	19.2
Cusk—*Brosmius brosme*	77.8	0.25	1.5	19.8

The similarity of composition of the members of the Orders Anacanthini and Percomorphi is striking, the exception being the fat and the TMAO values. This is also evident in the data of Braekkan (1958), summarized in Table VI, which include other closely related species. It appears that there is very good agreement in samples from various parts of the world.

Comparison of Composition of the Sections of Above Various Species with Those of Halibut, Mackerel, Tuna and Swordfish (Mannan *et al.*, 1961a,b)

Fat. The white meat varied from about 0.7% in haddock and similar lean fish to about 6.5%, except for mackerel which reached 16%. The flesh of the belly flap had a much higher lipid content in the halibut and mackerel group. The reddish-brown lateral layer was also much richer in lipid than the white meat, ranging from about 2% in haddock, 4 to 8% in halibut to about 22% in mackerel.

Moisture. This varied from 74.2 to 83.4% in the white muscle, except in fat mackerel where it was only 64%. It was lower in the belly flap and dark meat, where fat was higher.

The sum of moisture and lipid varied between 77.5% and 82%, except for the belly flap of the fat mackerel with 37.2% fat, where the sum was 86.5%, and the sturgeon and chimaera, where it was 84 and 84.1%. In the latter, the protein was also much lower, about 9 to 12%.

Total nitrogen. This ranged from 2.8 to 3.6%, except for a value of 2.3% in the sturgeon, while protein had a very narrow range of 14.8 to 16.2% for most species. It was higher in the halibut, mackerel and tuna, lying between 18.9 and 19.5%, and lower in the sturgeon and chimaera, with only 12.1 and 9.6% as noted above. Both total nitrogen and protein were lower in the belly flap and in the dark brown lateral line muscle, indicating that in these fatty tissues some protein as well as moisture is displaced by fat.

Non-protein nitrogen. NPN varied from 0.31 to 0.46%, but was higher in the mackerel and swordfish families, 0.58 to 0.73%, and very much higher in the chimaera, 1.4%. As a proportion of the total nitrogen, it ranged from 11 to 16%, with values of 19 to 20% for tuna and swordfish and 47% for chimaera. Except for a high value in the belly flap of the halibut, there was little difference between the white, dark or belly flap meat. TMAO was lower in the belly flap muscle of halibut, haddock, and mackerel, but higher in the brown muscle of the latter. These data confirm and extend Shewan's results (1951), which ranged from 9 to 14% (of total N) in the flatfish and gadoids, and 14 to 18% in the herring group with much higher values (34 to 38%) in the elasmobranchs.

Protein extractability. This was generally 90 to 97%, with lower values for the belly flap and dark brown muscles. The non-actomyosin fraction or "albumin", soluble at low ionic strength, appeared to be very constant, 20 to 23%, except for one species, the tuna, where it was 31% of the protein nitrogen.

Free fatty acid (FFA). These values in the very fresh fish ranged from 0.2 to about 5% of the extracted fat. They appeared to be lower in the more fatty samples, probably because the acid phospholipid components contribute a large proportion of the acidity in the lean fish where phospholipid makes up half or more of the total fat (Olley and Lovern, 1960; Bligh, 1961), whereas in the fatty species the constitutional lipid is effectively diluted by the large amounts of triglyceride present (Dill, 1921). In those few samples which were stored frozen for 2 to 3 months prior to analysis, large increases in free fatty acid occurred in the white sucker and haddock, but little if any increase was observed in halibut or mackerel. It appears that hydrolysis, presumably enzymic, occurs in the lipid of the haddock and the white sucker, as it does in cod (Dyer and Fraser, 1959).

Proportion of brown lateral-line tissue, and other fatty tissues. In the mackerel, the brown fatty layer accounted for about 14% of the weight of the edible part, in halibut about 6 to 7%, in haddock about 8% in the tail section and only 1% in the thick part. It was also prominent in the tuna and swordfish. Only a trace was present in the wolffish, spiny eel, chimaera and white sucker.

A layer of blubber or white fatty tissue, about two-thirds fat, was present in some specimens, e.g. tuna and the large spiny eel. It was thickest around the dorsal fin and appeared as a separate layer enclosed in connective tissue beneath the skin, and was separate from the brown fatty lateral-line tissue.

These results show that while the average composition of most of the species of fish discussed is very similar and varies little with season or area, in others there is a great variation, not only with season or maturity, but in the different sections of the individual specimens. To compare the nutritional value, the composition of the white meat should first be considered; then, if any considerable portion of the dark meat or other fatty parts will be included in the actual portion consumed during a meal, the calculation should be adjusted accordingly.

Note added in proof:

It has been brought to our attention that Braekkan (1959) has provided a good description of the occurrence of red muscle in several fish species, and suggests that the red muscle provides a storehouse for fat, glycogen and other metabolites in close proximity to the white or ordinary muscle. The position and amount of the red muscle varies from the anterior to the caudal ends of the fish and the arrangement in the tuna and shark families was found to differ considerably, being present as a distinct muscle embedded in the main trunk muscle rather than being situated under the skin along the lateral line as in most species. The fat content of the red meat was higher by 1.5 to 7 times that of the ordinary muscle in the species examined, in agreement with the present results.

REFERENCES

AMERICAN FISHERIES SOCIETY. 1960. A list of common and scientific names of fishes from the United States and Canada, 2nd ed. Special publication No. 2. Ann Arbor, Michigan, U.S.A. 102 pp.

ASSOCIATION OFFICIAL AGRICULTURAL CHEMISTS (A.O.A.C.). 1955. Official and tentative methods of analysis. 8th ed., p. 311. Washington.

BLIGH, E. G. 1961. *J. Fish. Res. Bd. Canada*, **18**: 143–145.

BRAEKKAN, O. R. 1958. *Fiskeridirektoratets Skrifter, Serie Teknologiske Undersokelser*, **III**(6): Pt. 3, 1–32.

1959. *Ibid.*, **III**(8): 1–42.

BRANDES, C. H., AND R. DIETRICH. 1953. *Fette, Seifen, Anstrichmittel*, **55**: 533–541.

CLARK, E. D., AND L. H. ALMY. 1918. *J. Biol. Chem.*, **33**: 483–498.

CROOKS, G. C., AND W. S. RITCHIE. 1939. *Food Research*, **4**: 159–172.

DAMBERGS, N. 1959. *J. Fish. Res. Bd. Canada*, **16**: 63–71.

DILL, D. B. 1921. *J. Biol. Chem.*, **48**: 73–82.

DINGLE, J. R., AND W. J. DYER. 1955. *J. Fish. Res. Bd. Canada*, **12**: 646–648.

DYER, W. J. 1952. *Ibid.*, **8**: 314–324.

DYER, W. J., AND D. I. FRASER. 1959. *Ibid.*, **16**: 43–52.

DYER, W. J., D. I. FRASER, D. G. ELLIS AND W. A. MACCALLUM. 1957. *Ibid.*, **14**: 627–635.

DYER, W. J., D. I. FRASER AND W. A. MACCALLUM. 1957. *Ibid.*, **14**: 925–929.

DYER, W. J., AND M. L. MORTON. 1956. *Ibid.*, **13**: 129–134.

DYER, W. J., M. L. MORTON, D. I. FRASER AND E. G. BLIGH. 1956. *Ibid.*, **13**: 569–579.

GRONINGER, H. S. 1959. The occurrence and significance of trimethylamine oxide in marine animals. *U.S. Fish and Wildlife Service, Special Scientific Rept., Fisheries*, No. 333, 22 pp.

HOMANS, R. E. S., AND V. D. VLADYKOV. 1954. *J. Fish. Res. Bd. Canada*, **11**: 535–542.

IDLER, D. R., AND I. BITNERS. 1958. *Can. J. Biochem. Physiol.*, **36**: 793–798.

JORDAN, D. S., AND B. W. EVERMANN. 1896–1900. The fishes of North and Middle America. *U.S. National Museum Bulletin* No. 47. Washington, Govt. Printing Office. 3313 pp.

KOMAROV, S. A. 1932. *Contrib. Canadian Biol. Fisheries*, **8**: 123–130.

LEIM, A. H. 1958. *J. Fish. Res. Bd. Canada*, **15**: 1259–1267.

LOVE, R. M. 1958. *J. Sci. Food Agric.*, **9**: 617–620.

MANNAN, A., D. I. FRASER AND W. J. DYER. 1961a. *J. Fish. Res. Bd. Canada*, **18**: 483–493. 1961b. *Ibid.*, **18**: 495–499.

McCANCE, R. A., AND E. M. WIDDOWSON. 1940. The chemical composition of foods. New York, Chemical Publishing Co., Inc. 150 pp.

NORRIS, E. R., AND G. J. BENOIT. 1945. *J. Biol. Chem.*, **158**: 433–438.

OLLEY, JUNE, AND J. A. LOVERN. 1960. *J. Sci. Food Agric.*, **11**: 644–652.

REAY, G. A., C. L. CUTTING AND J. M. SHEWAN. 1943. *J. Soc. Chem. Ind.* (London), **62**: 77–85T.

SHEWAN, J. M. 1951. *Biochem. Soc. Symposia* (Cambridge, Engl.), No. 6, 28–47.

THURSTON, C. E. 1958. *Food Research*, **23**: 619–625.

THURSTON, C. E., AND H. S. GRONINGER. 1959. *J. Agric. Food Chem.*, **7**: 282–284.

TIBBO, S. N., AND J. E. H. LEGARÉ. 1960. *J. Fish. Res. Bd. Canada*, **17**: 933–942.

VINOGRADOV, A. P. 1953. The elementary chemical composition of marine organisms (Efron and Setlow, translators). New Haven, U.S.A., Sears Foundation for Marine Research. 647 pp.

WATT, B. K., AND A. L. MERRILL. 1950. Composition of foods—raw, processed, prepared. *U.S. Dept. of Agric., Agric. Handbook* No. 8, Washington. 147 pp.

Oceanographic Features of Inlets in the British Columbia Mainland Coast[1]

BY G. L. PICKARD

Institute of Oceanography,
University of British Columbia, Vancouver, B.C.

CONTENTS

[1]Received for publication May 15, 1961.

J. FISH. RES. BD. CANADA, 18(6), 1961.
Printed in Canada.

CONTENTS

ABSTRACT

The inlets of the British Columbia mainland coast are morphologically fjords but few possess sills of depth less than 15 m.

The most significant influence in them is the fresh water runoff, chiefly from rivers. It is large in many of the inlets fed by rivers from glaciers, is seasonal in flow, and determines the estuarine character and circulation of the inlets and thereby the distribution of water characteristics.

In the large-runoff inlets the surface salinity increases from zero at the head to coastal sea values at the mouth. In winter the surface temperature is low and uniform but in summer it increases from the head, reaches a maximum where the salinity is about 8‰ and then diminishes toward the mouth. The water is highly stratified, particularly from the surface to about 20 m depth where the salinity rises to 90% or more of the deep water value. The marked halocline in the upper layer is accompanied by a marked thermocline. Below 50 m the salinity and temperature do not change much along the length of an individual inlet.

There is a pronounced geographical change of deep water characteristics from 30.7‰ and 8.3°C in the southern to 33.2‰ and 6.3°C in the northern inlets. In general, seasonal changes of temperature can be detected to 100 m but of salinity to only 30 m, suggesting a difference in the rates of eddy diffusion. Changes of deep water characteristics occur irregularly.

In many of the inlets a temperature minimum at 20 to 100 m depth is common in the inner reaches in the spring and diminishes in intensity later in the year.

In the inlets with medium or small runoff the surface salinity is generally higher and changes less along an inlet, and the halocline and thermocline are less marked. The homogeneous surface layer characteristic of the large-runoff inlets is usually absent.

Generally the large-runoff inlets show less variable dissolved oxygen values along an inlet at any depth than do the small-runoff inlets. Supersaturation of the upper layers is common, and there is often an oxygen maximum just below the halocline of the larger-runoff inlets. A few small-runoff inlets have a mid-depth oxygen minimum in which the lowest values are at the inlet head. Dissolved oxygen values of less than 2 ml/l are not common in any mainland inlets and zero values have not been definitely recorded.

The optical turbidity in large-runoff inlets is high in the surface layer, lower in the main body of water, and often increases in the bottom 50 to 100 m. At the heads of the large-runoff inlets Secchi-disc depths of 0.1 to 0.3 m are common in the summer. In the inlets with smaller runoff the turbidity is less. In both types the turbidity is at a maximum in the summer and a minimum in the winter, and the particulate material in the water is largely minerogenic.

Internal waves of period 1 to 4 minutes and amplitude up to 5 m occur in the upper layers. At mid-depth (20 to 150 m), vertical oscillations of the isotherms with semidiurnal tidal period are common, the amplitude being from 5 to 75 m.

A waxy substance sometimes found floating or washed ashore in Bute Inlet during cold winters appears to be peculiar to that inlet as no reference has been found to any similar substance being observed elsewhere in the world.

1. INTRODUCTION

THE MAINLAND COAST of British Columbia is indented by many long, relatively narrow, deep bodies of water opening on to the sea at one end and generally having a river at the other. These indentations are variously and unsystematically named "inlet", "arm", "channel", "canal", etc. on the charts. For simplicity, and following the practice of Vancouver (1798) who was the first to present a systematic description of the coast, the term "inlet" will be used as a generic term in the present discussion. The appellation "inlet", "canal", etc. will generally be omitted when referring to inlets by name.

An outline of the coast is given in Fig. 1 and 2 in which the more important inlets are named. There are 42 inlets (named in Table I) of 10 (nautical*) miles (18.5 km) or more length in the mainland coast, and in addition 15 in Vancouver Island and one in the Queen Charlotte Islands.

Their shape and location and the inflow of fresh water which gives rise to a brackish surface layer identifies most of these inlets as estuaries in the sense in which the term is currently used to describe a "semi-enclosed body of water having a free connection with the open sea and containing a measurable quantity of sea salt" (Pritchard, 1952, p. 245). The considerable depth and other characteristics of the British Columbia inlets suggest a comparison with the fjords of the Norwegian and New Zealand coasts and the deep inlets on the Pacific coast of South America, and a distinction from shallow estuaries such as Chesapeake Bay. It will be made clear however that there are some significant differences from the Norwegian fjords.

The investigation of estuarine circulation has attracted considerable attention in recent years and the Institute of Oceanography of the University of British Columbia has selected as one problem the study of the circulation in these deep estuaries.

Before the commencement of the present study, Alberni Inlet in Vancouver Island had been studied in detail by Tully (1949), and a limited amount of information, chiefly for the surface layers, was available for several others. These included Indian Arm, Howe Sound and Bute Inlet (Hutchinson and Lucas, 1931), Howe Sound, Jervis, Sechelt and Toba Inlets (Carter, 1932, 1934) in the mainland, and Saanich (Carter, 1934) and Nootka Sound (including Muchalat, Tlupana and Tahsis Inlets) (Tully, 1937) in Vancouver Island. The remainder of the inlets were unexplored oceanographically in 1950. As it was not possible to study all of the inlets in detail it was necessary to make some selection. To assist in this selection and to guide theoretical studies it was therefore necessary to extend the data to determine what characteristics were common to this type of water body and independent of local influence such as shape, wind stress etc. Since the study of the dynamics of the estuarine circulation was to be the salient feature it was appropriate to examine the inlets during the early summer when the fresh water run-off from the rivers was at its maximum.

*All sea distances given in this paper are in nautical miles.

FIG. 1. British Columbia mainland coast, northern portion, showing main inlets.

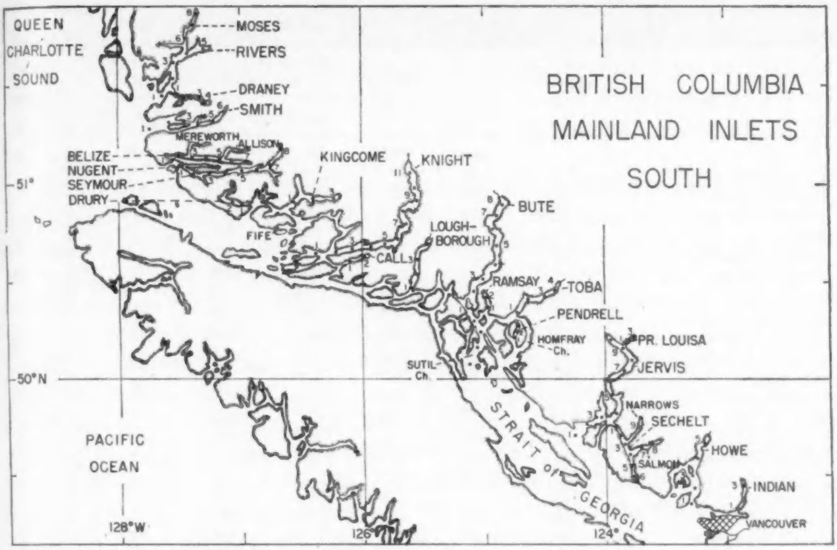

FIG. 2. British Columbia mainland coast, southern portion, showing main inlets.

To provide the general cover, an extensive 3-month cruise to 21 of the inlets was made in 1951. Most of the other mainland inlets were visited between 1952 and 1960. In addition, several of the typical southern inlets were visited a number of times between 1951 and 1960. Most of the cruises were made in the spring or summer, but some year-round data are available for Bute (1950–52; Tabata and Pickard, 1957), Bute and Jervis (1957–58), and Indian (1956-60; Gilmartin, 1960). The detailed data are available in the form of Data Reports, Institute of Oceanography, University of British Columbia (1953–1960) for the individual cruises.

The object of the present paper is to provide a summary of some of the oceanographic characteristics of the British Columbia mainland inlets, for reference and for comparison with similar coastal areas, and to draw attention to particular aspects of the inlet characteristics and of problems associated with them.

The 39 inlets included in this study are listed in Table I together with 5 whose oceanography has not yet been studied. All but 3 of the inlets are in the mainland coast proper; these three, Surf, Laredo and Pendrell, are in islands but are so closely associated with the mainland coast that they have been included in the present study.

When referring to position along the inlets, the term "head" is applied to the inland end and the term "mouth" to the seaward end. In several cases, the complicated topography makes it difficult to determine the mouth precisely, and the selection of its location from a chart alone may be rather arbitrary.

The chief observations made during the cruises were of depth, salinity, temperature, oxygen content, and turbidity of the water, plankton distribution, and bottom material.

TABLE I. Salient dimensions of British Columbia mainland inlets.

Name	Abbreviation	Length	Mean width	Mean mid-inlet depth	Maximum depth	Outer sill depth (Note 1)	Notes
		nautical miles		*m*	*m*	*m*	
Portland Canal	PoC	62	1.2	255	385	98	2
Portland Inlet	PoI	24	2.9	400	715	183	2
Observatory Inlet	Ob	41	1.2	385	530	46	3
Alice Arm	AA	10	0.7	240	385	18	2
Khutzeymateen Inlet	Kh	20	0.6	110	150	55	2,4
Work Channel	Wo	29	1.1	240	330	21	3
Porcher Inlet	Por	10	0.6	75	190	6	2,4
Douglas Channel	Do	45	1.9	330	455	210	2
Kildala Arm	Ki	10	0.8	175	240	162	2
Gardner Canal	Ga	70	1.0	275	500	37	2,5
Surf Inlet	Su	12	0.5	220	330	107	2
Laredo Inlet	La	21	0.8	295	400	128	2
Mussel Inlet	SM	18	0.8	275	435	146	3,6
Kynoch Inlet	MK	30	1.1	435	640	330	3,7
Spiller Channel	Sp	25	1.0	255	455	183	3
Briggs Inlet	Br	10	0.5	...	...	...	8
Roscoe Inlet	Ro	23	0.6	135	240	128	3
Cascade Inlet	Cas	14	0.6	250	305	128	3
Dean Channel	De	60	1.3	420	550	275	2,3
Kwatna Inlet	Kw	13	1.1	345	580	400	3
Burke Channel	Bur	56	1.4	400	550	43	3,9
South Bentinck Arm	SB	20	1.2	240	455	73	3
Rivers Inlet	Ri	25	1.6	295	365	137	2
Moses Inlet	Mo	14	0.5	200	290	37	2
Draney Inlet	Dr	13	0.5	90	145	11	3
Smith Inlet	Sm	18	0.7	270	365	122	2,3
Alison Sound	Al	11	0.5	...	185	...	4,10,11
Mereworth Sound	Me	10	0.5	...	185	...	4,10,11
Belize Inlet	Be	28	0.6	255	400	18	3,11
Nugent Sound	Nu	13	0.4	75	150	18	4,11
Seymour Inlet	Se	36	0.9	420	620	18	3,11
Drury Inlet	Dru	12	0.7	...	100	17	2
Kingcome Inlet	Kin	36	1.3	335	483	128	2
Knight Inlet	Kn	70	1.6	295	540	64	2
Call Inlet	Ca	15	0.8	135	209	48	2
Loughborough Inlet	Lo	19	0.9	190	260	128	2
Bute Inlet	Bu	41	2.0	510	660	355	2,12
Toba Inlet	To	20	1.4	390	505	490	2,12
Pendrell Sound	Pe	6	0.7	200	440	200	3
Jervis Inlet	Je	48	1.7	495	730	385	2
Princess Louisa Inlet	PL	4	0.4	120	180	6	2
Sechelt Inlet	Sec	22	0.8	190	300	14	2
Howe Sound	Ho	23	3.8	225	325	70	2
Indian Arm	Ind	14	0.7	130	218	20	2

NOTES:

(1) Depths are given for lowest normal tides. The tidal range varies from about 4 m at the south (Indian Arm) to 7 m at the north (Portland Inlet) and therefore the depth of water over the sills will periodically be increased by 4 to 7 m.

(2) Soundings from Canadian Hydrographic Service charts or field sheets (Portland Inlet and Canal from Admiralty Charts).

(3) Soundings during oceanographic cruises of Institute of Oceanography, University of British Columbia.

(4) Not yet visited by University of British Columbia.

(5) Sill depth quoted for exit through Ursula Passage, but Gardner also connects to Douglas through Devastation Channel, minimum depth 103 m.

(*See additional notes at foot of opposite page.*)

The depth measurements were made because before 1951 the majority of the inlets visited had either not been sounded or only partly sounded principally for navigation purposes. From echo sounder records and wire soundings, longitudinal profiles were prepared, but this part of the work was only incidental to the remainder of the program.

The main program consisted in the occupation of oceanographic stations at approximately 5-mile (9-km) intervals along the centre lines of the inlets, the locations being chosen as far as possible on straight sections rather than at bends. At each station serial observations were made of temperature, salinity and oxygen content of the water at as many as thirteen depths between the surface and close to the bottom. In each inlet and at each station the sampling depths were selected to permit the drawing of the salinity–depth curve with the minimum of individual interpolation. The necessity to adjust the depths arose chiefly in the surface layers (to about 30 m) because the main change in salinity takes place within this range. Temperatures were measured both with Richter and Wiese reversing thermometers, mounted on Atlas, Ekman or Fjarlie water sampling bottles, and with bathythermographs. Supplementary bathythermograph casts were frequently taken between the oceanographic stations.

The salinity was determined by titration of 10-ml samples by the Mohr method while the oxygen content was determined by the Winkler method using 250-ml samples.

At each station a Secchi-disc reading was taken together with observations of wind, air temperature, cloud cover and sea state.

Samples of the bottom sediments were obtained at some stations with either (a) a LaFond–Dietz bottom snapper (LaFond and Dietz, 1948) for the surface layers or (b) an Emery–Dietz-type gravity corer (Emery and Dietz, 1941) using a 3-foot by 1½-inch (1-m by 3.7-cm) core tube with lead weights to give a total weight of 70 lb (32 kg).

Some observations were made of internal waves with a direct-reading electrical resistance thermometer using a thermistor bead as temperature-sensitive element on a 25-m cable. For observations at greater depths a series of bathythermograph casts was used.

A vertical plankton haul and horizontal tows at four depths were made with Clarke–Bumpus samplers at alternate stations. The plankton distribution has been described by LeBrasseur (1954, 1955).

TABLE I.—NOTES—*Continued*

(6) From mouth of Sheep Inlet to head of Mussel Inlet.

(7) From west end of Oscar Passage, up Mathieson Channel to head of Kynoch Inlet.

(8) Not sounded; maximum of a few soundings in Briggs Inlet in 1956 was 70 m.

(9) Sill depth quoted for junction with Fitzhugh Sound, but Burke also connects with Dean through Labouchere Channel which is at least 400 m deep. (Ref. Note 2 above.)

(10) Not sounded in detail.

(11) Thompson and Barkey, 1938.

(12) But both Bute and Toba communicate with the Strait of Georgia through Sutil Channel which has a sill of depth 252 m.

Bute was the first inlet visited in 1951. Two weeks were spent in occupying each station a number of times to gain some familiarity with the distribution of characteristics and the effects of the tide in order to assist in planning the remainder of the 1951 study. In the other inlets the stations were occupied during a single visit to the inlet. In some cases the stations were occupied once only; in other cases it was possible to occupy stations both while proceeding to the head of the inlet and also on the return. During subsequent cruises many of the stations were reoccupied and a number of anchor stations were occupied for periods of several days.

2. GENERAL CHARACTERISTICS

2.1 Inlet Depth Profiles

Of the inlets in the mainland coast, twelve had been surveyed and detailed charts published by the Canadian Hydrographic Service before 1950, and since that time charts have been published for four others. The majority of the remainder have been surveyed by 1960. For those for which Canadian charts are not published it is necessary to rely upon the older Admiralty charts in which the shoreline is delineated reasonably well but in which depths are given only in isolated shallow localities. As the bottom profile is an inlet characteristic which may have a considerable influence on the water circulation, the echo sounder records were retained from cruises in those inlets not previously surveyed. From these, and from wire soundings obtained when bottom sampling, longitudinal depth profiles were prepared. The physical features of the inlets obtained from these data have been described previously (Pickard, 1956) but as some of the characteristics are relevant to the present discussion they are summarized here. The dimensions at sea level, and the average and maximum depths for the inlets obtained from the published charts or from cruise soundings are included in Table I. Longitudinal profiles are shown in Fig. 3, 4, and 5.

The general form of the southern inlets from Howe to Toba has been described by Carter (1934) and his description is applicable to most of the mainland inlets. They are generally deep, and narrow in relation to their length. The origin of the inlets has been discussed (e.g. Bancroft, 1913; Carter, 1934; Peacock; 1935) and it appears that both structural changes and glacial action contributed to their formation. The bottom profiles of the inlets generally show considerable variations in depth from head to mouth, the chief exceptions being Toba, Bute, Knight, Kingcome, Rivers and Douglas. The detailed Canadian Hydrographic Service surveys of Jervis, Bute, Kingcome, Douglas and Gardner show that there are considerable stretches of flat and often level mud bottom in these inlets. The significance of this is commented upon later.

Very shallow entrance sills, such as those in some Norwegian fjords (Strøm, 1936) where the sill depth is less than the depth of the brackish surface layer,

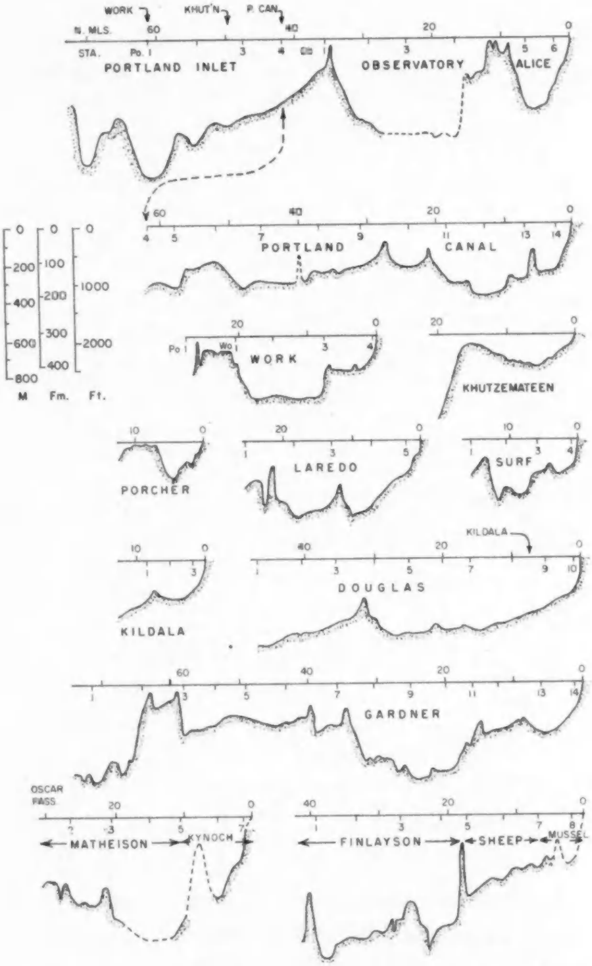

FIG. 3. Longitudinal sections along British Columbia mainland inlets, northern group.

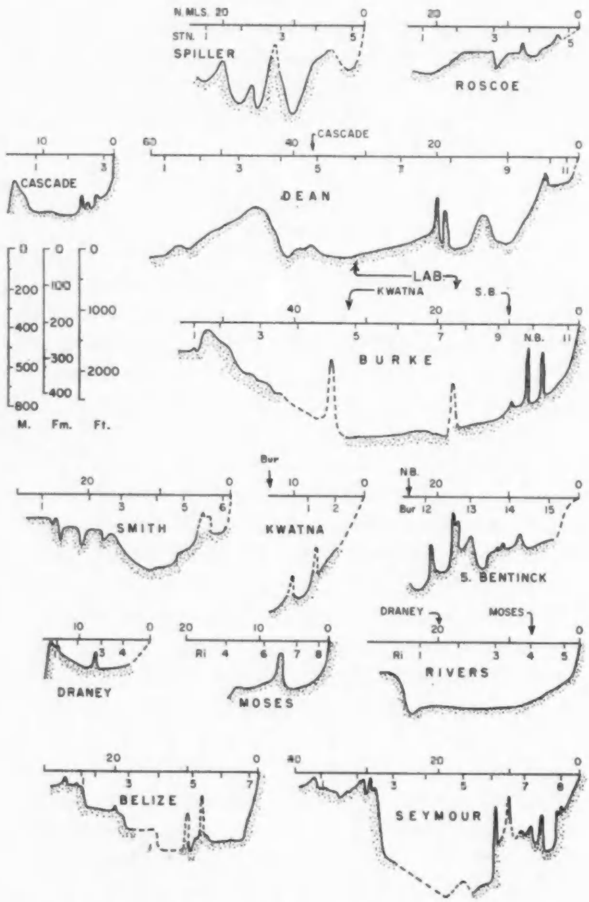

FIG. 4. Longitudinal sections along British Columbia mainland inlets, middle coast group.

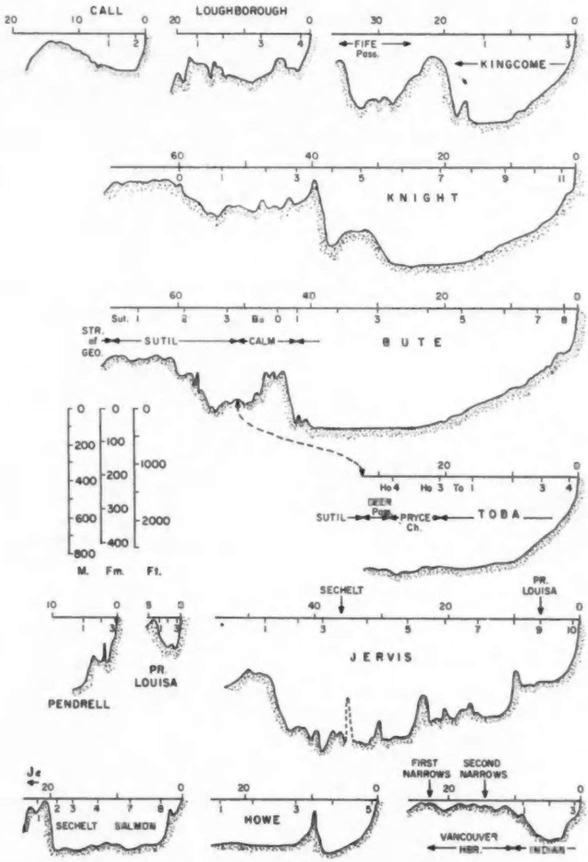

Fig. 5. Longitudinal sections along British Columbia mainland inlets, southern group.

are not found at all. A few inlets, as indicated in Table I, have sills of moderate depth (6 to 21 m) but in most cases the sills are deep. At the same time it must be remembered that the coastal seas into which all the inlets open are appreciably shallower (110 to 170 m) than the average in the inlets themselves. This feature is said to be typical of fjord coasts (Dinse, 1894).

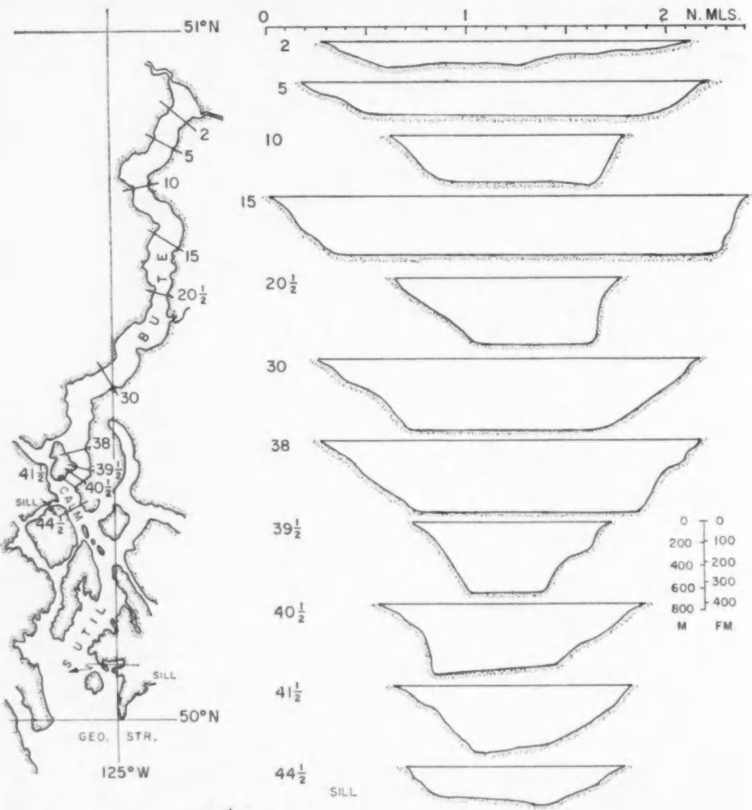

FIG. 6. Bute Inlet: transverse sections with same scale vertical and horizontal.

Figure 6 shows a selection of transverse sections across Bute drawn with no vertical-to-horizontal scale exaggeration. The distinctive features of these sections are the steep sides and the flat floor for the greater part of the inlet length. This flat floor appears to be characteristic of many of the large inlets into which considerable rivers flow. The superficial sediments are glacial silts (Toombs, 1956) and it is presumed that the flat floor is the result of a uniform settlement of this material from the water, the sediment being carried along the inlet either in the outflowing surface layer or by the agency of turbidity currents.

The relatively small amount of sediment found in the surface water layer suggests that the turbidity currents are probably the chief agent.

Figure 7 shows a selection of sections across Jervis, again with undistorted scale. The most notable difference from Bute is the absence of a flat bottom to seaward of section 7. The river inflow to Jervis is smaller than into Bute and there is a smaller concentration of suspended material in it. Presumably the material brought in at the head is trapped by the inner sill at about section 10. However, the fact that it reaches to this sill, and in fact is most conspicuous just inside the sill where the inlet is deeper than near the head, is regarded as significant. It again suggests that mud slides may take place from the inlet

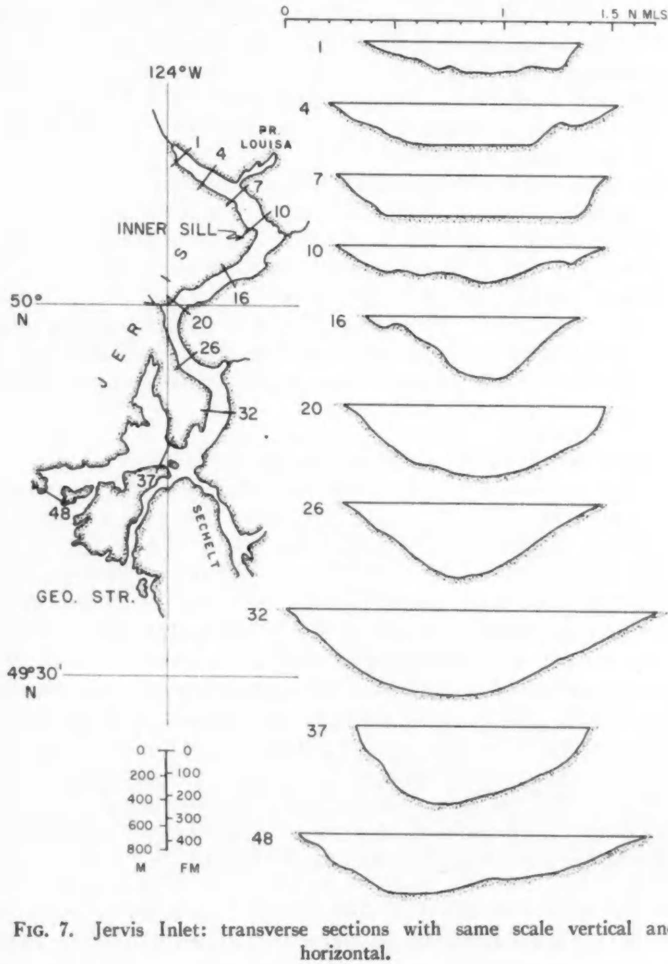

FIG. 7. Jervis Inlet: transverse sections with same scale vertical and horizontal.

head and cause turbidity currents which carry material along the bottom to the deepest part of the basin inside the sill. This hypothesis is supported by the evidence from Bute and Kingcome which have no inner sill and in which the very flat section is inside the outer sill and some 30 and 15 miles (56 and 28 km) respectively from the head. Further evidence for the frequent occurrence of turbidity currents has been put forward as a result of studies of optical turbidity due to particulate material in the inlet waters (Pickard and Giovando, 1960).

In Gardner (not illustrated), flat bottom sections are found to seaward of rivers entering at the head and at the side. This suggests that they are the result of direct deposition of river-transported material. A conspicuous flat section is found just to seaward of the Kemano River, but in this case it is not terminated at a sill. A deeper section with irregular bottom topography in transverse section is found only 3 miles beyond the flat one.

The profiles in Fig. 6 and 7 are drawn with no vertical-to-horizontal scale exaggeration and show that in many cases it will probably be possible, for theoretical study, to approximate the cross-section by a simple rectangular or trapezoidal form without significant error.

In plan form, on the other hand, the charts show that very few of the inlets are regular in shape. Sharp bends of 90° or more and variations in width by a factor of 2 are common (e.g. Fig. 1, 2, 6, 7). Observations of currents during cruises in 1952, 1953 and 1955 indicate that both the tortuous form of the inlets and the bottom irregularities where they occur have a profound influence on the local character of the flow. These irregularities in form are factors which have in the main been largely ignored in theoretical studies but which make it difficult to obtain representative current measurements for comparison with theory.

2.2 Bottom Materials

The character of samples of the bottom materials obtained with a snapper or a small gravity corer at 5- or 10-mile intervals has been described briefly (Pickard, 1956). The material was predominantly fine-grained mud, with sand in some samples, and occasionally pebbles or shells. About 75% of the mud samples were light to dark grey in colour when wet (from inlets with large run-off) and the remainder were greenish brown (from low-runoff inlets). Only a small percentage of samples smelled of H_2S. These were in the green–brown colour group, the grey samples having no smell.

The samples obtained in 1951 and 1952 in Bute were examined and described by Toombs (1956). He reported that the predominant minerals were quartz, feldspar, and biotite, while the organic content was very low (1 to 4%). No detailed study has been made of samples from other inlets but from field examination it is believed that the Bute results may be regarded as typical for the inlets with glacial runoff. It is probable that the bottom sediments in the small-runoff inlets have a higher organic content than those in Bute.

2.3 Fresh Water Discharge into the Inlets

Since the inlets are estuarine in character, information on the fresh water discharge into them is important but is unfortunately very scanty. However,

Trites (1955) has combined what data are available for river flow with data on precipitation for the watersheds concerned and has estimated the fresh water runoff into many of the inlets. Some idea of the amount of runoff and of the variation between inlets is given in Table II in which are presented Trites' values for the mean annual discharge.

TABLE II. Mean annual discharge of fresh water into some British Columbia inlets (after Trites, 1955).

Inlet	Group[1]	Fresh water discharge
		m³/sec
Portland Canal	A.1	260
Portland Inlet (Nass River)	A.1	990
Observatory	A.1	160
Gardner	A.1	580
Dean (above Labouchere)	A.1	280
Dean (total)	A.1	730
Burke	A.1	420
Rivers	A.1	540
Draney	A.2	40
Smith	A.2	120
Belize	A.2	80
Seymour	A.2	100
Knight	A.1	410
Loughborough	A.2	100
Bute	A.1	410
Toba	A.1	270
Jervis (above Sechelt)	A.2	180
Sechelt	A.2	110
Howe	A.1	460

[1]The significance of the grouping is explained in the text together with Table III and Fig. 4.

A method for estimating the fresh water transport along an inlet from the heat budget has been described and examples of its application are given by Pickard and Trites (1957). This offers a means for estimating the fresh water runoff into an inlet from observations of the distribution of temperature and salinity in the upper layers along the length of the inlet.

A pronounced seasonal variation in runoff occurs and the character of this is shown in Fig. 8. The majority of the inlets, including all the longer ones except Jervis and Observatory, have a considerable discharge, most of which comes from the summer melting of precipitation occurring during the winter as snow on higher inland elevations. The runoff to the majority group of inlets is a minimum during January–March and a maximum during May–July, with a secondary maximum in October. These inlets are combined as Group A.1 in Fig. 8, and examples of the annual variation are given for two southern inlets, (Bute and Knight) and for a northern inlet (Portland). The remainder of this group

fall between these limits. The lower minimum and higher maximum for Portland as compared to Bute are presumably due to climatic difference.

The minority of the inlets, mostly short ones, are not fed from stored runoff and show a different annual cycle as in Group A.2 in Fig. 8. Among this group the runoff is above average in the spring and in the winter months and below average during July–September, following the coastal rainfall pattern closely. The effect of this variation of runoff pattern on the surface layer of the coastal waters has been described by Pickard and McLeod (1953).

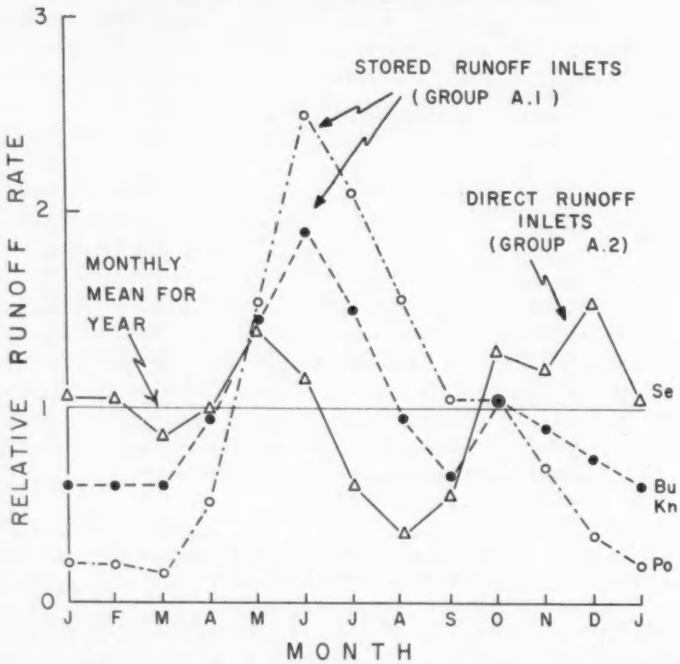

FIG. 8. Monthly runoff typical of stored runoff (Group A.1) and of direct runoff (Group A.2) inlets expressed as multiple of monthly mean for whole year.

2.4 TIDES

The principal characteristics of the tides of the British Columbia coast are that they are semi-diurnal and markedly declinational (having a marked inequality between the heights of successive low waters), and that the range increases from south to north. In the south at Point Atkinson near Vancouver the maximum range between low and high waters of large tides is 4.8 m, while at Prince Rupert in the north it is 7.6 m and at Stewart at the head of Portland Canal it is 8.0 m. Between the mouth and head of each inlet there is little difference in tide. At the head the time of high or low water is later by not more than 10

minutes than at the mouth, while the range is only from 1 to 10% greater than at the mouth (Dawson, 1920; Canadian Hydrographic Service, 1960).

2.5 Non-tidal or Estuarine Circulation

In his journal (1798, Vol. I, p. 309) Vancouver remarks: "In all these arms of the sea we had constantly observed, even to their utmost extremity, a visible, and sometimes a material rise and fall of the tide, without experiencing any other current than a constant drain down to the seaward, excepting just in the neighbourhood of the gulf." This net seaward motion is now recognized as a consequence of the discharge of fresh water into the heads of the inlets. The low-salinity surface layer so formed flows seaward, gaining in volume by entrainment of saline water from below as it does so and gaining in speed as it approaches the inlet mouth. The resulting unidirectional flow is superimposed on the flood and ebb due to the tide to decrease the speed of the former and increase that of the latter. It may even prevail over the flood to the extent of preventing any inward flow, the resultant being a seaward flow at all times but fluctuating in speed with tidal period. A further consequence of the entrainment of saline water into the outflowing surface layer is a subsurface inflow. The whole pattern of surface outflow and subsurface inflow is referred to as an "estuarine circulation". It has been described in detail for Alberni Inlet by Tully (1949), the dynamics have been discussed theoretically by Cameron (1951), and Pritchard (1952) has brought together the results of these and other workers with his own studies. Pickard and Rodgers (1959) have described more recent direct measurements of current in Knight. These suggest that the water movements in a deep inlet may be more complex than previous theoretical studies have assumed but support the net circulation pattern described above. Therefore in the present paper the estuarine circulation will be considered an established and expected feature of the British Columbia inlets.

3. SALINITY AND TEMPERATURE

The waters of all the inlets show marked horizontal stratification of both salinity and temperature, particularly near the surface. The water becomes more saline and, with some exceptions to be discussed later, colder with increase in depth. The salinity stratification is a consequence of the inflow of fresh water from the rivers, while the temperature stratification is a consequence of solar heating combined with the marked stability of the surface waters due to the salinity structure.

In describing the salinity and temperature distributions it is convenient to divide the water into two main depth zones, shallow and deep. The water in the first is fresh or brackish, while in the second it approximates in salinity to the water of the coastal seas. When considering the dynamics of the flow and the process of mixing between the fresh and salt waters it is necessary to subdivide the shallow zone into a surface zone and an intermediate or mixing zone (Tully, 1949). The depths of the surface and mixing zones vary from inlet to inlet, and

from time to time, and may be considered oceanographic characteristics of these bodies of water.

The inlets can be divided broadly into two groups:

A. those with a low surface salinity at the head, and

B. those with a relatively high surface salinity at the head.

Group A can be subdivided into possibly two subgroups (A.1 and A.2) in terms of salinity at the head and mouth. This division is shown in Table III,

TABLE III. Surface salinities, Secchi-disc readings and types of salinity profile in British Columbia inlets[1].

Group A.1				Group A.2				Group B			
Surface salinity											
Head	0.1– 2‰				1–11‰				18–29‰		
Mouth	5 –20‰				15–29‰				20–31‰		
Secchi-disc depth											
Head	0.3–1 m				4–7 m				6–10 m		
Mouth	2 –8 m				3–7 m				4–11 m		
Salinity profile type[2]											
	Mo	Mi	Hd[3]		Mo	Mi	Hd		Mo	Mi	Hd
Portland C.	1a	1b	1a	Sheep	2	2	2	Work	1c	1c	2
Observatory	1b	1b	1b	Spiller	2	1c	1b	Surf	2	2	2
Kildala	1b	1b	2	Roscoe	2	2	2	Laredo	2	2	2
Douglas[4]	1c	1b	1b	Draney	2	2	1b	Kynoch	1c	1c	2
Gardner	2	1b	1a	Smith	2	2	1b	Briggs	2	2	...
Cascade	1b	1b	2	Belize	1a	1b	2	Drury	2	2	...
Dean	1b	1b	1a	Seymour	2	2	2	Call	1c	...	1c
Burke	2	1b	1a	Loughborough	2	1b	1b	Pendrell	1c	...	1c
Rivers[4]	2	2	1a	Jervis	1c	2	2		or		or
Kingcome	1b	1b	1a	Sechelt	2	2	1b		2	...	2
Knight	1b	1b	1a	Indian	1b	1b	1b				
Bute	1c	1b	1a								
Toba	1c	1b	1a								
Howe	1b	1b	1a								

[1]A number of the smaller inlets, particularly those which are side arms of larger inlets, are special cases and have been omitted from this tabulation.

[2]The types of salinity profile are indicated in Fig. 15 and described in the text.

[3]Mo = mouth; Mi = middle; Hd = head of inlet.

[4]At head, surface salinity = 1 to 3‰, Secchi-disc depth = 1 to 2 m.

together with some data on salinity–depth profiles and on Secchi-disc depths which it is convenient to associate with the salinity data for subsequent discussion of the significance of the division. Group A.1 includes the inlets with the larger runoffs, in most cases from glaciers or snowfields, and Fig. 9 shows vertical profiles of temperature, salinity and oxygen for a typical example (Bute). Group A.2 includes inlets with medium runoff with little or no contribution from glaciers, etc. Figure 10 shows profiles of the water characteristics for Seymour as an example.

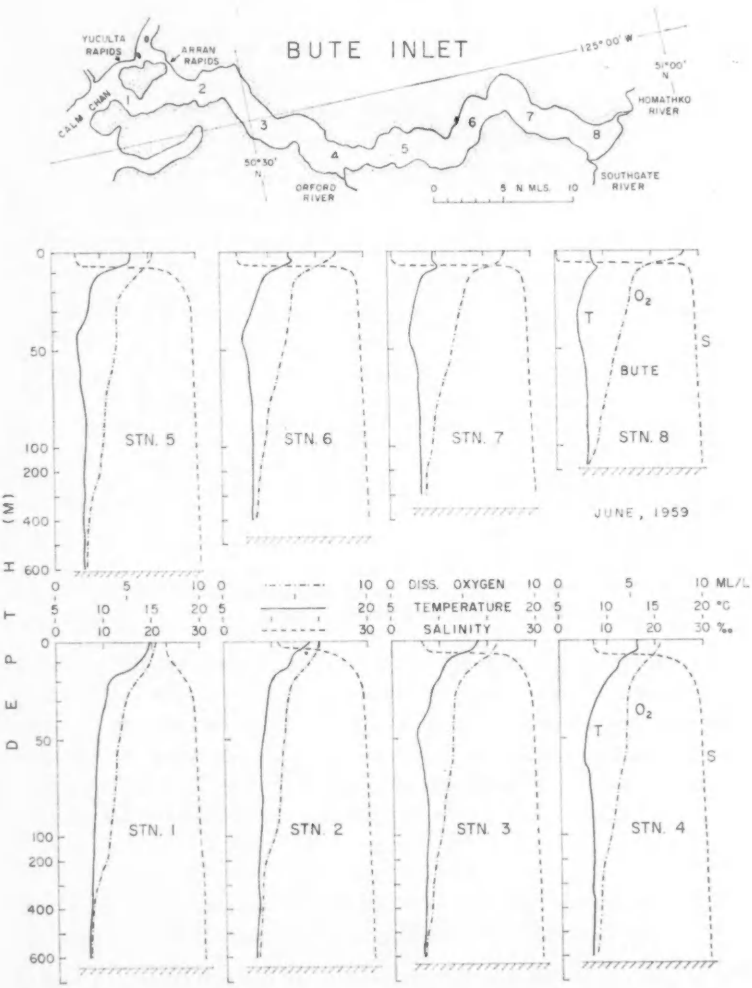

FIG. 9. Vertical profiles of salinity, temperature and dissolved oxygen in a large-runoff inlet (Bute).

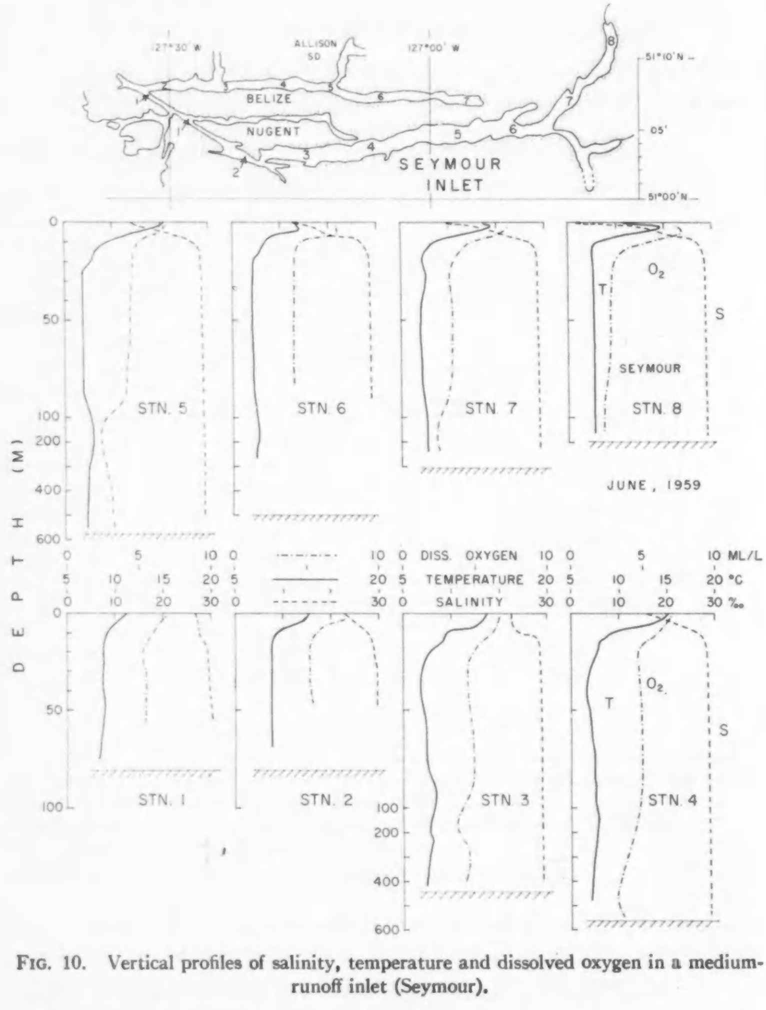

FIG. 10. Vertical profiles of salinity, temperature and dissolved oxygen in a medium-runoff inlet (Seymour).

Group B is a small one including the inlets with small runoff and consequently higher surface salinities, particularly near the head. Figure 11 shows profiles of water characteristics for Laredo as an example.

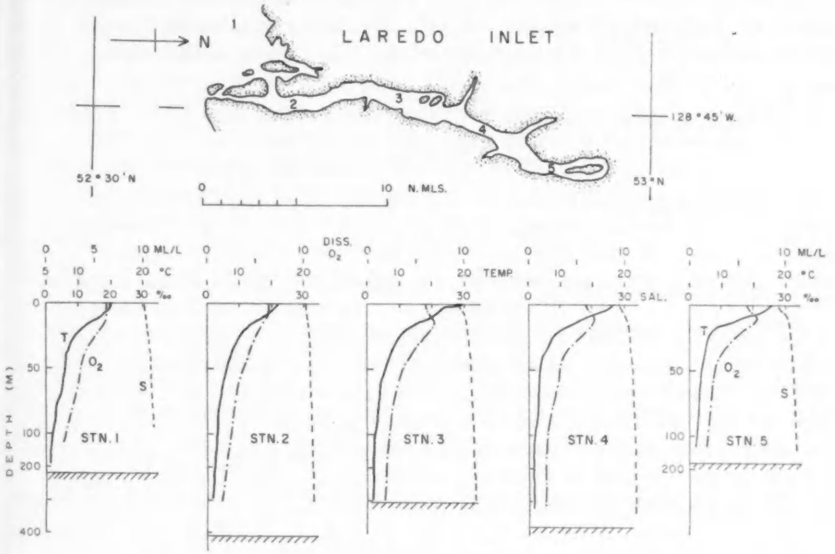

FIG. 11. Vertical profiles of salinity, temperature and dissolved oxygen in a small-runoff inlet (Laredo).

In the majority of cases the salinity of the water at a depth of 20 m in an inlet is at least 90% of that of the deepest water in the particular inlet. Since it is convenient to describe the shallow and the deep zones separately this depth of 20 m is arbitrarily taken to divide the two zones in the following description of the main characteristics. The actual depth of the halocline in the different inlets will be discussed in a subsequent section.

3.1 Shallow Zone

The major characteristics of the shallow zone are the general presence of (1) variations of both salinity and temperature along the length of an inlet, and (2) variations in vertical profiles of salinity and temperature along individual inlets and between inlets.

3.11 Salinity distribution at the surface

The surface sample was drawn either from a bucket sample or from a reversing water bottle with its upper end just beneath the surface. It is taken as characteristic of the top $\frac{1}{2}$-m layer of water.

The general character of the distribution of surface salinity (and temperature) along the inlets is shown in Fig. 12–14. Figure 12 shows a selection of longitudinal profiles for a Group A.1 inlet, Bute, and its continuation along Calm and Sutil Channels to the Strait of Georgia. The profiles are for different months and show that a marked seasonal variation occurs. The first profile, for February, is typical of the winter, when the river runoff is least. The salinity is then almost uniform

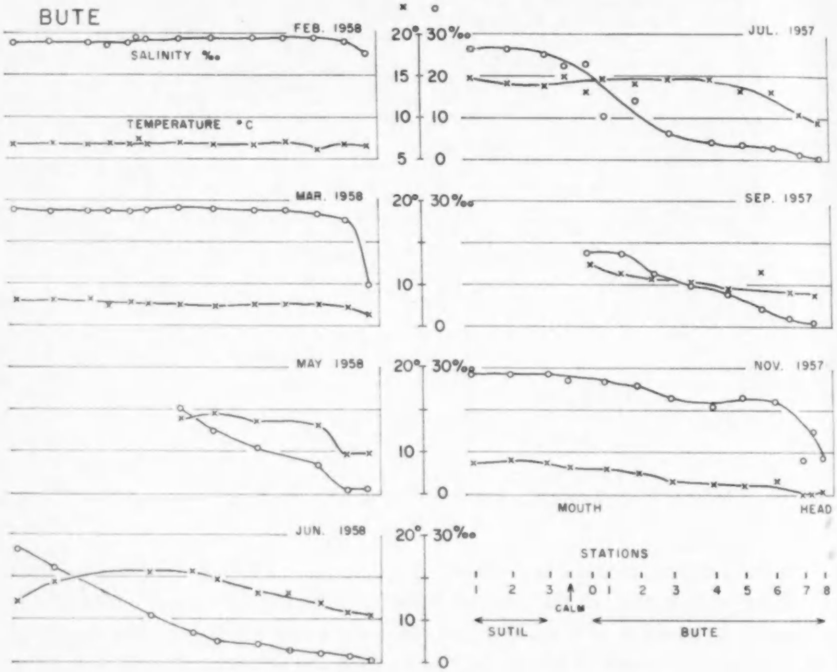

FIG. 12. Longitudinal profiles of salinity and temperature at the surface in a large-runoff inlet (Bute) showing seasonal variation.

along the inlet and channels and has its highest value for the year. The March profile shows a fall in salinity at the head as the river runoff starts to increase, probably chiefly from snow melt at lower elevations at this time. By May the salinity along the greater part of the inlet length has fallen below 20‰, and by June below 10‰. The abrupt change between Sta. 7 and 6 in the May profile is characteristic for a brief period at that time of the year. It is evidence of a low-salinity front which is a consequence of the rapid rise in runoff in the spring. The low-salinity water is silty and it can be seen to advance down the inlet in a period of a few days to change the surface salinity quickly from the high values of the winter regime to the low values typical of the summer as shown for June. The July profile shows low salinities still in the inner half of the inlet itself but a rise to Strait of Georgia surface values near the mouth (about Sta. 1) and along the

channels. This is because the runoff generally decreases in July and is insufficient to maintain low values in the outer passages (Calm and Sutil). The September and November profiles show a progressive return to the winter regime of high surface salinity.

Figure 13 shows some summer profiles for Knight, another Group A.1 inlet, having longitudinal distributions similar to those of Bute. No winter data are available for Knight. The same Figure also shows summer and winter profiles for Jervis which has a smaller runoff than Bute and is in Group A.2. The winter condition, of which the November profile is typical, is again one of uniform salinity along the inlet. The earlier decrease in salinity in Jervis (February) compared to Bute (March) may be due to differences in the pattern of precipitation or direct runoff which is the main source of fresh water in Jervis. The minimum salinity values are observed during June–July, the values not being as low as in Bute. Note that in Fig. 13 and 14 all the inlets have been scaled to the same length for convenience in comparison.

Figure 14 shows, on the left, summer profiles for some of the inlets further north. Portland, Gardner and Dean in Group A.1 show profiles similar to Bute and Knight. The longitudinal profile for Douglas, which is classed as a Group A.1 inlet in Table III on the basis of vertical profiles, is more like that for Jervis in Group A.2. The rapid rise in salinity midway along Burke, which has a large runoff from the Bella Coola River, may be the result of some of this surface low-salinity water moving to the right out of Burke through Labouchere Channel into Dean (see Fig. 1).

On the right in Fig. 14 are profiles for Smith and Seymour which are Group A.2 inlets (medium-runoff, non-glacial). Belize has only a very small runoff at the head, most of the fresh water appearing to enter at the north side from Alison Sound at the position corresponding to the dip in the salinity profile. Spiller might be expected to be one of the lower-runoff Group A.2 inlets, and the moderately low values of salinity at the head may be a consequence of the long restricted mid-section of the inlet limiting exchange with the outside. The profile for Surf is typical of the Group B very-low-runoff inlets with little longitudinal variation of salinity.

The distribution of surface salinity probably affords a better criterion of the location of the inlet mouth than does the mere geometry of the shorelines. For instance, it is clear that the influence of Bute runoff can be traced as far as Sutil Channel in summer and a synoptic survey to describe Bute should be continued out to this region. On the other hand, the salinity (and temperature) profiles for Jervis reach steady values within the inlet even in summer. (It must be pointed out that the values of salinity in the Strait of Georgia at the mouth of Jervis fall from about 28‰ in winter to 20‰ or less in summer (Waldichuk, 1957).) By this criterion, Dean in 1956 was not followed to its oceanographic mouth, which appears from 1951 data to be where Fitzhugh Sound opens into Queen Charlotte Sound.

The above comments all refer to observations taken along the approximate centreline of each inlet. A limited number of transverse sections across Bute have shown small salinity differences of up to 0.5‰ and temperature differences of

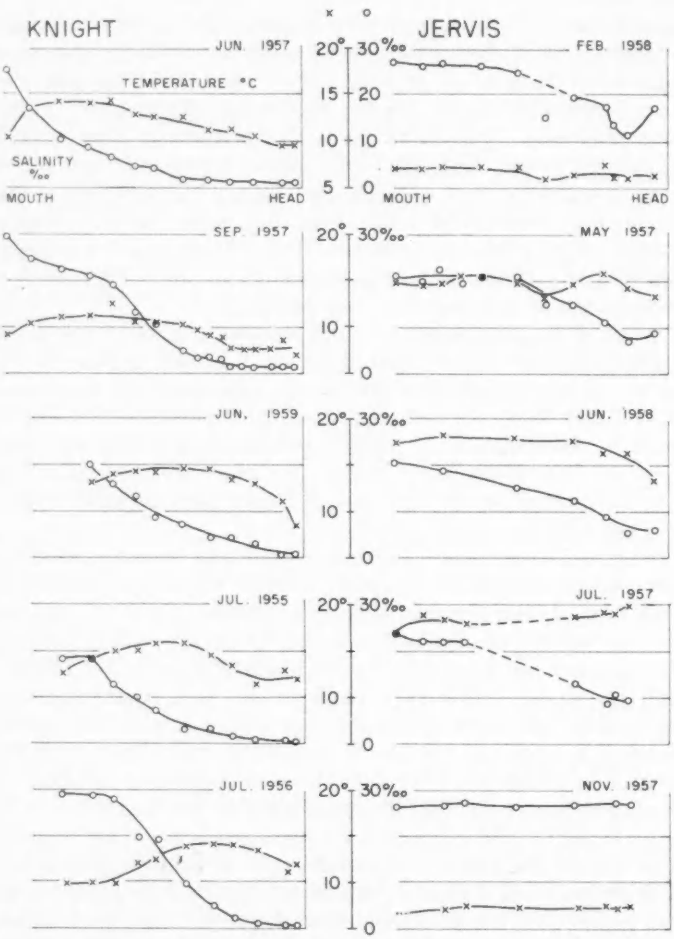

FIG. 13. Longitudinal profiles of salinity and temperature at the surface in large-runoff (Knight) and in medium-runoff (Jervis) inlets, showing seasonal variation in the latter.

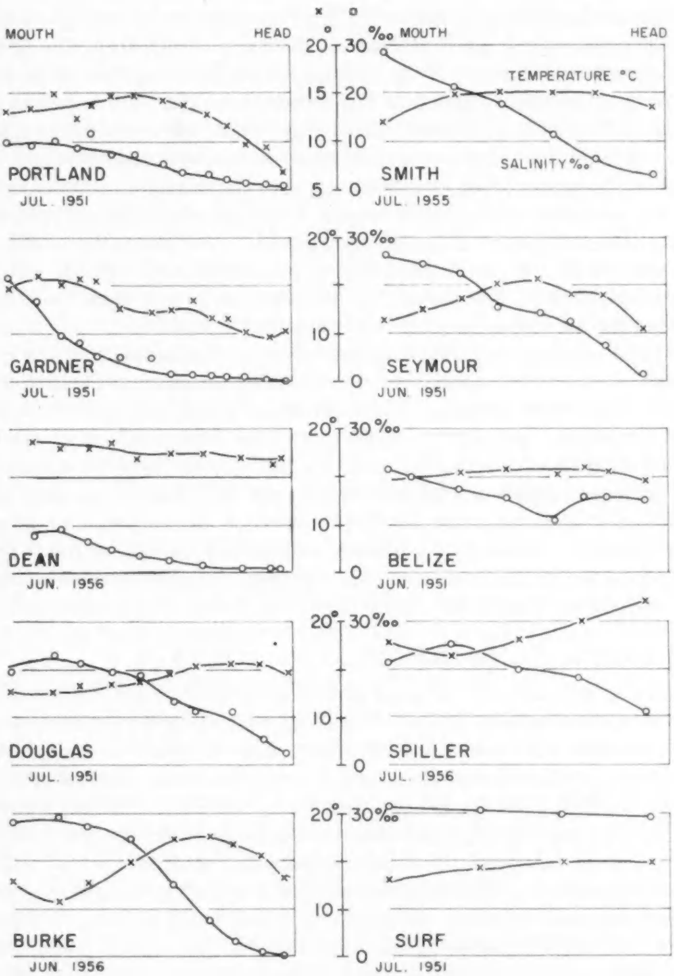

FIG. 14. Longitudinal profiles of salinity and temperature at the surface in large-, medium- and small-runoff inlets.

0.5 C degrees across the width of the inlet (Tabata and Pickard, 1957), the lower salinities and higher temperatures being on the west side (i.e. on the right when looking in the direction of net flow of the surface layer).

It is surprising that the group of inlets north of Ocean Falls, i.e. Roscoe, Spiller, Kynoch and Mussel, are in Groups A.2 or B since these inlets are in one of the regions of highest precipitation on the coast (over 150 inches (3.8 m) per year; Chapman and Turner, 1956). When visited in July 1956 these inlets had higher surface salinity values and lower total amounts of fresh water in the shallow zone than had most of the other large inlets. The probable explanations are that (a) these inlets have relatively small watersheds and therefore the large precipitation does not result in a large inflow of fresh water; (b) the runoff into these inlets probably occurs with only a short lag after the precipitation (the maximum values of precipitation occur in the winter but the only available oceanographic observations are from the summer period of small runoff); (c) there are only small glaciers or snowfields in the watersheds and therefore the stored runoff contribution to be expected in the summer is small.

Pendrell, although included in Group B, is unique among the inlets studied in that there is sometimes a salinity maximum at the head. The reason is that this inlet is located in a small island from which there is very little fresh water runoff. The salinity structure of the water in the body of the inlet is similar to that at the mouth of Toba and it is probable that the seasonal changes in salinity in Pendrell are the result of exchange of water with Toba via Homfray Channel. The surface temperature at the head of Pendrell in the summer is usually higher than elsewhere in this inlet or anywhere in the other southern inlets, and it is presumed that the salinity maximum here is the result of an excess of evaporation over precipitation plus runoff.

3.12 Temperature distribution at the surface

Figures 12–14 also show typical temperature profiles for the surface water along the lengths of several inlets. Figure 12 shows profiles for Bute to demonstrate the seasonal variation from minimum values in winter to maximum values in summer, and to show the association between temperature and salinity profiles. The typical winter profile for February shows substantially uniform low temperatures along the inlet length and the channels connecting it to the Strait of Georgia. In May it is seen that with the rise in salinity between Sta. 7 and 6 there is a change in temperature. The low values at Sta. 8 and 7 to the right of the surface-water front emphasize the low temperature of the runoff water. In June, when a steady state has been reached, it is seen that the cold runoff water warms up as it moves along the inlet. It is this fact which was made the basis for the method for determining the fresh water runoff from heat budget considerations (Pickard and Trites, 1957).

It should also be noted that the temperature at the surface in June reaches a maximum at about Sta. 1, while in July the maximum is further up the inlet at Sta. 4. This longitudinal temperature maximum is characteristic of the large-runoff inlets, and other examples may be seen in Fig. 13 and 14. It is noted that this maximum occurs where the salinity starts to rise rapidly, and the

decrease to seaward is considered to be a consequence of increased upward mixing of cool, saline water from below. Examination of all longitudinal profiles available indicates that the temperature maximum along the Group A.1 inlets usually occurs where the surface salinity rises to between 6 and 10‰, usually at about 8‰. There is no obvious reason why 8‰ should be a magic value. It would be more reasonable to expect the increased vertical mixing to be determined by the stability of the water in the shallow zone rather than be associated with an absolute value of salinity, i.e. density. The possible significance of the association of the temperature maximum with the 8‰ isohaline remains to be investigated.

In Fig. 13, Knight again shows characteristics similar to Bute, with the exception that the temperature maximum occurs where the surface salinity is about 6‰. In Jervis, the higher temperatures at the head than in Bute are because the main runoff does not originate in glaciers and is of smaller volume.

In Fig. 14, Portland shows a low surface temperature at the head because much of the runoff comes only a short distance from glaciers and snowfields. The runoff into Gardner, Douglas, Burke and Dean, particularly the latter, travels considerable distances before reaching the inlets and is warmed by the sun and atmosphere more than are the rivers which flow into Bute and Knight.

The high temperatures at the head of Spiller are characteristic of the complex of inlets between Dean and Gardner. These inlets appear to have little stored runoff, and hence the speed of net outward flow in the summer in the surface layer is small and the water reaches relatively high temperatures in the inner reaches of the inlets. The highest temperature recorded in a mainland inlet in these studies was 24.3°C in Roscoe, one of this group. In Surf and Laredo the lower temperatures combined with high salinities must be due to the direct communication between the waters of these inlets and the waters of Hecate Strait which have similar temperature–salinity (T–S) characteristics.

3.13 Salinity distribution with depth in the shallow zone

Immediately below the surface there is either a homogeneous layer or the salinity increases with depth. At the head of the inlets in Group A.1 there is a nearly homogeneous surface layer of low salinity whose lower limit is clearly defined at a depth of 3 to 10 m (e.g. Fig. 9, 16, 30). The depth depends upon the river inflow and the state of the tide. Below this depth the salinity increases rapidly to 25‰ or more at a depth of 5 to 12 m, the salinity gradient not uncommonly approaching 30‰ per metre in this halocline.

Near the mouths of the inlets of Group A.1 the salinity–depth profile shows a more gradual change from the surface salinity value to that in the deeper zone. Along the intervening length of the inlets a series of salinity–depth curves will show a steady transition from the two-layer system at the head to the more gradual change at the mouth. Figure 9 shows examples of such curves (cf. Tully, 1949, fig. 3, 4 and 5). Observations of the current distribution through the shallow layer have shown that there is often a marked velocity shear between the brackish surface water and the more saline water below it (Pickard and Rodgers, 1959). This shear is undoubtedly accompanied by turbulence which is chiefly responsible for the dilution of the originally fresh river water with salt water

entrained from below. The details of this process are at present imperfectly understood but are being studied.

The above remarks describe the variation of salinity with depth in broad terms. As this variation is the chief feature of these estuarial bodies of water it will be described in more detail.

The salinity–depth profiles are chiefly of one of two types. In Type 1 there is a more or less homogeneous surface layer and below it a distinct halocline, or region of large rate of change of salinity with depth, which separates the surface layer from the deeper zone of smaller rate of change. In Type 2 there is no homogeneous layer and the salinity increases with depth from the surface at a rate which decreases as the depth increases. Curves 1b and 2 in Fig. 15 show these basic types. In the case of Type 1 several variations occur. Type 1a,

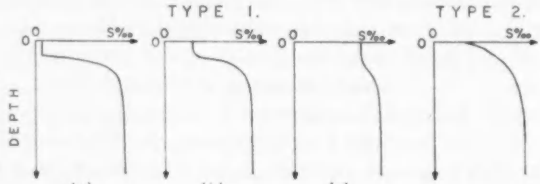

FIG. 15. Types of vertical profile of salinity in the shallow zone in British Columbia inlets.

in which the upper layer is nearly homogeneous, of low salinity, and with a clearly defined lower limit, is common at the heads of inlets with large runoff. A very large rate of increase of salinity with depth in the halocline is characteristic of these situations. Type 1c in which the surface layer is also homogeneous but of higher salinity is more common near the mouths of inlets, and the rate of increase of salinity with depth in the halocline is much less than in Type 1a. Occasionally the salinity–depth profile indicates the presence of more than one homogeneous layer in the surface zone.

The types of salinity–depth profile characteristics of the runoff period (May–August) are included in Table III. It will be seen that the distinct two-layer situation (Type 1a) is common in the inner parts of the inlets having low salinities (Group A.1 in Table III) because of the high runoff. Toward the mouth the curves change through Type 1b to Type 1c or 2 as mixing between the layers occurs. The inlets with low runoff generally have Type 2 curves even at the head. The Type 1c profile which is often seen at the mouth as a variant of the Type 2 is probably due to wind mixing of a previous Type 2 situation.

In comparing the shallow-zone salinity profiles of the various inlets a tabulation was made of the profile type and "dimensions". The latter include the surface salinity and a minimum of data necessary to indicate the location of the curve on a salinity–depth plot. The data used for this purpose were (a) the depth of the homogeneous zone (for Type 1 curves), (b) the depth at which the salinity reaches 50% of the deep water salinity (base salinity) for the inlet, (c) the depth at which the salinity reaches 90% of the base salinity. Table IV summarizes these values for the majority of the inlets.

The low-salinity homogeneous layer at the surface is characteristic of the inner part of an inlet. It is most sharply defined near the head and generally

TABLE IV. Dimensions of salinity–depth profile in shallow zone in British Columbia inlets.

	Depth of homogeneous layer near inlet head		50% depth			90% depth		Number of cruises
	Mean	Range	Mo	Mi	Hd	Mean	Range	
	m	*m*	*m*	*m*	*m*	*m*	*m*	
Portland C.	6	4.5–7.5	1.5	6.5	8	17	14–18	1
Observatory	8	6.5–9	7	-	8.5	14	13–15	1
Alice	9	6–12	-	-	9	20	19–21	1
Work	none	—	0	0	0	10	9–11	1
Kildala	none	—	5	6	5	11	10–12	1
Douglas	5	3–7	0	3	6.5	17	9–21	4
Gardner	6	4.5–7	1	4	6.5	10	9.5–10.5	1
Surf	none	—	0	0	0	0.5	0–1	1
Laredo	none	—	0	0	0	4.5	0–8	1
Sheep	none	—	0	0	1.5	8	0–18	1
Kynoch	none	—	0	0	0	8	4–11	1
Spiller	4	. . .	0	0	4	9	6–12	1
Briggs	none	—	0	0	—	4	2–6	1
Roscoe	none	—	2.5	0.5	2	6	5–7	1
Cascade	none	—	5	5	7	12	11–13	1
Dean	6	5.5–6.5	3	7	7	13	11–14	2
Burke	5	4.5–7	0	0.5	6	10	8–12	2
S. Bentinck	8	7.5–9	7.5	—	10	13	. . .	1
Moses	2	1.5–3	4	4.5	4.5	8.5	7.5–10	2
Rivers	2	1.5–3	0.5	3	3.5	6.5	5–8.5	2
Draney	1.5	1.5	0	1.5	2.5	7	6.5–8	1
Smith	1.5	1.5	0	—	2.5	5	. . .	1
Belize	0.5	0–1	0	1	0	6	3.5–8.8	1
Seymour	none	—	0	1	3	10	6.5–12	1
Kingcome	3	2.5–3.5	—	3	3.5	8	6.5–10	3
Knight	5	3–7	0	5.5	6.5	12	10–14.5	7
Call	6	5–7	0	—	0	0	. . .	3
Loughborough	1.5	1–3	0.5	—	2	3	2.5–4.5	3
Bute	4.5	3–6	0.5	4	5.5	9.5	7–14	12
Toba	2	1.5–3.5	2	—	3.5	15	9–20	5
Pendrell	none	—	0	—	0	11	6–18	5
Jervis	none	—	0	1	2	15	7–21	6
Sechelt	1.5	. . .	0	0	1.5	24	20–30	1
Howe	6	. . .	4	5	7	10	10–11	1
Indian	2	1–4	0	1	1	25	20–30	8

the depth of the layer decreases somewhat from the head toward the mouth. Eventually the salinity–depth profile becomes so rounded that it is difficult to select a specific depth for the layer. The homogeneous layer sometimes observed near the mouth (Type 1c profile) is generally much deeper than that at the head and is of much greater salinity.

The depth at which the salinity reaches 50 and 90% respectively of the base salinity may be read without ambiguity from the salinity–depth profiles. In the inlets with considerable runoff the 50% depth is not more than 2 m greater than that of the homogeneous layer. It decreases from head to mouth of an inlet, and in most cases is at or close to the surface at the mouth. The chief exceptions are those inlets which terminate part way along another inlet (e.g. Observatory opening into Portland, South Bentinck opening into Burke).

The 90% depth does not show the same regular decrease toward the mouth. In many cases, the 90% depth is relatively constant from station to station in

the inner half of an inlet but fluctuates considerably in the outer half. The values in Table IV indicate the mean value and the range of values observed for each inlet as a whole.

Occasional salinity inversions have been noted, usually toward the heads of inlets between the surface sample (taken with a bucket) and the next below it (taken with a water sampling bottle). These inversions are considered only to be significant of a cloudy structure in the water which is to be expected in the immediate vicinity of river inflow.

3.14 Temperature distribution with depth in the shallow zone

It is generally true that the shallow-zone temperature profile with depth is qualitatively a mirror image about a vertical axis of the salinity profile if both are plotted in the conventional manner with both temperature and salinity increasing to the right (e.g. Fig. 9 and 10). That is to say, an inlet with a salinity profile of Type 1 (Fig. 15) will have an isothermal layer below which there is a thermocline and then a reduced temperature gradient. With Type 2 salinity profiles the temperature generally decreases with depth from the surface, the gradient decreasing as the depth increases, e.g. Fig. 11.

In the Type 1 salinity profile inlets the thermocline is closely associated in depth with the halocline. In order to examine this association, a series of casts was made in Knight in 1955 with closely spaced Fjarlie water sampling bottles while a cast was made with a 20-m range bathythermograph close to the bottles as the messenger was dropped. A selection of salinity and temperature profiles from this series is shown in Fig. 16. The minimum water bottle spacing practicable with the 0.3-m-long Fjarlie bottles was 1 m and attempts were made to arrange a closely spaced group of bottles in the thermocline as determined from a preliminary bathythermograph cast. The bathythermograph used had only a small

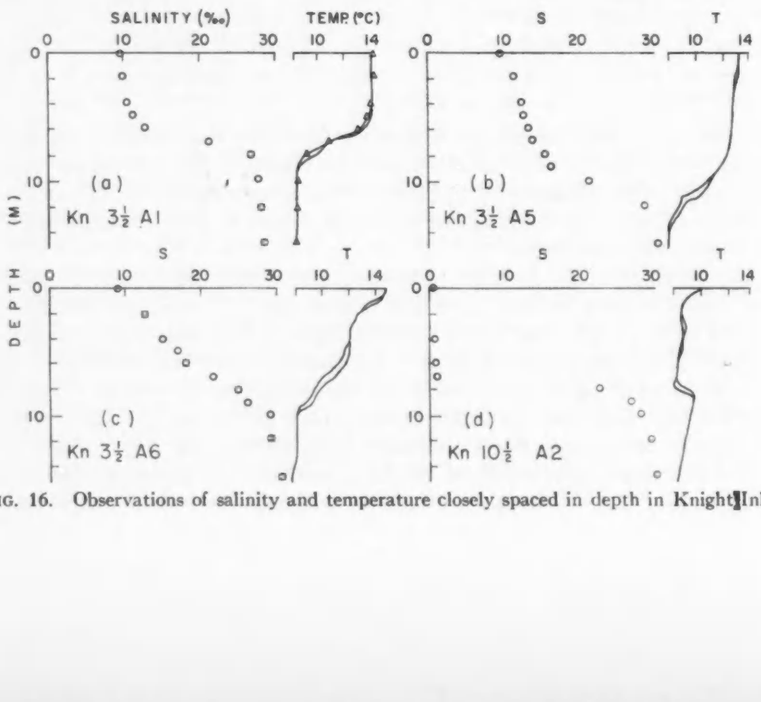

Fig. 16. Observations of salinity and temperature closely spaced in depth in Knight Inlet.

hysteresis, and previous and subsequent comparisons with reversing thermometers showed it to be a reliable instrument. The reversing thermometer temperatures observed are shown as an example in Fig. 16(a). It is clear from Fig. 16 that within the limitations imposed by the discrete character of the salinity observations the halocline and thermocline coincide in depth.

The T-S diagram corresponding to Fig. 16(a) is shown in Fig. 17. It is an excellent example of a water mass resulting from the mixing of only two water

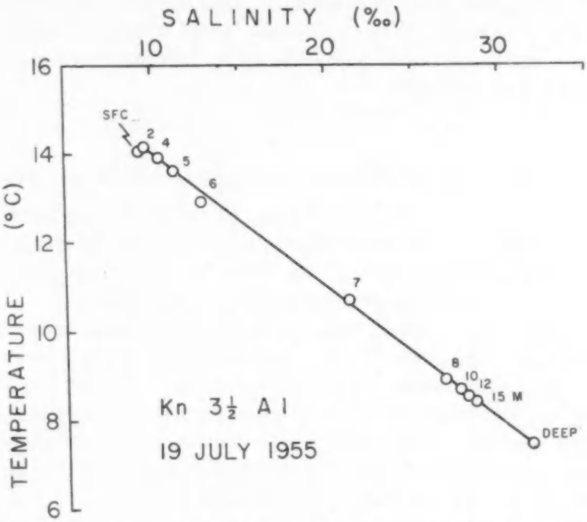

FIG. 17. Temperature–salinity diagram for Sta. Knight 3½ A (cf. Fig. 16(a)).

types, the low-salinity warm surface layer of 2 to 3 m depth with the cooler, more saline deep water.

The profiles in Fig. 16(d) were obtained near the head of Knight, and the surface layer of low-salinity water was cold as it had just entered the inlet from a river originating in glaciers. The sharp increase in temperature at 8 to 9 m depth is seen to be substantially coincident with the very sharp halocline.

The data of which the profiles in Fig. 16 are representative indicate that when a pronounced halocline and thermocline are both present the two agree closely in depth. However, neither is necessarily found with the other. Near the head of a large-runoff inlet with a conspicuous halocline there may be no significant thermocline (although irregularities in the temperature–depth profile are often present in such a case). In low-runoff inlets the shallow zone may have a marked thermocline even when the water is almost isohaline. It is, in fact, not practical to divide the inlets into types in terms of temperature profiles as has been done for salinity. This is the opposite of the open ocean situation where it is easier to categorize the temperature profiles than the salinity profiles.

The reason for the variety of combinations of temperature–depth and salinity–depth profiles found is that the stratification in the shallow zone is dominated

by the effect of salinity on density, with temperature playing a minor or even insignificant role. In the large-runoff inlets the fresh water at the head, on entry from the rivers, is at or below the temperature of the cool deeper saline water. It forms a low-density surface layer and as this flows along the inlet it absorbs heat from the sun and atmosphere and its temperature therefore rises and a thermocline develops. Mixing with the underlying saline water occurs during the passage along the inlet and the stability of the water diminishes; mixing then takes place over greater depths and the intensity of both halocline and thermocline decreases. Therefore while most marked haloclines are found at the heads of the large-runoff inlets, the most marked thermoclines are found toward mid-length of the inlets.

3.2 Deep Zone

3.21 Main features of salinity and temperature distributions

In the characteristics of the deep water (20 m and deeper) there is a marked gradation from south to north along the coast. In the southern inlets the salinity is lower and the temperature higher at the same depths than in the northern ones. The southern inlets include those from Indian to Loughborough. The northern inlets include Smith and all those north of it except for two side arms, Moses and Alice. Call, Knight, Kingcome, Draney and Moses in the mid-coast region have deep water with characteristics intermediate between those of the southern and northern groups. The water characteristics in Seymour and Belize fall into the southern group category, while Alice has salinities similar to the intermediate group but lower temperatures than in other inlets in the north. Possible explanations for these differences are offered and discussed later.

Mean values of temperature and salinity are summarized in Table V for comparison. The mean values are also displayed in the diagrams of Fig. 18 for

Table V. Mean values of subsurface temperature and salinity of the water in the inlets of the British Columbia mainland coast.

Inlets	Depth									
	20 m		50 m		100 m		200 m		400 m	
	T	S	T	S	T	S	T	S	T	S
	°C	‰	°C	‰	°C	‰	°C	‰	°C	‰
Northern group:	7	31.0	6.5	32.0	6.5	32.7	6.3	33.0	6.3	33.2
Except:										
Alice	6.5	29.0	5.5	30.5	5.2	31.0	4.3	31.4	–	–
Surf and Laredo	10	31.5	8.0	32.0	...	...	...	...	–	–
Intermediate group:	8	29.5	7.0	30.5	6.6	30.8	7.3	31.2	7.3	31.2
Except:										
Moses	...	...	7.1	31.5	7.1	31.6	7.3	32.0	–	–
Southern group:	8	29.0	8.0	29.5	7.5	30.0	8.1	30.5	8.3	30.7
Except:										
Seymour	8	28.5	7.3	28.8	7.4	29.0	7.8	29.0	7.4	29.0
Princess Louisa	11	23.5	8.8	26.5	7.7	28.2	–	–	–	–
Sechelt	11	26.0	8.8	27.5	7.5	28.5	7.4	28.6	–	–
Indian	11	25.5	10.0	26.4	7.9	27.2	7.0	27.2	–	–

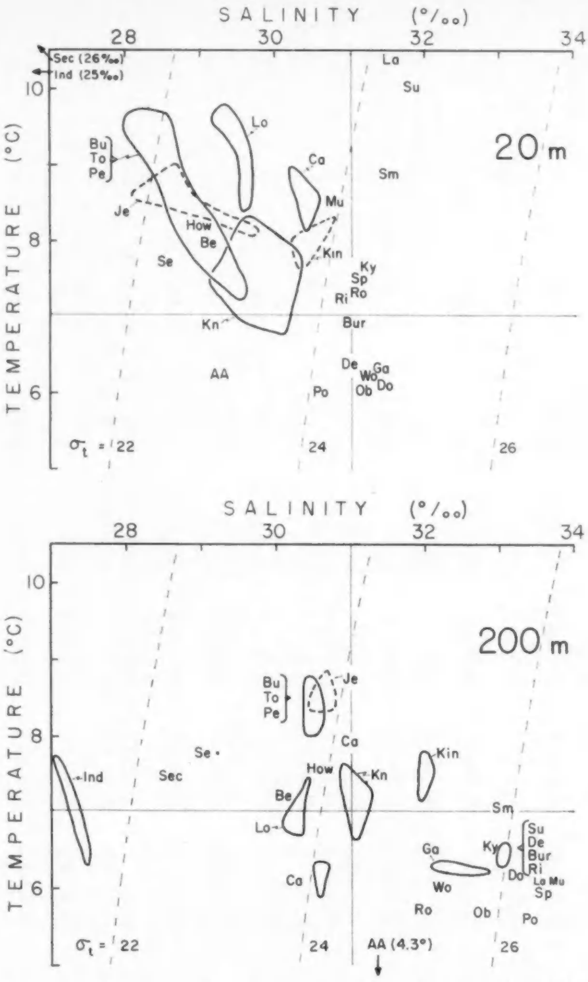

FIG. 18. Summary of temperature–salinity characteristics of the water at 20 and 200 m depth in British Columbia mainland inlets.

depths of 20 and 200 m which are considered to be sufficiently representative of the upper and lower parts of the deep zone.

The latter diagrams clearly show the difference in water characteristics between the southern and northern inlets. The mean difference in temperature is 1 to 1.5 C degrees and in salinity is 2 to 2.5‰. The wider distribution of temperature at 20 m than below this depth is attributed to climatic effects.

More detailed values of salinity and temperature are given in Tables VI and VII. In these are listed for depths of 20 m and greater for each cruise for each

TABLE VI. Mean values of salinity (‰) along the length of each inlet for each cruise, with range of salinity about mean which includes at least 75% of all values for each cruise (Note 1).

Inlet	Date		DEPTH (METRES) 20	50	100	200	300	400	500	600 (Notes)
Portland C.	Jul.	51	30.7 ±1.0	32.0 ±0.2	32.8 ±0.2	33.1 ±0.2	33.34	33.40	–	–
Observatory	Jul.	51	30.8 ±0.8	32.0 ±0.2	32.6 ±0.3	32.66	...	32.66	...	–
Hastings	Jul.	51	30.5 ±0.1	31.86	32.10	32.14	–	–	–	–
Alice	Jul.	51	29.4 ±0.8	30.7 ±0.1	30.96	31.32	...	–	–	–
Work	Jul.	51	31.3 ±0.3	31.8 ±0.1	31.96	32.10	32.14	–	–	–
Douglas	Jul.	51	31.5 ±0.3	32.3 ±0.3	32.9 ±0.1	33.2 ±0.2	...	33.32	–	–
	Jun.	52	30.5 ±0.1	31.7 ±0.1	32.4 ±0.1	32.7 ±0.1	...	...	–	(2)
	Jul.	52	30.7 ±0.4	31.9 ±0.2	32.6 ±0.2	32.7	...	...	–	(2)
	Aug.	52	31.1 ±0.7	31.8 ±0.2	32.6	32.96	...	...	–	(2)
	Aug.	54	31.2 ±0.1	31.9 ±0.2	32.76	33.0 ±0.1	33.08	33.24	–	(3)
Kildala	Jul.	51	31.6 ±0.1	32.00	32.86	...	–	–	–	–
Gardner	Jul.	51	31.6 ±0.4	31.9 ±0.1	32.0 ±0.1	32.2 ±0.1	...	33.16	–	(4)
			...	...	32.4 ±0.2	32.5	...	...	–	(5)
			...	32.5 ±0.2	32.8 ±0.1	33.7	...	33.3 ±0.1	–	(6)
	Aug.	54	31.2 ±0.5	31.8 ±0.2	32.2 ±0.1	32.4 ±0.2	33.00	...	–	(7)
Surf	Jul.	51	31.8 ±0.1	32.3 ±0.1	32.9 ±0.1	33.06	...	–	–	–
Laredo	Jul.	51	31.5 ±0.2	32.2 ±0.1	33.2 ±0.2	33.4 ±0.1	33.46	–	–	–
Sheep	Jul.	56	30.5 ±0.4	31.8 ±0.2	33.10	33.30	33.36	–	–	–
Kynoch	Jul.	56	31.0 ±0.2	32.26	32.76	32.86	32.96	32.98	32.98	33.04
Spiller	Jul.	56	31.1 ±0.5	32.0 ±0.2	33.2 ±0.2	33.40	33.42	...	–	–
			...	...	32.8	33.0	...	...	–	(8)

Briggs	Jul.	56	29.4	29.8	. . .	. . .	. . .	. . .	. . .	. . .
Roscoe	Jul.	56	30.0	31.5±0.1	31.9	. . .	–	–	–	–
Dean	Jun.	51	31.0±0.3	31.9±0.1	32.8±0.2	33.1	33.1	33.1	. . .	–
	Jul.	56	30.7±0.2	31.6±0.2	32.6±0.1	33.0±0.1	33.0±0.1	33.0±0.1	33.0	–
Cascade	Jul.	56	30.8	31.8±0.1	32.66	32.86	32.98	–	–	–
Burke	Jun.	56	31.1±0.8	32.1±0.4	32.8±0.1	33.0±0.1	33.05	33.10	. . .	–
	Jul.	56	30.7±0.4	31.8±0.2	32.6±0.1	32.9±0.1	33.0±0.1	33.08	33.2	–
Kwatna	Jul.	56	30.9	31.7	32.5	32.9	32.9	33.0	. . .	–
S. Bentinck	Jun.	51	30.6±0.2	32.0±0.1	32.7±0.1	33.0	33.1	. . .	–	–
Rivers	Jun.	51	30.8±0.3	31.8±0.1	32.8±0.1	33.06	33.10	–	–	–
	Jul.	56	31.1±0.2	32.0±0.1	32.8±0.1	33.06	33.06	–	–	–
Moses	Jun.	51	30.7	31.5	31.6	31.7	–	–	–	–
	Jul.	56	30.6	31.3	31.7	31.9	–	–	–	–
Draney	Jun.	51	29.4±0.2	30.0±0.1	30.80	–	–	–	–	–
Smith	Jul.	55	31.5±0.2	32.2±0.2	32.9±0.1	33.0	33.0	–	–	–
Belize	Jun.	51	29.3±0.2	29.8±0.2	30.0±0.1	30.1±0.1	30.1	–	–	–
Seymour	Jun.	51	28.4±0.1	28.8±0.1	28.8±0.1	29.0	29.0	29.0	29.0	. . .
Drury	Jul.	55	29.9	30.1	–	–	–	–	–	–
Kingcome	Jul.	53	30.2±0.1	30.7±0.1	31.5±0.1	31.9±0.1	32.0	. . .	–	–
	Jul.	55	30.8	31.2±0.1	31.80	31.98	32.00	. . .	–	–
	Jun.	57	30.3±0.1	30.8±0.2	31.40	31.78	32.1±0.1	32.2	–	–
Knight	Jun.	51	29.3±0.5	30.6±0.1	30.8±0.1	31.0	31.1	31.16	31.18	(9)
			30.0±0.3	30.8±0.1	31.3	31.5	–	–	–	–
	Jun.	52	30.0±0.3	30.7±0.2	30.7±0.1	31.0	31.2	31.3	. . .	–
			30.5	31.0	31.3	. . .	–	–	–	–

TABLE VI.—*Continued*

Inlet	Date	DEPTH (METRES)							
		20	50	100	200	300	400	500	600
Knight (*Cont.*)									(Notes)
	Jul. 53	29.8 ± 0.5	30.4 ± 0.2	30.9 ± 0.2	31.0 ± 0.1	31.0 ± 0.1	31.1 ± 0.1	31.1	–
		30.1 ± 0.3	30.9 ± 0.1	31.1 ± 0.2	31.5 ± 0.1	–	–	–	–
	Jul. 55	30.3 ± 0.3	30.9	31.14	31.20	31.22	31.24	31.26	–
		30.6 ± 0.1	31.1 ± 0.1	31.76	. . .	–	–	–	–
	Jul. 56	29.0 ± 0.5	30.4 ± 0.1	30.7 ± 0.2	31.0 ± 0.1	31.1 ± 0.1	31.2 ± 0.1	31.26	–
		29.6 ± 0.9	30.9	31.2 ± 0.1	. . .	–	–	–	–
	Jun. 57	30.0 ± 0.1	30.7 ± 0.1	30.9 ± 0.1	31.06	31.18	31.24	31.28	–
		30.4 ± 0.2	30.9 ± 0.2	31.2 ± 0.1	31.4	–	–	–	–
	Sep. 57	29.5 ± 0.5	30.3 ± 0.2	30.6 ± 0.1	30.9 ± 0.1	30.9	30.96	. . .	(10)
		30.0 ± 0.5	30.86	31.42	31.48	–	–	–	–
	Jun. 58	29.6 ± 0.1	30.3 ± 0.1	30.62	30.86	31.04	31.12	. . .	–
		29.95	30.6	31.3	. . .	–	–	–	–
	Jun. 59	29.8 ± 0.1	30.5 ± 0.1	30.66	30.90	31.00	31.10	31.10	–
		30.24	30.72	31.22	. . .	–	–	–	–
Call	Jul. 53	30.4	30.7	30.7	. . .	–	–	–	–
	Aug. 53	30.4 ± 0.1	30.66	30.76	30.96	–	–	–	–
	Jul. 55	30.5	30.8 ± 0.1	30.9	31.0	–	–	–	–
	Jul. 56	30.2	30.40	30.42	30.5	–	–	–	–
	Jun. 57	30.4 ± 0.1	30.64	30.66	30.7	–	–	–	–
	Sep. 57	30.2	30.50	30.46	. . .	–	–	–	–
Loughborough	Jul. 53	29.4 ± 0.2	29.6 ± 0.1	30.1 ± 0.1	30.36	–	–	–	–
	Jul. 55	29.6	29.8 ± 0.1	30.3	30.5	–	–	–	–
	Jul. 56	29.2 ± 0.1	29.50	29.98	30.16	–	–	–	–
	Jun. 57	29.6 ± 0.1	29.9 ± 0.2	30.08	30.30	–	–	–	–
	Sep. 57	29.3 ± 0.1	29.5 ± 0.2	29.8 ± 0.2	30.08	–	–	–	(10)
Bute	May 51	29.0 ± 0.4	29.2 ± 0.2	29.9 ± 0.2	30.4 ± 0.1	30.5 ± 0.1	30.5 ± 0.1	30.5 ± 0.1	30.6
	Aug. 51	28.3 ± 0.2	29.1 ± 0.1	30.1 ± 0.1	30.5 ± 0.1	30.5	. . .	. . .	. . .
	Oct. 51	28.8 ± 0.1	29.3 ± 0.2	30.1 ± 0.2	30.4 ± 0.1	. . .	30.56	30.58	. . .
	Mar. 52	29.0 ± 0.8	29.8 ± 0.2	30.0 ± 0.2	30.6 ± 0.1	30.6 ± 0.1	30.70	30.70	. . .
	May 52	29.3 ± 0.2	29.6 ± 0.2	30.2 ± 0.1	30.52	30.56	30.56	30.60	. . .

	Mar. 52	29.0±0.8	29.8±0.2	30.0±0.2	30.6±0.1	30.6±0.1	30.70	30.70	. . .
	May 52	29.3±0.2	29.6±0.2	30.2±0.1	30.52	30.56	30.56	30.60	. . .
	Aug. 52	28.7±0.2	29.4±0.1	30.2±0.1	30.6±0.1	30.60	30.62	30.7	. . .
	Mar. 53	29.1±0.2	29.4±0.1	29.9±0.1	30.6±0.1	30.6	30.7	30.7	30.7
	Jul. 53	28.3±0.6	29.3±0.2	30.3±0.2	30.7±0.1	30.6±0.1	30.6	30.6	. . .
	Aug. 53	28.7±0.3	29.2±0.2	30.2±0.2	30.6+0.1	30.7±0.1	30.74	30.76	30.78
	Jan. 54	28.8±0.2	29.5±0.3	29.9±0.1	30.4	30.62	. . .	. . .	. . .
	Jul. 55	28.5±0.3	29.7±0.1	30.3±0.2	30.6±0.1	30.6	30.6±0.1	. . .	30.7
	Jul. 56	28.6±0.2	29.3±0.1	30.2±0.1	30.4±0.1	30.5±0.1	30.56	30.58	30.58
	May 57	29.5±0.2	29.8±0.2	30.2±0.2	30.64	30.66	30.68	30.68	30.72
	Jul. 57	28.5±0.2	29.4±0.2	30.2±0.1	30.5±0.1	30.62	30.64	30.64	30.66
	Sep. 57	28.1±0.3	29.0±0.1	30.0±0.1	30.28	30.34	30.36	30.38	(10)
	Nov. 57	29.0±0.2	29.5±0.1	30.0±0.1	30.48	30.48	30.52	30.54	30.64
	Feb. 58	29.1±0.3	29.6	30.1±0.1	30.6±0.1	30.62	30.64	30.66	30.68
	Mar. 58	28.7±0.3	29.2±0.1	29.6±0.1	30.5±0.1	30.60	30.62	30.64	. . .
	May 58	28.9±0.1	29.4±0.1	29.8±0.1	30.38	30.54	30.56	. . .	. . .
	Jun. 58	28.2±0.2	28.96	30.00	30.46	30.56	30.62	30.62	30.64
	Jun. 59	28.6±0.1	29.3±0.1	29.90	30.40	30.48	30.50	30.56	30.56
	Jun. 60	28.3±0.3	29.1±0.2	30.0±0.2	30.5	30.56	30.6	30.62	30.62
Ramsay	Jun. 54	28.7	29.5	30.1	30.4	30.6	–	–	–
	Jun. 56	28.0	29.4	30.1	30.4	30.5	–	–	–
Toba	Aug. 51	28.6±0.1	29.2±0.1	30.0	30.5	. . .	30.5	. . .	–
	Mar. 53	29.1±0.1	29.4±0.2	30.0±0.1	30.5±0.1	30.6±0.1	30.7	30.7	–
	Jun. 54	28.5±0.1	29.6±0.1	30.04	30.38	30.5	. . .	. . .	–
	Jun. 55	27.4±0.1	29.8±0.1	30.4	30.6	30.6	30.6	30.6	–
	Jun. 56	28.1±0.4	29.7±0.2	30.28	30.52	30.56	30.58	30.64	–
	Sep. 57	28.4±0.4	29.3±0.1	30.2±0.1	30.48	30.52	30.56	. . .	–
	Feb. 58	28.5±0.2	29.3±0.1	30.16	30.5±0.1	30.56	30.58	. . .	–
	Mar. 58	28.1±0.4	29.1±0.1	29.76	30.46	30.54	30.56	. . .	–
	May 58	28.9±0.1	29.4±0.1	29.86	30.36	30.54	30.56	. . .	–
	Jun. 58	28.3±0.1	29.5±0.2	29.98	30.44	30.54	30.62	. . .	–
Pendrell	May 51	28.8±0.1	29.5±0.1	30.1	30.5	30.5	. . .	–	–
	Aug. 51	28.9±0.1	29.2±0.1	30.1	30.5	. . .	. . .	–	–
	Mar. 53	28.9±0.2	29.4	30.1	30.6	30.7	30.7	–	–
	Jul. 53	28.5	29.3±0.1	30.2	30.5	30.6	. . .	–	–
	Aug. 53	28.0±0.2	29.2±0.1	30.2±0.1	30.66	30.70	. . .	–	–

TABLE VI.—*Continued*

Inlet	Date	DEPTH (METRES) 20	50	100	200	300	400	500	600
Pendrell (*Cont.*)									(Notes)
	Jun. 54	28.7 ± 0.2	29.6 ± 0.1	30.10	30.44	30.5	. . .	–	–
	Jun. 56	28.1	29.34	30.16	30.46	30.56	. . .	–	–
	Sep. 57	28.3 ± 0.1	29.28	30.10	30.54	30.5	. . .	–	–
Jervis	May 52	29.9 ± 0.2	30.3 ± 0.2	30.5 ± 0.2	30.88	31.04	31.1	31.1	31.1
	Jun. 54	28.4 ± 0.5	30.0 ± 0.1	30.2 ± 0.1	30.58	30.82	. . .	. . .	. . .
	Jun. 56	28.1 ± 0.2	29.6 ± 0.2	29.8 ± 0.3	30.5 ± 0.2	30.6	30.6 ± 0.1	30.68	30.7
	May 57	28.5 ± 0.4	30.2 ± 0.1	30.4 ± 0.1	30.76	30.94	31.08	31.12	31.08
	Jul. 57	28.7 ± 0.1	29.7 ± 0.1	30.1 ± 0.1	30.7 ± 0.1	30.9 ± 0.1	30.98	31.04	31.04
	Nov. 57	28.8 ± 0.4	29.8 ± 0.4	30.3 ± 0.3	30.7 ± 0.1	30.8 ± 0.1	30.86	30.92	30.94
	Feb. 58	28.0 ± 0.2	29.6 ± 0.2	30.1 ± 0.1	30.6 ± 0.2	30.9 ± 0.1	30.98	30.98	31.00
	May 58	28.7 ± 0.1	29.58	29.86	30.48	30.78	30.92	. . .	. . .
	Jun. 58	28.5 ± 0.4	29.64	29.98	30.48	30.78	30.92	30.94	30.96
	Jun. 59	27.5 ± 0.2	29.76	30.18	30.68	30.86	30.94	30.98	31.00
	Jun. 60	29.0 ± 0.5	29.9 ± 0.1	30.2 ± 0.1	30.7	30.88	30.94	30.96	30.98
Pr. Louisa	May 52	23.6	27.2	28.8	. . .	–	–	–	–
	Jun. 60	22.8	26.1	28.2	28.2 at 176 m				
Sechelt	Jul. 57	25.8 ± 0.2	27.5 ± 0.2	28.46	28.58	–	–	–	–
Howe	Mar. 53	29.7 ± 0.2	30.3 ± 0.2	30.5 ± 0.1	30.6	. . .	–	–	–
	Jun. 57	29.2 ± 0.1	29.8 + 0.1	30.2 ± 0.2	30.5 ± 0.2	. . .	–	–	–
Indian	Jun. 53	24.8 ± 0.2	26.6 ± 0.4	27.8	. . .	–	–	–	–
	Sep. 53	26.3 ± 0.3	26.7 ± 0.2	27.9	28.0	–	–	–	–
	Win. 56	26.0 ± 0.3	26.6 ± 0.3	27.2 ± 0.2	27.3 ± 0.1	–	–	–	(11)
	Sum. 56	26.4 ± 0.5	26.6 ± 0.2	27.2 ± 0.2	27.4	–	–	–	–
	Win. 57	26.9 ± 0.3	27.1 ± 0.3	27.3 ± 0.2	27.4 ± 0.3	–	–	–	–
	Sum. 57	25.4 ± 1.0	26.2 ± 0.3	27.3 ± 0.2	27.5 ± 0.1	–	–	–	–
	Win. 58	26.3 ± 0.5	26.8 ± 0.3	27.2	27.3	–	–	–	–
	Sum. 58	25.2 ± 0.8	26.1 ± 0.3	27.1 ± 0.1	27.3	–	–	–	–
	Win. 59	26.1 ± 0.7	26.5 ± 0.4	26.9 ± 0.2	27.1 ± 0.1	–	–	–	–
	Sum. 59	25.0 ± 1.0	26.1 ± 0.1	26.9 ± 0.1	27.1 ± 0.1	–	–	–	–

Win.	59	26.1 ±0.7	26.5 ±0.4	26.9 ±0.2	27.1 ±0.1	–	–	–	–
Sum.	59	25.0 ±1.0	26.1 ±0.1	26.9 ±0.1	27.1 ±0.1	–	–	–	–

Notes:

(1) When the ± range including at least 75% of the values at a particular depth ("75% range") was 0.02‰ or less its value has been omitted and the mean salinity quoted to the nearest 0.02‰. When the "75% range" was between 0.03 and 0.07‰ its value has been omitted and the mean salinity quoted to the nearest 0.1‰. When the "75% range" was 0.08‰ or over its value has been quoted to the nearest 0.1‰.

(2) Data collected by Canadian Hydrographic Service.

(3) Data collected by Pacific Oceanographic Group, Sta. Do 6, 8 and 10 only.

(4) Stations Ga 4–14 at 50 m, Ga 8–14 at 100, 200 and 400 m.

(5) Stations Ga 3–7 at 100, 200 m.

(6) Stations Ga 1 and 2 at 50 m and deeper.

(7) Data collected by Pacific Oceanographic Group, Sta. Ga 4, 6 and 10 only.

(8) Station Sp 5 only.

(9) For Knight Inlet for each cruise the first line of data refers to Sta. 4–11 inside the sill, and the second line to Sta. 1–3 outside the sill.

(10) The salinity data for Bute, Loughborough and Knight for the cruise of September 1957 appear to be low by about 0.25‰ compared to values on previous and later cruises and should be regarded with caution.

(11) The information available for Indian Arm for 1956 to 1959 is more extensive than for any other inlet (36 cruises) and is the subject of a separate study (Gilmartin, 1960). Here it has been summarized in two groups each year: June to October (Summer) and November to May (Winter).

inlet the mean values together with a value referred to as the "75% range". The 75% range in Tables VI and VII is a range, above and below the mean value, which includes at least 75% of the values for the particular inlet and depth. It is intended simply as an indication of the range of values experienced, the number of values available being so variable and in many cases so small that the calculation of standard deviations would be of doubtful significance.

These Tables show clearly the change in salinity and temperature from north to south, and also show that both seasonal and year-to-year changes evidently occur.

The most noticeable change with location is the decrease in salinity and increase in temperature which occurs in the region between Smith and Knight. The details of this change, together with a comparison of water characteristics and topography, lead to possible explanations of the north–south variation in which both meteorological and oceanographic conditions play their part. The mean annual air temperature differences between south and north are not large, since the annual mean isotherms are only slightly inclined to the coastline. However from south to north there is a decrease in mean air temperature of the order of 3 C degrees (Thomas, 1953; Kendrew and Kerr, 1955) which must contribute to the observed decrease in mean water temperature to the north.

Nordgaard (1903) states that in Norwegian fjords with shallow sills the deep water temperature is close to the mean air temperature in the region, indicating a long-term climatic influence.

The annual precipitation, on the other hand, does not show a similar south to north decrease. In fact the areas of highest precipitation are north of Smith (Thomas, 1953; Chapman and Turner, 1956). It seems more likely that the variation of deep water salinity is associated with the directness or otherwise of the connection to the Pacific (as the source of the most saline water). The inlets from Smith to the north have deep sills and connect more or less directly through Hecate Strait to the Pacific at depths of the order of 130 m and through Dixon Entrance at depths of 160 m for the most northerly inlets. On the other hand the inlets from Bute southward open into the Strait of Georgia. This receives considerable quantities of fresh water runoff from several rivers; it is almost closed to the north and has only restricted connection at the south end with the Pacific. Since the salinities in Hecate Strait are 2 to 3‰ greater at the same depths than in the Strait of Georgia (e.g. Pacific Oceanographic Group, 1955; Waldichuk, 1957) a corresponding difference is to be expected between the northern and southern inlets.

The local differences in the Smith–Knight region previously mentioned may be seen in Table VI. Smith, with a moderately deep sill and opening directly to Queen Charlotte Sound and the Pacific Ocean, has a salinity at 200 m of 33.0‰. In Knight with a shallower sill and a less direct connection to the Pacific the salinity at 200 m is only 31.2‰. Kingcome which has a deeper sill than Knight and is between the previous two has a salinity of 32.0‰. Belize and Seymour, between Smith and Kingcome, show lower values than any of these (29 and 28‰ respectively). These two inlets have a common shallow sill which restricts the

TABLE VII. Mean values of temperature (°C) along the length of each inlet for each cruise, with range of temperature about mean which includes at least 75% of all values for that cruise.

Inlet	Date		DEPTH (METRES) 20	50	100	200	300	400	500	600 (Notes)
Portland C.	Jul.	51	6.9±1.4	5.8±0.7	5.6±0.1	5.6±0.1	5.6±0.1	5.63	–	–
Observatory	Jul.	51	6.8±0.8	5.8±0.3	5.5±0.1	5.7±0.1	. . .	5.72	. . .	–
Hastings	Jul.	51	6.0±0.1	5.31	5.61	5.62	–	–	–	–
Alice	Jul.	51	6.5±0.4	5.3±0.1	5.3±0.2	4.30	. . .	–	–	–
Work	Jul.	51	6.1±0.4	5.8±0.1	5.9±0.1	5.95	5.95	–	–	–
Douglas	Jul.	51	6.2±0.6	6.5±0.2	6.2±0.1	6.20	6.16	6.02	–	–
	Jun.	52	6.2±0.7	6.2±0.7	6.7	6.4	. . .	. . .	–	(2)
	Jul.	52	6.6±0.3	6.4±0.3	6.7	. . .	. . .	. . .	–	(2)
	Aug.	52	8.9±1.5	7.1±1.2	6.7±0.1	6.4	. . .	. . .	–	(2)
	Aug.	54	7.5±0.1	7.3	6.8	6.7	6.68	6.64	–	(3)
Kildala	Jul.	51	5.9±0.2	6.5±0.2	6.18	. . .	–	–	–	–
Gardner	Jul.	51	6.4±0.3	6.3±0.1	6.3±0.1	6.4±0.1	. . .	6.48	–	(4)
			6.8±0.2	6.3±0.1	6.3±0.1	6.2	. . .	6.10	–	(5)
	Aug.	54	7.4±0.1	7.2±0.1	7.1	7.1±0.1	7.13	. . .	–	(6)
Surf	Jul.	51	10.3±1.5	8.0±0.4	6.7±0.1	6.40	. . .	–	–	–
Laredo	Jul.	51	10.0±1.5	7.5±0.6	6.54	6.20	6.00	–	–	–
Sheep	Jul.	56	7.9±0.7	6.7±0.5	6.2±0.1	6.09	6.07	–	–	–
Kynoch	Jul.	56	7.6±0.6	6.3±0.3	6.4±0.2	6.5±0.1	6.65	6.66	6.66	6.67
Spiller	Jul.	56	7.7±1.0	6.9±0.3	6.4±0.1	6.05	. . .	. . .	–	–
			. . .	. . .	6.98	6.99	. . .	. . .	–	(7)
Briggs	Jul.	56	9.4	7.9	. . .	. . .	. . .	. . .	. . .	. . .
Roscoe	Jul.	56	7.3±0.4	5.8±0.1	5.8±0.2	. . .	–	–	–	–
Dean	Jun.	51	6.0±0.8	6.4±0.3	6.6±0.2	6.5±0.1	6.4±0.1	6.48	6.47	–
	Jul.	56	5.5±1.0	6.5±0.7	6.5±0.4	6.4±0.2	6.3±0.1	6.5±0.3	6.4±0.2	–

TABLE VII.—*Continued*

Inlet	Date		DEPTH (METRES) 20	50	100	200	300	400	500	600
										(Notes)
Cascade	Jul.	56	5.6±0.2	5.8±0.2	6.5	6.4±0.1	6.7	–	–	–
Burke	Jun.	51	7.2±0.6	6.9±0.3	6.6±0.2	6.5±0.1	6.50	6.46	6.38	–
	Jul.	56	6.9±1.1	5.6±0.6	6.6±0.2	6.5±0.2	6.4±0.2	6.6±0.1	6.65	–
Kwatna	Jul.	56	6.4	5.7	6.0	6.6	6.6	6.7	...	–
S. Bentinck	Jun.	51	7.1±0.2	6.5+0.1	6.6±0.1	6.5±0.1	...	6.45	–	–
Rivers	Jun.	51	7.4±0.2	7.1±0.2	6.9±0.2	6.5±0.1	6.45	–	–	–
	Jul.	56	7.1±0.2	6.9±0.2	6.6±0.2	6.4±0.2	6.28	–	–	–
Moses	Jun.	51	7.6±0.2	7.1±0.1	7.0	6.95	–	–	–	–
	Jul.	56	7.3	7.0	7.0	7.7	–	–	–	–
Draney	Jun.	51	7.9±0.2	7.8±0.2	6.9±0.1	–	–	–	–	–
Smith	Jul.	55	8.9±0.1	7.6±0.1	7.1±0.1	7.0±0.1	...	–	–	–
Belize	Jun.	51	8.2±0.8	7.8±0.7	7.5±0.4	7.4±0.3	7.04	–	–	–
Seymour	Jun.	51	7.7±0.5	7.3±0.3	7.4±0.3	7.9±0.1	7.93	7.45	7.35	7.35
Drury	Jul.	55	9.7	9.3	–	–	–	–	–	–
Kingcome	Jul.	53	8.0±0.6	7.3±0.3	7.48	7.9±0.2	7.52	...	–	–
	Jul.	55	8.3±0.1	7.6±0.2	7.5±0.1	7.56	7.53	...	–	–
	Jun.	57	7.8±0.3	6.8±0.1	6.8±0.1	7.2±0.2	7.53	7.58	–	–
Knight	Jun.	51	7.3±0.5	6.6±0.4	6.6±0.1	6.7±0.1	6.80	6.83	6.88	(8)
			7.0±0.5	7.1±0.4	6.9±0.2	6.95	–	–	–	–
	Jun.	52	6.9±0.4	6.7±0.4	6.5±0.3	6.7±0.3	6.95	7.15	...	–
			7.3	7.0	7.0	...	–	–	–	–
	Jul.	53	7.8±0.3	7.3±0.5	7.2±0.5	7.3±0.5	7.3±0.2	7.1±0.1	7.2	–
			8.3±0.2	8.0±0.3	7.9±0.1	7.9	–	–	–	–
	Jul.	55	7.9±0.2	7.4±0.2	7.3±0.1	7.3±0.1	7.40	7.42	7.43	–
			8.0±0.4	7.4±0.1	7.5	...	–	–	–	–

	Jul.	55	7.9±0.2	7.4±0.2	7.3±0.1	7.3±0.1	7.40	7.42	7.43	–
			8.0±0.4	7.4±0.1	7.5	. . .	–	–	–	–
	Jul.	56	7.4±0.4	6.3±0.5	6.0±0.4	6.7±0.3	7.0±0.3	7.3±0.2	7.45	–
			8.1±0.9	7.1±0.5	7.0±0.1	. . .	–	–	–	–
	Jun.	57	7.3±0.1	6.8±0.2	6.6±0.2	6.6±0.2	6.8±0.3	7.1±0.1	7.15	–
			7.7±0.2	7.3±0.1	7.2±0.1	7.3	–	–	–	–
	Sep.	57	7.5±0.4	7.2±0.5	6.7±0.3	6.9±0.4	6.9±0.2	6.95	. . .	–
			8.5±0.4	8.3±0.2	8.20	8.22	–	–	–	–
	Jun.	58	8.2±0.2	7.4±0.1	7.6±0.3	7.3±0.3	6.9±0.1	6.9	. . .	–
			8.5±0.3	8.5±0.4	8.5	. . .	–	–	–	–
	Jun.	59	7.7±0.2	7.6±0.1	7.6±0.2	7.6±0.2	7.4±0.2	7.55	7.48	–
			8.1	8.0±0.2	8.0	. . .	–	–	–	–
Call	Jul.	53	8.7±0.3	8.1±0.2	7.5±0.1	. . .	–	–	–	–
	Aug.	53	9.3±0.2	8.4±0.3	7.9	8.0	–	–	–	–
	Jul.	55	8.5±0.3	7.6±0.2	7.7±0.1	7.9	–	–	–	–
	Jul.	56	7.5±0.2	6.8±0.4	6.0±0.1	5.8	–	–	–	–
	Jun.	57	8.2±0.1	7.1±0.1	6.4	6.3	–	–	–	–
	Sep.	57	8.6±0.2	8.3±0.3	6.9±0.2	. . .	–	–	–	–
Loughborough	Jul.	53	9.9±0.3	9.1±0.1	8.2±0.2	8.1±0.1	–	–	–	–
	Jul.	55	9.1±0.1	8.6±0.2	7.8±0.4	7.7	–	–	–	–
	Jul.	56	8.6±0.1	7.8±0.3	7.6±0.4	7.3±0.1	–	–	–	–
	Jun.	57	8.5±0.2	8.0±0.4	7.2±0.4	6.6	–	–	–	–
	Sep.	57	9.5±0.3	9.1±0.5	8.6±0.9	6.7±0.1	–	–	–	–
Bute	May	51	7.6±0.2	6.4±0.3	7.3±0.2	7.6±0.2	7.9±0.1	7.9±0.1	. . .	7.98
	Aug.	51	8.9±0.2	8.1±0.4	7.8±0.2	8.0	. . .	. . .	. . .	. . .
	Oct.	51	8.4±0.2	7.7±0.7	7.6±0.2	7.9	. . .	7.9±0.1	7.91	. . .
	Mar.	52	6.9±0.4	6.8±0.5	7.0±0.6	8.0±0.3	8.1±0.2	8.2±0.2	7.93	. . .
	May	52	7.8±0.5	6.6±0.3	7.4±0.3	8.2±0.1	8.2±0.2	. . .	8.2±0.2	. . .
	Aug.	52	8.5±0.2	8.1±0.2	7.4±0.5	8.1±0.1	8.15	8.20	. . .	8.09
	Mar.	53	7.5	7.4±0.4	7.6±0.4	8.4±0.2	8.6	8.64	8.65	8.68
	Jul.	53	9.5±0.3	8.4±0.5	7.8±0.4	8.4±0.1	8.4±0.1	8.5±0.1	8.6	8.66
	Aug.	53	9.0±0.2	8.3±0.5	8.0±0.3	8.30	. . .	8.52	. . .	8.66
	Jun.	54	8.0±0.7	7.6±1.1	7.9±0.4	8.4±0.2	8.6±0.1	. . .	. . .	. . .
	Jul.	55	9.4±0.2	8.4±0.2	8.4±0.1	8.4±0.1	8.4±0.1	8.44	8.46	8.48
	Jul.	56	8.3±0.1	7.8±0.1	7.8±0.3	8.0±0.2	8.20	8.22	8.25	8.29
	May	57	7.5±0.9	7.0±1.0	7.4±0.4	8.2±0.1	8.16	8.1±0.1	8.2±0.2	8.05
	Jul.	57	8.8±0.1	8.0±0.2	7.5±0.1	7.9±0.3	8.0±0.2	8.1±0.1	8.11	8.11
	Sep.	57	8.9±0.2	8.2±0.3	7.9±0.5	7.8±0.3	8.0±0.2	8.0±0.2	8.1±0.1	. . .
	Nov.	57	7.9±0.4	8.0±0.3	7.8±0.4	8.0±0.2	8.0±0.2	8.0±0.1	8.1±0.1	. . .

TABLE VII.—*Continued*

Inlet	Date	DEPTH (METRES) 20	50	100	200	300	400	500	600
									(Notes)
Bute (*Cont.*)	Feb. 58	7.4 ±0.4	7.9 ±0.1	8.0 ±0.5	8.3 ±0.3	8.2 ±0.3	8.0 ±0.1	8.06	8.11
	Mar. 58	7.6 ±0.3	7.8 ±0.2	8.0 ±0.2	8.2 ±0.3	8.2 ±0.2	8.07	8.05	. . .
	May 58	7.7 ±0.3	8.2 ±0.5	8.2 ±0.4	8.2 ±0.3	8.2 ±0.2	8.08	. . .	. . .
	Jun. 58	9.3 ±0.3	7.9 ±0.3	8.3 ±0.1	8.3 ±0.1	8.2 ±0.1	8.06	8.05	8.06
	Jun. 59	8.9 ±0.9	7.7 ±0.2	8.5 ±0.2	8.6 ±0.3	8.6 ±0.3	8.4 ±0.1	8.36	8.19
	Jun. 60	9.6 ±0.3	8.2 ±0.7	8.3 ±0.2	8.6 ±0.1	8.8 ±0.1	8.8 ±0.1	8.8 ±0.1	8.6
Ramsay	Jun. 54	10.1	7.4	8.5	8.7	8.7	–	–	–
	Jun. 56	9.9	7.3	7.7	8.1	8.2	–	–	–
Toba	Aug. 51	9.5 ±0.1	8.1 ±0.1	7.9 ±0.1	8.0	. . .	8.0	. . .	–
	Mar. 53	7.2 ±0.1	7.6 ±0.1	8.0 ±0.1	8.3 ±0.1	8.54	8.70	8.8	–
	Jun. 54	9.8 ±0.5	8.4 ±0.1	8.6 ±0.1	8.6	8.6 ±0.1	. . .	. . .	–
	Jun. 55	11.2 ±0.3	8.6	8.6	8.5 ±0.1	8.4	7.8	7.8	–
	Jun. 56	9.6 ±0.8	7.7 ±0.2	8.0 ±0.2	7.9 ±0.2	8.0 ±0.2	8.14	8.16	–
	Sep. 57	8.8 ±0.6	8.1 ±0.5	7.9	7.9 ±0.2	7.9 ±0.3	7.85	. . .	–
	Feb. 58	7.5 ±0.1	8.1 ±0.1	8.0 ±0.2	8.2 ±0.2	8.2 ±0.2	8.0 ±0.1	. . .	–
	Mar. 58	7.6	7.9	8.0 ±0.2	8.2 ±0.2	8.2 ±0.2	8.1 ±0.1	. . .	–
	May 58	7.91	8.1 ±0.1	8.2 ±0.1	8.2 ±0.1	8.2 ±0.2	8.3 ±0.1	. . .	–
	Jun. 58	8.2 ±0.4	8.1	8.1 ±0.1	8.2 ±0.2	8.2 ±0.2	8.3 ±0.1	. . .	–
Pendrell	May 51	7.9 ±0.3	7.8 ±0.1	8.1	8.04	. . .	7.94	–	–
	Aug. 51	11.3 ±0.9	8.2 ±0.2	8.0	8.00	. . .	. . .	–	–
	Mar. 53	7.3	7.6 ±0.1	8.0 ±0.1	8.4	8.6	8.7	–	–
	Jul. 53	10.1 ±0.3	8.5 ±0.1	8.2	8.5	8.4	. . .	–	–
	Aug. 53	11.5 ±0.6	8.9 ±0.1	8.2 ±0.1	8.4	8.5	. . .	–	–
	Jun. 54	9.6 ±0.3	8.2	8.65	8.63	8.5	. . .	–	–
	Jun. 56	11.2 ±0.6	7.5 ±0.3	7.9 ±0.2	8.18	8.23	. . .	–	–
	Sep. 57	9.6 ±0.2	8.1 ±0.1	7.86	8.00	7.9	. . .	–	–
Jervis	May 52	8.1 ±0.2	8.0 ±0.3	8.0 ±0.5	8.4 ±0.2	8.4 ±0.1	8.47	8.50	8.5
	Jun. 54	9.3 ±1.0	8.5 ±0.4	8.6 ±0.1	8.6 ±0.2	87. ±0.1	. . .	. . .	. . .
	Jun. 56	8.7 ±0.3	7.6 ±0.2	7.8 ±0.6	8.3 ±0.2	8.5	8.47	8.49	8.48
	May 57	8.4 ±0.5	7.7 ±0.4	7.7 ±0.5	8.3 ±0.2	8.4 ±0.1	8.44	8.48	8.47

	Jul.	57	7.9 ± 0.5	8.2 ± 0.4	7.7 ± 0.2	8.3 ± 0.2	8.44	8.45	8.45	8.45
	Nov.	57	8.9 ± 0.2	8.4 ± 0.6	8.4 ± 0.5	8.3 ± 0.2	8.4 ± 0.1	8.42	8.44	8.44
	Feb.	58	7.6 ± 0.4	8.15	8.4 ± 0.2	8.4 ± 0.2	8.4 ± 0.1	8.39	8.42	8.42
	May	58	8.5 ± 0.4	8.2 ± 0.1	8.25	8.4 ± 0.2	8.40	8.41	. . .	. . .
	Jun.	58	8.4 ± 0.2	8.2	8.35	8.5 ± 0.2	8.41	8.40	8.40	8.39
	Jun.	59	9.9 ± 0.4	8.6 ± 0.1	8.8 ± 0.1	8.7 ± 0.2	8.7 ± 0.2	8.6 ± 0.1	8.7 ± 0.1	8.75
	Jun.	60	8.4 ± 0.2	8.3 ± 0.2	8.4 ± 0.4	8.8 ± 0.1	8.8 + 0.1	8.8 ± 0.1	8.9	8.94
Pr. Louisa	May	52	10.8	8.8	7.7	. . .	–	–	–	–
	Jun.	60	10.7	8.7	7.7	7.7 at 176 m		–	–	–
Sechelt	Jul.	57	11.1 ± 0.4	8.8 ± 0.4	7.5 ± 0.2	7.43	–	–	–	–
Howe	Mar.	53	7.8 ± 0.1	8.0 ± 0.2	8.3 ± 0.3	8.6	. . .	–	–	–
	Jun.	57	8.3 ± 0.7	8.0 ± 0.4	7.5 ± 0.2	7.45	. . .	–	–	–
Indian	Jun.	53	10.3 ± 0.3	8.4 ± 0.4	7.9	. . .	–	–	–	–
	Sep.	53	11.3 ± 1.1	10.7 ± 0.8	7.92	7.91	–	–	–	–
	Win.	56	9.4 ± 1.3	8.3 ± 1.3	6.7 ± 0.5	6.4 ± 0.1	–	–	–	(9)
	Sum.	56	11.0 ± 0.1	9.8 ± 1.0	6.6 ± 0.1	6.3	–	–	–	–
	Win.	57	8.5 ± 2.0	8.3 ± 1.8	7.0 ± 0.6	6.5 ± 0.2	–	–	–	–
	Sum.	57	10.8 ± 0.3	9.6 ± 1.2	6.6 ± 0.2	6.4	–	–	–	–
	Win.	58	8.8 ± 0.8	9.0 ± 0.8	7.9 ± 0.2	6.8 ± 0.3	–	–	–	–
	Sum.	58	11.9 ± 0.9	10.2 ± 1.2	7.9 ± 0.1	7.2 ± 0.2	–	–	–	–
	Win.	59	9.3 ± 1.2	8.8 ± 1.3	8.2 ± 0.6	7.7 ± 0.1	–	–	–	–
	Sum.	59	11.5 ± 0.6	10.4 ± 1.6	7.9 ± 0.2	7.7 ± 0.1	–	–	–	–

Notes:

(1) When the ± range including at least 75% of the values at a particular depth (75% range) was ±0.02 C degree or less its value has been omitted and the mean temperature has been quoted to the nearest 0.01 C degree. When the 75% range was between 0.03 and 0.07 C degree its value has been omitted and the mean temperature quoted to the nearest 0.1 C degree. When the 75% range was 0.08 C degree or over, its value has been quoted to the nearest 0.1 C degree.

(2) Data collected by Canadian Hydrographic Service.

(3) Data collected by Pacific Oceanographic Group, Sta. Do 6, 8, 10 only.

(4) Station Ga 4–14.

(5) Stations Ga 1–3.

(6) Data collected by Pacific Oceanographic Group, Sta. Ga 4, 6 and 10 only.

(7) Station Sp 5 only.

(8) See Note (9), Table VI.

(9) See Note (11), Table VI.

entrance of saline water. The difference between the two is attributed to the larger runoff into Seymour (Table II).

It is also noted that in any region, inlets with shallow sills have deep water of lower salinity than at the same depth outside, but of higher salinity than at the sill depth outside. The water temperature however is sometimes higher and sometimes lower than outside. These facts may be related to the character of the circulation which is discussed later.

The salinity in the deep zone generally increases with depth. A few inversions have been noted in the deepest water where the salinity gradients are small but these are usually within the limits of error of salinity determination with the method in use.

3.22 Temperature minimum

In contrast to the vertical salinity distribution which shows a continuous increase from surface to bottom, the temperature profiles often show maxima or minima at intermediate depths. In the spring and summer the surface water is the warmest in any vertical column and the temperature decreases as depth increases in the shallow zone except occasionally when wind mixing has created an isothermal layer, or where at the head of an inlet cold fresh water is overlying warmer saline water. Usually there is a thermocline closely associated with the halocline and below this in many of the inlets the temperature decreases to a minimum at 15 to 100 m depth. It then rises and becomes isothermal or nearly so in the deep water. Sometimes there is a temperature maximum at 40 to 200 m between the minimum and the isothermal deep layer. There are twelve inlets, mostly shorter ones, in which a temperature minimum has not been observed or is uncommon.

The temperature minimum appears most marked and is generally a feature in Bute. The minimum temperature is as much as 2 C degrees less than that of the deep isothermal water, but, as Fig. 19 shows, the extent of the minimum varies from year to year. During the extensive survey of 1951 a marked minimum was also observed in Seymour and Douglas. It was less conspicuous elsewhere (i.e. less than 1 degree) but was evident to some extent in most inlets. In 1956 and 1957 the minimum was very conspicuous in several of the large inlets (Jervis, Bute, Knight, Kingcome, Burke and Dean). On the other hand, in 1958 the minimum was much less conspicuous that usual in Jervis, Toba and Bute although more conspicuous in Knight.

Figure 19 shows that the minimum differs in appearance in different years and also indicates a change in appearance during a year (e.g. 1951, 1952, 1957, 1958). Figure 20 shows a series of vertical temperature profiles in Bute which illustrates in more detail the variation in appearance of the minimum during a period of 14 months.

This temperature minimum has been attributed (Pickard, 1953) to winter cooling of the upper part of the water column followed in spring and summer by warming from the surface. The temperature of the minimum, the difference

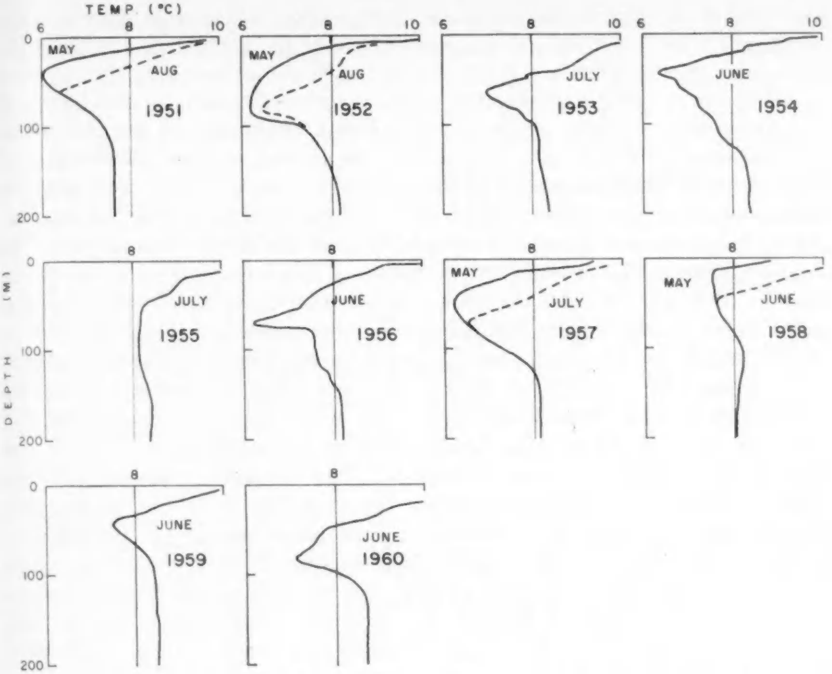

FIG. 19. Temperature minimum at Sta. 6, Bute Inlet, 1951–1960.

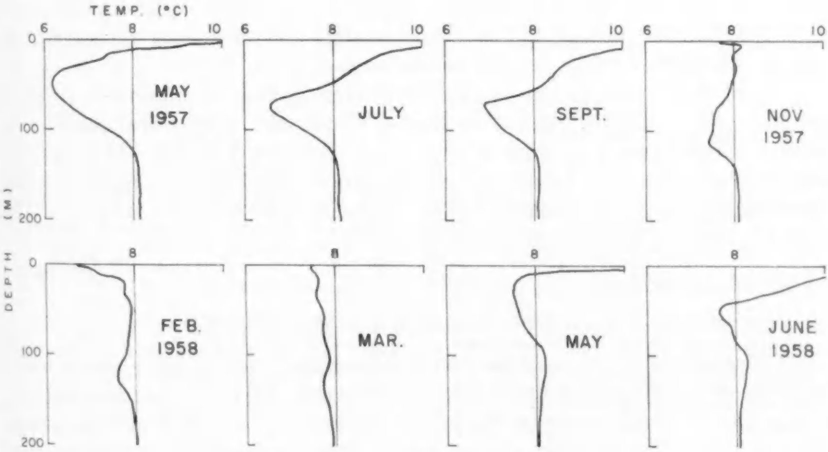

FIG. 20. Temperature minimum at Sta. 6, Bute Inlet from May 1957 to June 1958.

from that of the deep isothermal water, and possibly the depth of the top of the isothermal layer, must then be some indication of the amount of cooling in the previous winter or winters. Unfortunately there are no meteorological stations in the southern inlets and therefore there is no opportunity to correlate local climate directly with the temperature minimum. However, an examination of the temperature records at a selection of the coastal stations (Meteorological Division, 1950–1958) indicates that the climatic fluctuations at all of these follow essentially the same pattern, and it may be legitimate to use the temperature records for Vancouver Airport for comparison with the water temperatures in the southern inlets. For instance the temperature minimum was very marked in Bute in 1951 (Fig. 19) and the value was low (6.0°C) in May. In succeeding years the minimum became less marked and the temperature rose to 8.2°C in 1955. In 1956 the minimum was again very marked and the value had fallen to 6.4°C and in 1957 to 6.3°C. In 1958 it had risen to 7.6°C. For comparison the mean temperature at Vancouver Airport was lower than usual during 1949–50, was close to the long-term mean during 1951–54, below this mean in the winter of 1955–56, and above it again in 1957–58. The temperature minimum in the water therefore shows some inclination to follow the mean air temperature. More specifically there is an indication that below-normal air temperatures during January–March may be particularly effective in determining the extent of the minimum. This is the time of year when the stability of the water column in the upper 100 m is least because the salinities are highest (see Section 4.2). It is also the time when strong winds ("Squamishes") bring cold air down from the interior plateau to the inlets. These may be a significant factor in causing turbulent mixing and cooling of the water. It would be interesting to follow the development of the temperature minimum by closely spaced cruises during the winter, studying the heat budget at the same time. The best series obtained so far was in 1957–58 (Fig. 20) but unfortunately the winter was not a cold one and the minimum in 1958 was not conspicuous.

Mohn (1887) describes an apparently similar temperature minimum at 10 to 100 m depth in certain Norwegian fjords. Nordgaard (1903) also describes a marked temperature minimum in By Fjord and Hjelte Fjord. It is at the surface in the winter and descends subsequently to 20 to 50 m in April. In By Fjord the temperature is substantially constant from 80 m to the bottom at 150 m and in Hjelte Fjord from 120 m to the bottom.

3.3 Periodic Changes

3.31 Seasonal changes in salinity and temperature

The character of the seasonal variation in salinity and temperature in Bute for 1950–52 was described by Tabata and Pickard (1957) and summarized by stating that an annual cycle of change was evident to a depth of 60 feet (about 20 m) in salinity but to about 150 feet (about 50 m) in temperature. Data from the series of eight cruises in 1957–58 are shown in Fig. 21 and 22 to supplement

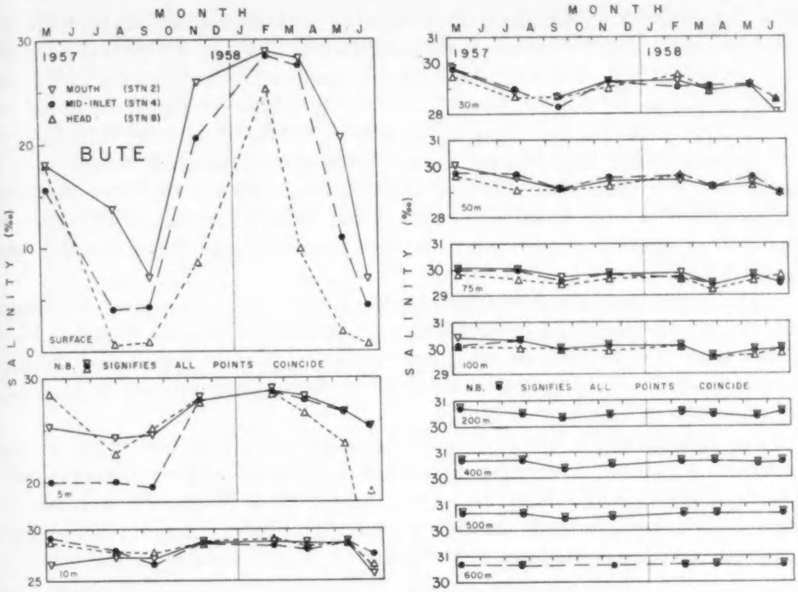

FIG. 21. Seasonal variation of salinity in Bute Inlet, 1957–1958.

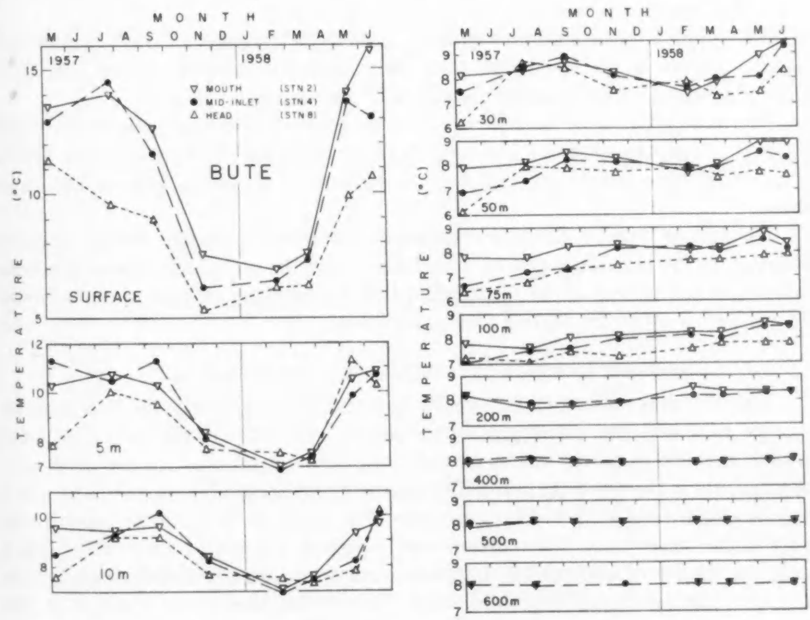

FIG. 22. Seasonal variation of temperature in Bute Inlet, 1957–1958.

those for 1950–52. The later series, together with data from successive winter and summer cruises at other times, suggests that the seasonal fluctuation in salinity may extend to 30 m, and that the seasonal temperature fluctuations may extend to 100 m particularly if the winter is unusually cold. (It should be noted that the salinity values for the cruise of September 1957 appear to be 0.15 to 0.25‰ low compared with neighbouring cruises while the temperature values show no significant difference. The accuracy of the salinity values is therefore questioned and the slight minima in salinity at 50 m and 75 m for September 1957 are not regarded as significant evidence of deeper penetration of the seasonal salinity fluctuations.)

The ranges of seasonal variations at the surface in Bute are from 6 C degrees and 25‰ at the inlet head to 10 C degrees and 22‰ at the inlet mouth. In the surface layer the temperature maximum occurs in July or August and the minimum in December or January, while at 50 m the maximum occurs in September and minimum in February or March.

The other inlet for which there are adequate data to determine the seasonal variations is Indian. Gilmartin (1960) has described a series of observations at approximately monthly intervals over a period of 3 years. In this inlet the seasonal variations of salinity are clearly evident to 50 m. There is some variation at 100 m but this is irregular and appears to be attributable to the occasional influx of water from outside rather than being a direct result of seasonal runoff variations. There is a seasonal temperature variation evident to 100 m. The ranges of seasonal variations at the surface in Indian are 12 to 17‰ in salinity and 10 to 17 C degrees in temperature.

The much larger runoff into Bute is taken to be the cause of the larger salinity variations than in Indian, while the low temperature of the runoff into Bute (from glaciers) limits the seasonal range of temperature in this inlet.

The only other inlet for which winter and summer observations are available is Jervis. The observations indicate that the variations in this inlet are similar to those in Bute which are taken to be typical of the situations in the larger inlets.

Nordgaard (1899) describes seasonal variations in some fjords as being observed to 200 m. This greater penetration may be a consequence of the lesser stability of the waters in the Norwegian fjords where the shallow water salinities are not as low as in the British Columbia inlets.

3.32 Long-term changes in salinity and temperature

The seasonal variations in salinity and temperature in the shallow zone are so large that with the infrequent observations over most of the period of study it is not possible to detect any significant long-term variation. In the deep water the situation is the opposite and while no significant seasonal variation is apparent there is evidence of year-to-year changes. For instance, in Bute the temperature range in the water from 300 to 600 m depth is generally within 0.1 to 0.2 C degree along the length of the inlet at any one time, and long-term differences greater than this can be considered significant. It will be seen from Table VII that

there was an increase in temperature of 0.6 to 0.7 C degree from 1951 to 1953 and then a decrease of about the same amount to a minimum in 1957 with a subsequent rise. The salinity showed a small rise in 1953, a decrease until 1956, a rise in 1957, a decrease in 1959, and then a small rise in 1960. These data for Bute are illustrated in Fig. 23. The data plotted are taken from Tables VI and VII and are the average values along the length of the inlet at each depth below the level of seasonal change. The scales for temperature and for salinity have been selected so that a displacement of the temperature line from the mean by

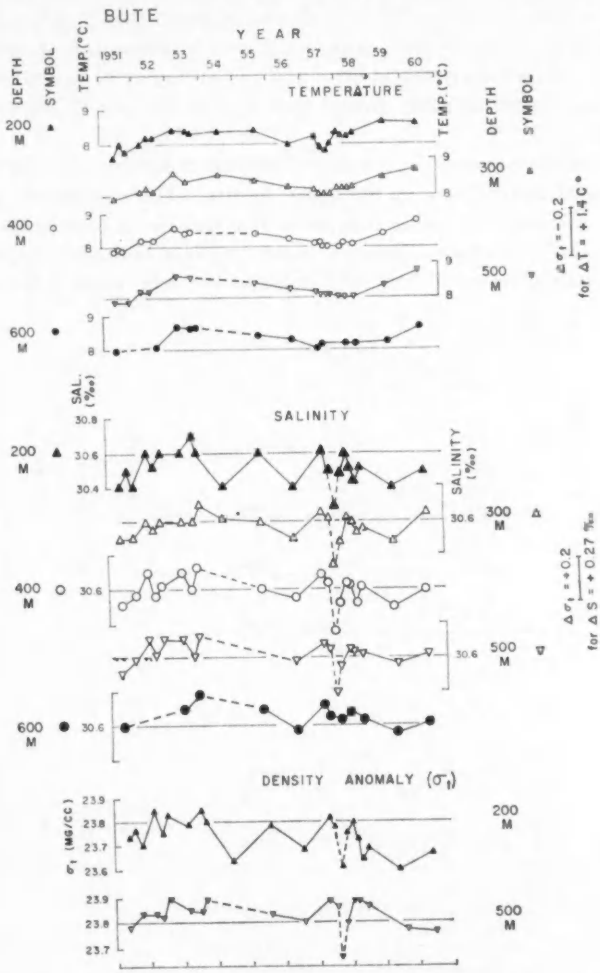

FIG. 23. Values of salinity, temperature and density anomaly of the deep water in Bute Inlet, 1951–1960.

a given distance (say 1 cm) represents the same change in σ_t as does the same displacement of the salinity line. This facilitates the comparison of the significance of fluctuations of these two quantities which are themselves independent and of different physical character but which together determine the density of sea water. This in turn determines the depth at which a particular water mass will find itself in static equilibrium. The graphs of σ_t for depths of 200 and 500 m at the bottom of Fig. 23 are again plotted to the same scale to show that the salinity is the main determining factor in density even in the deep water of this inlet. When reading Fig. 23 it should be noted that in terms of the effect on density the precision of the temperature points (estimated at about ± 0.1 C degree including the experimental error and the averaging of several points along the inlet length) is considerably greater than that of the salinity points (estimated at ± 0.05 to 0.1‰).

In Fig. 23 there is some indication of the rise in temperature occurring more abruptly at 600 meters than at the lesser depths. The number of observations are too few to warrant stressing this point, particularly as the change in salinity appears to occur much less abruptly. However, since both the temperature and salinity generally increase slightly with depth in the deep water it is clear that an

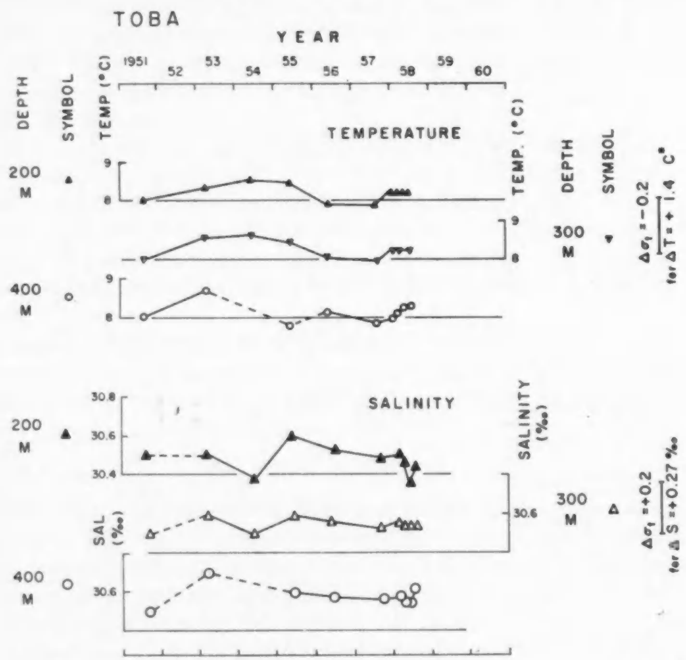

FIG. 24. Values of salinity and temperature of the deep water in Toba Inlet, 1951–1958.

increase in either cannot be explained by downward diffusion and it is concluded that the increases in the 1951 and 1959 periods must be due to an inflow of deep water from outside the inlet. The slow decrease in temperature and salinity after 1953 could be explained by diffusion upward with an eddy diffusion coefficient of the order of 0.02 cm² sec⁻¹. This may be compared with the values of 0.2 to 1.2 cm² sec⁻¹ estimated for depths of 90 to 130 m just below the temperature minimum (Tabata and Pickard, 1957) where the gradients of temperature and salinity are greater.

The amount of data available for other inlets is less than for Bute. Toba (Fig. 24) shows essentially the same pattern as Bute at 300 and 400 m from 1951 to 1958. Jervis (Fig. 25) shows a smaller rise in temperature at 300 m, 0.4 C

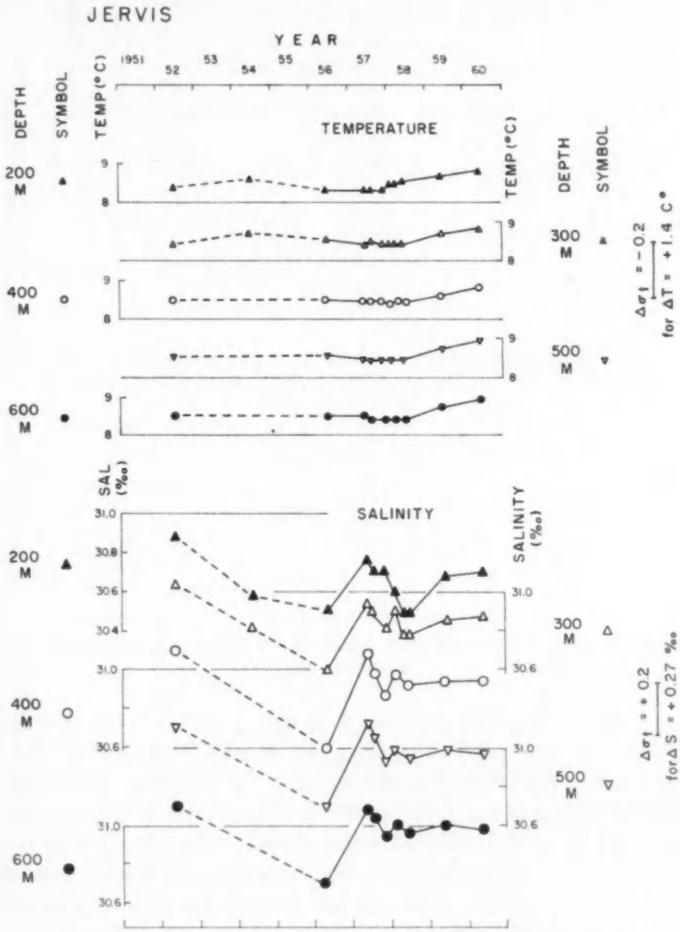

FIG. 25. Values of the salinity and temperature of the deep water in Jervis Inlet, 1952–1960.

degree compared to 0.7 in Bute. The changes in salinity in Toba are somewhat similar to those in Bute but less marked. Those in Jervis differ in showing a decrease from 1952 to 1956 before the rise to 1957 values and, except at 200 m, less change from 1958 to 1960 compared to Bute.

Outside the group which opens on to the Strait of Georgia the only inlet for which there are many data for the period of study is Knight (Fig. 26). The

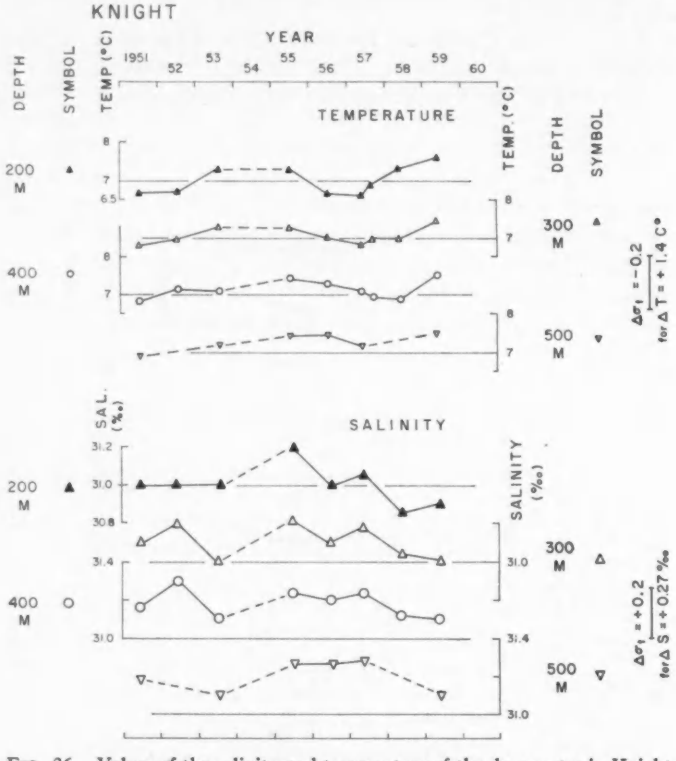

FIG. 26. Values of the salinity and temperature of the deep water in Knight Inlet, 1951–1959.

temperature pattern is similar to that in Bute with a rise from 1951 to 1954 or 1955, a fall until 1957 or 1958 and a subsequent rise to 1959. The last is more marked at the lesser depths than in the deepest water. The variations in salinity are not the same as in Bute and the year-to-year variations are not as consistent at the different depths as in the more southerly inlets. (Note that when comparing inlets it is necessary to compare only the values for years for which there are observations in both inlets, otherwise an exaggerated idea of the differences between inlets may be obtained.)

For the inlets further north there are only a few scattered observations which are summarized in Table VIII in terms of the change from the earlier year quoted to the later, while the observations of Thompson and Barkey (1938) are given in Table IX with the present author's observations in 1951 for comparison.

TABLE VIII. Changes of temperature and salinity of deeper waters in some northern inlets between the years stated.

Inlet	Years	Depth range	Change of: Temperature	Salinity
		m	C°	‰
Douglas	1951 to 1954	100–400	+0.5	−0.1
Gardner	1951 to 1954	100–300	+0.6	−0.1
Dean	1951 to 1956	100–300	−0.1	−0.1
		400–500	nil	nil
Burke	1951 to 1956	100–300	−0.1	−0.2
		300–500	+0.2	nil
Rivers	1951 to 1956	100–300	−0.2	nil
Moses	1951 to 1956	200	+0.7	+0.2
Kingcome	1953 to 1955	100	nil	+0.3
		200–300	nil	nil
Kingcome	1955 to 1957	100–200	−0.5	−0.3
		300	nil	+0.1

TABLE IX. Temperature and salinity in Seymour Inlet in 1937–38 and in 1951. (Data for 1937 and 1938 from Thompson and Barkey, 1938.)

	September 1937	March 1938	June 1951
Temperature (°C):			
Surface	14.73–16.04	6.83–7.19	9.5–15.8
75 m	7.87–8.49	7.06–7.95	7.1–8.3
550 m	7.02	7.19	7.35
600 m	7.15	7.47	. . .
Salinity (‰):			
Surface	5.5–12.7	25.3	1–23
Deep	28.95–29.02	. . .	29.02–29.06

It is concluded from the evidence available that there is no annual cycle of change of properties below 100 m but that changes do take place irregularly at intervals of a year or more. The question remains as to whether these changes represent changes in the properties of basically static water masses or are evidence of replacement of significant proportions of the deep-water masses from outside. The latter process is believed to be the more probable and in any event is the only means whereby an *increase* in salinity of the deep water can occur.

4. DENSITY

4.1 Density Distribution in Shallow and Deep Zones

In the shallow zone and to about 50 m the density of the water is determined almost entirely by the salinity, particularly in the Group A inlets, and there is no point in describing the density distribution separately. However, in the deep water the effect of temperature is not insignificant and the density distribution which includes the effect of both salinity and temperature shows some features which should be mentioned.

A plot (not given) of the density at a selection of depths from 20 to 500 m against the latitude of the approximate middle of the inlet length suggests that very broadly the inlets might be divided into two groups. The northern inlets from Portland to Smith, with some exceptions, have much the same density at the same respective depths. For the remaining inlets the density at any depth tends to decrease to the southward. Looking more closely one can pick out basic groups of northern and southern inlets, similar to those selected on the basis of temperature and salinity, also an intermediate group. The mean values of σ_t are given in Table X, and also shown graphically in Fig. 27. There are exceptions from the main groups and these are included in the Table for subsequent comment. The intermediate inlets are given individually, since the change of mean values from one to another, in relation to the variation in any one of them, is such that grouping them together would obscure certain features on which it is desired to comment.

The broad feature of greater density in the northern than in the southern group is attributed to their more direct connection with the Pacific Ocean as the ultimate source of the densest water along the coast. The lesser density in the southern group is attributed to the fact that these open into the Strait of Georgia where the water is of lesser density than in the Pacific. It will be noted that the difference in σ_t between the southern and the northern groups is very significant (about 2.2 mg/cc).

The southern inlets which depart from the main group (Sechelt, Princess Louisa and Indian) are those which have a restricted entrance and it is assumed that it is this feature which holds the lower-density surface water in these inlets. At the same time it should be noted that it is not only the surface but also the deeper water which is of lesser density by 1 to 2 mg/cc within the inlets than outside. Of the northern inlets, only Alice, Work and Draney have comparatively narrow entrances and these all have water of lesser density than other inlets in their region. The low values in Gardner are attributed to its shallow sill.

Among the intermediate group, Seymour and Belize have restricted entrances and again show lesser densities than others in the region. Although these two inlets have a common entrance there is a significant difference between their waters at all depths listed, that in Seymour being less dense by 0.6 to 0.9 mg/cc

TABLE X. Mean values of σ_t for British Columbia mainland inlet waters.

Inlets	Depth (metres)					
	20	50	100	200	300	500
Northern group:						
Portland C. to Smith	24.3	25.1	25.8	26.1	26.2	26.2
Exceptions:						
Alice and Observatory	23.5	24.5	24.6	24.8	25.0	–
Work, Gardner (Sta. 8 to head)	. . .	. . .	25.2	25.2	25.2	–
Draney	22.8	23.5	24.3	–	–	–
Intermediate group:						
Belize	22.7	23.3	23.5	23.6	23.6	–
Seymour	22.2	22.4	22.6	22.7	22.7	22.8
Kingcome	23.7	24.2	24.7	24.9	25.1	–
Knight, Call	23.2	23.9	24.2	24.3	24.4	24.5
Southern group:						
Bute to Howe	22.5	23.1	23.5	23.7	23.8	24.0
Exceptions:						
Princess Louisa, Sechelt, Indian	18.9	20.9	22.0	22.1	–	–

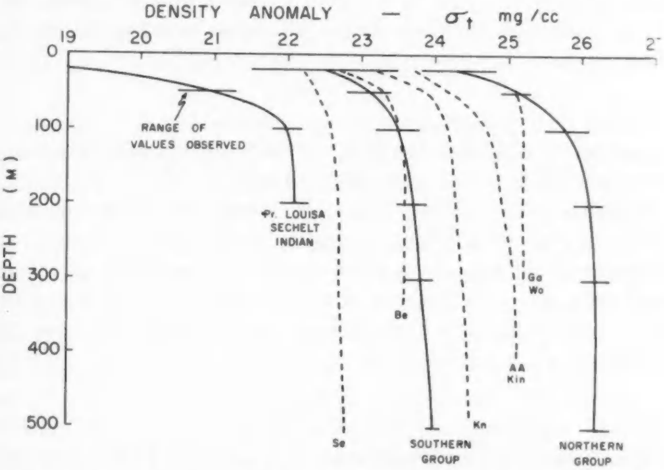

FIG. 27. Mean vertical profiles of σ_t in British Columbia mainland inlets.

than that in Belize. According to the best information available (Trites, 1955) the former inlet has more fresh water runoff than the latter and this is taken to be the reason for the difference in densities through the difference in salinities. Since the deep water as well as the shallow has a lesser density in Seymour it must be deduced that despite the conclusion (Tully, 1949, p. 10) that the chief mixing process in these estuaries is that of more saline deep water *upward* into the less

saline upper layer, yet there must be some downward diffusion of fresh water sufficient to maintain the observed difference between the two inlets which differ essentially only in fresh water supply. Even in low-runoff inlets, as long as the entrance is restricted the water is less saline than outside.

Generally the difference in σ_t between the 100-m level and the deepest water in any inlet is less than 0.5 mg/cc. In some inlets with shallow sills the difference in density between the sill depth and the deepest water is smaller than this, e.g. Observatory, Work, Gardner inside Sta. 8, Belize and Seymour; but in other cases this is not so, e.g. Alice, Draney. The reason for near homogeneity of the water below sill depth in one group but not in the other is not known, no feature which might suggest a reason common to one group but not to the other having been recognized. It is pointed out that the above statement is based on only one survey of some of the inlets mentioned and it might be suggested that the distinction observed between the two groups may not be a permanent feature. However, for the inlets for which more than one survey has been made it appears that although there may be long-term variations in the values of the temperature and salinity that determine the density, the character of the vertical distribution does not change radically. It is therefore assumed for the present that homogeneity or otherwise of the water below sill depth is a feature which requires explanation.

4.2 Stability

In the previous section it has been shown that the large changes of salinity and temperature with depth, particularly those of salinity, give rise to large changes in density with depth (Fig. 27). Hesselberg and Sverdrup (1915) showed that the vertical gradient of density determines the magnitude of the Archimedean restoring force on a water mass displaced from its natural depth. This in turn determines the amount of energy needed for the displacement of a water mass as the first step in a mixing process between different levels. Hesselberg (1918) introduced the term "stability" defined as:

$$E = \frac{1}{\rho} \times \frac{d\rho}{dz}$$

as a measure of the unwillingness of a water mass to undertake vertical motion. For the depths (z) of only a few hundred metres in the inlets the pressure effects on density (ρ) are small and the stability may be approximated by:

$$E = \frac{1}{\rho} \times \frac{d\sigma_t}{dz} \times 10^{-3}.$$

Using units of grams per cubic centimetre (g/cc) for density, milligrams per cubic centimetre (mg/cc) for σ_t, and metres for depth, the units of E are metres^{-1}. The numerical values of E found in nature range from high values of the order of 10^{-2} to low values of 10^{-8} which approach the limit of experimental error.

As the stability of the water column exerts an influence on the rate of vertical mixing, and also determines the period of internal waves, it may be regarded as a significant characteristic of the inlet waters. Values of the stability have been calculated for a number of inlets. Typically the highest values are found in the upper 10 m, and seasonal variations occur in the upper 20 m as a consequence chiefly of the seasonal variations of salinity. The range of values observed in a large-runoff inlet is indicated for Bute in Fig. 28 where stability is plotted on a logarithmic scale as $\log_{10}E$ against depth. The depth scale has been magnified between 100 and 20 m and further between 20 m and the surface to show in more detail the regions where the greatest values and variations occur. The values shown are for four cruises during the summer period of large runoff in 1957 and 1958 and a smooth line has been drawn through them. The dashed line shows the smoothed line drawn through values calculated for the winter period of 1957–58 for comparison. The highest values of $E = 10^{-3}$ to 10^{-2}m^{-1} occur in the halocline. Figure 30 compares in more detail the distribution of temperature, salinity and stability in the upper 20 m near the head of Bute.

It may be noted for comparison that values of stability in the coastal waters outside the inlets are of the order of 10^{-5} while values typical for open ocean areas are from 10^{-5} to 10^{-8} m^{-1}. The values in the surface layers of the large-runoff inlets are therefore 100 to 1000 times as great as open ocean values in the upper layers.

The seasonal variations below 50 m are not significant. It is pointed out that in the deeper water where the stability is least the accuracy of determination of E becomes small, being determined chiefly by the probable error in the determination of salinity. If it is assumed that individual salinity determinations are accurate to $\pm$ 0.02‰ this puts a limit of approximately $\pm 30 \times 10^{-8}$ m^{-1} on the calculated values of stability where the observed depth interval is 100 m.

It should be noted that the values of stability have been calculated from the values of density at observed depths. Except for special cases, such as those described by Fig. 30, the observations available are usually not more closely spaced than 2 m. Calculation of the stability from such data will give minimum values and there are indications that the gradient of the pycnocline is often greater than obtained by linear interpolation between observed depths. The highest value of stability recorded in the British Columbia inlets is 1.1×10^{-2} m^{-1} but it is possible that values as high as 2×10^{-2} m^{-1} occur.

It is seen from Fig. 28 that the seasonal variations in Bute are chiefly in the upper 10 to 20 m and it is apparent that in the winter the stability at Sta. 8, near the inlet head, does not decrease as much as elsewhere. The probable explanation is that the smaller runoff in the winter is the prime cause of the smaller stability and that a secondary cause is the mixing due to the stronger winds which occur in winter than summer. These effect greater mixing in the upper

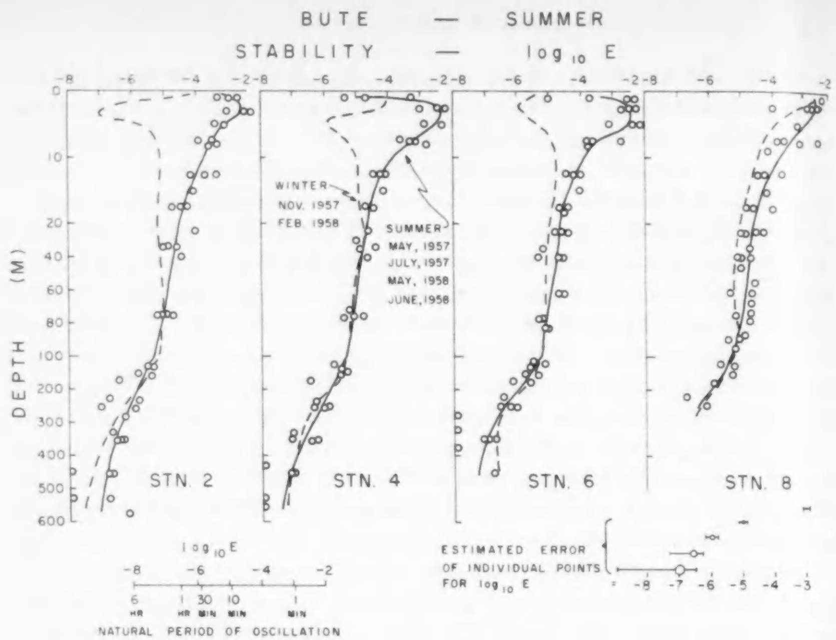

FIG. 28. Vertical profiles of the stability of the water at some stations in Bute Inlet, summer and winter.

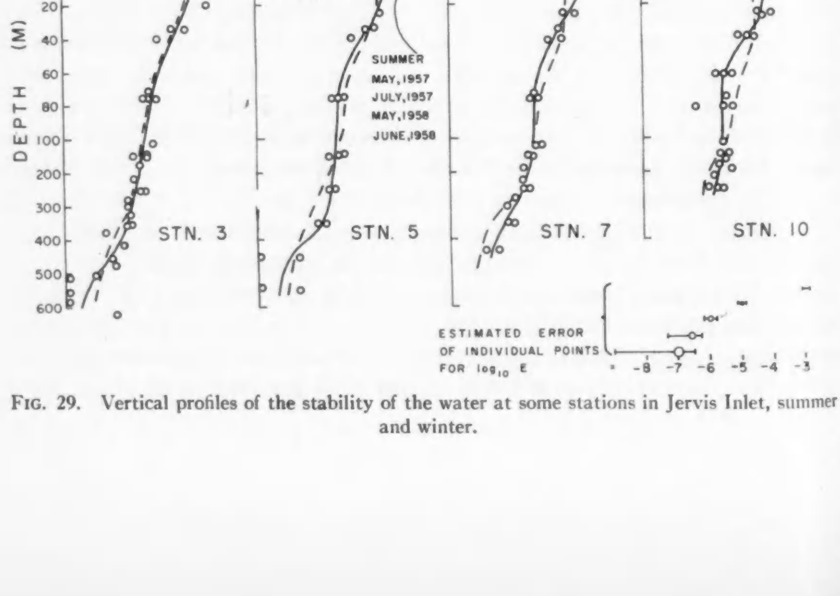

FIG. 29. Vertical profiles of the stability of the water at some stations in Jervis Inlet, summer and winter.

20 m particularly away from the stabilizing effect of the fresh water entering at the inlet head.

Figure 29 shows stability data for Jervis, a deep inlet with a smaller runoff than Bute. The difference in stability between winter and summer in the upper 10 m is less than in Bute but below 50 m there is no significant difference in the stability of the water in the two inlets.

On examining the values for stability in other inlets it is found that there is little difference between high- and low-runoff inlets below the surface layer of depth 20 to 30 m directly influenced by runoff. Values in some of the inlets with

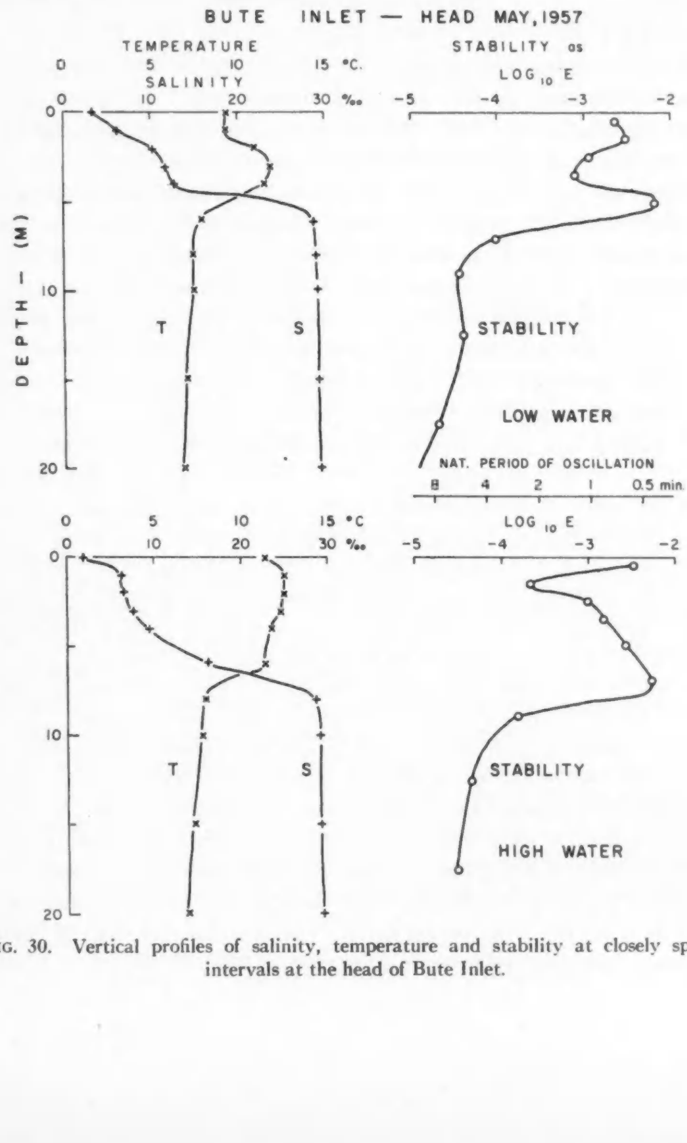

FIG. 30. Vertical profiles of salinity, temperature and stability at closely spaced intervals at the head of Bute Inlet.

deep basins such as Matheison–Kynoch are less than in Bute by a factor of 2 to 4 between 100 and 300 m but at greater depths the stability values in all the inlets are between $30 \times 10^{-8}\,m^{-1}$ and zero, i.e. not significantly different.

It can be shown that the period of vertical oscillation of a displaced water mass is determined chiefly by the stability of the water for moderate depths (Eckart, 1960). A few representative values for the period corresponding to different values of stability are shown in Fig. 28 for reference. In the surface layer the period is of the order of minutes, increasing to an hour or more in the deep water.

5. DISSOLVED OXYGEN

5.1 Main Features

It is much less easy to generalize on the distribution of dissolved oxygen in the inlet waters than on the salinity or temperature. In the surface layer, values are usually at or above saturation, while in the deeper water they are below saturation. Maxima and minima in the vertical direction are common but do not follow a regular pattern. One of the few broad statements that can be made is that very low values (e.g. below 2 ml/l) are uncommon, and no zero values have been observed in the mainland inlets during the studies now being reported except occasionally in water in contact with the bottom in small-runoff inlets. (Very low and zero values for dissolved oxygen have been recorded in Saanich Inlet on the east coast of Vancouver Island, e.g. Carter (1934); I.O.U.B.C. Data Reports No. 4 and 5 (1955); Herlinveaux (1962, in press).)

It does appear, however, that the large-runoff inlets show smaller ranges of dissolved oxygen content along their length and with depth, than do the small-runoff inlets. Some of the oxygen data are summarized in Fig. 31, 32, 33 and 34 for the surface and for a series of depths to 500 m. In these Figures the oxygen content is presented against relative position in the inlet, i.e. all inlets have been normalized to the same length with the head at the right and the mouth at the left. In considering the oxygen data, graphs of oxygen content against relative position along the inlet were first plotted for each depth. In contrast to similar salinity and temperature plots, the oxygen plots do not show any particularly consistent patterns which themselves suggest groupings of inlets. The oxygen content curves vary considerably from inlet to inlet and from cruise to cruise. As it is not practicable to present all the individual curves, the Figures simply show shaded areas within which the curves for the particular classification lie. The combinations of inlets here presented are based on the fresh water runoff characteristics of the inlets. They do show some similarities and contrasts but it is quite possible that some other significant grouping may exist at present unrecognized.

The data for the surface layer must be regarded as less reliable than the remainder as there are fewer actual surface observations and some of the values were obtained by extrapolation from subsurface values.

The large-runoff inlets included in Fig. 31(a) are Portland, Douglas, Gardner, Dean, Burke, Rivers, Knight, Bute and Toba. Figure 32(a) includes the same group except for Knight which appears to be anomalous at the greater depths. The small-runoff inlets included in Fig. 31(b) are Observatory, Work, Surf, Laredo, Mussel, Kynoch, Spiller, Roscoe, Draney, Smith, Belize, Seymour, Loughborough, Jervis and Sechelt. Fig. 32(b) includes the same group except for Belize and Seymour. The curves for these two inlets are shown separately in Fig. 31(c) and 32(c) for subsequent comment. Figures 33(a) and 34(a) show the values for all cruises on record in Bute, Fig. 33(b) and 34(b) for all in Knight, and Fig. 33(c) and 34(c) for all in Jervis.

In the shallow zone from the surface to 20 m, while there is in most cases a somewhat larger range of values in the small-runoff inlets as a group than in those with large runoff, the differences are not very marked. The difference is more marked between individual inlets such as Bute and Jervis (Fig. 33(a) and (c)).

At depths of 50 m and more there is a more consistent difference between the large- and small-runoff inlets as groups, the latter showing a greater range of values (e.g. Fig. 32). The spread of the shaded area toward the inlet head in the plots for these small-runoff inlets is chiefly because in some the oxygen content decreases toward the head whereas in others it increases. This behaviour is less evident in the large-runoff inlets. Seymour and Belize are shown separately in Fig. 31(c) and 32(c) to emphasize the difference between these neighbouring inlets which have a common outlet to the sea. Seymour would fall essentially into the small-runoff category. Belize is definitely a small-runoff inlet but appears to be extreme in oxygen distribution. The situation in these two inlets will be discussed later.

Of the remaining inlets, whose oxygen content distributions are shown in Fig. 32, Bute falls into the large-runoff group as might be expected. It is shown separately in Fig. 33(a) and 34(a) because so many more data are available (13 cruises from 1951 to 1959) than for the others listed in the large-runoff category (one or two cruises). Knight (seven cruises from 1952 to 1959, Fig. 33(b) and 34(b)) is certainly a large-runoff inlet but the oxygen values in it depart markedly from those in the remainder of this group, showing both a wider range at the lesser depths and generally larger values at the greater depths. Jervis, although physically a long and deep inlet, has a small runoff and its oxygen values fall within the areas on the plots in Fig. 31(b) and 32(b) for small-runoff inlets. It is shown separately in Fig. 33(c) and 34(c) to indicate two of the characteristics of this group, the marked change from head to mouth at the lesser depths and the consistency of the values, particularly at 200 m and below, from eight cruises from 1952 to 1959.

There is no evident geographical variation of oxygen values.

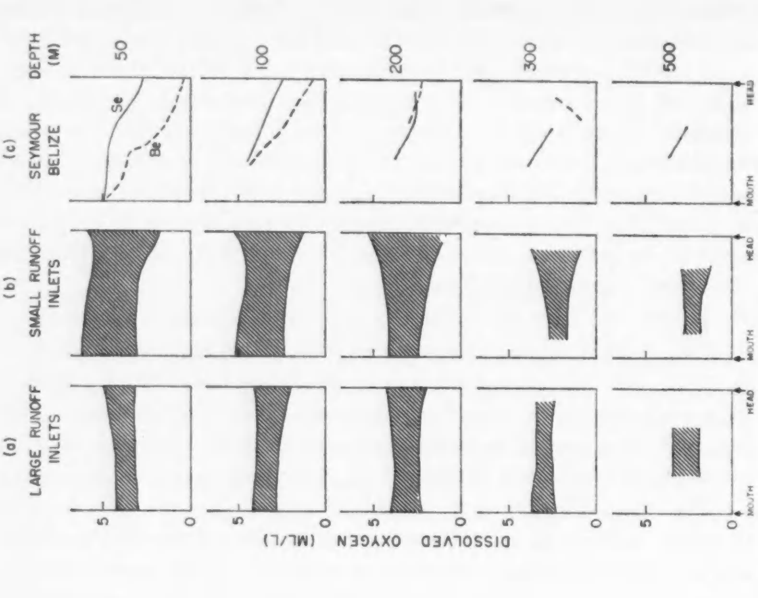

FIG. 32. Ranges of dissolved oxygen values at depths of 50 to 500 m along the length of large- and small-runoff inlets and of Seymour and Belize Inlets.

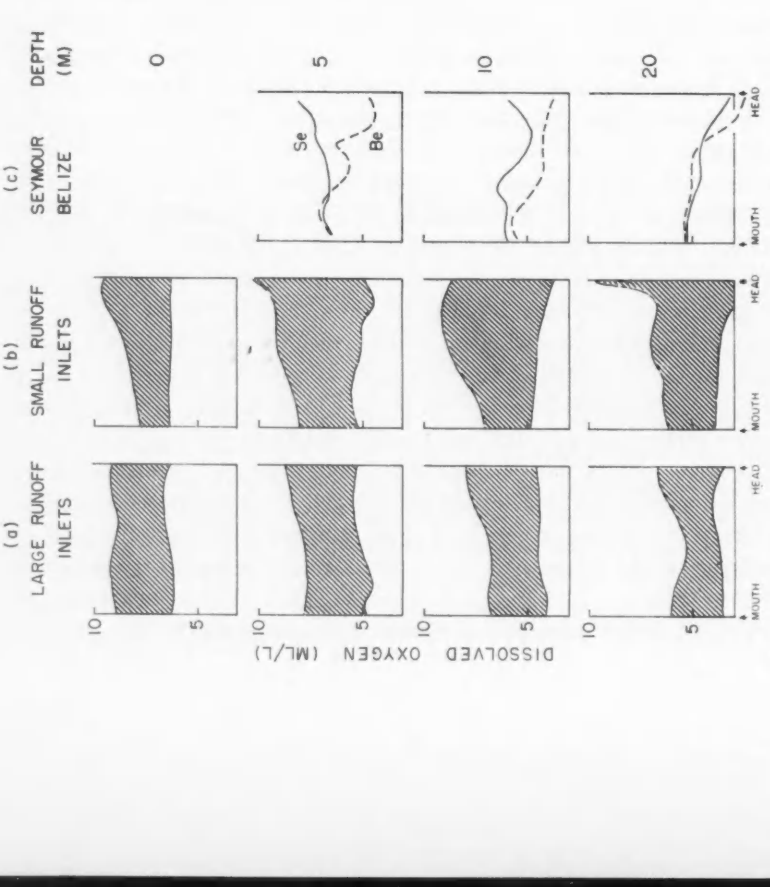

FIG. 31. Ranges of dissolved oxygen values at depths of 0 to 20 m along the length of large- and small-runoff inlets and of Seymour and Belize Inlets.

along the length of large- and small-runoff inlets and of Seymour and Belize Inlets.

along the length of large- and small-runoff inlets and of Seymour and Belize Inlets.

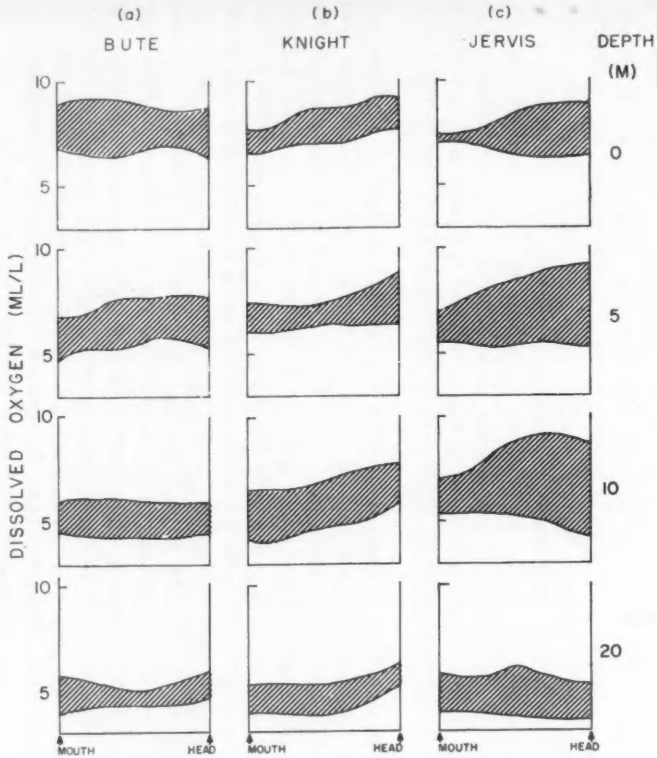

FIG. 33. Ranges of dissolved oxygen values at depths of 0 to 20 m for all cruises, 1951–60, in Bute Knight and Jervis Inlets.

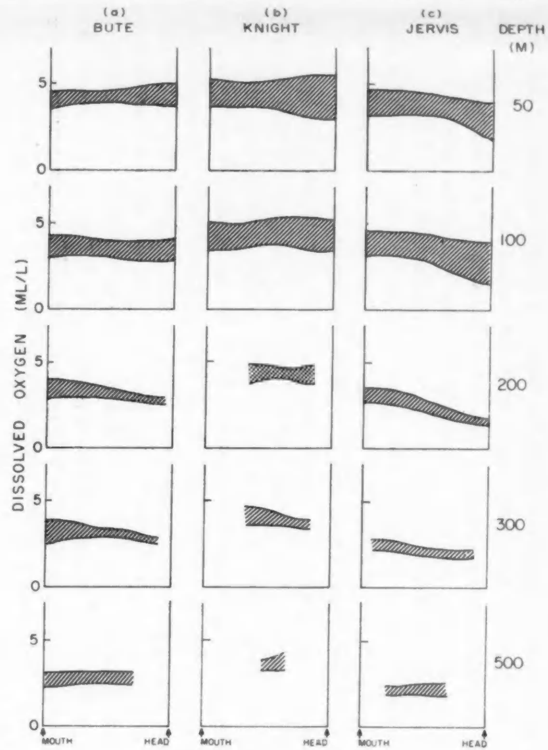

FIG. 34. Ranges of dissolved oxygen values at depths of 50 to 500 m for all cruises, 1951–60, in Bute, Knight and Jervis Inlets.

5.2 Oxygen Maxima

It was mentioned above that when the dissolved oxygen content of the water is plotted against depth at individual stations, maximum and/or minimum values are frequently observed in the vertical distribution. The existence of either a maximum or a minimum automatically implies the existence of one or more of the other and it is sometimes difficult to say which is the more significant. However, when one examines a considerable number of profiles for a particular inlet or type of inlet, these features may sometimes be present, sometimes absent, and therefore require description and, if possible, explanation.

Before continuing with the description of the oxygen distribution it will be well to define the term "saturation" or "saturation value" which will be used frequently. In this paper the term "saturation value" for dissolved oxygen is used to refer to the amount of oxygen which sea water is capable of holding in solution at the temperature and salinity of the water and at a pressure of one atmosphere, not at the *in situ* pressure. That is, it is implied that the normal source of dissolved oxygen is the atmosphere and that the oxygen dissolved in water at the surface will be in equilibrium with the atmosphere. Variations of actual barometric pressure from 76 cm of mercury are ignored. The nomogram of Tully (1949) based on the data of Whipple and Whipple was used to determine the solubility. The errors in the Whipple and Whipple data pointed out by Richards and Corwin (1956) are noted but are not significant in the present discussion. The oxygen content for saturation is markedly dependent upon the salinity and temperature of the water, decreasing as these two quantities increase. In the saline water below the halocline the saturation value is about 7 ml/l and in the less saline surface water it is up to 8 ml/l. In the plots of Fig. 35 and 36 which demonstrate some features to be discussed later, saturation values appropriate to the temperature and salinity of the surface water and to the temperature and salinity at 40 m depth are shown by arrows and the letter S. It should be noted that the saturation value generally increases slightly with depth in the low-salinity surface layer due to decrease in temperature and then in the halocline region drops by about 10% to the deeper value due to the rise in salinity.

Water which is homogeneous with respect to dissolved oxygen content over the full depth is never found in the inlets, though it may be found in some of the turbulent outside passages. The oxygen content is generally greatest at or near the surface and diminishes as depth increases. A single oxygen maximum at the surface is found either near the head of the large-runoff inlets or near the mouth (e.g. Fig. 9). In the former case, the value is very close to saturation for the temperature and salinity of the water, the salinity in these situations usually being small. This water is mainly river water, and as most of the rivers entering the inlets are turbulent it is assumed that the water attains its saturation value by solution from the atmosphere. On the other hand, maxima occurring near the mouth of an inlet usually have values greater than the saturation value and these are attributed to the oxygen production by phytoplankton which are usually present in these regions in the summer. Under these circumstances, an oxygen content of 110 to 130% of saturation is quite common (values up to 215%

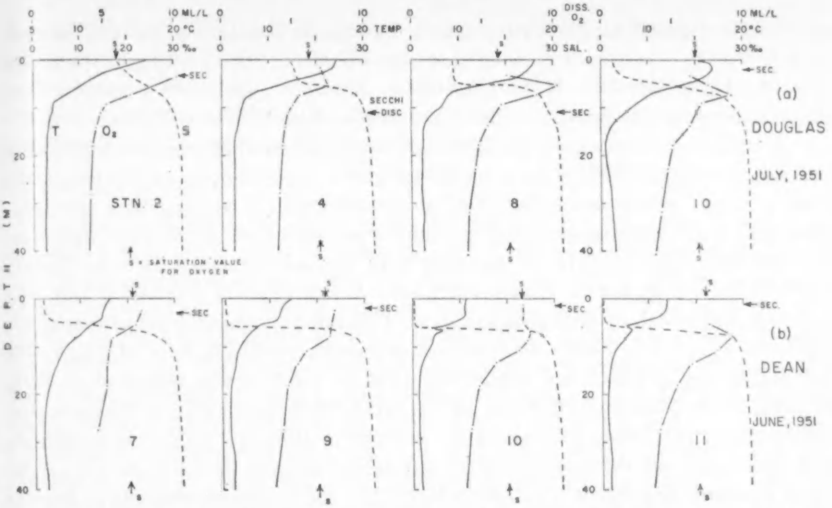

Fig. 35. Vertical profiles of salinity, temperature and dissolved oxygen in the upper 40 m in Douglas and Dean Channels.

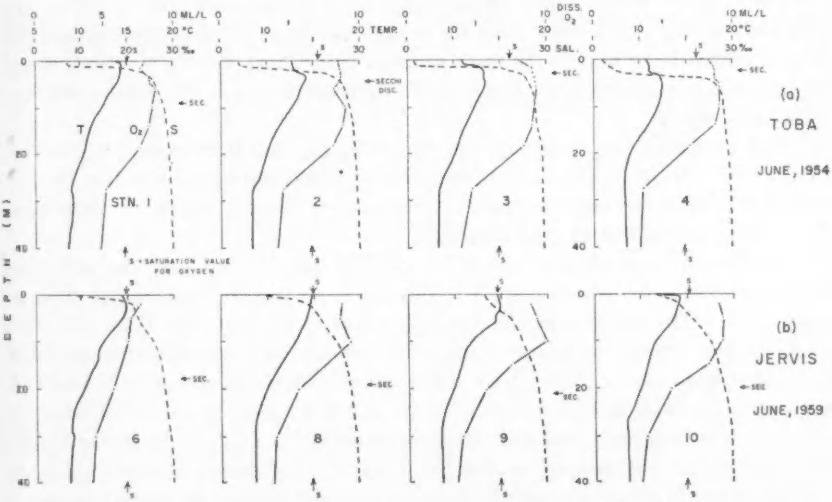

Fig. 36. Vertical profiles of salinity, temperature and dissolved oxygen in the upper 40 m in Toba and Jervis Inlets.

of saturation have been recorded in Saanich Inlet, I.O.U.B.C. Data Report No. 5). The actual value when highly supersaturated is not regarded as very significant, since experiments by the author have shown that it may be appreciably affected by the handling of the water sample. For instance, if a sample of such supersaturated water is shaken for about 15 seconds, the content may

decrease by several milliliters per liter. In standard sampling procedures such violent physical treatment is avoided, but it would not be surprising if the action of drawing samples into B.O.D. bottles might not cause some variation from the *in situ* value if the oxygen in its supersaturated state is so unstable.

Alternatively to a maximum at the surface, a maximum is common at 3 to 8 m depth and occasionally as deep as 20 m, the values being greater than 100% of saturation. More significant than the actual depth is the fact that the maximum generally appears to be at, or more frequently just below, the halocline. It sometimes appears only at the inlet head, sometimes along the inlet length. The feature is observed most frequently in large-runoff inlets (Fig. 35(a) and (b)) but does occur in those with small runoff. It is not an invariable feature of either type or of a particular inlet. For instance it was observed in Bute in 1951 and 1954 but not in any of the other years from 1951 to 1960; it was observed in Toba in 1951, 1954, 1955 and 1958 but not in 1952, 1956 and 1957; in Jervis it was observed in 1952, 1954, 1958 and 1959 but not in 1956 and 1957. It is difficult to be precise about the location of the maximum because of the finite size of the water sampling bottles (0.3 to 0.45 m long) and their minimum practical spacing (1 to 1.5 m) but it appears that when the halocline is well defined, the oxygen maximum lies just below it and is sharply defined.

The layer of water whose oxygen content is above saturation is then only a few metres thick. At other times the oxygen maximum is much broader and the supersaturated layer may be 10 to 20 m thick (Fig. 36(a) and (b)). Both sharp and broad maxima have been observed (in different years) in the same inlet, e.g. Toba and Jervis.

Strøm's curves for many of the fjords in the southern coast of Norway (Strøm, 1936) show this feature of a maximum in oxygen content in the vicinity of the halocline, although the observations were at too few depths to determine any of the detail of the pattern of distribution.

The broad maxima are relatively common phenomena and the existence of a maximum below the surface (by day) is common in waters other than in these inlets. The explanation for the sharp maximum (e.g. Fig. 35(a) and (b)) is not known. Since the oxygen content is above saturation one must attribute it to phytoplankton, and the sharp differentiation between the surface brackish layer where the saturation is close to 100% and the deeper saline water where it is much higher suggests that the phytoplankton are limited to the saline water. The most remarkable feature is that this oxygen maximum is generally sharpest and has its highest value near the head of an inlet where the surface water is most turbid and therefore transmits least light. The maximum diminishes to seaward along the inlet where the water becomes less turbid and transmits more light.

The above-described maxima are clear anomalies from a condition of 100% or less saturation in the upper 30 m. Less well marked oxygen maxima are observed at 30 to 50 m in some inlets such as Gardner, Burke, Draney, Seymour,

Bute and Jervis. The oxygen content at these depths is always less than 100% and it is often difficult to say whether the maximum or the concomitant minimum is the more significant. Somewhat arbitrarily it has been decided to focus attention upon the minima rather than the maxima in the deeper waters and these are described in the next section.

5.3 Oxygen Minima

In the cases discussed above where there is an oxygen maximum below the halocline, the surface value is smaller and constitutes one type of minimum. This is not regarded as particularly significant. Below the surface maximum, or the sub-halocline maximum, the oxygen content generally decreases to a value of 2.5 to 4 ml/l which is about 35 to 60% of the saturation value. In some cases the lowest value is at or near the inlet bottom, in others the deep water is nearly homogeneous in oxygen content (as well as in salinity and temperature) from a depth of 200 to 300 m to the bottom.

Most of the large-runoff inlets fall into one or other of the above two categories. Bute almost always has substantially homogeneous water from 300 to 650 m depth. Knight usually shows its minimum oxygen content near the bottom. In a minority of cases a slight mid-depth minimum appears. Such mid-depth minima, or sometimes just points of inflexion in the oxygen–depth curve, occur at the same depth as the bottom of the low temperature water forming the mid-depth temperature minimum layer (e.g. Fig. 37).

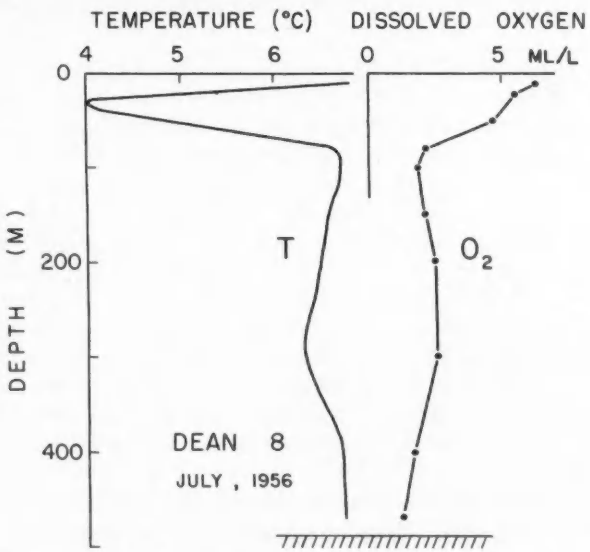

FIG. 37. Dissolved oxygen minimum below the temperature minimum at Sta. 8, Dean Channel.

Only a few inlets have water with an oxygen content of less than 1.5 ml/l. In Smith, in 1955 the oxygen content decreased to 1.2 ml/l at the bottom but only near the inlet head. Call has shown low oxygen values but the conditions in this inlet have varied from year to year. In Dean, in 1956 the oxygen content in the bottom water (161 m) at Sta. 10 near the inlet head was 0.5 ml/l. Between this station and the outer part of the inlet there is a sill with a maximum depth believed to be at 75 to 80 m and this presumably isolates the deeper water inside it. The measurements in 1951 did not extend as deep as those in 1956 but there was a marked decrease in oxygen content in the deeper water at Sta. 10 and 11.

Carter (1934) states that in Saanich Inlet, Princess Louisa Inlet, and the Narrows Inlet (of Sechelt) the "dissolved oxygen rapidly decreases to almost zero, [and] the density is greater than that of water at an equal depth in the Strait of Georgia". The observations in the present series do not entirely agree with this statement. The minimum oxygen content observed in Princess Louisa in 1952 was 1.7 ml/l at 140 m depth (the maximum depth in the inlet is 179 m). This was *greater* than that (1.5 ml/l) at the same depth in Jervis just outside the sill separating the two inlets. Furthermore, the oxygen content at lesser depths in Princess Louisa was considerably greater than that in Jervis, and not markedly different from values in the Strait of Georgia. In June 1960 the oxygen content to within 3 m from the bottom of the two basins of Princess Louisa was 3.3 ml/l compared to only 1.4 ml/l at the same depth in Jervis outside. Observations in the Narrows Inlet of Sechelt in 1957 did show a content of 0.15 ml/l at 1 m from the bottom, and the zero values in the deep water in Saanich have been mentioned previously.

In respect to the second part of Carter's statement above, the present observations disagree. As described previously it has been found that the density in basins such as Princess Louisa is *less* than that outside.

The most noticeable oxygen minima are those in the Belize–Seymour group and in Sechelt. In Belize there is an oxygen minimum layer which is most pronounced at the inlet head where the minimum value observed is 0.4 ml/l at 75 m. The distribution is shown in Fig 38(a) as a series of profiles and in Fig. 38(b) as a longitudinal section. The 8 miles at the head of Belize is an anomalous region. There appears to be very little runoff into it and the surface salinity is higher at the head than at Sta. 5 where Alison Sound joins Belize and presumably brings in the main fresh water flow. The Secchi-disc reading at the head of Belize is greater (up to 8 m) than further along the inlet (5 m) and the water is of an unusual yellowish-green colour. Thompson and Barkey (1938) observed a similar oxygen distribution at the head of Belize, with a minimum of 0.2 ml/l at 75 m depth.

In Seymour there is a less pronounced oxygen minimum of 2.5 ml/l between 150 and 180 m (Fig. 10). Again the observations of Thompson and Barkey showed a similar situation with a minimum of the same value at 150 to 200 m. Seymour differs from Belize in that there is an appreciable river runoff at its

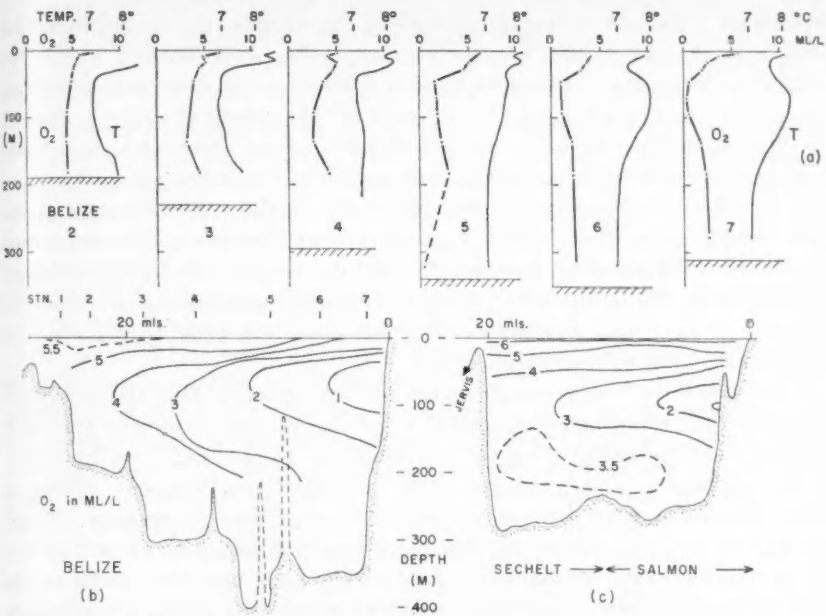

FIG. 38. (a). Vertical profiles of temperature and dissolved oxygen in Belize Inlet.
(b and c). Longitudinal sections of dissolved oxygen in Belize and Sechelt Inlets showing mid-depth minimum.

head although the water is apparently not of glacial origin (Secchi-disc readings were as great as 5.8 m in 1951).

A very similar distribution to that in Belize was observed in Sechelt in 1957 with a minimum layer at about 100 m depth both in Sechelt Inlet proper (Fig. 38(c)) and in the connecting Salmon Inlet. The oxygen minimum was more pronounced (1.3 ml/l) in Salmon than in Sechelt (1.4 ml/l).

Thompson and Barkey (1938) suggested that the mid-depth minimum was due to a flow of water from a shallower section of an inlet, or from a side arm, where it had been in contact with a reducing bottom. Although this seems to be a logical explanation, the details of a circulation to maintain this distribution are not clear. The character of the low oxygen content tongue suggests flow away from the head of the inlet toward the mouth and this requires a supply of mid-depth water to the head. The only likely source of this mid-depth water is by sinking of shallower water and it is considered that the head of the inlet is generally the least likely place for this to occur because of the relatively low density of the water above the oxygen minimum compared with elsewhere in the inlet. The real questions are why the oxygen minimum should be at mid-depth and not at the bottom in these inlets, and why this distribution occurs in only a

few inlets. The area of bottom with which the water at the oxygen minimum level is in contact is only a small fraction of the whole bottom area. One suggestion offered here is that reduction takes place over the whole bottom volume for some years until eventually an intrusion of saline water of sufficient density to displace the bottom water upward occurs. At the same time the greater tidal currents near the mouth might cause greater mixing and more rapid dissipation of the low-oxygen water than at the head. In this case the tongue at the head would represent a vestigial remnant of a layer which earlier spread over most of the inlet bottom. However, the fact that almost identical distributions were found in 1951 as in 1937 in Belize and Seymour suggests that the observed distribution is a steady-state one and that some continuing process for its maintenance must be assumed to exist.

An alternative suggestion, favoured by the author, is that the mid-depth minimum is a consequence of several simultaneous and continuous processes. Sinking organic material along the full length of the inlet may use up oxygen in the subsurface water. At the same time small but frequent inflows of oxygenated saline water from outside may take place over the entrance sill and spread over the inlet bottom, so that the oxygen-deficient water is held at mid depth. In addition, the maximum tidal currents are near the mouth of the inlet and therefore vertical mixing is probably greatest there, tending to eliminate the oxygen minimum and leaving it more conspicuous at the inlet head. The inlets in which the mid-depth minimum occurs are ones with small fresh water runoff and consequently the induced estuarine circulation is not sufficient to replace the oxygen deficient layer entirely, as it does in the large-runoff inlets. Another contributing factor may be that the relatively low stability in the upper layers in these inlets may aid vertical mixing to reduce the density of the deep waters. This would mean that water from outside at sill depth could be denser than even the deepest water in the inlet basin and hence it could sink along the bottom after entry.

It is suggested that a comparison of the bottom sediments near the inlet head at the oxygen minimum level in Belize and Sechelt with other inlets not showing the minimum might be profitable, and a study of the mid-depth oxygen minimum might yield useful information on the circulation in the inlets.

One other locality in which very low oxygen values were found was in Minette Bay at the head of Douglas. It is a basin some 3 miles long by $\frac{3}{4}$ mile wide, supplied by small streams. The maximum depth measured was 38 m and Minette is connected to Douglas by a shallow channel only a metre or so deep at low water. The salinity and temperature of the water in Minette in 1951 corresponded to that at the head of Douglas but the oxygen content was less. It decreased from 6.9 ml/l at 3 m to 0.55 ml/l at 25 m, compared to 6.9 ml/l and 4.9 ml/l in Douglas at the same depths.

6. OPTICAL TURBIDITY

6.1 Optical Turbidity of the Surface Waters

A conspicuous visual feature of the inlet waters is the colour and the turbidity or otherwise of the upper layer. In the inlets which receive runoff from glacial rivers, the surface water at the head during the summer is milky white in appearance and of high turbidity. It changes through a milky green along the inlet to green with a lower turbidity near the mouth. In contrast, in the inlets which do not receive much runoff the water is green and of more or less uniform and lower turbidity along the whole length of the inlet. (In the inner reach of Belize in 1951 the water was of an unusual yellowish colour.)

In Table XI are listed values of the Secchi-disc depths in the majority of the inlets during the runoff period, May to September. For some inlets visited a number of times (e.g. Bute, Knight) the range of values observed is quoted. The first group of inlets includes those for which the large rivers are definitely glacial in origin, those of the second group receive runoff from large rivers to which the glacial contribution is believed to be small or negligible, while the third group includes those having relatively little runoff at all.

In Fig. 39 are shown values of Secchi-disc depths for some typical examples of the three groups in Table XI. For Gardner and Knight the small values toward the head are also shown on an enlarged scale. For Jervis values for 2 years show the differences observed in inlets with small rivers, while Kynoch and Work are examples of very-low-runoff inlets.

Vancouver (1798, Vol. I, pp. 304, 305, 308, etc.) was probably the first to draw attention to the white appearance of the water at the heads of some of the inlets, e.g. Howe, Bute, Knight, Kingcome, but not Jervis. On first observing it in Howe he "attributed [it] to the melting of the snow, and its water passing rapidly over a chalky surface, which appeared probable by the white aspect of some of the chasms that seemed formerly to have been the course of water falls, but were now become dry." Later he noted that in Jervis "The cataracts here rushed from the rugged snowy mountains in greater number, and with more impetuosity than in Howe's sound; yet the colour of the water was not changed, though in some of the gullies there was the same chalky aspect. Hence it is probable, that the white appearance of the water in Howe's sound, may arise from a cause more remote, and which we had no opportunity of discovering." Vancouver's observations and deduction were acute and it is probably only because his instructions forbade him from making excursions up the rivers that he was prevented from determining the "cause more remote". This is the grinding of rock against rock in the motion of the glaciers on the mountains which produces a finely divided "rock flour" which is brought down by the rivers. Much of this remains in suspension for a considerable time and is carried along the inlet by the outflowing surface layer. During the winter months the water in the greater part of the length of Bute is relatively clear and greenish in colour. Then in the spring when the runoff starts (usually in May) a sharp front of silty water moves

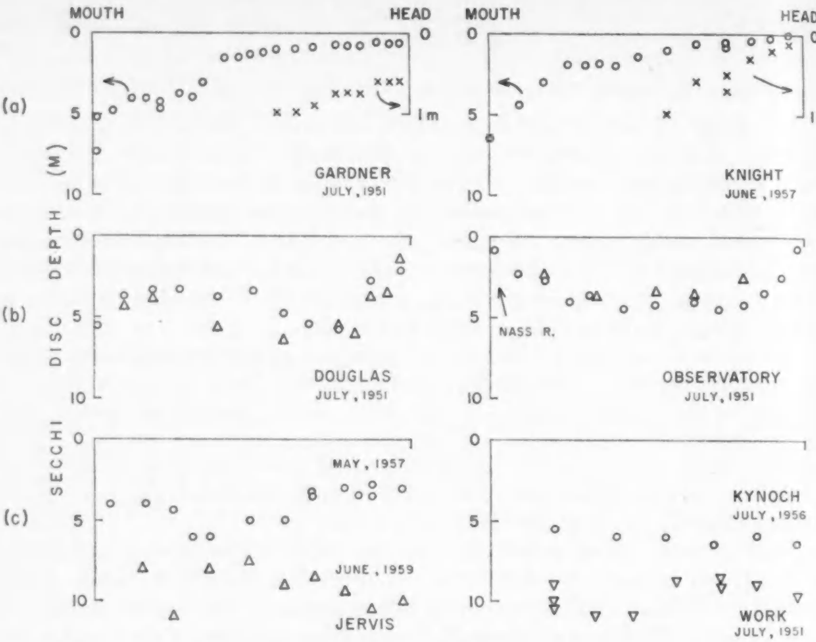

FIG. 39. Longitudinal profiles of Secchi-disc depths in large and small runoff inlets.

down inlet in a few days and for the rest of the spring, summer and fall the water has its characteristic silty appearance. Occasional observations while skin diving in these inlets have shown that near the inlet head the lower boundary of the silty surface water is quite sharp and appears to be close to the halocline. A very marked increase in the clarity of the water is evident when one swims down through the halocline–thermocline into the more saline water below. When the silty layer is only 2 to 3 m thick, the propeller of a ship will often bring the clear water to the surface and the track of a vessel moving near an inlet head may remain visible for some time. In such a region, when a Secchi disc or a bucket is lowered through the silty layer and then pulled smartly back to the surface it will bring with it a "bubble" of the clearer saline water.

The illumination in the clear water below the silty layer is much greater than would be calculated from the loss of light in the upper layer on the basis of an absorption coefficient k obtained from the Secchi-disc reading D using the formula $k = 1.7/D$ determined by Poole and Atkins (1929). For example, for a typical value of $D = 0.3$ m, the formula yields $k = 5.7$, and for a silty zone thickness of 4 m the illumination below this zone would be reduced to about 10^{-10} of that at the surface. That is, for full sunlight at the surface (about 10^4 foot-candles) the illumination below the silty water would then apparently be reduced to about 10^{-6} f-c, or about one-hundredth of the illumination on a clear

TABLE XI. Secchi-disc depths in British Columbia mainland inlets (May–September).

Inlets	Mouth	Middle	Head
Inlets with large river of glacial origin:			
Portland Canal	3.5	2.5	0.3
Portland Inlet	2.5	...	1.0*
Gardner	6	1.5	0.6
Dean	3–6	1.5–3.5	1.0
Burke	2.5–6	5–5.5	0.4
Rivers	4.5	3.5	1
Kingcome	1.5–3	...	0.5
Knight	4–8	1.5–4	0.1–0.5
Bute	3–8	1.5–3	0.1–0.3
Toba	4–6	1–3	0.3–1
Howe	3	1.5	0.5
Inlets with large rivers having small glacial contribution:			
Observatory–Alice	1*	4	3
Douglas	4	5.5	2
Inlets with small rivers or streams only:			
Work	10	8.5	9.5
Surf	6	6	6
Laredo	7.5	6.5	7.5
Sheep–Mussel	3	6	5.5
Matheison–Kynoch	5.5	6.5	6.5
Spiller	5	7	5
Roscoe	7	7.5	6
Cascade	6	8	7
Draney	5	5	...
Smith	3.5	4.5	4.5
Belize	4.5	5.5	7
Seymour	5	8	5
Call	3.5–9	...	4.5–8
Loughborough	3–6	4–8	3–10
Pendrell	6–9	7–10	7–9
Jervis	4–6	6–10	3–10
Sechelt	6	5.5	3.5
Indian	4	7	6.5

*The Nass River enters at the junction of Portland Inlet (head) and Observatory Inlet (mouth).

starlit night. Direct observation indicates that the illumination is much greater than this. It might be inferred that the formula of Poole and Atkins, which was determined for Secchi-disc readings of 10 to 50 m, gives too large a value for the absorption coefficient at the very small Secchi-disc readings observed in the inlets. However, measurements of the turbidity described in the next section yield even greater values than 5.7 for the scattering coefficient τ which is related to k. The probable explanation for this apparent paradox is that the quantities k in the Poole and Atkins formula or τ in the next section properly describe the rate of loss of light from a narrow parallel beam of light by scattering out of the beam

as well as by true absorption which implies conversion to some other form of energy. This is not the case at the head of an inlet where the surface layer is very extensive in relation to its thickness and light is passing through all parts of it. Then at any small area at the lower surface of the silty layer the part of the light which has been lost by scattering from the direct beam to that area is to some extent replaced by light scattered from neighbouring beams. The illumination is therefore not reduced as much as it would be if true absorbtion occurred to the extent of the k or τ values calculated.

The decrease of Secchi-disc readings toward the mouth of some inlets can often be attributed to the effect of phytoplankton blooms which are common in the spring and summer.

The relatively low turbidity in Burke seaward of Sta. 8 supports the suggestion made on the basis of surface salinity that a large proportion of the runoff into the North and South Bentinck Arms (head of Burke) moves out through the connecting Labouchere Channel into Dean, rather than along the seaward reaches of Burke.

6.2 Optical Turbidity of the Subsurface Waters

Measurements have been made of the turbidity of both surface and deeper water in some of the southern inlets and the results have been described previously (Pickard and Giovando, 1960). As some of the observations and the conclusions from them are relevant to the present description of inlet water properties they are summarized here.

The measurements were made on board ship by means of a commercial light-scattering microphotometer on samples obtained with reversing water bottles internally coated with ceresin wax to reduce contamination of the water sample by particulate material from the metal bottles. A light-scattering method was used, rather than a transmission method, in order to see how much information could be obtained on the nature of the particulate material in the water, as well as on the turbidity or light attenuation itself. One object in making the measurements was to investigate the possibility of using the turbidity as a tracer of deep water movements.

Polar diagrams of the scattered light show predominantly forward scattering with a broad minimum from 100 to 120° from the forward direction of the light beam through the sample. There is little difference in shape of the polar diagram with turbidity or wavelength of light, confirming that the particle size is generally large compared to the wavelength of light. Polarization measurements indicate that the material is optically anisotropic. These results suggest that the material is largely that brought down by the rivers from glacial abrasion of the granitic rocks in the region, the "rock flour" referred to above.

A number of typical samples have been filtered through 0.5-μ "Millipore" filters. The water passing through these filters has a very low turbidity, not much greater than that of distilled water, indicating that there are very few particles smaller than 0.5 μ diameter in the inlet waters. The particles retained by the filters appear to be chiefly minerogenic in character with a size range from 0.5 to 50 μ.

In Table XII are given some typical values of turbidity of the water and corresponding particle size. The turbidity τ is defined by the usual equation:

$$I = I_0 \times e^{-\tau L}$$

where I_0 and I are respectively the incident and emergent intensities of a beam of parallel light passing through a layer of thickness L metres of water of turbidity τ expressed in reciprocal metres (m^{-1}). Measurements were made with green light (5460 A) for all samples and with other wavelengths for some.

TABLE XII. Mean values of optical turbidity in waters of Jervis and Bute Inlets for winter and summer, and of size of particulate material in Bute.

Depth (m)	Winter		Summer	
	Jervis Inlet optical turbidity (m^{-1})			
	Outer basin	Inner basin	Outer basin	Inner basin
0–50	0.14	0.9	2	11
50–250	0.1	0.2	0.6–0.9	2
250–600	0.1	–	1–1.3	–
Bottom	0.15	0.45	1.3	3
	Bute Inlet optical turbidity (m^{-1})			
	Mouth	Head	Mouth	Head
0–50	0.2	0.7	7	18
100–550	0.10	0.12	0.7	0.7–1
550–650	0.16	0.4	0.9	1.5
	Bute Inlet particle size (microns)			
Mean:	7	10.5	8	17
Range:	0.5–15		0.8–49	

Volume concentrations of particulate material range up to 105 ppm and weight concentrations to 285 ppm. The material is 90% minerogenic in winter and 99% so in summer.

The major features of the turbidity distributions are (a) the difference between large- and small-runoff inlets, (b) differences between values at different depths in a vertical column at any point, (c) seasonal variations in both types of inlet.

Bute and Knight both show larger values of turbidity than Loughborough and Jervis at similar depths. This is in accord with the observation that the particulate material is chiefly glacial rock flour. The largest turbidity values are found at the heads of the inlets in the low-salinity surface layer. The values in the main body of the water in an inlet between the surface layer and a layer near the bottom are generally fairly uniform. Values in a layer 50 to 100 m thick in contact with the bottom are often higher than in the main body above. The seasonal variation in turbidity values is evident in both large- and small-runoff inlets.

From the above findings it is concluded that the rivers flowing into the inlets are the chief source of particulate material in the inlet waters. The silt

introduced by the rivers is carried along in the surface layer which acts as an extended source of particles which shower down into the main body of water. For this reason the turbidity has severe limitations as a tracer of deep water influx from outside.

The increase of turbidity near the bottom is interesting. In describing a similar distribution in the shallow Gullmar Fjord, Jerlov (1953) attributes it to the stirring action of tidal currents. However, such data as are available for the deeper British Columbia inlets (Pickard and Rodgers, 1959) suggest that the bottom currents in these flow at only a few centimetres per second and are unlikely to be sufficient to maintain material in suspension in a layer of 50 to 100 m depth. An alternative hypothesis favoured is that the increase in turbidity near the bottom is a consequence of mud slumps on the slopes at the head of an inlet starting turbidity currents which flow along the inlet bottom. There are several pieces of evidence to support this hypothesis. For instance, in Bute the high-turbidity bottom layer stops abruptly at the sill. It is less common in the outside passages where tidal currents may be expected to be greater. In Jervis, the increase near the bottom occurs only inside the inner sill where tidal currents should be least. Another point is that in many inlets there is an area of flat bottom in the deepest part of the basin inside the sill (ref. Sub-sect. 2.1, page 914). These flat areas are probably the result of settling out of material from turbidity currents trapped by the sill. There is no other source of the material in these regions than the mud banks deposited by the rivers at the inlet head. A third point is that the water in Bute and other inlets, below sill depth, is generally nearly homogeneous despite the evidence of inflow of deep water from outside from time to time. This homogeneity may be attributed to the stirring action of the turbidity currents. The fact that the increase of turbidity near the bottom was evident in each survey, combined with calculations of settling rate, suggests that these turbidity currents occur quite frequently.

From the difference between winter and summer concentrations of particulate material, it is possible to calculate an average rate of deposition of sediment of 35 cm per 1000 years. Near river mouths the value may be as high as 600 cm per 1000 years.

7. WIND AND WAVES

7.1 Wind and Surface Waves

The wind can be expected to affect oceanographic conditions in the inlets in several ways. The frictional stress on the surface influences the motion of the surface layer and so may increase or decrease the mean surface-layer flow along an inlet. In addition, the waves generated by the wind will cause mixing in the surface layer tending to make it homogeneous. During the cruises therefore, observations of wind velocity were made at each station by means of an anemometer at 4 to 10 m above sea level, and the significant wave height was estimated visually at the same time. In Table XIII are presented these correlated wind-wave data for the cruises from 1951 and 1959 all lumped together. The totals

TABLE XIII. Frequency of occurrence of wind speeds and wave heights in British Columbia inlets for summer months from 1951 to 1959 inclusive (percentage of 1653 observations).

Wave height		Wind speed					Wave-height frequency totals
Beaufort scale	Feet	Beaufort force: Knots:	0 and 1 0–3	2 and 3 4–12	4 and 5 13–24	6 25+	
			%	%	%	%	%
0	Calm		27	4	0	0	31
1	0 to 1		14	28	5	0	47
2	1 to 3		1	5	14	½	20½
3	3 to 5		0	0	1	½	1½
Wind speed frequency totals:			42	37	20	1	100

have been normalized to show the percentage frequency of occurrence of the stated ranges of wind speed and of wave height and of the combinations thereof. The data for individual cruises vary considerably from these means but there does not seem to be any significant pattern and therefore the details are not presented. 95% of the observations were made during daytime between about 0600 and 2000 hours.

It is seen that for about 80% of the time during the summer the wind speed is not over 12 knots nor the wave height greater than 3 feet. It may be added that on no occasion during summer cruises have oceanographic observations been prevented by wind or waves, although there have been occasions when the drift of the ship due to the wind has caused some anxiety for the safety of equipment over the side when operating in these narrow inlets where the depth often changes considerably in a short distance. The waves referred to in Table XIII are all short-period (2- to 4-second) wind waves or "sea" generated locally in the inlet and progressing along the inlet, i.e. with their crests approximately at right angles to the longitudinal axis of the inlet. At no time is there any indication of "swell" or long-period waves penetrating from the ocean. For this reason, shipboard operations are not hindered by rolling of the ship, except on rare occasions at anchor station when, due to the opposing action of wind and current, the ship lies across-inlet and therefore parallel to the waves. The stability of even a small vessel permits operations and the use of instruments which would be quite impossible in less protected waters. This is an important factor to bear in mind when considering the practicability of equipment for oceanographic work in these regions.

The wind direction in the inlets is almost invariably along the length of the inlet, following the bends, and most often directed *up*-inlet during the summer. The along-inlet direction of the wind is a consequence of the channelling action of the steep sides of most of the inlets. In addition the wind speed is significantly affected by the inlet width, and an increase of wind speed is often experienced in the narrower, steeper-sided reaches. This is probably of some consequence since in a narrow part of the inlet the speed of the surface flow will also increase and there is likely to be increased turbulence. This, with the increased wave

action due to the stronger wind, promotes mixing in the upper layer and therefore such narrow portions of an inlet may be regions where much of the mixing takes place. The wind speed is generally greatest near the mouths of the inlets and least near the head. The up-inlet wind is usually diurnal in character, springing up during the morning and dying away in the late evening. Ship operations are therefore often facilitated by scheduling work in the seaward reaches of an inlet for the early morning and working up to the head in the afternoon.

7.2 Internal Waves

During the first cruise in 1951 it was observed that the depth of isotherms at a fixed station showed distinct variations with time. In the upper layers (5 to 20 m) these oscillations had periods of 1 to 3 minutes, while at mid-depth (50 to 100 m) the period appeared to be several hours. These observations were verified and extended in subsequent cruises and there is no doubt that in the upper layer the vertical oscillations are the result of progressive internal waves occurring in the pycnocline associated with the halocline (Pickard, 1954). The precise character of the mid-depth oscillations is not yet determined but for convenience both these and the shallow ones are referred to as internal waves. The observations in subsequent years have confirmed that both the shallow and the deeper internal waves are common features in some inlets.

7.21 Shallow internal waves

These were observed on a number of occasions in Knight particularly, and measurements of their amplitude and apparent period were made with an electrical resistance thermometer using a thermistor bead on the end of a cable marked in metres. With this device the depth of an isotherm in the thermocline was followed and recorded at short intervals to reveal the characteristics of the shallow internal waves. This was done on a number of occasions when the sea state was slight and the ship so steady that variations in the length of cable out could be taken as variations in depth of the selected isotherms. Sample records of these internal waves are shown in Fig. 40 together with a record showing typical "quiet" conditions. On the records obtained, the intervals between successive crests range from 1 to 5 minutes. Although it is tempting to identify these intervals with the periods of the waves, it must be pointed out that when the waves occur between the surface low-salinity layer and the deeper more saline water both of these layers are generally in motion, often in opposite directions as a result of estuarine and tidal currents (Pickard and Rodgers, 1959). Since the observations were usually made from an anchored ship, the observed time intervals between wave crests might differ from the true period of vertical oscillation of a water mass. When current measurements were available at or close to the time of the internal wave oscillations it was estimated that the observed time intervals probably did not differ from the true period by more than a factor of $\frac{1}{2}$ to 2. The wavelengths of the waves were estimated from associated surface manifestations ("ruffled bands" described below), either in relation to ship's

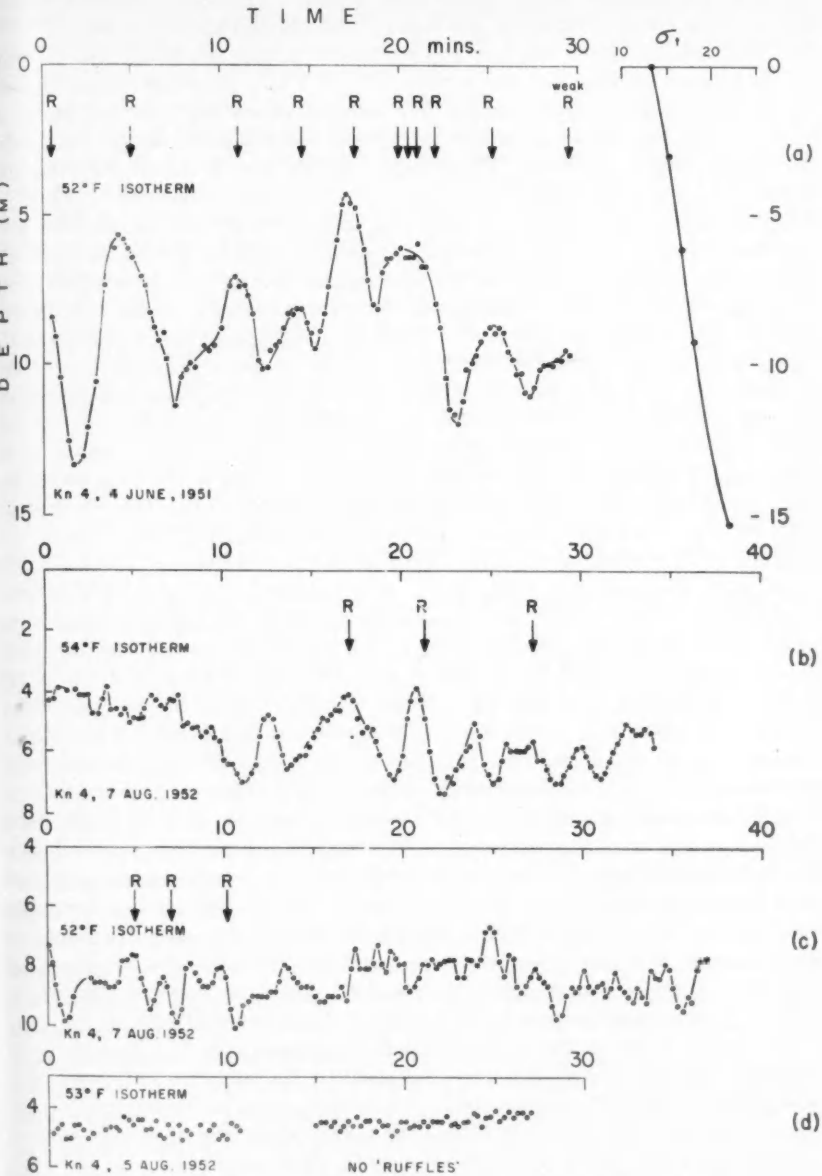

FIG. 40. Time–depth plots for selected isotherms in Knight Inlet to show the presence (a), (b), (c) or absence (d) of shallow internal waves.

length or by time and ship's speed when sailing. They were between 50 and 200 m. The speed of travel in still water would then be about 1 m/sec.

The appearance of the sea surface accompanying these shallow internal waves is quite striking and merits description. On a calm day, when the sea surface is otherwise mirror smooth, the internal waves are accompanied by a series of narrow (10 to 30 m wide) "ruffled" bands on the water with wider smooth patches in between. These ruffled bands stretch across the inlet and usually progress with a speed of up to 1 m/sec relative to the shore. They are generally located just behind the advancing internal wave crest as observed with the thermometer. The word "ruffled" is used to describe the bands since the surface asperities do not consist of series of ripples such as those generated by the wind but of randomly distributed peaked protuberances of some 5 to 10 cm height. The passage of the ruffled band is accompanied by a characteristic hissing noise similar to that caused by rain falling on water. It appears to be due to water from the peaks of the ruffles breaking off and falling back into the water. When these ruffles have been seen in calm water it becomes quite easy to pick them out even when superimposed on wind waves up to 3 feet height. The explanation suggested for these ruffles is that they indicate the location of the region of convergence behind the crest of the moving wave (e.g. Sverdrup *et al.*, 1942, p. 588). In many cases in the inlets, the amplitude of the waves in the halocline is comparable to the mean depth of the halocline and consequently the convergence is very strong. The motion of the water in the upper layer is often made evident by the motion of the ship relative to the hydrographic wire if the latter extends an appreciable distance into the relatively stationary deeper water. If the ship happens to be lying parallel to the wave crests, the wire will alternately trend under the ship and then away from the ship as the latter is moved back and forth by the surface flows associated with the internal waves. The presence of these internal waves may be indicated by an apparently anomalously large hysteresis at the thermocline in bathythermograms taken at the time. This evidence often reveals the presence of internal waves even if their amplitude is not large enough to make the ruffled band effect conspicuous. Some idea of the amplitude of the internal waves may be obtained by lowering a bathythermograph through a ruffled band and then raising it through the succeeding smooth patch, or vice versa. There is little point in attempting to make a conventional bottle cast in the upper 50 m or so when such internal waves are evident, and as the hydrographic wire is likely to be carried under the ship it is prudent to suspend operations with overside equipment in the presence of such waves.

It should be made clear that the surface phenomenon just described and interpreted differs in detail from that described by Ewing (1950), although both are associated with the convergence in the surface layer accompanying internal waves. The essential difference is that the phenomenon described here consists of narrow bands of ruffles on otherwise smooth water, whereas Ewing describes narrow slicks or smooth bands on otherwise wind-rippled water. Ewing ascribes the slicks to the ripple-smoothing action associated with surface contaminants being concentrated by the water convergence, whereas the effect observed in the

British Columbia inlets is ascribed here to a purely mechanical process in the intensely convergent water flow. The slick patterns described by Ewing have been observed frequently by the author in local coastal waters, for instance in English Bay near Vancouver, but rarely in the inlets.

The shallow internal waves have been observed most frequently in the vicinity of the sill (between Sta. 3 and 4) in Knight. Current measurements in this region (Pickard and Rodgers, 1959) have shown that at times a strong shear develops between the low-salinity surface layer flowing seaward and the deeper more saline water, particularly during the first part of the flood tide. The waves are sometimes observed at other times than this however. They are not often observed more than about 10 miles from the sill in Knight, presumably having dissipated their energy within this distance. Similar waves are sometimes observed in Bute near Sta. 2 and are probably associated with the strong currents flowing in through Arran Rapids where water from the northern passages enters the inlet. Surface ruffles have also been observed by the author in Burke and in Observatory. Comments in the British Columbia Coast Pilot (Canadian Hydrographic Service, 1953, p. 2) suggest that they may be common in Burke (although the phenomena described in the Pilot are not there interpreted in terms of internal waves). Annotations on Admiralty Chart 2458 together with the strong ship movement experienced during a University of British Columbia oceanographic cruise in Observatory suggest that internal waves occur frequently in the latter.

On calm days when there is a distinct surface layer of 2 to 3 m depth it is quite common when the ship is brought to a stop at a station to see a series of several ruffles move on ahead and to the beam of the ship as it comes to a halt. These are assumed to be associated with bow waves generated by the ship at the internal boundary as it slows down through the speed of propagation of internal waves at this boundary.

When flying over the southern Strait of Georgia in the spring and summer, when the water is stratified due to the runoff of the Fraser River, one frequently sees extensive systems of ruffles apparently originating at the passages between islands in the southern part of the strait. Shand (1953) has described this phenomenon and interpreted it as evidence of internal waves. Although simultaneous measurements in the water were not available to him there is no doubt that his explanation is correct as the writer has observed the phenomenon at close hand while making current observations in the strait. In this region the surface layer is usually turbid while the deeper water is much clearer. Under these conditions, internal waves are often visually evident as a series of turbid bands (over the troughs of the internal waves) separated by darker bands (of clearer water over the crests of the waves). A similar distribution of turbid (low-density) water overlying clearer (more dense) water is found regularly toward the heads of the inlets but internal wave evidence has not been observed. This is possibly because no generating mechanism in the form of a marked shear flow occurs in these localities.

7.22 Mid-depth internal waves

The mid-depth internal waves have been observed on many occasions in Bute and Knight and appear to be a regular feature. A good example of the observed phenomenon is shown in Fig. 41. The data for the Figure were obtained in Bute by making bathythermograph casts at 30-minute intervals for about 3 days

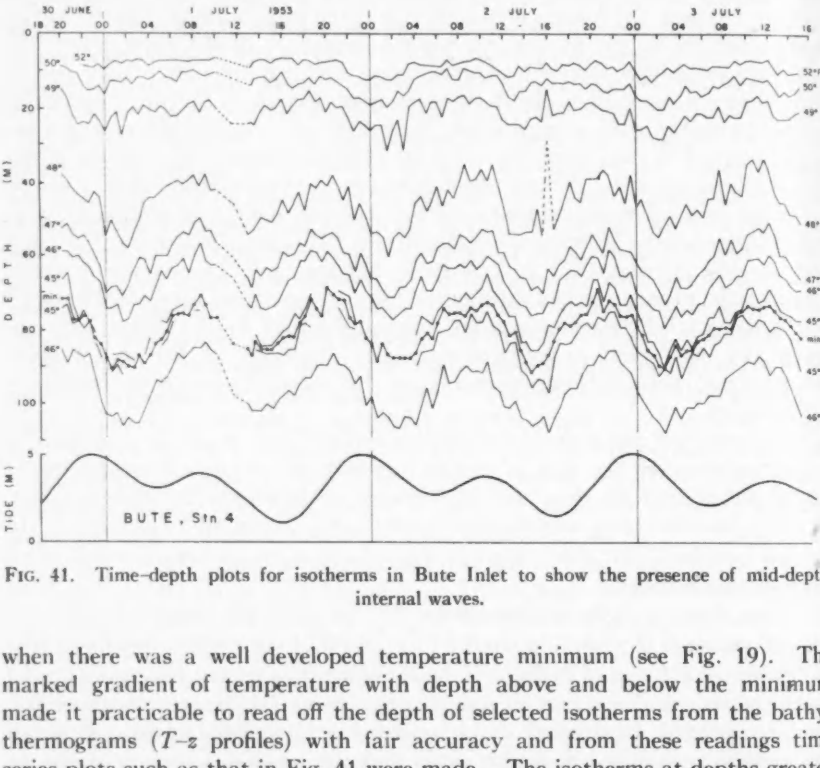

FIG. 41. Time–depth plots for isotherms in Bute Inlet to show the presence of mid-depth internal waves.

when there was a well developed temperature minimum (see Fig. 19). The marked gradient of temperature with depth above and below the minimum made it practicable to read off the depth of selected isotherms from the bathythermograms (T–z profiles) with fair accuracy and from these readings time series plots such as that in Fig. 41 were made. The isotherms at depths greater than about 40 m show both a gross variation in depth with time and a fine structure. The gross oscillation is seen to have a period similar to that of the surface tide and to be about 40° advanced in phase. The fine structure may either be real or be indicative of the possible inaccuracy of the method as used to determine the depth of a particular isotherm, or be a combination of both. Real short-period fluctuations in depth of a given isotherm about its mean value could be due to and indicative of turbulent motion of the water. Apparent short-period fluctuations could be attributable to instrumental inconsistency, improper technique in inserting the slide in the bathythermograph, or to errors in reading the bathythermogram. The only likely error in technique is to fail to push the slide fully home when inserting it in the bathythermograph. The

result is then a decrease in apparent depth of isotherms above the temperature minimum and a simultaneous increase in apparent depth below the temperature minimum when the slide is read in the viewer. An isolated example of this is apparent in Fig. 41 at 1600 hours on July 2. To investigate the personal errors, several series of bathythermograms were read and time series plots prepared independently by different individuals. Differences certainly were found between such plots, particularly at depths where the temperature gradient was small, but at the same time much of the fine structure was found to be common to the independently prepared plots. This suggests that human error in reading is not entirely responsible for this feature, but it does not determine the relative contributions of instrument inconsistency and of real fluctuations in depth. However, most of the series of observations were made with selected bathythermographs having small hysteresis and histories of close correspondence with temperatures determined with reversing thermometers. Sometimes a recognizable detail in the bathythermogram could be tracked for several hours, and its vertical motion generally followed that of the isotherms near to it. It is therefore considered probable that the fine structure on the plots has some reality.

It has not proved possible to follow oscillations at depths much greater than 100 to 120 m by this simple technique because the temperature gradient becomes too small for the depths of isotherms to be read with any confidence. At depths of less than about 20 m the vertical oscillations become too small and too rapid to be followed conveniently by this bathythermograph method because the stability of the water becomes very great. A more sensitive electrical resistance type of thermometer, or an isotherm-follower of the type described by LaFond (1961) would be useful to extend the observations of these mid-depth internal waves.

The observed amplitude of the vertical oscillations varies from series to series. In Fig. 41 the total amplitude of vertical oscillation in the vicinity of the temperature minimum is about 20 m with the amplitude decreasing at lesser depths. In other series the amplitudes have been from 5 to 75 m.

The interpretation of these time series observations is not certain. Possible explanations are that (a) they are evidence of progressive internal waves, (b) they are evidence of standing internal waves, (c) they are simply an incidental consequence of the back-and-forth tidal movement of water having isotherms inclined to the horizontal along the length of the inlet.

The last alternative is rejected for two reasons. The required longitudinal inclination of the isotherms to the horizontal is not generally observed either in regular surveys along the inlets or in special quasi-synoptic series made by taking a series of bathythermograph casts rapidly at half-mile intervals through the anchor station positions. The data at present available do not permit one to distinguish between alternatives (a) and (b). All but one set of observations have been made by a single ship at any one time. This set consisted of simultaneous observations in Bute at two points approximately one quarter and one half the length of the inlet from the head and it revealed internal waves out of phase by 180° within the accuracy of observation. This could be explained either

in terms of progressive waves, or of standing waves with a node between the two observation stations. A critical experiment would be to make a series of simultaneous observations at two points at different separations to see if the phase difference varied continuously along the inlet at any instant (progressive waves) or had eigenvalues of 0° or 180° only (stationary waves).

The density distribution in the inlets is such that, except for the wind-mixed surface layer of a few metres depth, the water is always gravitationally stable. The free period of vertical oscillation of a small mass of water calculated from the observed density gradient ranges from about half a minute in the halocline at 5 to 10 m depth to one hour at 300 m depth (see Fig. 28). These values are much smaller than the gross period of oscillation observed in the time series, but of the same order as that of the fine-structure components (as far as can be judged from observations at 30-minute intervals).

If the observed continuous density distribution is approximated by a two-layer system with an upper layer of thickness 100 m and average density difference of 1 mg/cc less than that of the deeper layer, and if Bute is regarded as a narrow bay closed at one end, the fundamental free period of an internal seiche at the boundary between the two layers would be about 8 hours and for a 50-m depth of upper layer it would be about 10.5 hours. Corresponding values for Knight would be about 11 and 14 hours. Such a two-layer approximation is crude, though the density difference is realistic, but it suggests that is not unlikely that mid-depth internal waves could occur, being driven by the tidal in-and-out flow in some manner.

These internal oscillations present interesting problems in themselves as to character and origin, but will need further properly designed observations for their elucidation. However, their frequent, if not invariable, occurrence must be borne in mind when longitudinal profiles of water properties are being considered. Without carrying out anchor stations during each survey of an inlet it would not be possible to eliminate the effect of the waves on apparent distributions of properties. In this connection it may be noted that when using conventional oceanographic techniques for water sampling from a 10-knot ship the time taken to complete eight oceanographic stations along the 40-mile length of Bute Inlet is 8 to 9 hours, a time of the same order as the period of the internal waves.

8. BUTE INLET WAX

About six times between 1922 and 1956 there have been reports of the appearance in Bute Inlet and occasionally at the mouth of the neighbouring Toba Inlet of a peculiar whitish waxy substance. The material appears only during some unusually cold winters and is then found on the shore and floating on the water in amounts variously reported as "bucketsful" to "scow loads". Examination of the material at the Fisheries Research Board of Canada Technological Station, Vancouver, (Anon., 1951) has shown the substance "to be essentially a wax, i.e., fatty alcohols combined with fatty acids. The wax contains almost no

glycerides, which are the major components of fish and marine mammal oils. It contains little, if any, hydrocarbons, which are the substances composing petroleum". The wax solidifies at about 11°C, its specific gravity is 0.87, and carbon-14 determinations give its age as 0 to 300 years (Swain, quoted by Williams, 1957). Above 11°C it is a brown liquid.

Williams has assembled the available information on the wax. He draws attention to the fact that one half of the total stands of lodgepole pine in British Columbia occur in the watershed of Bute Inlet and that the pollen is often observed in considerable quantities on the water in Bute but not elsewhere. He suggests that it is possible that the wax may be a decomposition product of this pollen.

The wax has not been reported from any other region in British Columbia and neither Williams nor the author has been able to find in the literature any description of such a material being found elsewhere. Any hypothesis to explain its occurence must take into account, since the wax is lighter than water, the fact that the surface layers of water in the inlet have a net motion out of the inlet both in winter and in summer.

9. SUMMARY AND DISCUSSION

The oceanographic studies of the inlets of the mainland coast of British Columbia have shown that as a consequence of the precipitation and the discharge into them of fresh water from rivers they are all essentially positive estuaries, the salinity of the water ranging from zero to that of the coastal waters outside. The inlet waters are markedly stratified and the density is determined chiefly by the salinity. The circulation in the inlets appears to be dominated by the influence of the river runoff, and in fact the differences between property distributions from inlet to inlet can be explained as a direct consequence of the fresh-water-induced estuarine circulation.

The inlets are often compared to the Norwegian fjords. Morphologically the comparison is appropriate but in one respect at least they differ—very few, if any, of the British Columbia mainland coast inlets are sufficiently stagnant to exhibit anaerobic conditions. Before pursuing this point one comment should be made. A frequently quoted reference for descriptions of Norwegian fjords is the paper by Strøm (1936), but it sometimes appears to be forgotten that this valuable paper was not intended to be a general description of Norwegian fjords. Its title is "Land-Locked Waters: hydrography and bottom deposits in badly-ventilated Norwegian fjords with remarks upon sedimentation under anaerobic conditions". Strøm restricts himself to the fjords in the southern quarter only of Norway's coastline, and further restricts himself to those which might be expected from their depths to be stagnant. Not all of those studied proved to be stagnant and Strøm presumably deliberately omitted the greater fjords, such as Sogne Fjord and Hardanger Fjord, in the region studied. The coast north of that studied by Strøm contains many fjords, and his paper is not and was not intended to be broadly descriptive of Norwegian fjords as a whole. To get a more complete

picture of the Norwegian fjords it is necessary to refer also to other descriptions such as those of Mohn (1887), Nordgaard (1899, 1903), Gaarder (1915) and others. These indicate that many of the fjords are not stagnant. However, even taking this broader view the basic distinction stated at the beginning of this paragraph still stands, namely that while many Norwegian fjords have no oxygen and do have hydrogen sulphide in their deep waters, this condition is uncommon in British Columbia, both in the mainland inlets as described above and, as other investigations have shown, in those in the large islands off the coast.

In discussing the causes of ventilation or lack of it in the Norwegian fjords studied, Strøm mentions several factors. He stresses (1936, p. 11) the effect of offshore winds in the spring carrying away the surface layer which induces an inward flow of subsurface saline water. He also refers to the effect of the fresh water, stating (*ibid.*, p. 58): "Freshwater supplies are of course essential to get more or less permanent density differences between surface and deep, but the degree of stagnation has nothing to do with the volumes of freshwater at the surface. Though very great freshwater supplies preserve deep waters against complete renewals, they cause a certain degree of partial ventilation". These two statements appear to be contradictory. The present writer is of the opinion, contrary to Strøm, that in bodies of water such as the British Columbia inlets and presumably the Norwegian fjords the distribution of subsurface water properties including the degree of stagnation *is* in large measure determined by the fresh water runoff into them. The effect of the fresh water runoff is to drive the estuarine circulation which promotes a renewal of the subsurface waters in the manner described by Tully (1949) and Pritchard (1952) subsequent to the publication of Strøm's work.

The influence of the fresh water runoff then is twofold. In the first place it determines the surface salinity values, decreasing them most in inlets where the runoff is large and giving rise to seasonal variations of surface salinity with a minimum in summer. The surface low salinity layer is 2 to 10 m thick, the salinity value ranging from 2 to 20‰ in summer. By about 20 m depth the salinity even in large-runoff inlets reaches 90 to 95% of the deep water value. In the inlets with small runoff the homogeneous surface layer is generally inconspicuous or absent. The temperature structure in the surface layer is influenced by the runoff to the extent that surface values in the large-runoff inlets are low, even in summer, because of the glacial or snowfield origin of the river water. In addition the very strong halocline is accompanied by a strong thermocline. Estimates which have been made of the vertical eddy mixing coefficients for heat and for salt in the upper 200 m indicate that the former is the larger, and seasonal variations of temperature penetrate to a greater depth than do those of salinity. The temperature minimum which is evident in many inlets is believed to be the result of late winter cooling which penetrates to 75 to 100 m although seasonal salinity variations are not noticeable much below 50 m.

The second influence of the fresh water runoff is in promoting the estuarine circulation. The river runoff into the head of an inlet gives rise to a surface outflow which picks up and carries out some of the underlying saline water. In

consequence of this there is a compensatory inflow below the surface layer of saline water from outside. There is evidence in the distribution of subsurface properties of the water in the inlets that the estuarine circulation is stronger in the inlets with large river runoff than in those with smaller runoff. Therefore the deep water characteristics are determined by the river runoff at the surface.

The distribution of dissolved oxygen shows greater variations between inlets than does the temperature, and some of these can be attributed to differences in river runoff. In the inlets with large runoff the surface layers are generally saturated or nearly so with 5 to 8 ml/l. Then, neglecting certain maxima and minima in the upper few tens of metres, the oxygen content decreases at greater depths to 2 to 4 ml/l. This is the general situation in inlets with large runoff. The inlets with small runoff on the other hand have a greater *range* of dissolved oxygen values at any given depth than do the large-runoff inlets. In the surface layers supersaturation is fairly common with values up to 11 ml/l, while in the deep waters the oxygen content is often lower than in the large-runoff inlets at 1 to 3 ml/l. It seems reasonable to suggest that the higher surface values in the low-runoff inlets are associated with the higher salinities which are conducive to greater phytoplankton growth and consequent photosynthetic production of oxygen, together with the slower net seaward movement of the surface layer which permits the phytoplankton populations to develop without being swept out of the inlet. In the deeper water there is a lesser inflow of saline and oxygenated water from outside because of the smaller surface outflow, and therefore the deeper water becomes more depleted of oxygen.

As examples of these last suggestions one may take Bute and Jervis which are geographically close, generally similar in depth and shape, open on to the same body of water in the Strait of Georgia, but show marked differences in some aspects of water structure. The deep water oxygen content in Jervis, particularly near the head, is markedly less than in Bute although the inlet is more directly connected with the Strait of Georgia and has a deeper sill. The chief difference between these inlets is that Jervis has less than 40% as much river runoff as Bute, and only one-quarter of this comes in at the head whereas in Bute three-quarters of the total enters at the head. The flushing effect of the large runoff into the head of Bute is expected to be greater on the whole of the inlet length than that of the smaller runoff distributed along the length of Jervis.

Another example is given by Belize and Seymour which have a common outlet to the sea, but the lower oxygen values in Belize are considered to be a consequence of lower runoff into that inlet. In addition, in Belize itself the main runoff comes in from the side about 8 miles from the head. The reach of the inlet between this junction and the head shows the lowest oxygen values in the length of the inlet and some of the lowest in any of the mainland coast inlets.

Although it is outside the area covered by this paper, Saanich Inlet provides an extreme example on the British Columbia coast of an inlet with small runoff. It does have water with H_2S in its deepest basin. This inlet has a relatively deep sill but an almost complete lack of river runoff into the head. As a result the estuarine circulation is slight and consequently there is stagnation. It is

possible that in the future somewhat more river water may flow into the head of this inlet through diversion and it will be interesting to observe if the extent of stagnation is reduced as a result.

It is remarked that several inlets show a different dissolved oxygen structure with a minimum at mid-depth rather than at the bottom. These are certain of the low-runoff inlets such as Belize and Sechelt. Thompson and Barkey's (1938) suggestion that this is due to reduction in contact with the bottom at mid-depth is questioned. The alternative suggestion is presented that the low runoff, by causing only a slight estuarine circulation, is the main cause of the mid-depth minimum.

In considering the vertical distribution of water properties, particularly in the large-runoff inlets, the fact that upward mixing into the saline zone occurs to a much greater extent than downward mixing, at least until the stability decreases near the inlet mouth, is a well known but not adequately explained feature of the inlet waters. At the same time there is evidence in the inlets with shallow sills that downward mixing does occur to a significant extent even in low-runoff inlets.

In examining the distribution with depth of water properties the possible influence of internal waves which appear to be common must be borne in mind.

10. ACKNOWLEDGMENT

The author wishes to acknowledge assistance from many sources. The Fisheries Research Board of Canada through Dr J. P. Tully of its Pacific Oceanographic Group, Nanaimo, B.C., loaned equipment for the early cruises and provided summer appointments. The Royal Canadian Navy through the Pacific Naval Laboratory, Esquimalt, B.C., made available the oceanographic research vessels C.N.A.V. *Ehkoli*, H.M.C.S. *Cedarwood* and C.N.A.V. *Whitethroat*, and the officers and crews of these vessels contributed materially to the progress of the work.

The greater part of the work reported here was carried out with the assistance of research grants from the National Research Council of Canada, while the work on current measurements and on turbidity described elsewhere and referred to here briefly was supported by the Defence Research Board of Canada under Grants Number 9520-05 and 9520-15.

The Canadian Hydrographic Service, Victoria, B.C., of the Department of Mines and Technical Surveys has been generous in permitting access to detailed field sheets of their surveys.

Finally, while the author directed the field work and took part in most of the cruises the greater part of the field observation and subsequent reduction of data was carried out by student assistants associated with the Institute of Oceanography, University of British Columbia. Reference is made to many of these assistants as authors of papers on specific investigations. Among others

are L. Regan, H. Wilke, T. H. Killam who also prepared the Figures, and G. S. Pond who assisted with data analysis.

For the generous assistance provided by all these organizations and individuals the author wishes to express his sincere thanks.

11. REFERENCES

ANON. 1951. Bute Inlet wax. *Fish. Res. Bd. Canada, Prog. Rept. Pac. Coast Sta.*, No. 86, 17–18.

BANCROFT, J. A. 1913. Geology of the coast and islands between the Strait of Georgia and Queen Charlotte Sound, British Columbia. Canada Dept. Mines, Geol. Survey, Mem. 23, Ottawa.

CAMERON, W. M. 1951. On the dynamics of inlet circulations. Doctoral dissertation, Scripps Inst. of Oceanography, University of California, Los Angeles.

CANADIAN HYDROGRAPHIC SERVICE. 1953. British Columbia Coast Pilot, Vol. II, Third Edn. Queen's Printer, Ottawa, 305 pp.

1960. Pacific coast tide and current tables. Queen's Printer, Ottawa, 257 pp.

CARTER N. M. 1932. The oceanography of the fiords of southern British Columbia. *Fish. Res. Bd. Canada, Prog. Rept. Pac. Coast Sta.*, No. 12, 7–11.

1934. Physiography and oceanography of some British Columbia fiords. *Proc. 5th Pac. Sci. Cong.*, 1933, Vol. I, pp. 721–733.

CHAPMAN, J. D., AND D. B. TURNER. 1956. British Columbia Atlas of Resources. B.C. Nat. Res. Conference, Victoria, B.C.

DAWSON, W. B. 1920. The tides and tidal streams with illustrative examples from Canadian waters. King's Printer, Ottawa, 43 pp.

DINSE, P. 1894. Fjord formations. A contribution to the morphography of coasts. *Zeit. Gesell. f. Erdkunde zu Berlin*, **29**: 189–259.

ECKART, C. 1960. Hydrodynamics of oceans and atmospheres. Pergamon Press, New York, 290 pp.

EMERY, K. O., AND R. S. DIETZ. 1941. Gravity coring instrument and mechanics of sediment coring. *Geol. Soc. Amer. Bull.*, **52**: 1685–1714.

EWING, G. 1950. Slicks, surface films and internal waves. *Jour. Mar. Res.*, **9**: 161–187.

GAARDER, T. 1915. Surstoffet i fjorden. (De vestlandske fjordes hydrografi. I). Bergens Museums Aarbok, 1915–16, Naturvidensk. Raekke, Nr. 2.

GILMARTIN, M. 1960. The primary production of a British Columbia fjord. Ph.D. thesis, University of British Columbia, Vancouver, B.C.

HERLINVEAUX, R. H. 1962. Oceanography of Saanich Inlet in Vancouver Island, British Columbia. *Jour. Fish. Res. Bd. Canada*, **19**(1): 1–37.

HESSELBERG, Th. 1918. Uber die Stabilitätsverhaltnisse bei vertikalen Verschiebungen in der Atmosphäre und im Meer. *Ann. d. Hydr. u. Mar. Meteor.*, 118–129.

HESSELBERG, Th., AND H. U. SVERDRUP. 1915. Die Stabilitätsverhaltnisse des Seewassers bei vertikalen Verschiebungen. Bergens Museums Aarbok, 1914–15, No. 15.

HUTCHINSON, A. H., AND C. C. LUCAS. 1931. The epithalassa of the Strait of Georgia. *Can. Jour. Res.*, **5**: 231–284.

I.O.U.B.C. REPORTS. (See list of Data Reports following these References.)

JERLOV, N. G. 1953. Influence of suspended and dissolved matter on the transparency of sea water. *Tellus*, **5**: 59–65.

KENDREW, W. G., AND D. KERR. 1955. The climate of British Columbia and the Yukon Territory. Queen's Printer, Ottawa, 222 pp.

LAFOND, E. C. 1961. The isotherm follower. *Jour. Mar. Res.*, **19**: 33–39.

LAFOND, E. C., AND R. S. DIETZ. 1948. New snapper type sea floor sediment sampler. *Jour. Sedi. Petr.*, **18**: 34–37.

LEBRASSEUR, R. J. 1954. The physical oceanographic features governing the plankton distribution in the British Columbia inlets. M.A. Thesis, University of British Columbia, Vancouver, B.C.

1955. Oceanography of British Columbia mainland inlets, VI. Plankton distribution. *Fish. Res. Bd. Canada, Prog. Rept. Pac. Coast Sta.*, No. 103, 19–21.

METEOROLOGICAL DIVISION. 1950–58. Monthly record, meteorological observations in Canada. Canada, Dept. Transport, Toronto.

MOHN, H. 1887. Nordhavets dybder, temperatur og strøminger. Norske nordhavseekspedisjon 1876–1878, XVIII. Christiania [Oslo].

NORDGAARD, O. 1899. Some hydrographical results from an expedition to the north of Norway during the winter of 1899. Bergens Mus. Aarbog, No. 8.

1903. Studier over naturforholdene i vestlanske fjorde. I. Hydrografi. Bergens Mus. Aarbog, No. 8.

PACIFIC OCEANOGRAPHIC GROUP. 1955. Physical and chemical data record, Hecate Project, 1954. Joint Comm. on Oceanography, Canada. [Fisheries Research Board of Canada.]

PEACOCK, M. A. 1935. Fiord-Land of British Columbia. *Bull. Geol. Soc. Amer.*, **46**: 633–696.

PICKARD, G. L. 1953. Oceanography of British Columbia mainland inlets. I. Water characteristics. *Fish. Res. Bd. Canada, Prog. Rept. Pac. Coast Sta.*, No. 96, 3–6.

1954. Oceanography of British Columbia mainland inlets. III. Internal waves. *Fish. Res. Bd. Canada, Prog. Rept. Pac. Coast Sta.*, No. 98, 13–16.

1956. Physical features of British Columbia inlets. *Trans. Roy. Soc. Canada*, Series III, 50: 47–58.

PICKARD, G. L., AND L. F. GIOVANDO. 1960. Some observations of turbidity in British Columbia inlets. *Limn. and Oceanog.*, **5**(2): 162–170.

PICKARD, G. L., AND D. C. MCLEOD. 1953. Seasonal variation of temperature and salinity of surface waters of the British Columbia coast. *Jour. Fish. Res. Bd. Canada*, **10**: 125–145.

PICKARD, G. L., AND KEITH RODGERS. 1959. Current measurements in Knight Inlet, British Columbia. *Jour. Fish. Res. Bd. Canada*, **16**(5), 635–678.

PICKARD, G. L., AND R. W. TRITES. 1957. Fresh water transport determination from the heat budget with applications to British Columbia inlets. *Jour. Fish. Res. Bd. Canada*, **14**(4): 605–616.

POOLE, H. H., AND W. R. G. ATKINS. 1929. Photoelectric measurements of submarine illumination throughout the year. *Jour. Mar. Biol. Assn. U.K.*, **16**: 297–324.

PRITCHARD, D. W. 1952. Estuarine hydrography. Advances in geophysics. Vol. I, pp. 243–280. Academic Press Inc., New York.

RICHARDS, F. A., AND N. CORWIN. 1956. Some oceanographic applications of recent determinations of the solubility of oxygen in sea water. *Limn. and Oceanog.*, **1**: 263–267.

SHAND, J. A. 1953. Internal waves in Georgia Strait. *Trans. Amer. Geophys. Union*, **34**: 849–856.

STRØM, K. M. 1936. Land-locked waters. Hydrography and bottom deposits in badly-ventilated Norwegian fjords with remarks upon sedimentation under anaerobic conditions. *Skr. Norske Vidensk. Akad. Oslo*, **1**(7): 1–85.

SVERDRUP, H. U., M. W. JOHNSON AND R. H. FLEMING. 1942. The oceans, their physics, chemistry and general biology. Prentice–Hall, Inc., New York. 1087 pp.

TABATA, S., AND G. L. PICKARD. 1957. The physical oceanography of Bute Inlet, British Columbia. *Jour. Fish. Res. Bd. Canada*, **14**(4): 487–520.

THOMAS, M. K. 1953. Climatological Atlas of Canada. Nat. Res. Council, Ottawa, 256 pp.

THOMPSON, T. G., AND K. T. BARKEY. 1938. Observations on fjord-waters. *Trans. Amer. Geophys. Union*, **19**: 254–260.

TOOMBS, R. B. 1956. Some characteristics of Bute Inlet sediments. *Trans. Roy. Soc. Canada*, Ser. III, **50**: 59–65.

TRITES, R. W. 1955. A study of the oceanographic structure in British Columbia inlets and some of the determining factors. Ph.D. thesis, University of British Columbia, Vancouver, B.C.

TULLY, J. P. 1937. Oceanography of Nootka Sound. *J. Biol. Bd. Canada*, **3**(1): 43–69.

1949. Oceanography and prediction of pulp mill pollution in Alberni Inlet. *Fish. Res. Bd. Canada Bull.* No. 83, 169 pp.

VANCOUVER, G. 1798. A voyage of discovery to the North Pacific Ocean and round the world. G. G. and J. Robinson, London. 3 Vol. and Atlas.

WALDICHUK, M. 1957. Physical oceanography of the Strait of Georgia, British Columbia. *Jour. Fish. Res. Bd. Canada*, **14**(3): 321–486.

WILLIAMS, M. Y. 1957. Bute Inlet wax. *Trans. Roy. Soc. Canada*, Ser. III, **51**: 13–17.

DATA REPORTS of the Institute of Oceanography, University of British Columbia, Vancouver, B.C.

No. 1. British Columbia Inlet Study, 1951. (March, 1953).

No. 2. British Columbia Inlet Cruises, 1952. (April, 1953).

No. 3. British Columbia Inlet Cruises, 1953. (April, 1954).

No. 4. C.G.M.V. "Cancolim II" Survey of the British Columbia coast, 1953. (December, 1955).

No. 5. Saanich Inlet Cruises, 1954, 1955. (December, 1955).

No. 6. British Columbia Inlet Cruise, 1954. (December, 1955).

No. 7. British Columbia Inlet Cruise, 1955. (December, 1955).

No. 8. British Columbia Inlet Cruise, 1956. (October, 1956).

No. 9. Queen Charlotte Strait, 1956. (November, 1956).

No. 10. Indian Arm, 1956. (December, 1956).

No. 11. British Columbia Inlet Cruises, 1957. (June, 1958).

No. 12. Indian Arm Cruises, 1957. Queen Charlotte Strait Cruise, 1957. (March, 1958).

No. 13. British Columbia Inlet Cruises, 1958. (December, 1958).

No. 14. Indian Arm Cruises, 1958. (June, 1959).

No. 15. British Columbia Inlet Cruise, 1959. (August, 1959).

No. 16. Indian Arm Cruises, 1959. (May, 1960).

No. 17. British Columbia Inlet Cruises, 1960. (March, 1961).

On the Chemical Composition of Eleven Species of Marine Phytoplankters[1]

By T. R. Parsons, K. Stephens and J. D. H. Strickland

Fisheries Research Board of Canada
Pacific Oceanographic Group, Nanaimo, B.C.

ABSTRACT

Eleven species of marine planktonic representatives of the Chlorophyceae, Chrysophyceae, Bacillariophyceae, Dinophyceae and Myxophyceae have been analyzed for their chemical composition. All species were grown under similar physical and chemical conditions and cells were analyzed during the exponential phase of growth. Chemical analyses consisted of a proximate analysis of each species for ash, protein, carbohydrate and lipid, and an analysis for carbon, silicon and phosphorus, as well as quantitative determinations of the monosaccharides and amino acids in hydrolysates of whole cells. The principal finding of this report is that marine phytoplankton have very similar organic composition when grown under similar physical and chemical conditions, regardless of the size of the organism or the class to which it belongs.

INTRODUCTION

There is a general scarcity of information on the chemical composition of marine phytoplankton. Analyses of natural crops and cells in pure culture (see reviews by Vinogradov, 1953; Strickland, 1960) have been performed on organisms grown under a variety of conditions and using different techniques for the estimation of their composition. Consequently there appears to be no comparative analysis of the different groups of algae which may contribute to a marine phytoplankton crop. In the following presentation an attempt has been made to analyze several representatives of different classes of marine phytoplankton, grown under very similar chemical and physical conditions, and employing standardized techniques for the chemical analyses.

The analytical techniques used are those which have been employed by our laboratory for the measurement of phytoplankton crops *in situ*, and as such are designed for shipboard as well as land-based laboratories. Most of the techniques have been described previously (Strickland and Parsons, 1960). Methods for the quantitative estimation of individual monosaccharides and amino acids, also for some of the other analyses, will be described in outline.

It should be emphasized that the composition of the algal cells reported here applies to vigorously growing cells in the exponential phase of growth, and results would have been different if the cells had been grown under conditions of nutrient deficiency or different conditions of light intensity and temperature. This is well illustrated by work on *Chlorella* by Spoehr and Milner (1949).

[1]Received for publication May 15, 1961.

J. Fish. Res. Bd. Canada, 18(6), 1961.
Printed in Canada.

MATERIALS AND METHODS

Algal Species

The eleven species employed in this investigation were two members of the Chlorophyceae, ***Tetraselmis maculata*** and ***Dunaliella salina***; two Chrysophyceae, ***Monochrysis lutheri*** and the coccolithophore ***Syracosphaera carterae***; four Bacillariophyceae, ***Skeletonema costatum***, ***Coscinodiscus*** sp., ***Chaetoceros*** sp. and ***Phaeodactylum tricornutum***; two Dinophyceae, ***Exuviella*** sp. and ***Amphidinium carteri***; and a representative of the Myxophyceae, ***Agmenellum quadruplicatum***.

All the cultures were unialgal but not bacteria free. The presence of bacteria during the exponential phase of growth was not apparent and their contribution to the biomass of harvested algal cells was considered insignificant.

Media

Two media were employed for the growth of the phytoplankton cells. The first was ASP 2 as described by Provasoli *et al.* (1957). The second was a medium very similar to ASP 2, but containing a concentration of magnesium, calcium, potassium, borate and bicarbonate ions representative of the concentration of these ions found in sea water. The composition of the latter medium was as follows:

At a salinity of 35‰, a litre of the medium contained 24 g NaCl, 10.9 g $MgCl_2.6H_2O$, 4 g Na_2SO_4, 0.68 g KCl, 1.5 g $CaCl_2.2H_2O$, 0.195 g $NaHCO_3$ and 0.026 g H_3BO_3. To obtain an artificial sea water of a salinity of 25‰, 1.0 volume of this solution was diluted to 1.4 volumes with distilled water. A dilution to 1.06 volumes was made to obtain a salinity of 33‰. All media contained 500 μg-atom N/l as KNO_3 and 50 μg-atom P/l as KH_2PO_4. Trace metals and vitamins were added in the same amount as employed in the ASP 2 medium. Silicon was provided to all media at a concentration of 200 μg-atom Si/l with the exception of the media for the growth of diatoms, where it was provided at a concentration of 1000 μg-atom/l. The silicon was added as a solution of sodium metasilicate and adjusted to pH 8 by the simultaneous addition of HCl.

The choice of the ASP 2 medium for the growth of *Monochrysis lutheri* and *Tetraselmis maculata* was made before the second medium was developed. It was later found that these two organisms grew equally well on the second medium at a salinity of 25‰. *Coscinodiscus* sp., *Skeletonema costatum*, *Chaetoceros* sp., *Phaeodactylum tricornutum* and ***Agmenellum quadruplicatum*** were all grown on the second medium described above at a salinity adjusted to 25‰. ***Dunaliella salina*** and *Syracosphaera carterae* were grown on the same medium adjusted to a salinity of 35‰, and the two dinoflagellates, ***Amphidinium carteri*** and *Exuviella* sp., on the same medium adjusted to a salinity of 33‰.

Culture Conditions

All cultures were grown in 20-l glass bottles under continuous illumination from cool white fluorescent lamps giving an illumination of *ca.* 0.04 cal/cm^2/min. Cultures were stirred and aerated with a stream of filtered air and the temperature was adjusted to 18 ± 2°C with a plastic cooling coil inserted into the medium.

The growth constants shown in Table I for the various algal species were obtained from the slope of the plot of $\log_{10}$ [Chlorophyll] *a* against time in hours. Algal cells were harvested at different times depending on the growth rate of the species, but in all cases this was during the exponential phase of growth.

Number, Volume and Dry Weight of Cells

Number of cells. Determined using a haemocytometer. The diatom *Coscinodiscus* sp. was too large to be determined by this method and counts were made on settled samples using an inverted biological microscope.

Cell volumes. Determined by direct measurement using a micrometer attachment to the ocular lens of a microscope. Volumes were approximated from the measurements using the closest-fitting geometrical form.

Dry weight. Determined by filtering a known volume of the medium containing the algal cells onto a Millipore Type AA filter that had been previously washed with distilled water, dried and weighed. The cells were rinsed with isotonic ammonium formate to remove any sodium chloride adhering to the Millipore filter, and dried for 2 hours at 105°C at which temperature any residual formate was volatilized. No measure was made of the amount of moisture that may have been retained after heating at 105°C.

Chemical Methods

The methods for the determination of protein, carbohydrate, crude fibre, hexosamine, fat, plant pigments, total oxidizable carbon and particulate phosphorus have been described in detail in Bulletin No. 125 of the Fisheries Research Board of Canada (Strickland and Parsons, 1960). The following standards were employed for the determination of the various metabolites:

Protein was estimated by direct Kjeldahl nitrogen determination using ammonium sulphate as a standard and multiplying by the factor 6.25 to give protein. A second method employed for the estimation of protein, using 2,5-hexanedione reagent, was standardized with casein. Carbohydrate, crude fibre and oxidizable carbon estimations were standardized using glucose. Stearic acid was employed as a standard for fat determinations. The method employed for hexosamine determination was that described in Bulletin No. 125 for the estimation of chitin using glucosamine as a standard.

Methods not reported in Bulletin No. 125 are described below:

Ash. Determined on a sample of algal cells dried at 105°C to constant weight and ashed in a muffle furnace at 550°C to constant weight.

Silicon. Determined as silicate after fusion of a weighed sample of dried cells with sodium carbonate. The melt was dissolved in water and the silicate determined colorimetrically with ammonium molybdate.

Sugars. Individual monosaccharides were determined by chromatographic separation after hydrolysis of a whole plant with sulphuric acid. The technique followed was that described by Wilson (1959) with the modification that the paper chromatography was carried out at 38 to 39°C which resulted in a better

separation of the individual sugars. The solvent employed was butanol : pyridine : water (6 : 4 : 3) and the spots were developed with aniline hydrogen phthalate. The quantity of the individual carbohydrates was determined after elution of the spots and the optical density of the eluate was measured with a Beckman DU spectrophotometer at wavelengths of 390 mμ for hexoses and methyl pentoses, and 360 mμ for pentoses. Hexuronic acids were not determined quantitatively and the presence of several minor unidentified sugars was recorded. For confirmation of the identity of certain sugars a second chromatographic solvent, phenol saturated with water, was employed. Use was made also of the orcinol reagent (1% orcinol, 15% trichloracetic acid in water-saturated butanol) for the detection of ketose sugars on chromatograms.

AMINO ACIDS. Determined using modifications of the techniques described by Consden *et al.* (1944) and Dent (1948). After acid hydrolysis of the plant cells the amino acids were separated by two-dimensional paper chromatography using water-saturated phenol for the first separation and 1 : 1 mixture of 2,4-lutidene and 2,4,6-collidine saturated with water for the second separation. The amino acids were developed with ninhydrin and the individual spots eluted from the paper and compared spectrophotometrically at a wavelength of 570 mμ with simultaneously run standards of known concentration of natural (L)-amino acids. Leucine, isoleucine and methionine were estimated as one fraction and the presence of minor quantities of some amino acids was noted but not quantitatively determined.

RESULTS AND DISCUSSION

Table I shows the size relations of the algal species to their growth rates.

TABLE I. Cell volumes and growth constants of algal species.

Species	Approximate cell volume	Number of cells per 100 mg dry weight	Growth constant (base 10)	Time required for one cell division
	μ^3		*hour*$^{-1}$	*hours*
CHLOROPHYCEAE				
Tetraselmis maculata	310	4.4×10^8	0.039	8
Dunaliella salina	400	7.6×10^8	0.021	14
CHRYSOPHYCEAE				
Monochrysis lutheri	28	2.9×10^9	0.016	19
Syracosphaera carterae	1,760	2.1×10^8	0.015	20
BACILLARIOPHYCEAE				
Chaetoceros sp.	650	4.4×10^8	0.018	17
Skeletonema costatum	1,390	1.5×10^8	0.023	13
Coscinodiscus sp.	3,420,000	1.4×10^5	0.0083	36
Phaeodactylum tricornutum	120	4.6×10^9	0.013	23
DINOPHYCEAE				
Amphidinium carteri	740	4.0×10^8	0.034	9
Exuviella sp.	780	3.8×10^8	0.0093	33
MYXOPHYCEAE				
Agmenellum quadruplicatum	1.5	1.2×10^{11}	0.020	15

The second column of data gives the number of cells contributing to 100 mg of dry weight. It may be noted that cells of the *Coscinodiscus* sp. had approximately a thousand times the volume of those of the next largest organisms and that they grew at the slowest rate. The sizes of the other organisms vary over a further thousandfold range in cell volume with no obvious correlation between the size of the cell and the growth constant or between pigment content (Table II) and growth constant. This is not unexpected, as the standard growth conditions are not necessarily equally effective for all species.

TABLE II. Proximate analysis of algal cells.

Species	Metabolites (percentage dry weight of cells)					
	Protein*	Carbohydrate	Fat	Total pigment**	Ash	Total
CHLOROPHYCEAE						
Tetraselmis maculata	52	15.0	2.9	2.1	23.8	96
Dunaliella salina	57	31.6	6.4	3.0	7.6	106
CHRYSOPHYCEAE						
Monochyrsis lutheri	49	31.4	11.6	0.8	6.4	99
Syracosphaera carterae	56	17.8	4.6	1.1	36.5	116
BACILLARIOPHYCEAE						
Chaetoceros sp.	35	6.6	6.9	1.5	28.0	78
Skeletonema costatum	37	20.8	4.7	1.8	39.0	103
Coscinodiscus sp.	17	4.1	1.8	0.5	57.0	81
Phaeodactylum tricornutum	33	24.0	6.6	2.9	7.6	73
DYNOPHYCEAE						
Amphidinium carteri	28	30.5	18.0	2.4	14.1	93
Exuviella sp.	31	37.0	15.0	1.1	8.3	92
MYXOPHYCEAE						
Agmenellum quadruplicatum	36	31.5	12.8	1.5	10.7	93

*Nitrogen × 6.25.
**Chlorophylls and carotenoids (sum of mg and MSPU/100 mg dry weight).

Table II shows the proximate analyses of the algal species studied. It may be seen that, with the exception of the two dinoflagellates, protein was the principal organic constituent of the algal cells. In the two dinoflagellates carbohydrate exceeded protein. The chief storage product of the algal cells was carbohydrate in every case except *Chaetoceros* sp. which contained slightly more fat than carbohydrate. The relatively high values for the fat content of the two dinoflagellates are in contrast with other species with the exception of *Monochrysis lutheri* and *Agmenellum quadruplicatum*. Large amounts of ash were found in the diatoms and the coccolithophore, *Syracosphaera carterae*, as was to be expected from previous reports (see review by Vinogradov, 1953). The ash of *Syracosphaera carterae* was approximately 24% calcium carbonate although the number of coccoliths on this organism has been found to vary under different growth conditions from a very heavy coating to a complete disappearance. The surprisingly high ash of *Tetraselmis maculata* was found to be mostly chloride.

The percentages of the different metabolites contributing to the total dry weight of the cells reported in the last column of Table II show some deviation

from a recovery of 100%. Many of the results reported for the analysis of phytoplankton have been obtained by analyzing certain metabolites and calculating at least one component by difference to obtain 100% recovery (e.g. Ketchum and Redfield, 1949). The results reported here show that certain cell constituents were not estimated in terms of the major metabolites reported. In this respect Lewin *et al.* (1958) showed that 12% of *Phaeodactylum tricornutum* was neither protein, lipid, carbohydrate or ash. In a number of the species reported in Table II the percentage recovery is greater than 100%. This may be attributed to the use of average constants for the conversion of biological values. There is no certainty, for example, that the commonly accepted factor 6.25 for the conversion of assayed nitrogen to protein is applicable in every case.

There is little information on which to base interpretation of the nutritional significance of the results in Table II. *Monochrysis lutheri* has been found by Davis and Guillard (1958) to be one of the best foods for oyster larvae. Shiraishi and Provasoli (1959) have reported that *Monochrysis lutheri* was the only organisms of a number tested that would support indefinite growth of the crustacean *Tigriopus japonicus*. One may surmise that the *Monochrysis* cultures fed in both the above experiments were in an exponential growth phase in order to continually produce enough food for the animal populations. It is reasonable to suggest, therefore, that on the basis of the proximate analysis alone, a protein, carbohydrate and fat ratio of approximately 4 : 3 : 1 is suitable for zooplankton nutrition.

Table III shows the carbon content of the species analyzed and the amount

TABLE III. Organic and inorganic composition of algal cells.

Species	Oxidizable carbon (a)	Carbon (by combustion)* (b)	Hydrogen*	Silicon (Si)	Phosphorus (P)	Ratio (b)/(a)
	percentage dry weight of cells					
CHLOROPHYCEAE						
Tetraselmis maculata	36.8	35.1	5.4	1.2	3.3	0.95
Dunaliella salina	39.6	45.4	6.3	0.2	3.3	1.15
CHRYSOPHYCEAE						
Monochrysis lutheri	53.2	44.6	6.6	1.6	3.0	0.84
Syracosphaera carterae	39.6	35.2	3.2	0.2	1.2	0.88
BACILLARIOPHYCEAE						
Chaetoceros sp.	31.0	(–)	(–)	(–)	1.5	(–)
Skeletonema costatum	26.0	31.3	4.4	14.3	1.7	1.20
Coscinodiscus sp.	15.9	18.8	2.9	22.1	0.4	1.18
Phaeodactylum tricornutum	37.5	49.5	6.7	0.3	2.0	1.32
DINOPHYCEAE						
Amphidinium carteri	40.7	47.1	6.7	<0.05	1.1	1.16
Exuviella sp.	44.5	47.4	6.5	0.2	1.3	1.06
MYXOPHYCEAE						
Agmenellum quadruplicatum	42.0	44.9	6.3	1.3	1.4	1.06
				Mean carbon ratio:		1.08 ± 0.12

(–)Samples not analyzed.

*Samples analyzed by Weiler and Strauss, Oxford, England.

of silicon and phosphorus in each species. A comparison has been made between the carbon content of the cells as determined by oxidation with dichromate, and by the classical method of direct combustion. The ratios of the results obtained by the two methods are reported in the last column of the Table. The mean of these ratios agrees with that of El Wakeel and Riley (1957) who suggested the factor of 1.05 for the conversion of dichromate-oxidizable carbon to true carbon in the estimation of the organic content of phytoplankton. High results are obtained by dichromate oxidation in the presence of fats (Johnson, 1949) or other compounds at a higher state of reduction than glucose. Low values may be due to incomplete oxidation by dichromate or to the volatilization of certain compounds during the phosphoric acid treatment employed to remove extraneous chloride (Strickland and Parsons, 1960).

From the values for silicon and phosphorus in Table III it may be seen that the diatoms are the only class of organisms to contain a substantial amount of silicon. The presence of different amounts of silicon in all the other species is of interest in view of the ubiquity of silicon in terrestial plants and animals (King and Belt, 1938; King *et al.*, 1933; Parry and Smithson, 1957). The phosphorus contents of the cells analyzed were found to be higher than those generally reported in the literature (see review by Strickland, 1960) and these values have been discussed in terms of the nitrogen-to-phosphorus ratios in Table VII.

Table IV presents a comparison between two different methods for the estimation of algal protein. The advantage of the 2,5-hexanedione reagent (Strickland and Parsons, 1960) for the colorimetric estimation of protein is that the method

TABLE IV. Comparison of results of two methods for estimation of proteins.

Species	Colorimetric method (a)	Nitrogen × 6.25 (b)	Ratio (b)/(a)
	percentage dry weight of cells		
CHLOROPHYCEAE			
Tetraselmis maculata	72	52	0.72
Dunaliella salina	68	57	0.84
CHRYSOPHYCEAE			
Monochrysis lutheri	49	49	1.00
Syracosphaera carterae	53	56	1.06
BACILLARIOPHYCEAE			
Skeletonema costatum	47	37	0.79
Coscinodiscus sp.	18	17	0.94
Phaeodactylum tricornutum	93	33	0.35
DINOPHYCEAE			
Amphidinium carteri	53	28	0.53
Exuviella sp.	36	31	0.86
MYXOPHYCEAE			
Agmenellum quadruplicatum	64	36	0.56
		Mean ratio:	0.77

is applicable under shipboard conditions where the use of fuming sulphuric acid, employed in the Kjeldahl nitrogen determination, is to be avoided. The other reason for employing a second measure of phytoplankton protein is that there appears to be a discrepancy in the determination of protein by the Kjeldahl method. In our own experiments (McAllister *et al.*, 1961) poor agreement between nitrate disappearing and protein being formed during a natural phytoplankton bloom has been reported. Similar discrepancies have been reported by Yentsch and Vaccaro (1959) in the analysis of *Phaeodactylum tricornutum* and by Krey (1958) in studies on natural phytoplankton populations.

The results in Table IV show that the algal species generally gave higher protein values with the 2,5-hexanedione reagent than by total Kjeldahl nitrogen determination. Keeler (1959) investigated the amino acids which react with the 2,5-hexanedione reagent. His results and our determinations of the amino acid composition of the algal species (Table VI) do not explain the variability shown in Table IV for the amount of protein estimated by the colorimetric method. It would appear that nitrogen compounds other than amino acids were present in appreciable amounts.

Table V shows the acid- and alkali-insoluble carbohydrate (crude fibre) as a percentage of the total carbohydrate, also the principal monosaccharides found in hydrolysates of the different algal species as a percentage of the dry weight of algae. The amount of crude fibre found in the different species may be interpreted as indicating the amount of carbohydrate that is employed by the cell for structural support (i.e. cell wall material) as opposed to the amount of carbohydrate stored within the cell. *Tetraselmis maculata*, *Exuviella* sp., *Agmenellum quadruplicatum*, *Coscinodiscus* sp. and *Chaetoceros* sp. were all found to have crude fibre contents greater than 10% of the total carbohydrate. The first three organisms just named were also found to be difficult to extract with 90% acetone for pigment analysis. It may be surmised that these organisms have relatively tough carbohydrate cell walls. The presence of large amounts of crude fibre in two of the four Bacillariophyceae is less readily explained. Diatoms are known to contain carbohydrate associated with the silica of the frustules (see review by Fogg, 1953). It seems reasonable to suggest that the amount of crude fibre associated with the species of *Coscinodiscus* and *Chaetoceros* was due to the relatively large size of the former and the elaborate structure of the latter compared, for example, with *Skeletonema costatum*. In all the other species studied the crude fibre was 10% or less of the total carbohydrate. In contrast, the crude fibre content of sea water has been found to reach 80% of the total carbohydrate when much detritus is present. It appears, therefore, that the level of crude fibre affords a measure of the level of particulate detritus in sea water.

Glucose, galactose and ribose were present in all the species analyzed, while hexuronic acids were detected in all species except the dinoflagellates (Table V). Glucose was always the predominant sugar. The amount of galactose present was variable. Although hexuronic acids were not measured quantitatively on the chromatograms, a measure of their relative amount was obtained using dichromatic

TABLE V. Carbohydrate composition of the algal cells.

Species	Crude fibre (percentage of total carbohydrate)	Principal sugars (percentage dry weight of cells)										
		Glucose	Galactose	Mannose	Ribose	Xylose	Arabinose	Rhamnose	Fucose	Fructose	Hexosamine	Hexuronic acids
CHLOROPHYCEAE												
Tetraselmis maculata	12.6	11.9	2.3	–	0.95	–	–	–	–	–	–	+
Dunaliella salina	9.8	17.2	11.8	–	1.7	–	–	–	–	–	–	+
CHRYSOPHYCEAE												
Monochrysis lutheri	3.6	22.1	4.4	–	1.3	3.5	–	–	–	–	–	+
Syracosphaera carterae	1.7	9.2	7.1	–	1.5	0.8	1.9	–	–	–	–	+
BACILLARIOPHYCEAE												
Chaetoceros sp.	22.8	3.3	1.5	0.79	0.71	0.4	–	2.8	+	–	–	+
Skeletonema costatum	9.6	16.4	1.8	0.87	1.2	–	–	1.0	0.9	–	–	+
Coscinodiscus sp.	29.0	2.1	0.4	0.41	+	–	–	0.7	0.5	–	–	+
Phaeodactylum tricornutum	2.5	10.7	2.7	3.7	0.72	0.7	–	1.5	–	–	–	+
DINOPHYCEAE												
Amphidinium carteri	2.0	19.0	8.4	–	0.9	–	–	+	–	–	–	–
Exuviella sp.	37.0	26.8	8.3	–	+	+	+	+	–	–	–	–
MYXOPHYCEAE												
Agmenellum quadruplicatum	17.4	17.4	3.2	–	1.5	–	–	–	–	3.5	0.3	+

+Sugars detected but not estimated.
–Sugars not detected.

readings of the colour produced by the anthrone reaction (Strickland and Parsons, 1960). The results of these measurements showed that hexuronic acids were not present in appreciable amounts. Mannose and rhamnose appeared to be present only in the representatives of the Bacillariophyceae, and fucose also may be a characteristic sugar of this class. Although fucose was not detected in *Phaeodactylum tricornutum*, Lewin *et al.* (1958) have reported its presence in this organism. Xylose appears to be a variable constituent of the algae analyzed while arabinose was only found in the coccolithophore *Syracosphaera carterae*, and the dinoflagellate *Exuviella* sp. Fructose and an unidentified hexosamine were only found in *Agmenellum quadruplicatum*. Two unidentified sugars were detected in the coccolithophore and one in *Chaetoceros* sp. These were minor constituents which appeared ahead of pentoses on the chromatograms.

The occurrence of ribose in every species analyzed is probably attributable to the presence of ribonucleic acid, which Jeener (1952) found to be present in *Polytomella caeca* to the extent of 6 to 10% of the protein.

The occurrence of glucose as the principal sugar in every species further justifies the use of the anthrone reaction (which gives a maximum colour with glucose) for the determinations of total particulate carbohydrate *in situ* (Strickland and Parsons, 1960). From metabolic considerations the amount of glucose occurring in each species reported in Table V further assists in evaluating the nutritional importance of the individual species. Thus in *Monochrysis lutheri*, *Tetraselmis maculata*, *Skeletonema costatum*, *Exuviella* sp. and *Agmenellum quadruplicatum* the amount of glucose is 70% or more of the total carbohydrate. When crude fibre is taken into consideration, however, it would appear that only *Monochrysis lutheri* and *Skeletonema costatum* contain carbohydrates which are both readily hydrolysable and nutritionally important. The importance of *Monochrysis lutheri* as a food for zooplankton has already been mentioned (*loc. cit.*). *Skeletonema costatum* appears to be an equally reliable food for many organisms (Nelson, 1947; Barnes, 1956).

Table VI shows the relative distribution of amino-acid nitrogen. The principal amino acids have been expressed as a percentage of the total estimated amino-acid nitrogen. The presence of other amino acids is recorded in the lower half of the Table. The fact that a number of amino acids were not detected on the chromatograms does not necessarily rule out their presence in the hydrolysates. These amino acids may have been minor constituents which were difficult to detect in the presence of the large amounts of major components.

From the results in Table VI it is apparent that algal protein is characterized by large amounts of aspartic and glutamic acids, glycine, alanine and lysine. The results are in general agreement with other reports (see review by Fogg, 1953) with the exception of the amino acid arginine. Some difficulty was encountered in the detection of arginine on the chromatograms and it was decided, therefore, to estimate arginine by the Sakaguchi reaction (Brand and Kassell, 1942). The

TABLE VI. Amino acid composition of the algal cells.

Amino acids	*Tetraselmis maculata*	*Dunaliella salina*	*Monochrysis lutheri*	*Syracosphaera carterae*	*Skeletonema costatum*	*Coscinodiscus* sp.	*Phaeodactylum tricornutum*	*Exuviella* sp.	*Agmenellum quadruplicatum*	*Amphidinium carteri*
	Amino-acid nitrogen as a percentage of the total amino-acid nitrogen									
Aspartic acid	26.0	16.5	25.3	35.5	28.0	15.6	14.8	20.0	17.0	15.4
Glutamic acid	8.1	13.6	5.9	5.1	13.5	15.6	12.9	13.1	17.7	11.0
Glycine	11.1	16.8	8.6	11.4	16.5	12.8	15.6	17.6	16.4	21.2
Alanine	15.0	19.0	26.0	11.4	7.5	13.8	17.0	13.1	15.7	28.5
Threonine	–	6.3	5.3	5.1	5.0	7.3	8.7	6.0	3.9	+
Lysine	21.0	12.0	19.6	17.8	+	12.9	7.2	16.6	13.8	+
Valine	5.1	4.2	3.7	5.1	8.5	7.3	6.4	4.0	2.6	7.1
Phenylalanine	7.5	4.5	1.5	2.5	8.0	7.3	11.0	3.5	5.2	8.6
Leucine, Isoleucine, Methionine	6.0	6.9	4.0	6.3	13.0	7.3	6.4	6.0	7.9	8.1
	Occurrence of other amino acids									
Serine	–	+	+	+	+	+	+	+	+	+
Proline	+	+	+	+	+	–	+	+	+	+
Tyrosine	–	+	+	+	–	+	–	–	+	+
Histidine	–	–	–	–	+	–	–	–	+	–
Arginine*	–	–	–	–	+	–	–	–	–	–
Cysteic acid	–	–	+	–	–	–	+	–	–	–
Methionine sulphoxide	–	+	+	+	–	–	–	+	–	+

+Amino acid detected but not estimated.
–Amino acid not detected.
*See text for additional values.

estimation was carried out on *Exuviella* sp., *Agmenellum quadruplicatum*, *Monochrysis lutheri* and *Phaeodactylum tricornutum*, and gave respective arginine contents of 1.5, 0.9, 1.2 and 1.5% dry weight of algal cells. These results indicate that arginine was one of the principal amino acids in the species investigated, although the possibility that the Sakaguchi reaction was being given by some other mono-substituted guanidine was not investigated.

Among the occurrences of minor amino acids reported in Table VI those of cysteic acid and methionine sulphoxide can be attributed to the formation of these compounds, during the acid hydrolysis, from cysteine (or cystine) and methionine, respectively. The occurrence of tryptophan in the species analyzed has not been investigated due to the destruction of this amino acid during acid hydrolysis.

A comparison of the distribution of the metabolites in the different species is obtained by comparing ratios of the metabolites to organic carbon. Results are shown in Table VII. Such ratios may be interpreted as an evaluation of

TABLE VII. Ratios involving (oxidizable) carbon values.

Species	$\frac{\text{Protein*}}{\text{C}}$	$\frac{\text{Carbohydrate}}{\text{C}}$	$\frac{\text{Fat}}{\text{C}}$	$\frac{\text{C}}{\text{P}}$	$\frac{\text{C}}{\text{N}}$	$\frac{\text{N}}{\text{P}}$(atoms)
CHLOROPHYCEAE						
Tetraselmis maculata	1.42	0.41	0.07	11	4.4	5.5
Dunaliella salina	1.43	0.80	0.15	12	4.3	6.1
CHRYSOPHYCEAE						
Monochrysis lutheri	0.94	0.59	0.22	19	6.8	5.8
Syracosphaera carterae	1.41	0.45	0.12	33	4.4	17.4
BACILLARIOPHYCEAE						
Chaetoceros sp.	1.12	0.22	0.21	21	5.5	8.3
Skeletonema costatum	1.38	0.79	0.17	15	4.4	7.7
Coscinodiscus sp.	1.08	0.27	0.11	40	5.9	15.0
Phaeodactylum tricornutum	0.88	0.64	0.17	19	7.0	5.9
DINOPHYCEAE						
Amphidinium carteri	0.69	0.75	0.44	37	9.0	13.2
Exuviella sp.	0.70	0.84	0.34	34	8.9	12.3
MYXOPHYCEAE						
Agmenellum quadruplicatum	0.86	0.75	0.31	30	7.2	10.6

*Nitrogen × 6.25.

the composition of the different species on an ash-free basis. Due to the difficulty involved in determining ash on natural populations it has been found necessary to use a direct estimation of total carbon as a measure of the organic material for *in situ* studies. Thus the ratios of metabolites to carbon represents an important comparison of the type of metabolites produced by different classes of marine phytoplankton grown under similar conditions. It may be seen that these ratios are considerably less variable than the proximate analysis values reported in Table II. Deviations from this generalization are most marked among the two Dinophyceae and *Agmenellum quadruplicatum.*

Considering the diversity of size and evolutionary origin of the species studied it is remarkable to find such a strong similarity in the composition of the species reported in Table VII. The governing factor in the composition of an algal cell appears to be, therefore, the physical and chemical environment in which it is grown (Spoehr and Milner, 1949). A similar conclusion was reached by Ketchum and Redfield (1949) from a less extensive study of five Chlorophyceae and one diatom.

The finding that different species of organisms grown under the same conditions have similar organic composition is of some advantage to *in situ* studies. Thus phytoplankton, which may be easily netted in large quantities, would be expected to have an organic composition similar to that of the nannoplankton in the same environment. The latter organisms are more difficult to obtain but

may constitute the largest fraction of a crop (e.g. McAllister *et al.*, 1960). Therefore, the organic analysis of a natural crop may be performed on the readily collectible net phytoplankton with reasonable certainty that the results are representative of the organic composition of the entire crop growing under the physical and chemical conditions prevailing at the time of collection. If such a determination is made, however, some measure of the total crop in terms of carbon or pigment is necessary in order to provide a quantitative reference basis for the proportions of protein, carbohydrate and fat.

The nitrogen-to-phosphorus ratios reported in Table VII are generally lower than the classical value of 15:1 (on an atom basis) assumed for *in situ* productivity studies. As mentioned in connection with Table III, this appears to be due to high phosphorus values rather than to low nitrogens (see review by Strickland, 1960). From our own studies (McAllister *et al.*, 1961) using a large plastic sphere to follow the growth of a natural population, it was found that during the exponential phase of growth the N/P ratio was at least as low (5 to 6) as some of the values reported in Table VII. It would appear, therefore, that vigorously growing cells in the presence of adequate nutrients may absorb more phosphorus than the N/P ratio of 15:1 predicts.

In Table VIII the ratios of different metabolites to chlorophyll *a* are reported.

TABLE VIII. Ratios involving chlorophyll *a*.

Species	Carbon / Chl. *a*	Carot.* / Chl. *a*	Protein** / Chl. *a*	Carbohydrate / Chl. *a*	Fat / Chl. *a*	N / Chl. *a*	P / Chl. *a*
CHLOROPHYCEAE							
Tetraselmis maculata	32	0.33	46	13	3	7	2.9
Dunaliella salina	19	0.47	26	14	3	4	1.5
CHRYSOPHYCEAE							
Monochrysis lutheri	97	0.40	90	57	21	14	5.5
Syracosphaera carterae	61	0.49	86	27	7	14	1.8
BACILLARIOPHYCEAE							
Chaetoceros sp.	44	0.26	50	10	10	8	2.1
Skeletonema costatum	26	0.28	36	21	5	6	1.7
Coscinodiscus sp.	69	0.31	75	19	8	12	1.7
Phaeodactylum tricornutum	26	0.44	23	17	5	4	1.4
DINOPHYCEAE							
Amphidinium carteri	48	0.59	48	36	21	5	1.4
Exuviella sp.	62	0.47	62	51	21	7	1.8
MYXOPHYCEAE							
Agmenellum quadruplicatum	45	0.56	45	34	14	6	1.5

*Carotenoids expressed in MSP units.
**Nitrogen × 6.25.

The amounts of chlorophyll *a* from which these ratios have been obtained were determined at the same time as the other analyses reported here. Complete results of the pigment analyses have been reported by Parsons (1961). In the

estimation of phytoplankton crops *in situ* it is impossible to obtain a direct measure of various metabolites present in the plants, because of the presence of large amounts of detritus in sea water (Parsons and Strickland, 1959; McAllister *et al.*, 1960). Consequently the amount of a plant metabolite must be calculated from a prior knowledge of the ratio between the pigment concentration in the naturally occurring species and the metabolite being measured. Thus Table VIII serves as a guide to the range of values to be expected from the various classes of organisms. These values are in general agreement with average values quoted by Strickland (1960) but one or two individual characteristics of the classes are worthy of note.

The ratio of carbon and protein to chlorophyll *a* (Table VIII) was found to be higher for the two Chrysophyceae than for any of the other groups. Fat and carbohydrate ratios were found to be high for the two Dinophyceae, *Agmenellum quadruplicatum* and the two Chrysophyceae. The representatives of the Bacillariophyceae show considerable variation while the two Chlorophyceae are characterized by the lowest ratios. The ratios of total carotenoids to chlorophyll *a* are remarkably constant throughout the different classes. A similar constancy in the chlorophyll *a*-to-carotenoid ratio has been found to occur in the natural populations of coastal waters throughout the year (Parsons, 1960) but its significance has not been interpreted.

ACKNOWLEDGMENTS

We would like to thank Dr R. R. L. Guillard (Woods Hole Oceanographic Institution), Dr V. L. Loosanoff (Biological Station, Milford), Dr C. Van Baalen (Kitchewan Research Laboratories) and Dr J. R. Stein (University of British Columbia) for cultures of organisms used in these experiments. We would like to thank also Mr A. Bursa (Arctic Unit, Fisheries Research Board, Montreal), Dr J. Stein and Dr E. M. Hulbert (Woods Hole Oceanographic Institution) for the identification of some of the species.

REFERENCES

BARNES, H. 1956. *Balanus balanoides* (L.) in the Firth of Clyde: The development and annual variation of the larval population, and causative factors. *J. Anim. Ecol.*, **25**: 72–84.

BRAND, E., AND B. KASSELL. 1942. Photometric determination of arginine. *J. Biol. Chem.*, **145**: 359–364.

CONSDEN, R., A. H. GORDON AND J. P. MARTIN. 1944. Quantitative analysis of protein: A partition chromatographic method using paper. *Biochem. J.*, **38**: 224–232.

DAVIS, H. C., AND R. R. L. GUILLARD. 1958. Relative value of ten genera of micro-organisms as foods for oysters and clam larvae. Fish. Bull. No. 136, *U.S. Fish. Wildlife Serv. Bull.*, **58**: 293–304.

DENT, C. E. 1948. A study of the behaviour of some sixty amino acids and other ninhydrin-reacting substances on phenol–collidine filter paper chromatograms, with notes as to the occurrence of some of them in biological fluids. *Biochem. J.*, **43**: 169–180.

El Wakeel, S. K., and J. P. Riley. 1957. The determination of organic carbon in marine muds. *J. Conseil Expl. Mer.*, **22**(2): 180–183.

Fogg, G. E. 1953. The metabolism of algae. Methuen and Co. Ltd., London, 149 pp.

Jeener, R. 1952. The evolution of nucleoprotein fractions in the cytoplasm during the growth of a culture of *Polytomella caeca*. I. Ribonucleic acid content of cells and growth rate. *Biochim. Biophys. Acta*, **8**: 125–133.

Johnson, M. J. 1949. A rapid micro-method for estimation of non-volatile organic matter. *J. Biol. Chem.*, **181**: 707–711.

Keeler, R. F. 1959. Color reaction for certain amino acids, amines and proteins. *Science*, **129**: 1617.

Ketchum, B. H., and A. C. Redfield. 1949. Some physical and chemical characteristics of algae growth in mass culture. *J. Cellular and Comp. Physiol.*, **33**: 281–299.

King, E. J., and T. H. Belt. 1938. The physiological and pathological aspects of silica. *Physiol. Rev.*, **18**: 329–365.

King, E. J., H. Stantial and M. Dolan. 1933. Silica in animal tissues. *Biochem. J.*, **27**: 1002–1006.

Krey, J. 1958. Chemical determination of net plankton, with special reference to equivalent albumin content. *J. Mar. Res.*, **17**: 312–324.

Lewin, J. C., R. A. Lewin and D. E. Philpott. 1958. Observations on *Phaeodactylum tricornutum*. *J. Gen. Microbiol.*, **18**: 418–426.

McAllister, C. D., T. R. Parsons, K. Stephens and J. D. H. Strickland. 1961. Measurements of primary production in coastal sea water using a large volume plastic sphere. *Limnol. and Oceanogr.*, **6**(3): 237–258.

McAllister, C. D., T. R. Parsons and J. D. H. Strickland. 1960. Primary productivity at Station "P" in the Northeast Pacific Ocean. *J. Conseil Expl. Mer*, **25**(3): 240–259.

Nelson, T. C. 1947. Some contributions from the land in determining conditions of life in the sea. *Ecol. Monographs*, **17**: 337–346.

Parry, D. W., and F. Smithson. 1957. Detection of opaline silica in grass leaves. *Nature*, **179**: 975–976.

Parsons, T. R. 1960. A data record and discussion of some observations made in 1958–1960 of significance to primary productivity. *Fish. Res. Bd. Canada, MS Rept.* (*Oceanogr. and Limnol. Ser.*) No. 81, 19 pp.

1961. On the pigment composition of eleven species of marine phytoplankters. *J. Fish. Res. Bd. Canada*, **18**: 1017–1025.

Parsons, T. R., and J. D. H. Strickland. 1959. The proximate analysis of marine standing crops. *Nature*, **184**: 2039.

Provasoli, L., J. J. A. McLaughlin and M. R. Droop. 1957. The development of artificial media for marine algae. *Arch. Mikrobiol.*, **25**: 392–428.

Shiraishi, K., and L. Provasoli. 1959. Growth factors as supplements to inadequate algal foods for *Tigriopus japonicus*. *Tohoku J. Agr. Res.*, **10**: 89–96.

Spoehr, H. A., and H. W. Milner. 1949. The chemical composition of *Chlorella*, effect of environmental conditions. *Plant Physiol.*, **24**: 120–149.

STRICKLAND, J. D. H. 1960. Measuring the production of marine phytoplankton. *Bull. Fish. Res. Bd. Canada*, No. 122, 172 pp.

STRICKLAND, J. D. H., AND T. R. PARSONS. 1960. A manual of sea water analysis. *Bull. Fish. Res. Bd. Canada*, No. 125, 185 pp.

VINOGRADOV, A. P. 1953. The elementary chemical composition of marine organisms. Translation by the Sears Foundation for Marine Research, Yale University, New Haven, U.S.A. 130–146.

WILSON, C. M. 1959. Quantitative determination of sugars on paper chromatograms. *Anal. Chem.*, **31**: 1199–1201.

YENTSCH, C. S., AND R. F. VACCARO. 1958. Phytoplankton nitrogens in the oceans. *Limnol. and Oceanogr.*, **3**: 443–448.

On the Pigment Composition of Eleven Species of Marine Phytoplankters[1]

By T. R. Parsons

Fisheries Research Board of Canada
Pacific Oceanographic Group, Nanaimo, B.C.

ABSTRACT

The amounts of different chlorophylls and carotenoids in eleven representatives of marine phytoplankton have been estimated. Representatives of the Chlorophyceae, Chrysophyceae, Bacillariophyceae, Dinophyceae and Myxophyceae were grown under similar chemical and physical conditions and their pigment content was determined during the exponential phase of growth. Particular attention was paid to the presence of chlorophyll *c* as well as to the identity of certain carotenoids.

In a previous publication (Parsons *et al.*, 1961) the chemical composition of eleven species of marine phytoplankton was studied. The results reported here are a continuation of this work with a view to establishing the quantitative and qualitative differences in the phytosynthetic pigments of these principal classes of marine phytoplankton. Considering the marked variation in pigment content of cells grown under different physical and chemical conditions described by previous investigators (Stanbury, 1931; Haskin, 1941; Strain *et al.*, 1944), the same precautions for standardizing growth conditions as described previously (Parsons *et al.*, 1961) were employed in the studies reported here.

MATERIALS AND METHODS

Algal Species and Culture Conditions

The unialgal cultures employed in this investigation were two members of the Chlorophyceae, *Tetraselmis maculata* and *Dunaliella salina*; three Chrysophyceae, *Monochrysis lutheri* and the coccolithophores *Syracosphaera carterae* and *Coccolithus huxleyi;* four Bacillariophyceae, *Skeletonema costatum*, *Coscinodiscus* sp., *Chaetoceros* sp. and *Phaeodactylum tricornutum*; two Dinophyceae, *Exuviella* sp. and *Amphidinium carteri*; and a representative of the Myxophyceae, *Agmenellum quadruplicatum.*

The media and growth conditions for the algal cultures were the same as reported previously (Parsons *et al.*, 1961) with the exception of conditions for the growth of *Coccolithus huxleyi.* This organism, which has been used here in connection with studies on chlorophyll *c*, was grown in a medium of 33‰ salinity (Parsons *et al.*, 1961) at a temperature of 16°C and under a light intensity of 0.065 cal/cm^2/min from cool white fluorescent bulbs.

[1]Received for publication May 15, 1961.

J. Fish. Res. Bd. Canada 18(6), 1961.
Printed in Canada.

Chemical Methods

Chlorophylls and total carotenoids

The method for the determination of chlorophylls *a*, *b* and *c* and the total plant carotenoids was that described by Richards with Thompson (1952), with the spectrophotometric corrections as modified by Strickland and Parsons (1960).

Individual carotenoids

The amounts of the individual algal carotenoids were determined by a chromatographic technique similar to that described by Strain *et al.* (1944) for the separation of algal pigments on columns of sugar.

Fresh cells were collected on a Millipore AA filter and extracted overnight (16 hours) in 90% acetone in the presence of a small amount of magnesium carbonate. Water was added to the acetone extract and the pigments were transferred to hexane in a separatory funnel. The hexane extract was taken to dryness by blowing with a stream of nitrogen, and the pigments were redissolved by washing with several small (0.5-ml) portions of hexane.

The chromatographic apparatus was obtained as a unit (No. 57824) from Scientific Glass Apparatus Co., Bloomfield, N.J. The column was prepared by the addition of a slurry of starch (Analar, reagent grade) in hexane and packed under pressure (100 cm of water) from a nitrogen cylinder to a height of 20 cm. The sample was applied to the top of the column, under the same pressure at which the column was packed, and washed on with two 10-ml portion of hexane. Approximately 200 ml of hexane was then added to the reservoir at the top of the column, and allowed to percolate through the column under pressure.

With representatives of the Chrysophyceae, Dinophyceae, Myxophyceae and Bacillariophyceae, a single chromatographic separation sufficed to resolve the pigments into their major components. No attempt was made to separate isomers of the different pigments or to resolve the different carotenes. Following the elution of the carotenes with hexane, the eluting solvent was changed to 0.5% *n*-propanol in hexane which removed chlorophyll *a* followed by the xanthophylls. Fucoxanthin, peridinin and an unidentified xanthophyll from *Agmenellum quadruplicatum* moved very slowly with 0.5% *n*-propanol in hexane, and usually were eluted with 2% *n*-propanol in hexane.

With representatives of the Chlorophyceae it was found that the chlorophylls would not separate from two xanthophylls (Fractions II and III in Table II) on elution with 0.5% *n*-propanol in hexane. The combined fraction of chlorophylls and xanthophylls was therefore chromatographed again on starch and eluted with hexane. The xanthophylls which ran ahead of the chlorophylls were cut out of the column and eluted with acetone. Two closely associated xanthophyll bands (Fractions IV(A) and (B) in Table II) which remained behind on the original column after elution with 0.5% *n*-propanol in hexane were similarly eluted with acetone.

Spectra of the various pigments were measured in hexane, also in carbon disulphide and chloroform when their identity was uncertain. Measurements

were made using a Beckman DU spectrophotometer and the pigments identified from absorption spectra reported by a number of authors (Strain *et al.*, 1944; Deuel, 1951; Goodwin, 1955; Dales, 1960). The quantity of carotenoid present in each fraction was estimated from the volume of the effluent and the optical density of the carotenoid at the wavelength of maximum absorption. When the specific absorption coefficient was not known, the specific absorption coefficient for β-carotene was used to calculate the approximate quantity of a pigment (Goodwin, 1955).

Preparation of Chlorophyll *c*

In order to confirm the presence of chlorophyll *c* in certain species a separation of this pigment from most of the carotenoids and chlorophyll *a* was achieved by the following procedure.

Plants were extracted with 90% acetone in the presence of a small amount of magnesium carbonate. An equal volume of water was added to the acetone extract and the aqueous mixture was extracted three times with hexane. The hexane layer was discarded after each extraction. The acetone–water mixture was then extracted once with chloroform and the chloroform evaporated with a stream of nitrogen. The dried residue was taken up in methanol or ether and the spectrum measured on a Beckman DU spectrophotometer.

RESULTS AND DISCUSSION

Table I shows the quantitative distribution of chlorophylls and total carotenoids in the species studied. Chlorophyll *a* was found to be the predominant pigment in all the species studied, except *Amphidinium carteri* in which chlorophyll *c* predominated. Quantitatively, the amount of chlorophyll *a* was quite variable. The two Chrysophyceae have the least chlorophyll *a* of any class,

Table I. Chlorophylls and total carotenoids.

Species	Chlorophyll *a*	Chlorophyll *b*	Chlorophyll *c*	Total carotenoids
	mg or MSPU per 100 mg dry weight			
CHLOROPHYCEAE				
Tetraselmis maculata	1.14	0.56	0	0.38
Dunaliella salina	2.19	0.50	0	1.02
CHRYSOPHYCEAE				
Monochrysis lutheri	0.55	0	0.03	0.22
Syracosphaera carterae	0.65	0	0.15	0.32
BACILLARIOPHYCEAE				
Skeletonema costatum	1.00	0	0.56	0.28
Coscinodiscus sp.	0.23	0	0.16	0.07
Phaeodactylum tricornutum	1.44	0	0.87	0.63
Chaetoceros sp.	0.70	0	0.56	0.18
DINOPHYCEAE				
Amphidinium carteri	0.85	0	1.10	0.50
Exuviella sp.	0.72	0	0.06	0.34
MYXOPHYCEAE				
Agmenellum quadruplicatum	0.93	0	0	0.52

while the two Chlorophyceae contain relatively large amounts of chlorophyll *a*. Chlorophyll *b* was only found in the Chlorophyceae, as was to be expected from earlier reports (see review by Strain, 1951).

The large amount of chlorophyll *c* in *Amphidinium carteri* and the presence of chlorophyll *c* in the two representatives of the Chrysophyceae required further investigation in view of the inaccuracy of determining this pigment by the Richards method (Richards with Thompson, 1952). An attempt was made, therefore, to extract the chlorophyll *c* from *Amphidinium carteri*, *Monochrysis lutheri* and *Coccolithus huxleyi*. The last-named organism has been employed in these studies because it has been found in our laboratory (unpublished result) to contain considerably more chlorophyll *c* (*ca*. 50% of the chlorophyll *a*) than is reported for the two other Chrysophyceae in Table I.

The spectra for chlorophyll *c* in ethyl ether, as extracted from *Amphidinium carteri* and *Coccolithus huxleyi*, are shown in Fig. 1 and 2 respectively. The chlorophyll *c* spectrum from *Amphidinium carteri* appears to be virtually free of chlorophyll *a* and has absorption maxima at 447, 578, and 627 mμ. In methanol, the same pigment gave absorption maxima at 450, 584 and 633 mμ. These values are in good agreement with values reported by Smith and Benitez (1955) for pure chlorophyll *c* in ether and methanol. The absorption minimum for chlorophyll *c* at 500 mμ, reported by those investigators, occurred at 510 mμ

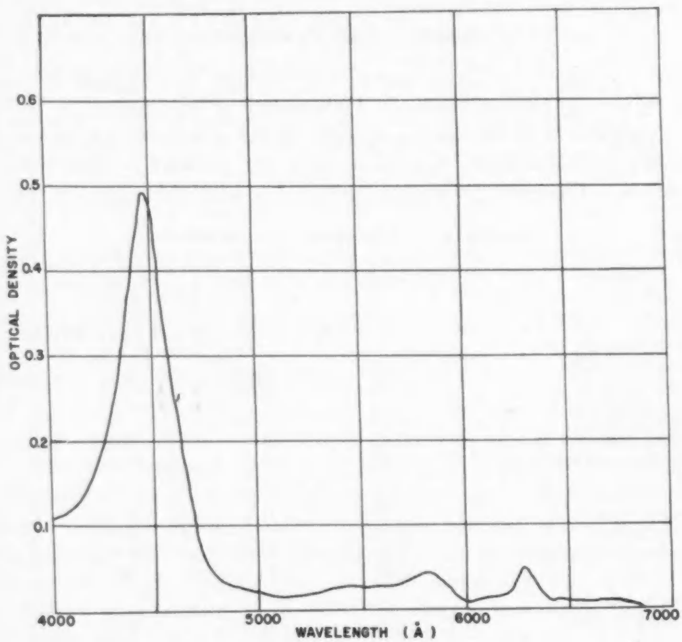

FIG. 1. Spectrum of chlorophyll *c* in ether extracted from *Amphidinium carteri*.

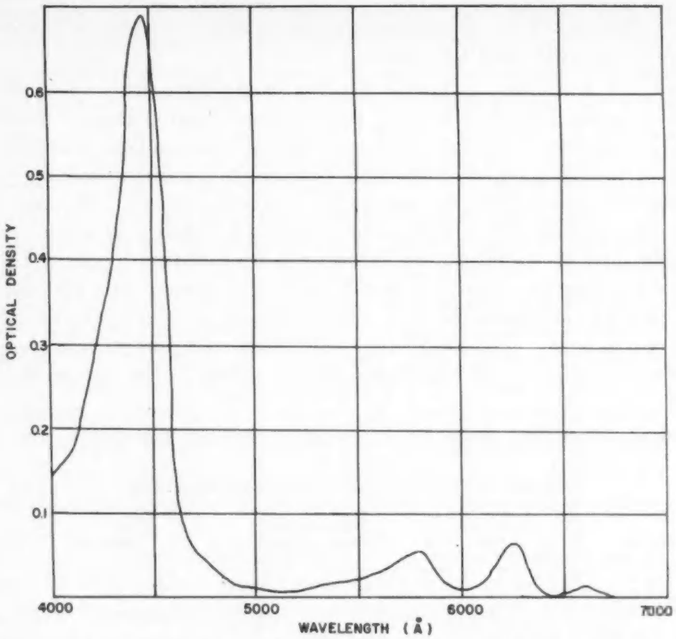

FIG. 2. Spectrum of chlorophyll *c* in ether extracted from *Coccolithus huxleyi*.

in the spectrum shown. This is probably due to contamination with a small amount of a carotenoid. The spectrum for chlorophyll *c* from *Coccolithus huxleyi* (Fig. 2) is similar to that shown for ***Amphidinium carteri*** having absorption peaks at 447, 578, 627 and 660 mμ. The small peak at 660 mμ is probably due to contamination with chlorophyll *a* which Smith and Benitez have reported as being difficult to remove completely from chlorophyll *c*. A spectrum similar to that shown for *Coccolithus huxleyi* was obtained with *Monochrysis lutheri*. Dales (1960) has reported that chlorophyll *c* is absent from the Chrysophyceae. In referring to a yellow, water-soluble pigment found in the Chrysophyceae by Gaidukov (1900), Dales concluded that this was a contaminant in the culture preparation. It would appear from the findings presented here that Gaidukov's water-soluble pigment was chlorophyll *c*.

The amount of chlorophyll *c* in *Syracosphaera carterae* and *Monochrysis lutheri* reported in Table I is quite small and could not be detected in a chromatogram. Under certain conditions, however, the amount of chlorophyll *c* in *Monochrysis lutheri* has been found to increase. The increase appears to be associated with a high light intensity, lower temperature and nutrient-deficient cells. The large amount of chlorophyll *c* in ***Amphidinium carteri*** was confirmed by measuring the amount of chlorophyll *c* obtained after removal of most of the chlorophyll *a* and carotenoids. This value was some 80% of the value found by the Richards

method (Richards with Thompson, 1952), which, considering losses during extraction, is in fairly good agreement.

There are a number of reports (Currie, 1958; Humphrey, 1960; McAllister *et al.*, 1960) showing that amounts of chlorophyll *c* often exceed chlorophyll *a* in plankton samples from ocean waters. In our own studies (McAllister *et al.*, 1960) the principal group of organisms believed to be responsible for the total crop in the Northeast Pacific Ocean are the coccolithophores. The inconsistency between this finding and Dales' (1960) reported absence of chlorophyll *c* in members of the Chrysophyceae now appears to be remedied in part. The largest amount of chlorophyll *c* found by us (*loc. cit.*) to be present in a Chrysophycean, however, was in ***Coccolithus huxleyi***. It contained about 50% of the amount of chlorophyll *a* present. This is still less than the values reported from ocean waters and further investigation of high chlorophyll *c* values in the oceans would seem necessary.

Table II shows the amount of the various carotenoids present in the different

TABLE II. Principal carotenoids of the algal cells.

Species	Fractions in order of elution	Wavelength of maximum absorption in hexane			Carotenoid	Amount
		mμ	mμ	mμ		% dry weight
CHLOROPHYCEAE						
Tetraselmis maculata	I (A)	~428,	452,	480 (β)	Carotenes	0.106
	(B)	~430,	462,	494 (α)		
	II	419,	446,	475	Lutein	0.070
	III	446,	472		Unidentified	0.041
	IV (A)	443,	476		Violoxanthin	0.039
	(B)	436,	468		Neoxanthin	
Dunaliella salina	I	~425,	450,	475	Carotenes	0.149
	II	422,	445,	477	Lutein	0.416
	III	442,	470		Unidentified	0.129
	IV	436,	467		Neoxanthin	0.049
CHRYSOPHYCEAE						
Monochrysis lutheri	I	~425,	450,	474	Carotenes	0.042
	II	447,	477		Diadinoxanthin	0.066
	III	450,	478		Fucoxanthin	0.069
Syracosphaera carterae	I	~425,	450,	480	Carotenes	0.048
	II	447,	476		Diadinoxanthin	0.107
	III	450,	480		Fucoxanthin	0.145
BACILLARIOPHYCEAE						
Skeletonema costatum	I	~425,	450,	479	Carotenes	0.050
	II	448,	477		Diadinoxanthin	0.051
	III	450,	480		Fucoxanthin	0.176
Coscinodiscus sp.	I	~425,	450,	475	Carotenes	0.012
	II	450,	480		Diatoxanthin	0.007
	III	448,	477		Diadinoxanthin	0.010
	IV	450,	480		Fucoxanthin	0.037
Phaeodactylum tricornutum	I	~425,	450,	478	Carotenes	0.059
	II	448,	477		Diadinoxanthin	0.154
	III	450,	480		Fucoxanthin	0.740
DINOPHYCEAE						
Amphidinium carteri	I	~425,	450,	478	Carotenes	0.042
	II	448,	477		Diadinoxanthin	0.129
	III	454,	485		Peridinin	0.258
Exuviella sp.	I	~425,	450,	477	Carotenes	0.025
	II	448,	477		Diadinoxanthin	0.081
	III	454,	485		Peridinin	0.130
MYXOPHYCEAE						
Agmenellum quadruplicatum	I	~425,	450,	478	Carotenes	0.213
	II	450,	479		Antherxanthin	0.162
	III	452,	480		Unidentified	0.033

~ Indicates an inflection.

species analyzed. It will be seen that fucoxanthin is the predominant carotenoid of the three Bacillariophyceae, and the two Chrysophyceae. The presence of diadinoxanthin in the Chrysophyceae agrees with results found by Dales (1960). This latter pigment was found during chromatography to run considerably slower than lutein but was inseparable from diadinoxanthin prepared from diatoms. An additional property of this compound was found to be that on treatment with dilute HCl there was a spectral shift in the wavelengths of maximum absorption in hexane from 447 and 477 mμ to 428 and 456 mμ. This shift of approximately 20 mμ is characteristic of the isomerization of 5,6-epoxides to 5,8-epoxides (Goodwin, 1955). The HCl derivative of diadinoxanthin ran above diadinoxanthin on the starch column. It was found, in fact, that if *Monochrysis lutheri* was extracted with acetone in the absence of magnesium carbonate then a second band appeared above diadinoxanthin. This was an artifact which did not occur if the cells were extracted in the presence of magnesium carbonate immediately following filtration. Allen *et al.* (1960) have not reported diadinoxanthin in the two representatives of the Chrysophyceae that they studied. However, these authors record several unknown pigments. At least one of these (Fraction D in the *Prymnesium parvum* analysis) appears to be similar to HCl-treated diadinoxanthin.

Diatoxanthin was only estimated in one diatom, *Coscinodiscus* sp. It was detected as running below diadinoxanthin in extracts of *Monochrysis lutheri* and *Phaeodactylum tricornutum* but was not observed at all in *Skeletonema costatum* or in *Syracosphaera carterae*. Its presence in the Bacillariophyceae and Chrysophyceae may be quite variable, however, since in old cultures of *Monochrysis lutheri*, grown under brighter illumination, it has been observed to occur in appreciable amounts. Allen *et al.* (1960) have reported the presence of diatoxanthin in the two Chrysophyceae they analyzed, while Dales (1960) has recorded it as being absent in the eight species studied by him.

In *Dunaliella salina* the predominant carotenoid was lutein while in *Tetraselmis maculata* it was associated with the carotene fraction. In the latter species there appeared to be two distinct carotenes present as determined by measuring the spectrum of the first part of Fraction I as compared with the last part of the fraction. The spectrum of the first part of this fraction (A) was similar to that of β-carotene while the last part (B) was similar to γ-carotene. The last fraction to be eluted from the column (Fraction IV) also was composed of two parts, the first of which (A) was spectroscopically similar to violoxanthin and the last (B) to neoxanthin. The identification of Fraction III reported for the Chlorophyceae is uncertain. The position of this fraction on the starch column would suggest that it was lutein-5,6-epoxide. However, the wavelengths of maximum absorption in carbon disulphide of 475 and 506 mμ were rather high compared with those reported by Goodwin (1955). In addition, the pigment was stable to treatment with dilute HCl, which indicated that it was not 5,6-epoxide (Deuel, 1951).

In the two dinoflagellates the principal carotenoid was peridinin. Dinoxanthin, reported to occur in dinoflagellates by Strain *et al.* (1944), was not observed. This pigment may have been, however, a minor constituent of these

species which was not detected in the presence of large amounts of the other carotenoids.

The carotenoids reported for the species of Myxophyceae, *Agmenellum quadruplicatum*, are in contrast with those reported to identify this class of organisms. Goodwin (1957) reported that the Myxophyceae are characterized by β-carotene, echinenone, zeaxanthin and myxoxanthophyll. With the exception of β-carotene, none of these pigments were found to occur in *Agmenellum quadruplicatum*. The identity of antherxanthin as one of the pigments of *Agmenellum quadruplicatum* has been based on its absorption maxima in chloroform at 460 and 490 mμ and in carbon disulphide at 480 and 510 mμ. Goodwin (1955) has reported that antherxanthin has absorption maxima at 460.5 and 490.5 mμ in chloroform and 482 and 510 mμ in carbon disulphide. On treatment with dilute HCl, the antherxanthin fraction, reported in Table II, showed a shift in the wavelengths of maximum absorption in hexane from 450 and 479 mμ to 450 and 424 mμ. Antherxanthin is the 5,6-epoxide of zeaxanthin and has been found to show an epoxide shift on treatment with HCl to give the 5,8-epoxide known as mutatoxanthin (Deuel, 1951). Mutatoxanthin has been reported by Deuel to have absorption maxima in petroleum ether at 426 and 456 mμ. While this is not a particularly close fit with the HCl-treated antherxanthin reported above, the HCl treatment was found to cause an eventual disappearance of all absorption maxima above 400 mμ which may account for the relatively poor agreement with the reported maxima.

The last fraction (Fraction III) to be separated from the *Agmenellum quadruplicatum* has not been identified. No attempt was made to characterize or estimate the phycobilin pigments in this species. On a quantitative basis the results reported here for *Agmenellum quadruplicatum* agree with the finding by Goodwin (1957) who has reported that β-carotene is the predominant carotenoid of the Myxophyceae. There have been other reports (for references see Goodwin, 1957) on the presence of xanthophylls in the Myxophyceae other than echinenone, zeaxanthin and myxoxanthophyll. None of the reported pigments agree with the finding presented here, however, and the only other reported occurrences of antherxanthin have been in the anthers of flowers (Deuel, 1951) and in the echinenoids and asteroids (Fox, 1953).

Recent experiments in this laboratory have shown that the specific absorption coefficient of peridinin is less than half that of β-carotene on which the determination of the former pigment was based. This would increase the amount of peridinin found in the two dinoflagellates by a factor of approximately 2.5. The specific absorption coefficient of chlorophyll *c* employed for the determinations cited above also is in doubt. Recent evidence indicates that the chlorophyll *c* determinations reported here have been overestimated by a factor of approximately 2.

ACKNOWLEDGMENT

The author would like to express his thanks to Mr Wing Wai for technical assistance during the course of these studies.

REFERENCES

ALLEN, M. B., T. W. GOODWIN AND S. PHAGPOLNGARM. 1960. Carotenoid distribution in certain naturally occurring algae and some artificially induced mutants of *Chlorella pryenoidosa*. *J. Gen. Microbiol.*, **23**: 93–103.

CURRIE, R. I. 1958. Some observations on organic production in the North East Atlantic. *Rapp. et Proc-Verb., Cons. Expl. Mer.*, **144**: 96–102.

DALES, R. P. 1960. On the pigments of the Chrysophyceae. *J. Mar. Biol. Ass. U.K.*, **39**: 693–699.

DEUEL, H. J. 1951. The Lipids. Interscience Publishers, Inc., New York, Vol. 1: 507–666.

FOX, D. L. 1953. Animal biochromes and structural colours. Cambridge Univ. Press, Cambridge, 378 pp.

GAIDUKOV, N. 1900. Ueber das Chrysochrom. *Ber. dtsh. bot. Ges.*, **18**: 331–335.

GOODWIN, T. W. 1955. Carotenoids. Modern Methods of Plant Analysis. Springer-Verlag, Berlin, Vol. III: 272–311.

1957. The nature and distribution of carotenoids in some blue-green algae. *J. Gen. Microbiol.*, **17**: 467–473.

HASKIN, H. H. 1941. The chloroplast pigments in *Chlorella pyrenoidosa*. Thesis, Dept. Biol., Harvard Univ.

HUMPHREY, G. F. 1960. Concentration of plankton pigments in Australian waters. C.S.I.R.O. Aust. Fish. Oceanogr. Tech. Pap. No. 9, Melbourne, 27 pp.

MCALLISTER, C. D., T. R. PARSONS AND J. D. H. STRICKLAND. 1960. Primary productivity at Station "P" in the North-East Pacific Ocean. *J. Conseil Expl. Mer*, **25**(3): 240–259.

PARSONS, T. R., K. STEPHENS AND J. D. H. STRICKLAND. 1961. On the chemical composition of eleven species of marine phytoplankters. *J. Fish. Res. Bd. Canada* **18**(6): 1001–1016.

RICHARDS, F. A., WITH T. G. THOMPSON. 1952. The estimation and characterization of plankton populations by pigment analysis. II. A spectrophotometric method for the estimation of plankton pigments. *J. Mar. Res.*, **11**: 152–172.

SMITH, J. H. C., AND A. BENITEZ. 1955. Chlorophylls: Analysis in plant materials. Modern Methods of Plant Analysis. Springer-Verlag, Berlin, Vol. IV: 143–196.

STANBURY, F. A. 1931. The effect of light of different intensities reduced selectively and non-selectively, upon the rate of growth of *Nitzschia closterium*. *J. Mar. Biol. Ass. U.K.*, **17**: 633–653.

STRAIN, H. H. 1951. The pigments of algae. Manual of Phycology. Chronica Botanica Co., Waltham, Mass., pp. 243–262.

STRAIN, H. H., W. M. MANNING AND G. HARDIN. 1944. Xanthophylls and carotenes of diatoms, brown algae, dinoflagellates and sea-anemones. *Biol. Bull.* **86**: 169–191.

STRICKLAND, J. D. H., AND T. R. PARSONS. 1960. A manual of seawater analysis. *Bull. Fish. Res. Bd. Canada*, No. 125, 185 pp.

ABS

INT

GEO
C
C

PRO
I
D
S

T

D

W

OBS
E
T

CON

thei
mec

par

J. F
Pri

Some Oceanographic Features of Juan de Fuca Strait[1]

By R. H. Herlinveaux and J. P. Tully

Fisheries Research Board of Canada
Pacific Oceanographic Group, Nanaimo, B.C.

CONTENTS

ABSTRACT

The distribution and structure of dissolved oxygen, salinity, temperature and density, and their seasonal and tidal variations are summarized, and related to the tidal and estuarine mechanisms.

Juan de Fuca Strait is a complex, deep, positive estuary. It is divided into inner and outer parts by a sill extending southward across the channel from Victoria, B.C. The Inner Strait

[1]Received for publication May 23, 1961.

J. Fish. Res. Bd. Canada, 18(6), 1961.
Printed in Canada.

is separated from the Strait of Georgia by the San Juan Archipelago. The water structure in the Strait of Georgia is highly stratified due to the shallow brackish upper zone maintained by the Fraser River discharge. This brackish water tends persistently seaward due to the estuarine mechanism. In the passages through the San Juan Archipelago the shallow and deep waters are mixed to near homogeneity by the turbulent tidal flows. In the Inner Strait the stratification is small. Part of this mixed water is fed back into the lower zone of the Strait of Georgia, and part escapes seaward in the upper zone of the outer part of Juan de Fuca Strait, where it overruns the intruding ocean water, creating a new stratification. The ebb flow is stronger than the flood in this upper zone, and the halocline is deepest on the northern side of the strait.

The flood flow, augmented by the deep inflow required by the estuarine mechanism, is strongest in the lower zone. Here the ocean waters advance over the sill during the flood flow, but do not retreat during the ebb flow, which is relatively weak. These ocean waters are incorporated with the mixed waters in the Inner Strait. This mechanism is a tidal pump.

The concentration of fresh water in the upper zone of Juan de Fuca Strait varies from 2 to 6% during the year. The amount (depth of fresh water when separated from the ocean water in the system) varies from 1 to 7 m. In this and all other properties there is a gradient from the Strait of Georgia into the Inner Strait. In the Outer Strait there are cross-channel gradients, but none longitudinally.

Throughout the system the density structure is salinity dominated. During the summer the thermocline coincides with the halocline. In winter the waters are isothermal, or the upper waters become slightly colder than the deep waters. Then the stability depends on the salinity structure alone.

The salinity is a linear function of temperature within 0.1 C°, except at the surface in summer. The slope of the relation varies with time (season) and location. The relation shows that the waters throughout the system are mixtures of ocean water and brackish water from the Strait of Georgia, and tributary inlets.

INTRODUCTION

Juan de Fuca Strait (Fig. 1) is the principal approach to the Strait of Georgia and Puget Sound from the sea. Therefore, it was desirable to have an oceanographic investigation to provide complete synoptic charts of the structure, and to establish the mechanics of sea water exchange between the Strait of Georgia and the sea.

GEOGRAPHY AND CLIMATE

Geography

As shown in Fig. 1 Juan de Fuca Strait is a submarine valley extending from the ocean (Cape Flattery) to the channels of the San Juan Archipelago. It is bounded on the north by the low (600-m) Seymour Range on Vancouver Island, and on the south by the high (1800-m) Olympic Range in the State of Washington. The eastern limit borders a low (100-m) coastal plain.

The strait contains two basins (Fig. 2) where depths greater than 100 m (55 fathoms) are found. These are separated by a sill, a cross-channel ridge lying southward from Victoria, B.C., at 60 m (33 fathoms) depth. The "Inner Strait" contains several shallow banks, through which the deepest channel leads into Haro Strait, and lesser channels lead to Rosario Strait and Admiralty Inlet.

The "Outer Strait" deepens gradually to seaward to more than 200 m at Cape Flattery. Beyond the cape (Fig. 1) this valley turns southward at right

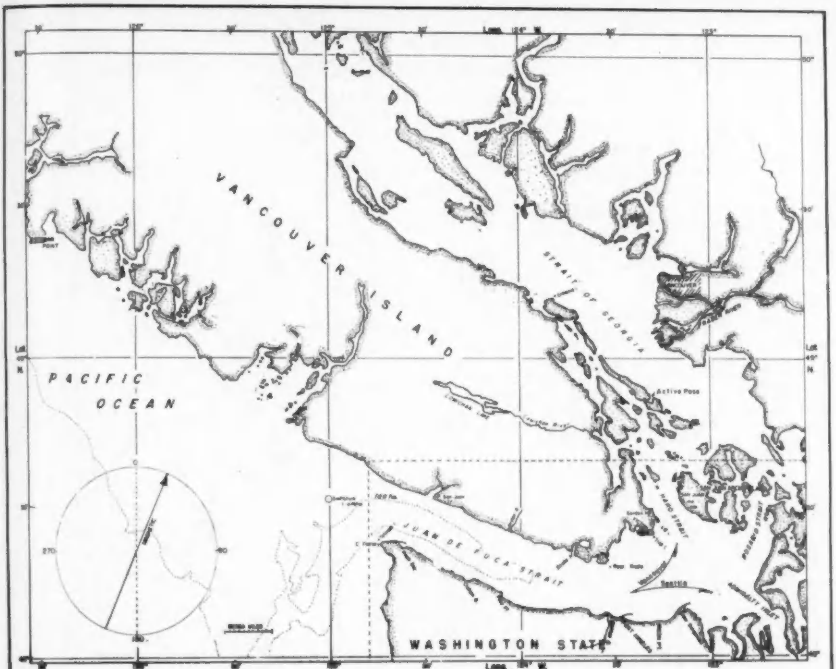

FIG. 1. Juan de Fuca Strait and adjacent sea regions (Chart 3607, Canadian Hydrographic Service, 1952).

angles and cuts through the continental shelf and down the continental slope to the ocean abyss.

CLIMATE

The weather data have been summarized by the Canadian Meteorological Service (1896–1957) and United States Weather Bureau (1953). Some features of the climate have been discussed by Kendrew and Kerr (1955).

AIR TEMPERATURE

The air temperature cycle at any one place in Juan de Fuca Strait is in phase with the air temperature cycle experienced along the whole British Columbia coast, but the range of the cycle varies along and across the channel. Figure 3 shows the annual air temperature cycle at several locations in the area. In the winter, the air at the entrance (Tatoosh Island) is warmer than in the Inner Strait (Port Angeles) by 2 C°. In summer this relation is reversed. The eastern extremity (Anacortes) is almost 10 C° warmer than Tatoosh Island during July. Across the channel, the air temperature shows a 2 C° difference from Jordan River to Clallam Bay.

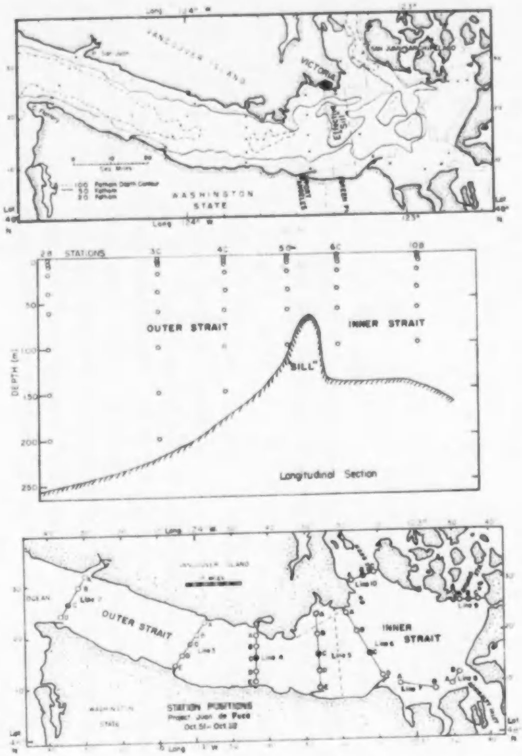

FIG. 2. Juan de Fuca Strait, showing bottom topography and locations of observations.

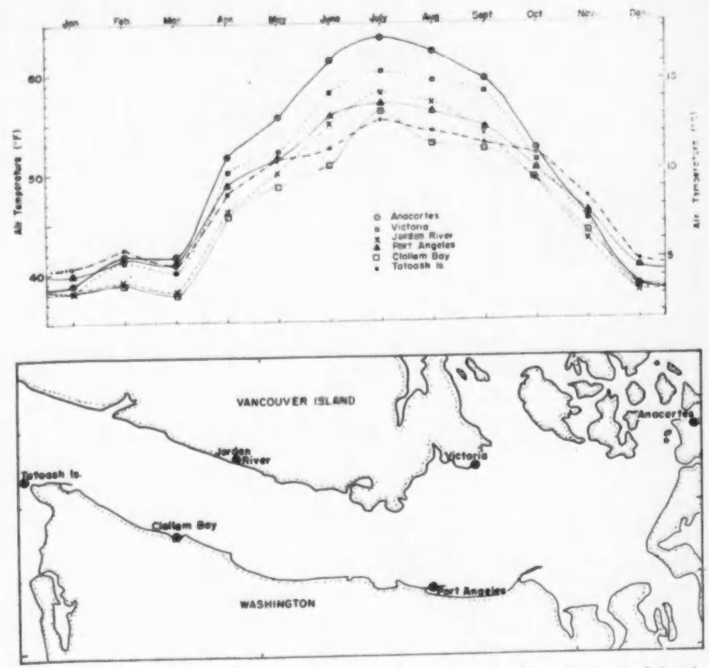

FIG. 3. Air temperatures in Juan de Fuca Strait 1952. Tatoosh Island, Port Angeles, Jordan River, Clallam Bay.

PRECIPITATION AND RUNOFF

The precipitation in Juan de Fuca Strait varies considerably from one end to the other (Fig. 4). The average precipitation at Neah Bay, at the entrance,

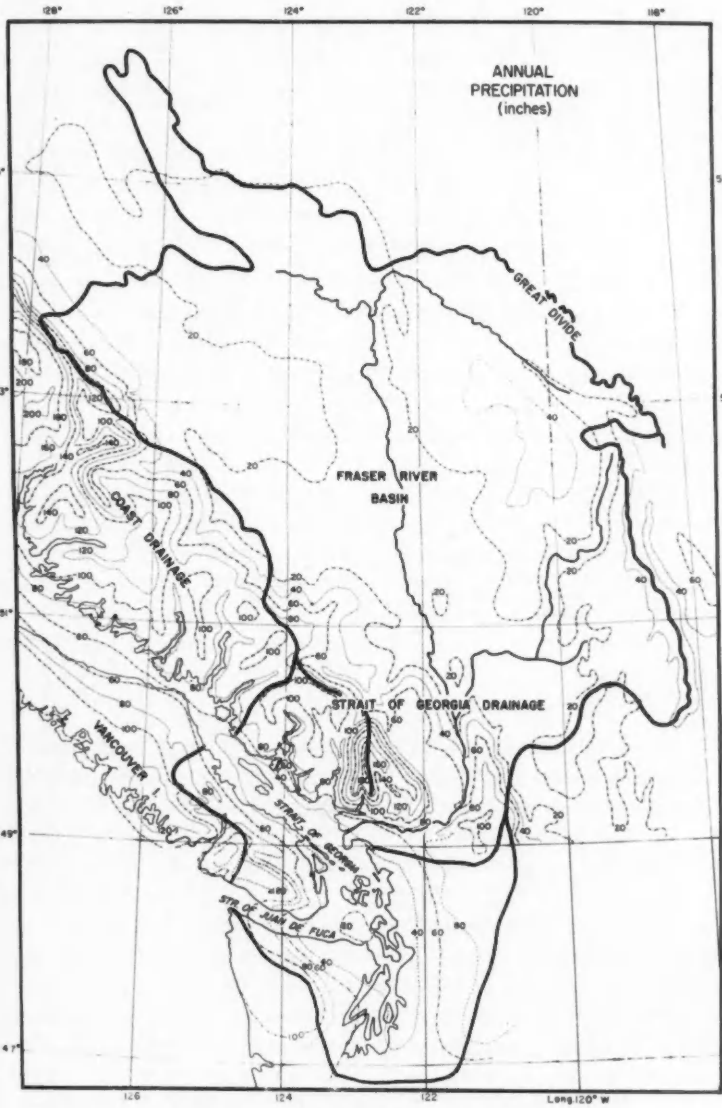

FIG. 4. Juan de Fuca drainage area and average annual precipitation.

is 272 cm (107 in) per year; at Port Angeles, 69.5 cm (27.4 in); and in the southern San Juan Islands, 49 cm (19.3 in) per year. It is noteworthy that the precipitation is much greater on the western side of the mountains than on the eastern side.

The drainage area into Juan de Fuca Strait (Fig. 4) includes the surface of the southern part of the Strait of Georgia (Waldichuk, 1957), Puget Sound, and the many smaller seaways. It also includes the islands of the San Juan Archipelago, adjacent islands, the southeastern coastal slopes of Vancouver Island, coastal slopes of the adjacent mainland, and the basin of the Fraser River, which extends inland for 1500 miles (2500 km).

In this area, precipitation varies from 40 to more than 250 cm (15 to 100 in) per year, depending on the location. Generally it is greatest on the western side of the mountains, and decreases from seaward to the interior of British Columbia. In general, the precipitation is greatest in winter and least in late summer (Fig. 5).

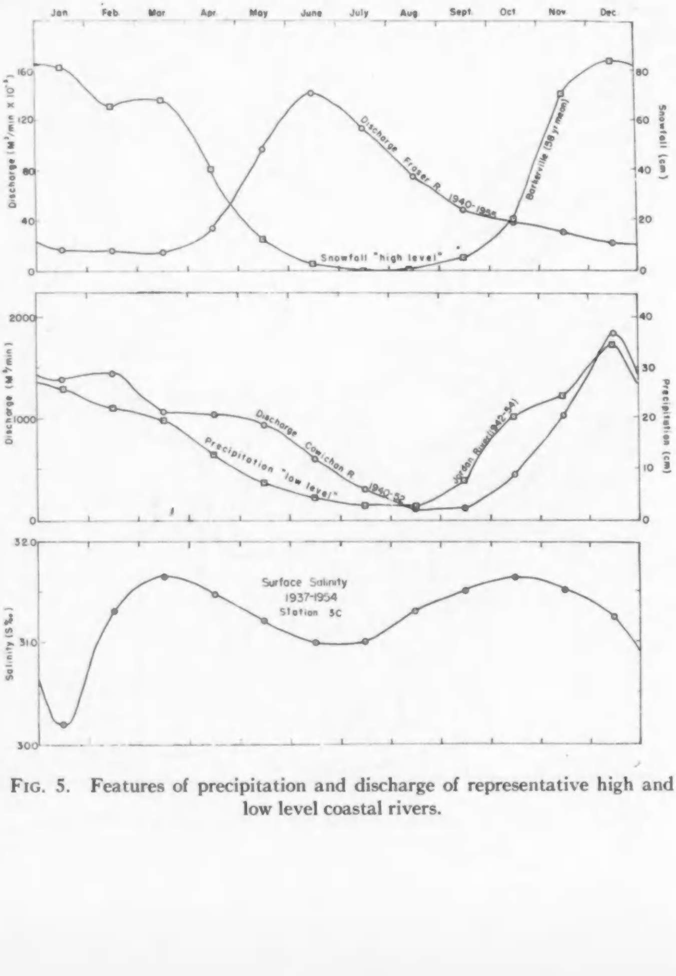

FIG. 5. Features of precipitation and discharge of representative high and low level coastal rivers.

Most of the drainage areas are high mountainous regions where winter snow storage plays a major part in regulating the runoff. The snow cover advances to sea level in January, and retreats to the permanent snow level at about 1500 m (5000 ft) altitude in September. The precipitation is greatest at high levels but drainage does not occur until the spring thaws, so that rivers draining the high levels commence to rise in late March, and reach their maximum discharge in June. This is particularly true of the Fraser River (Fig. 5) (Canadian Water Resources Branch, Annual).

The coastal climate at sea level is mild, and in the winter, when precipitation is greatest, this usually occurs as rain. Even when there is snow, this seldom lies as long as a month (January). The land drainage at low levels near the sea closely follows the precipitation and is greatest in winter. This is illustrated in the discharge of the Cowichan River in the middle diagram of Fig. 5.

The average annual precipitation in the Fraser River basin was compared to the precipitation into the whole drainage basin of the Straits of Georgia and Juan de Fuca. From this study it was deduced that 70 to 75% of the fresh water in the system is supplied by this one river. Undoubtedly the proportion is greater in June and less in January, but it is the principal fresh water source, and all others may be regarded as local.

The rivers discharging into Juan de Fuca Strait from the northern (Canadian) side are generally the "low level" type similar to the Cowichan River (Fig. 5) whose maximum discharge occurs in winter. On the southern side of the strait, the head waters of the rivers are in the high Olympic Mountains where the winter precipitation is stored as snow. The maximum discharge of these rivers occurs in the summer. Thus there are two periods of high runoff; one associated with the melting snow at high levels, and lesser, local maxima in winter associated with the peak of coastal precipitation.

WINDS

The principal winds (Canadian Meteorological Service, 1896–1957) along the ocean coast (Fig. 6) are southeasterly in winter, and northwesterly in summer, parallel to the general coastline. However, there is considerable diversion in the Strait of Juan de Fuca where the southerly winds tend to blow seaward along the strait, while the northwesterly winds tend to blow inwards (Harris and Rattray, 1954).

In Juan de Fuca Strait the winds are limited by the geography, as in most of the coast inlets. The seaward, easterly winds are generally associated with southeast winds along the coast, and increase in strength to seaward. Reed (1931) suggested that these coastal winds had a venturi effect, accelerating the normally light easterly winds in the outer reaches of the strait. Out of 75 occurrences of winds greater than 50 mph at Tatoosh, the average was 60 mph. The average of the corresponding winds at Port Angeles was 16 mph.

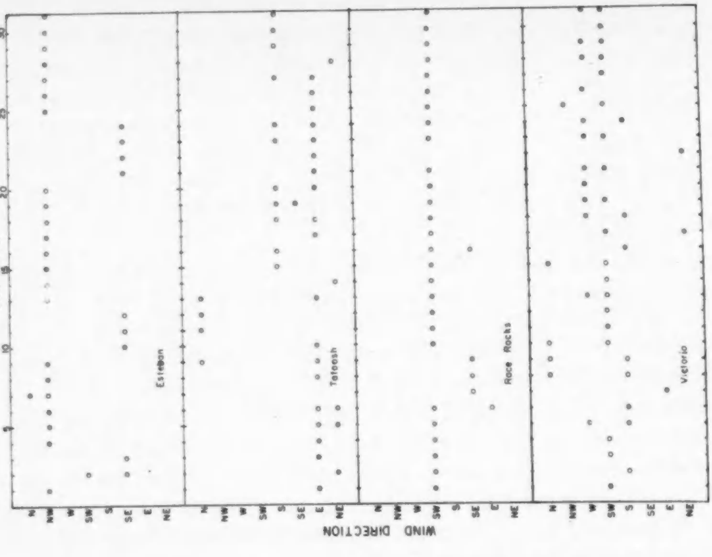

FIG. 7. Semi-daily observations of wind directions along the ocean coast and in the Juan de Fuca region.

FIG. 6. Principal winds along the ocean coast and in the Juan de Fuca region.

The westerly winds, blowing inward in the strait, are usually associated with northwest winds along the coast. They are diverted and channelled up the strait by the orographic effect of adjoining mountains. However, they also occur as strong afternoon winds during summer, when the coastal winds are light. Generally these winds are strongest off Victoria and in the Inner Strait.

It may be deduced from a study of Fig. 7 and similar data that the winds at Tatoosh, at the entrance to Juan de Fuca Strait, are affected by the wind systems in the strait and along the coast. They show no definite trends, and evidently exhibit characteristics of both. Observations made during oceanographic surveys indicate that a few miles seaward of the entrance, the coastal winds, as recorded at Esteban (Estevan) Point, are dominant. A few miles into the strait, the Juan de Fuca winds, as recorded at Victoria or at points along the strait, are dominant.

The observed winds at Victoria (Fig. 1) through the period 1922 to 1946 have been summarized by Boughner and Thomas (1948) as shown in Table I.

TABLE I. Analyses of wind data from Victoria, B.C., January 1922–December 1945. (Boughner and Thomas, 1948).

	Jan.	Feb.	Mar.	Apr.	May	June	July	Aug.	Sept.	Oct.	Nov.	Dec.
Percentage frequency (by directions)												
North	30	31	19	14	10	6	4	5	14	24	31	28
Northeast	18	15	10	9	6	4	4	5	10	12	15	14
East	14	12	10	8	6	4	4	5	8	11	14	14
Southeast	11	10	8	6	4	2	2	2	4	8	10	14
South	7	7	9	10	13	15	16	17	15	12	8	9
Southwest	7	8	16	22	29	34	40	37	21	12	11	7
West	11	14	24	28	30	33	29	26	24	17	12	12
Northwest	2	2	3	2	1	1	*	1	1	2	2	1
Calm	*	1	1	1	1	1	1	2	3	2	1	1
Average wind speed in miles per hour (by directions)												
North	10.4	10.3	10.0	9.0	8.5	7.1	5.5	6.1	7.2	8.7	9.2	9.7
Northeast	12.8	10.5	8.2	8.6	7.5	6.3	6.1	6.1	7.3	7.3	8.8	12.3
East	8.2	7.8	7.8	7.1	6.2	5.5	4.7	5.2	5.3	5.8	7.3	8.6
Southeast	16.1	16.8	14.3	12.5	11.2	7.0	5.4	6.1	8.4	12.2	15.8	17.7
South	10.8	8.9	8.1	7.8	8.6	9.2	8.4	8.4	6.9	7.2	9.3	11.7
Southwest	20.5	18.4	17.8	16.0	15.7	14.7	15.1	13.5	11.5	11.2	17.8	21.5
West	16.2	14.4	14.2	13.9	13.7	14.5	12.6	12.0	11.2	12.0	14.8	16.8
Northwest	7.0	6.3	6.3	6.5	5.0	4.7	3.6	4.1	4.5	5.0	6.5	6.4
Average wind speed in miles per hour												
	12.4	11.6	11.6	11.7	12.0	12.3	11.9	10.6	8.7	8.9	10.7	12.8

*Indicates less than 0.5%.

The analysis of percentage frequency shows that there is no direction from which the winds predominate. Rather, the outward-blowing winds (N, NE, E, SE) occur more than 50% of the time during the winter (October through March). The inward-blowing winds (S, SW, W) predominate during the summer (April

through September). Furthermore, the inward-blowing winds (westerly), whenever they occur, are always stronger than the outward-blowing (easterly) winds.

The principal oceanographic effect of the winds in Juan de Fuca Strait is to accelerate or retard the surface seaward transport. It is probable that the occasionally observed intrusions of ocean water along the southern side of the strait are associated with periods of westerly winds.

FOG

Figure 8 shows that the frequency of fog reaches its maximum from July through October, and is a minimum in the winter and spring months. From observations taken in 1952, there seems to be a tendency for the fog to hold to

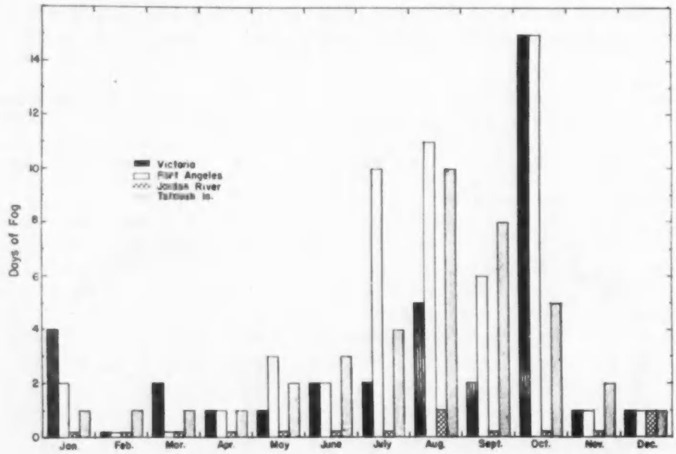

FIG. 8. Occurrence of fog in Juan de Fuca Strait at Victoria, Port Angeles, Jordan River and Tatoosh Island (1952).

the Washington side of Juan de Fuca Strait. This may be due to the cold air coming off the Olympics, meeting the warm moist air coming in off the Pacific, or it may be due to the cool water intrusion from the sea along the Washington coast.

PROPERTIES AND STRUCTURE OF THE WATER

INVESTIGATIONS

The properties of the water currents in Juan de Fuca Strait were observed at approximately bi-monthly intervals from October 1951 to October 1952, according to the plan shown in Fig. 2 (bottom diagram), and the schedule shown in Table II. This was a joint project carried out by the Pacific Oceanographic Group of the Fisheries Research Board of Canada, and the Pacific Naval

Laboratory of the Defence Research Board of Canada, in the oceanographic research vessel CNAV *Ehkoli*, operated by the Royal Canadian Navy. The whole undertaking was directed and published by the Joint Committee on Oceanography (1955). There was a series of observations (Fig. 2) across the strait and

TABLE II. Schedule of observations.

*Cruise number**	*Period*
I	Oct. 2–13, 1951
II	Nov. 5–17, 1951
III	Feb. 28–Mar. 8, 1952
V	Apr. 16–25, 1952
VII	Jun. 3–13, 1952
IX	Jul. 10–17, 1952
X	Aug. 13–20, 1952
XI	Sep. 23–Oct. 2, 1952

*Cruise numbers are those given in the Data Record (Joint Committee on Oceanography, 1955).

across the mouths of the principal passages leading to the Strait of Georgia and Puget Sound. The stations in each section were observed in sequence while the tide was rising (or falling) and again during the opposite tidal phase on the same or following day. The bi-monthly repetition of the surveys provided periodic observations of the annual cycle of properties, while the semi-diurnal repetition provided an assessment of tidal variation.

At each station a cast was made with Mark III Fjarlie water sampling bottles (Fjarlie, 1953) at depths of 0, 2, 6, 10, 20, 40, 60, 100, 150, and 200 m, or as many of these as the depth of water allowed. The bottles carried Richter & Wiese reversing thermometers. The temperature readings were taken and corrected on board ship. Salinity samples were sealed (McCracken, 1956) and determined at the base laboratory (McCracken, 1955). Dissolved oxygen was determined by the modified Winkler method adapted for shipboard use by Tully (1949).

The oceanographic laboratories of the University of Washington (1954; 1956a,b,c) made regular monthly observations at a number of stations from 1934 through 1938, as well as a number of surveys in the area. These data have not been published, but were made available in manuscript form. Later data, 1952–56, have been published (University of Washington, 1954–1956) and have been used in this report.

The oceanography of the Strait of Georgia has been fully discussed by Waldichuk (1957) and Tully and Dodimead (1957). The properties of the water in the ocean approaches to Juan de Fuca Strait have been observed (Joint Committee on Oceanography, 1956) and some aspects of circulation have been discussed by Tully (1941).

Dissolved Oxygen

Figure 9 shows the dissolved oxygen distribution and structure observed in June 1952. The lowest surface concentrations occurred in the Inner Strait in the vicinity of the passages through the San Juan Archipelago, and particularly those leading to Puget Sound. From the Inner Strait the surface oxygen concentration increased seaward. The cross and longitudinal sections show that the concentration decreased with depth, and the iso-oxys sloped downwards to the north, i.e. to the right when looking seaward, in all parts of the system. The structure and range of concentration were markedly different in the Inner and Outer Straits. In the Inner Strait the concentration was moderate, from 5.5 to 7.5 mg/l with a uniform gradient from surface to bottom. This water (from surface to 150 m depth) was continuous with the water between 40 and 60 m depth in the Outer Strait. There was marked stratification from a high concentration in the upper zone, to the deep zone whose waters were less than 40% saturated with dissolved oxygen.

As indicated by the representative seasonal longitudinal sections in Fig. 10, the principal features of dissolved oxygen structure and distribution persist throughout the year, although the values and range of values vary somewhat. The monthly sequence of dissolved oxygen concentrations in the upper and deep zones of the Outer Strait have been assembled from all available data (1934–1952) in the bottom diagram of Fig. 10. In both the surface and the deep waters (100 m) there is a simple annual cycle with a maximum in later winter (end of February), and a minimum at the end of summer (September). The range of dissolved oxygen concentration from surface to 100 m depth appears to be greatest in July and least in February.

The cross-sections in Fig. 11 show that at any position in the strait the dissolved oxygen concentration was slightly less during the flood than during the ebb tidal phase. It is notable that the cross-channel slope of the iso-oxys was most marked during the ebb. In the illustrated longitudinal sections (October) they indicate marked differences of structure in the vicinity of the sill. During the flood, the deep iso-oxys from the Outer Strait advanced up the seaward slope of the sill, and waters having oxygen concentrations as low as 4.0 mg/l were continuous over the sill into the Inner Strait. During the ebb, the deep iso-oxys in the Outer Strait were depressed, and waters having less than 4.8 mg/l were not continuous over the sill. The phenomenon occurred throughout the year, although the critical oxygen values varied with season as shown in Fig. 10.

Salinity

Figure 12 shows the salinity distribution and structures observed in June 1952. The lowest salinities occurred in the passages through the San Juan Archipelago, and extended into the inner part of Juan de Fuca Strait. From there the salinity increased towards Admiralty Inlet and to seaward. The

cross and longitudinal sections show that the salinity increased with depth, and the isohalines sloped downward to the north, i.e. to the right when looking seaward in all parts of the system. The structure and range of salinity were markedly different in the Inner and Outer Strait. In the Inner Strait the salinity was everywhere less than 32‰. This water (from near surface to 150 m depth) was continuous with the water above 50 m depth in the Outer Strait. There it formed a distinct upper zone, separated by a halocline from a deep zone whose salinity exceeded 33.5‰.

As indicated by the representative seasonal longitudinal sections in Fig. 13, the principal features of salinity structure and distribution persist throughout the year, although the values, and the range of values, vary somewhat. The monthly sequence of salinities in the upper and deep zones of the Outer Strait have been assembled from all available data (1934–1952) in the last diagram of the Figure. In the surface waters there is a marked minimum in January and a broad minimum through June and July. Maxima occur in March and October. At 100 m depth there is a single annual cycle of salinity having a minimum near the end of February and a maximum in August. Evidently the range of salinity from the surface to 100 m depth is least in March (and November) and greatest in July (and January).

The cross-sections in Fig. 14 show that at any position the salinity is slightly greater during the flood than during the ebb tidal phase. The cross-channel slope of the isohalines is steepest during the ebb. In the illustrated longitudinal sections (October) they indicate marked differences of structure in the vicinity of the sill. During the flood the deep isohalines from the Outer Strait advance up the seaward slope of the sill, and waters of salinities 32 to 33‰ are continuous over the sill into the Inner Strait. During the ebb, the deep isohalines in the Outer Strait are depressed, and waters of salinity greater than 32‰ are not continuous over the sill. This phenomenon occurs throughout the year, although the critical salinity values vary with season as shown in Fig. 13.

ZONE STRUCTURE

Tully (1958) has shown that there are definite features of salinity structure associated with estuarine systems which distinguish the regimes of fresh and sea water: He noted that there usually was an *upper zone* in which the salinity was nearly constant to a limited depth, but increased seaward. Below this was a *halocline* which was most marked near the major fresh water sources, and became less distinct to seaward, as the salinity of the upper zone increased. Below this was a *lower zone* of saline (ocean) water which was nearly homogeneous from head to mouth of the seaway, and with depth.

He deduced that the halocline is due to internal mixing and in the absence of wind it would extend to the surface. Herlinveaux (1962) observed this structure in Saanich Inlet. In the presence of wind, the waters are mixed to

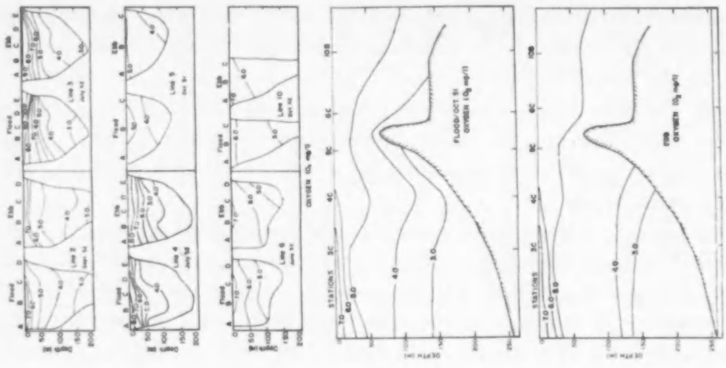

FIG. 11. Structures of dissolved oxygen observed in Juan de Fuca Strait during the flood and ebb phases of the tide.

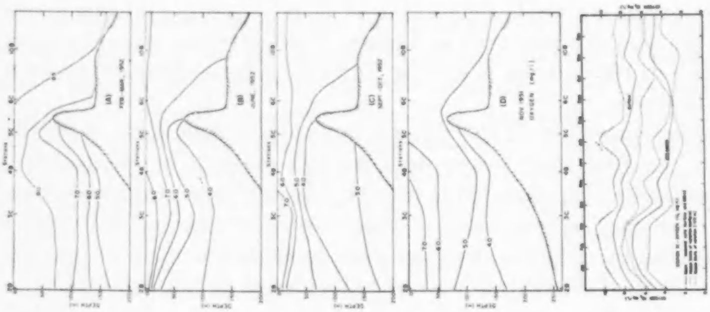

FIG. 10. Representative seasonal structures of dissolved oxygen observed in Juan de Fuca Strait, and the average monthly values at the surface and 100 m depth.

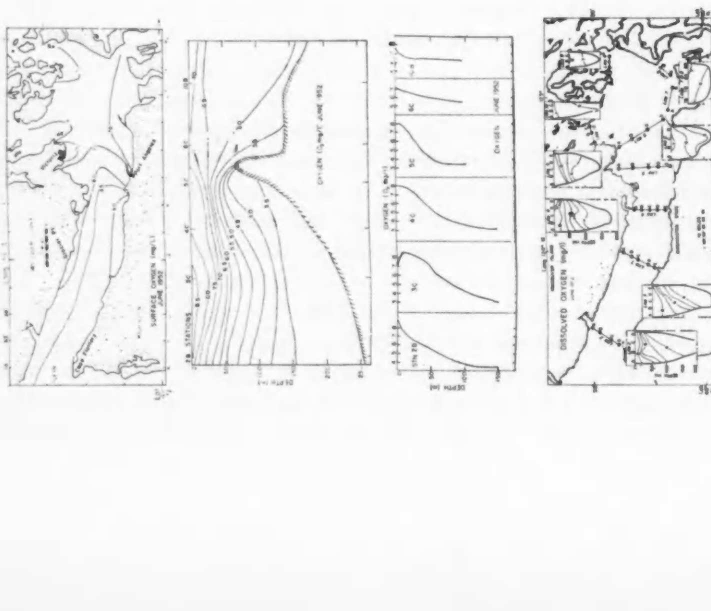

FIG. 9. Dissolved oxygen distributions and structures observed in Juan de Fuca Strait, June 1952.

FIG. 12. Salinity distribution and structures observed in Juan de Fuca Strait, June 1952.

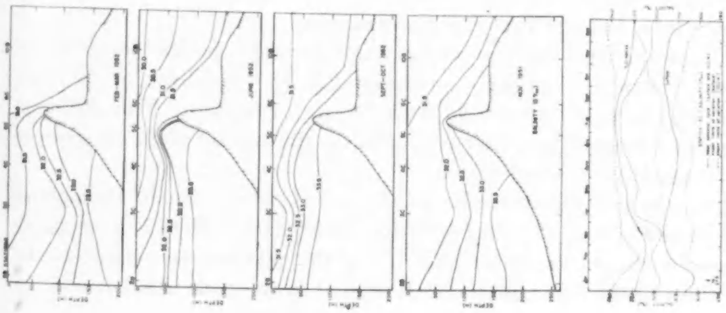

FIG. 13. Representative seasonal salinity structures observed in Juan de Fuca Strait and the average monthly values at the surface and 100 metres depth.

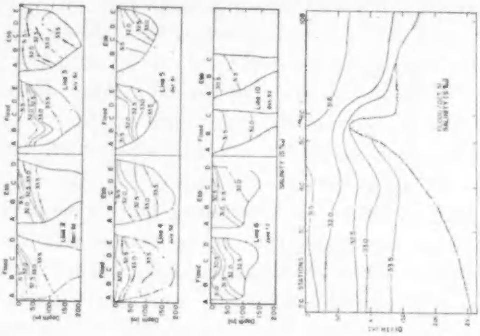

FIG. 14. Salinity structures observed in Juan de Fuca Strait during the flood and ebb phases of the tide.

homogeneity to the depth of wind influence, as Tully observed in Alberni Inlet, and Dodimead (1961) observed in the subarctic Pacific Ocean.

He also showed that when the observed salinities were plotted as functions of the logarithm of depth, the zones were defined by straight-line segments (Fig. 15) and their limits by the intersection of the segments. He designated the upper limit of the halocline as (*D*) and the lower limit as (*L*).

Tully (1952) studied this structure in Alberni Inlet where he found the zone structure simply defined as shown in the first diagram of Fig. 15. In the Strait of Georgia there was a step-structure of alternating homogeneous zones and haloclines. This resulted from the upper zone being successively over-run by successive fresh water outflows. The lower diagrams of the Figure show the zone structure in the outer basin of Juan de Fuca Strait. Here, there are two distinct segments in the halocline structure, which are characteristic of this region.

Figure 16 shows depths of the limits (*D*) and (*L*) in the several seasons. As in the corresponding salinity data (Fig. 12 to 14) there was a cross-channel slope of the surfaces, but no clear gradient to seaward.

Figure 17 shows the limits in mid-channel section. In the Outer Strait the zone structure can be identified, as shown in Fig. 15. However, in the Inner Strait the halocline extends effectively from surface to bottom. This structure is similar to that observed by Pritchard (1956) in the coastal plain estuaries of the Atlantic coast of the United States.

The depths and salinities at the limits (*D*) and (*L*) at Station 3C throughout the year are shown in Fig. 18, along with the runoff data. Here it is apparent that the characteristics of the upper limit (*D*) of the halocline are related to the runoff while those of the lower limit (*L*) are related to the cycle of salinity in the deep zone.

FRESH WATER BUDGET

It is evident that the system contains two fluids, fresh and sea water. It is of interest to consider the proportions of each.

The concentration (*C*) of fresh water in an interval of depth $(Z_1–Z_0)$ at any position, is:

$$C = \frac{S^x(Z_1-Z_0) - \int_{z_2}^{z_1} S dz}{S^x(Z_1-Z_0)}$$

where S is the observed salinity and S^x is the salinity of undiluted ocean water. This has been called the base salinity by Waldichuk (1957) and the *Index Salinity* by Tully (1958).

Ignoring the zone structure, Waldichuk solved this relation through arbitrary depth intervals (0–10 m, 10–50 m, 50–100 m) along a section through the Strait of Georgia and Juan de Fuca Strait as shown in Fig. 19. From a study of the data he concluded that the index salinity 33.8‰ was representative of the ocean water being supplied to the system at the time (September 1952). Figure 18

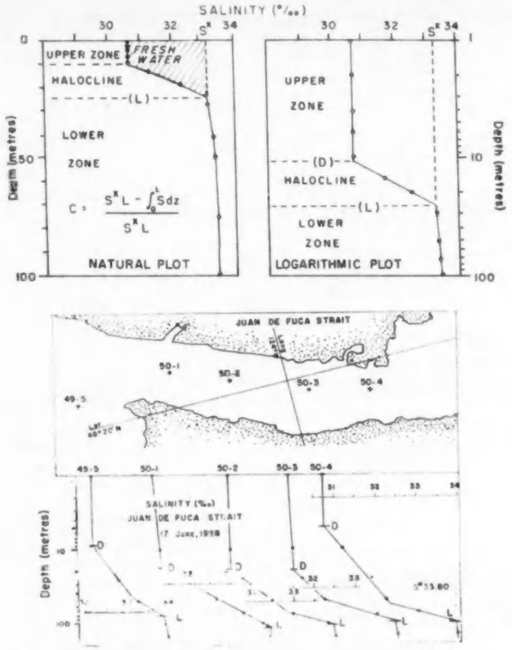

FIG. 15. Features of zone structure, and zones in Juan de Fuca Strait.

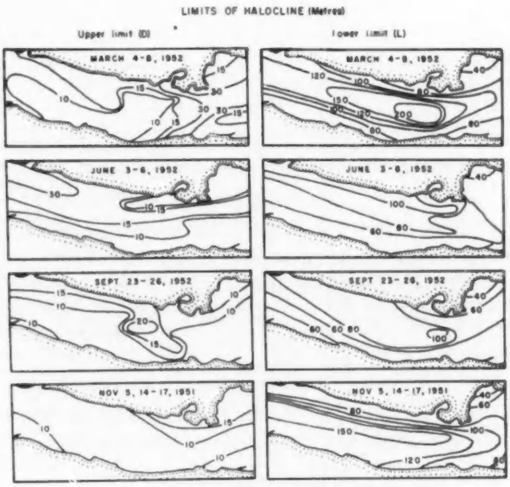

FIG. 16. Depth in metres of the upper (D) and lower (L) limits of the halocline in Juan de Fuca Strait.

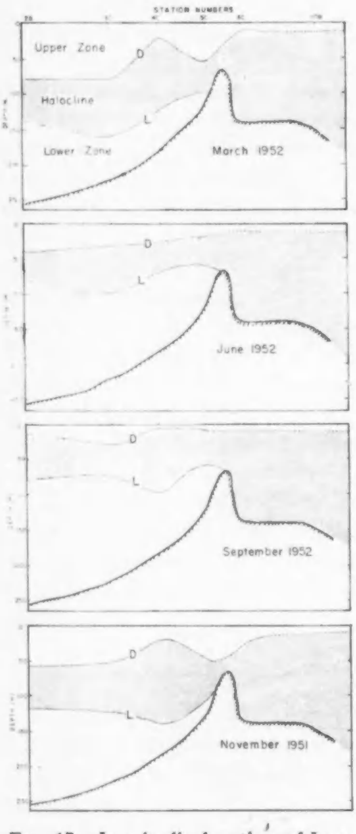

FIG. 17. Longitudinal sections of Juan de Fuca Strait showing the depth (metres) of the upper (D) and lower (L) limits of the halocline.

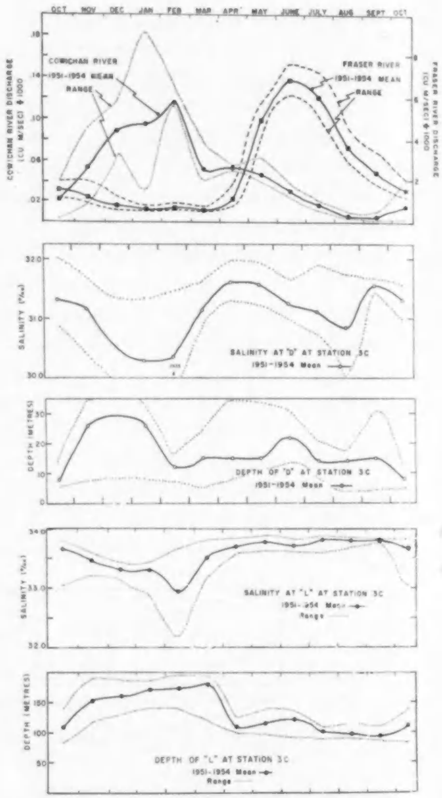

FIG. 18. Depth and salinity of the limits (D and L) of the halocline at station 3C, compared to the runoff and deep salinity.

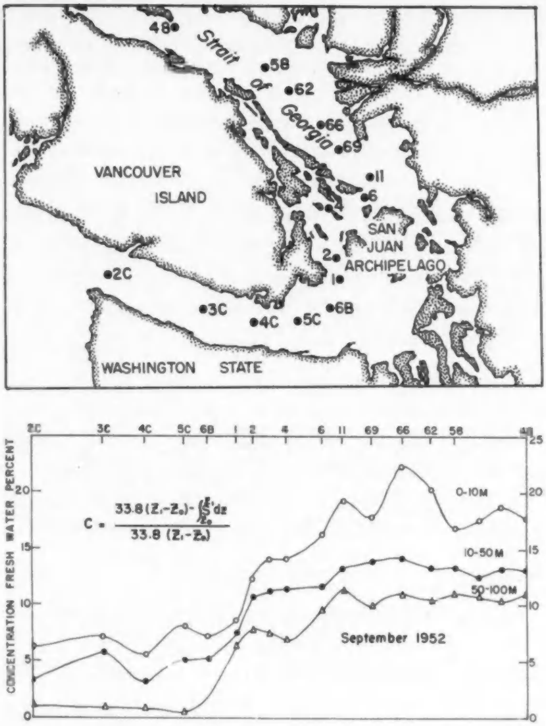

FIG. 19. Concentration (C%) of fresh water in a section through the Strait of Georgia and Juan de Fuca Strait, September 1952. (From Waldichuk, 1957.)

shows that this value coincides with the salinity at the lower limit of the halocline. He showed conclusively that the concentration (C) of fresh water decreased to seaward, and was a function of the depth interval (Z_1–Z_0) considered.

Tully (1958) deduced that when fresh water enters an embayment it moves persistently seaward through the upper zone and halocline. En route it entrains sea water from the lower zone, where there is a persistent inward transport sufficient to supply the entrainment demand. It follows that *all* the local fresh water is contained above the limit (L). The lower zone contains only intruding sea water. The character of the water being entrained into the halocline is defined by the index salinity (S^x) at the limit (L) of the halocline. Then the concentration (C) of fresh water contained in the upper zone and halocline is:

$$C = \frac{S^x L - \int_0^L S dz}{S^x L}.$$

Re-arranging this equation, the total amount of fresh water at any position may be expressed as the depth (CL) of fresh water in a unit column segregated from sea water of index salinity (S^x):

$$CL = \frac{S^xL - \int_0^L S\mathrm{d}z}{S^x}.$$

In practice, the depth of the lower limit (L) of the halocline and the corresponding index salinity (S^x) were determined in a logarithmic plot (Fig. 15). From these data a plot on a natural scale was made. Then the numerator of the equations was readily obtained by planimeter integration of the area between the salinity–depth graph, and the index salinity, as shown in the Figure.

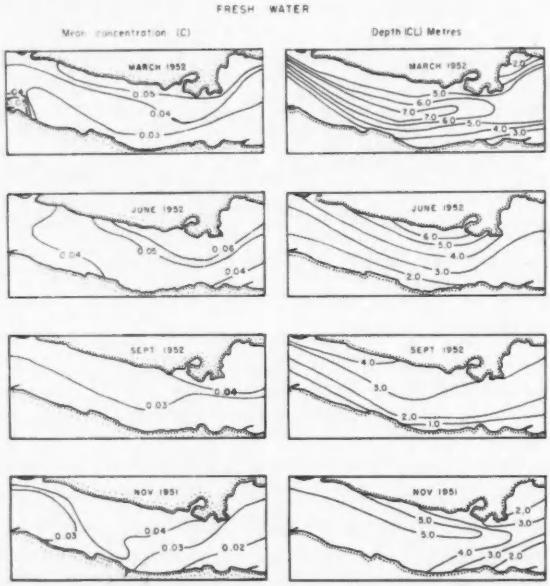

Fig. 20. The mean concentration (C) and the amount, or depth (CL metres) of fresh water contained in the upper zone and halocline in Juan de Fuca Strait.

Contours of concentration (C) and amount or depth (CL) of fresh water in the upper zone and halocline are shown in Fig. 20. Here S^x varies seasonally as shown in Fig. 18. These diagrams emphasize the cross-channel gradient of fresh water, and the lack of longitudinal gradients. Comparison with Fig. 19 shows that the concentrations of fresh water were similar to those computed by Waldichuk (1957) considering the difference in basis of computation.

Temperature

Figure 21 shows the temperature distribution and structures observed in June 1952. There was no marked horizontal gradient over the area, although the lowest surface temperatures occurred in the vicinity of the sill. The cross and longitudinal sections show that the temperature decreased with depth, and that the isotherms generally sloped downward to the north, in all parts of the system. The structure and range of the temperature were markedly different in the Inner and Outer Strait. In the Inner Strait the temperature was everywhere greater than 7.5°C and there was no distinct thermocline. This water, from surface to 150 m depth, was continuous with the water above 50 m depth in the Outer Strait. There it formed a distinct upper zone, separated by a thermocline from a deep zone, whose temperature was less than 7.0°C.

It is notable that the summer thermocline was coincident with the halocline; hence the zone structure, based on salinity, can be extended to temperature. This is quite different from conditions in the ocean, where Dodimead (1961) has shown that the thermocline structure occurs wholly within the upper zone.

As indicated by the representative seasonal longitudinal sections in Fig. 22 these features of temperature structure and distribution persist through spring, summer and autumn (June, September, November), although the range of values varies considerably. In winter (March) the structure is reversed, the coldest water being on the surface and the warmest in the depths. The monthly sequence of temperatures in the upper and deep zones of the Outer Strait has been assembled from all available data (1934–1952) in the bottom diagram of the Figure. In the surface waters there is a single annual cycle of temperature with a marked minimum in February and a broad maximum through June, July, and August. In the deep zone, as represented by the data from 100 m depth, there is a simple annual cycle, opposite in phase to that at the surface. A marked maximum occurs in January and a broad minimum occurs through the summer.

The temperature decreases with depth (negative gradient) from March to December, and the maximum range occurs in August. The temperatures increase with depth (positive gradient) from December to March and the range is greatest in February. The waters are generally isothermal in December and late March.

The cross-sections in Fig. 23 show that during the summer at every position, the water is slightly colder during the flood than during the ebb tidal phase. Further, the cross-channel slope of the isotherms is most marked during the ebb. In the illustrated longitudinal sections (October) the isotherms indicate marked differences of structure in the vicinity of the sill. During the flood, the deep isotherms from the Outer Strait advance up the seaward slope of the sill, and waters of temperatures 8 to 9°C are continuous over the sill into the Inner Strait. During the ebb, the deep isotherms in the Outer Strait are depressed and waters colder than 9°C are not continuous over the sill. This phenomenon occurs throughout the year, although the definitive temperatures vary with season as shown in Fig. 22.

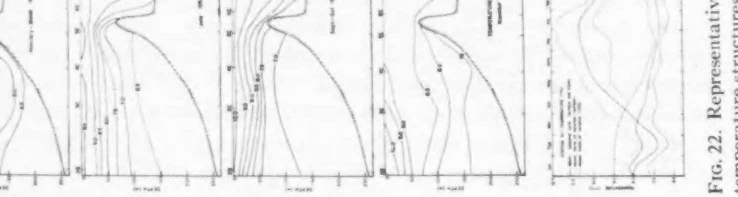

FIG. 21. Temperature distribution and structures observed in Juan de Fuca Strait, June 1952.

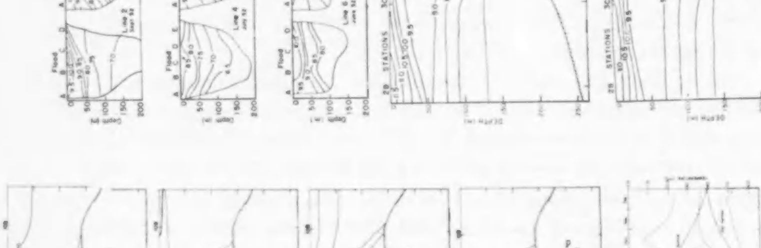

FIG. 22. Representative seasonal temperature structures observed in Juan de Fuca Strait, and the average monthly values observed at the surface and 100 m depth.

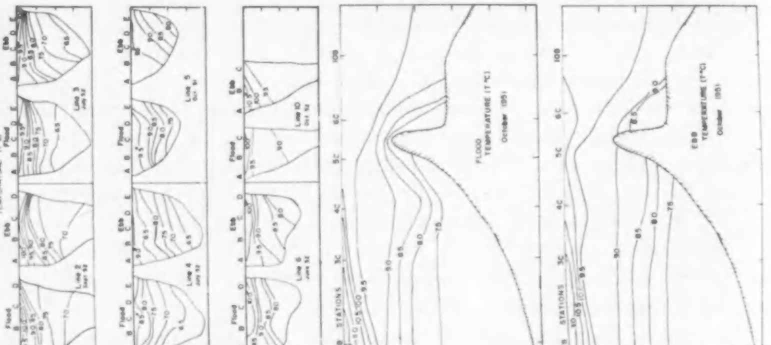

FIG. 23. Temperature structures observed in Juan de Fuca Strait during the flood and ebb phases of the tide.

HEAT BUDGET

Waldichuk (1957) studied the heat budget in the Strait of Georgia and Juan de Fuca Strait, on the basis of data observed in 1950. It is expedient to summarize some of the major features here for ready reference.

The net heat exchanges between the sea and atmosphere, computed from Waldichuk's data, are shown in Fig. 24. These include the heat gain from the sun, corrected for reflection and cloud cover; and the heat losses due to back radiation from the sea surface, evaporation, and conduction. These show that there is a heating situation through the warm months from the end of March through September. A cooling situation exists through the rest of the year. Further the heat exchange follows the same general cycle in the Strait of Georgia (Entrance Island) as in Juan de Fuca Strait (Victoria).

It may be argued that in a stagnant basin the water temperatures would be a simple function of the heat content, and would follow the integral of the heat-exchange curve. The maximum temperatures would occur in September and the minimum in March. This is not quite the case in Juan de Fuca Strait, as shown in the middle diagram of Fig. 24.

Waldichuk computed the discrepancy between the heat exchange and the heat contained in the water, and concluded that heat was being transported out of (and into) the system as indicated in the bottom diagram of Fig. 24.

While passing from the Strait of Georgia to Juan de Fuca Strait the surface water temperatures decrease in the San Juan Passages during the summer, as shown in Fig. 25. This decrease in surface temperature is due to the extensive tidal mixing in the passages. As the shallow (10-m) warm upper zone progresses seaward, it is mixed to near homogeneity with almost 100 m of cool lower-zone water. Hence there is a heat transport out of the Strait of Georgia. In winter (March) the relation is reversed because the surface waters of the Strait of Georgia become colder than the deep waters. At this time there is a heat transport into the region.

DENSITY[2]

Figure 26 shows examples of the density (σ_t) structures observed in June 1952. The lowest values occurred in the passages through the San Juan Archipelago, and extended into the Inner Strait. From there, the density increased toward the Washington State side of the strait and to seaward. The cross and longitudinal sections show that the density increased with depth, and the isopycnal surfaces sloped downward to the north, in all parts of the system. The structure and range of density were markedly different in the Inner and Outer Strait. In the Inner Strait, σ_t was everywhere less than 25.0. This water (from surface to 150 m depth) was continuous with the water above 50 m depth in the Outer Strait. There it formed a distinct upper zone separated by a pycnocline from a deep zone whose σ_t value exceeded 26.5.

[2]In this paper density is expressed as σ_t = (specific gravity−1)1000 (Sverdrup *et al.*, 1946).

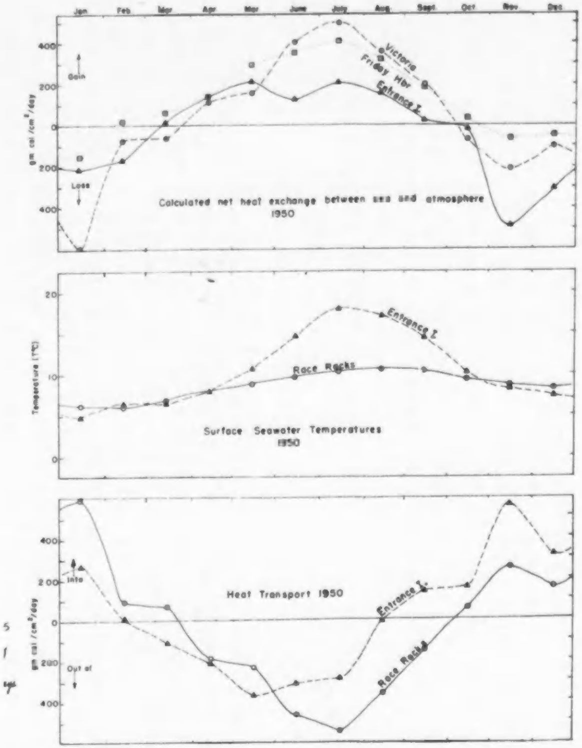

FIG. 24. Heat exchange between the sea and atmosphere, and resultant seawater temperature at locations in the Strait of Georgia and Juan de Fuca Strait, and heat transport into and out of the system (from Waldichuk, 1957).

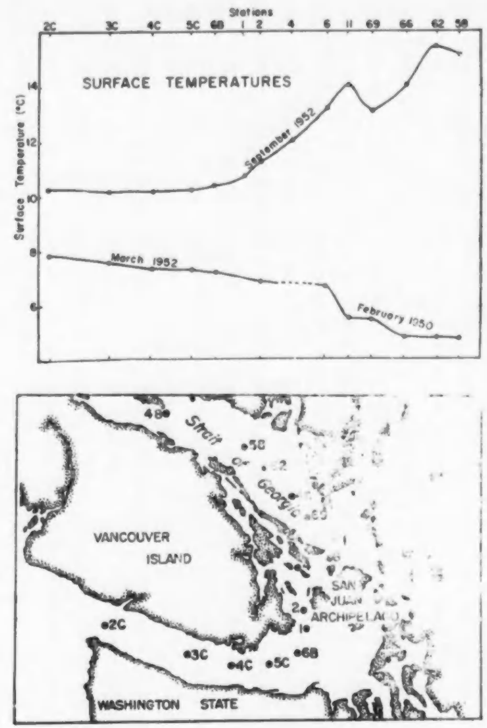

FIG. 25. Surface water temperatures through the Strait of Georgia and Juan de Fuca Strait in September and March 1952.

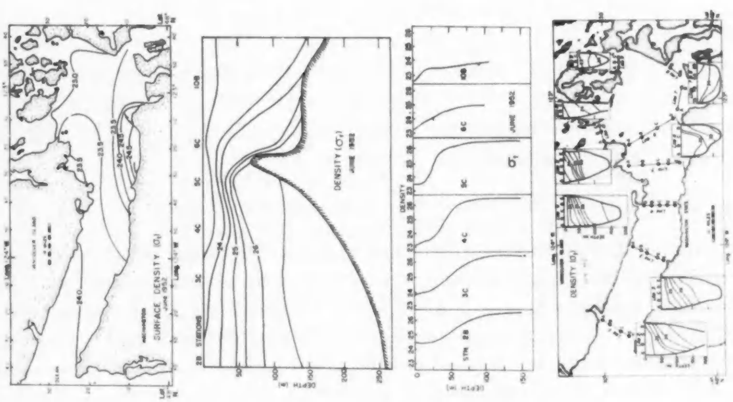

FIG. 26. Density (σ_t) structures observed in Juan de Fuca Strait, June 1952.

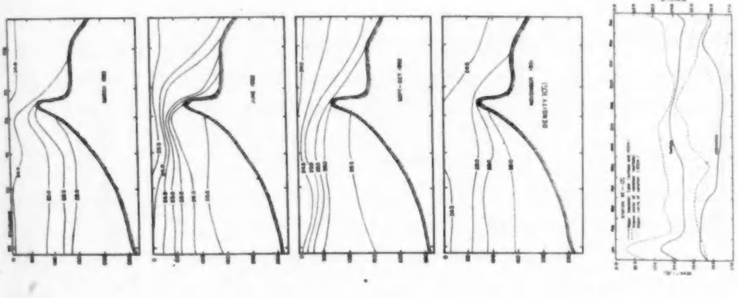

FIG. 27. Representative seasonal density (σ_t) structures observed in Juan de Fuca Strait, and the average monthly values at the surface and 100 metres depth.

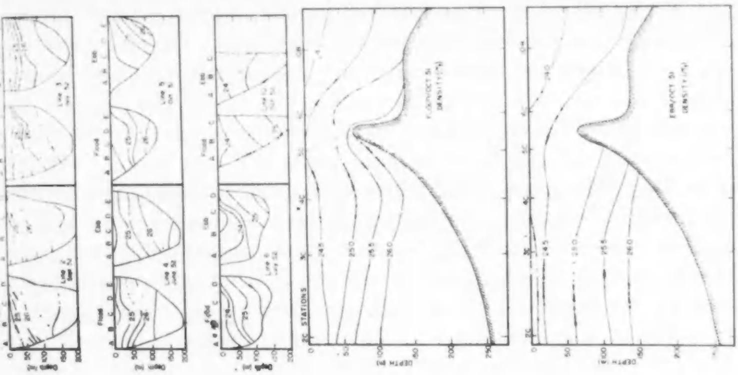

FIG. 28. Density (σ_t) structures in Juan de Fuca Strait observed during the flood and ebb phases of the tide.

As indicated by the representative seasonal longitudinal sections in Fig. 27 the principal features of density structure and distribution persist throughout the year, although the values and range vary somewhat. The monthly sequence of density in the upper and deep zones of the Outer Strait have been assembled from all available data (1934–1952) in the last diagram of the Figure. In the surface waters there is a marked minimum in January and a broad minimum through June to July. Maxima occur in early and late winter. At 100 m depth there is a single annual cycle of density having a broad minimum in winter and a maximum in summer. Evidently the range of density from surface to 100 m depth is least in February and November and greatest in July and January.

The cross-sections in Fig. 28 show that at any position the density is slightly greater during the flood than during the ebb tidal phase. The cross-channel slope of the isopycnal surfaces is most marked during the ebb. In the illustrated longitudinal sections (October) they indicate marked differences of structure in the vicinity of the sill. During the flood the deep isopycnals from the Outer Strait advance up the seaward slope of the sill, and waters of σ_t 25.0 to 26.0 are continuous over the sill into the Inner Strait. During the ebb the deep isopycnals in the Outer Strait are depressed, and waters of σ_t greater than 25.0 are not continuous over the sill. This phenomenon occurs throughout the year, although the definitive density values vary with season as shown in Fig. 27.

RELATION OF TEMPERATURE AND SALINITY TO DENSITY

Throughout this seaway system the influence of temperature on the density structure is always secondary to the effect of salinity. This is illustrated in the scatter diagrams of Fig. 29 which show the relations of the observed temperature and salinity to σ_t (density) in the outer and inner parts of Juan de Fuca Strait, and in the Strait of Georgia. It is evident that there is a very close relation between salinity and density, but no clear relation with temperature.

In both the Strait of Georgia and Juan de Fuca Strait there are vertical temperature gradients in summer, coincident with the salinity gradients. The only effect is to reinforce the density structure which is predetermined by the salinity gradients. In winter, the temperature gradients vanish, and the density structure is determined solely by the salinity.

Water Masses

Following the procedure of Helland-Hansen (1916) the relations of temperature to salinity were plotted using the comprehensive data from Line 3 in July 1952. Each station (A, B, C, D, E) was observed 10 times during the week July 2 through 7. The top row of diagrams in Fig. 30 shows that, except for the surface observations, the relations were linear, and coincident within 0.1 C°. Since each observation was made at a different time of day, the surface values varied in accord with the diurnal heating and cooling cycle (Tully and Dodimead, 1957). At greater depths the temperature may be regarded as a conservative

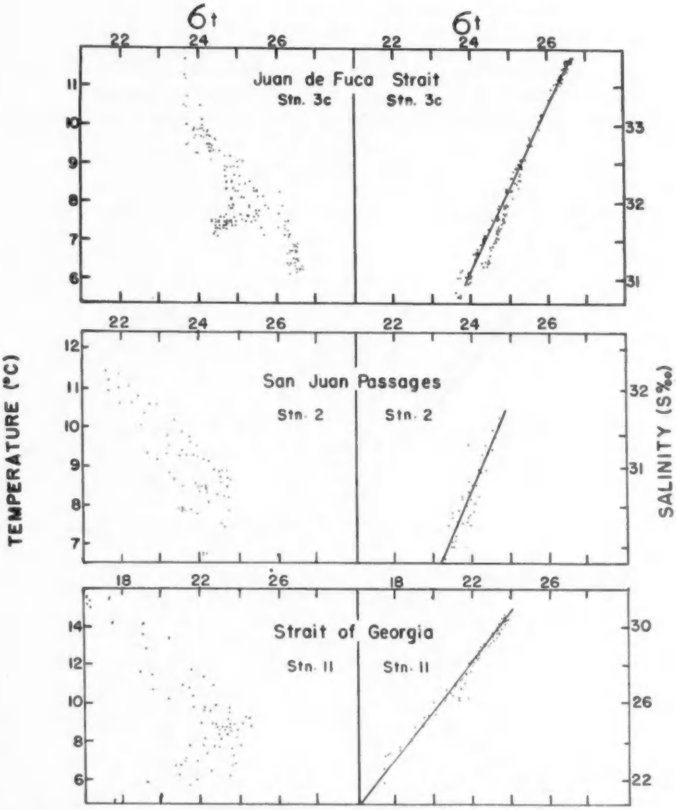

FIG. 29. Relation of temperature and salinity to density in Juan de Fuca Strait, the San Juan Passages, and the Strait of Georgia.

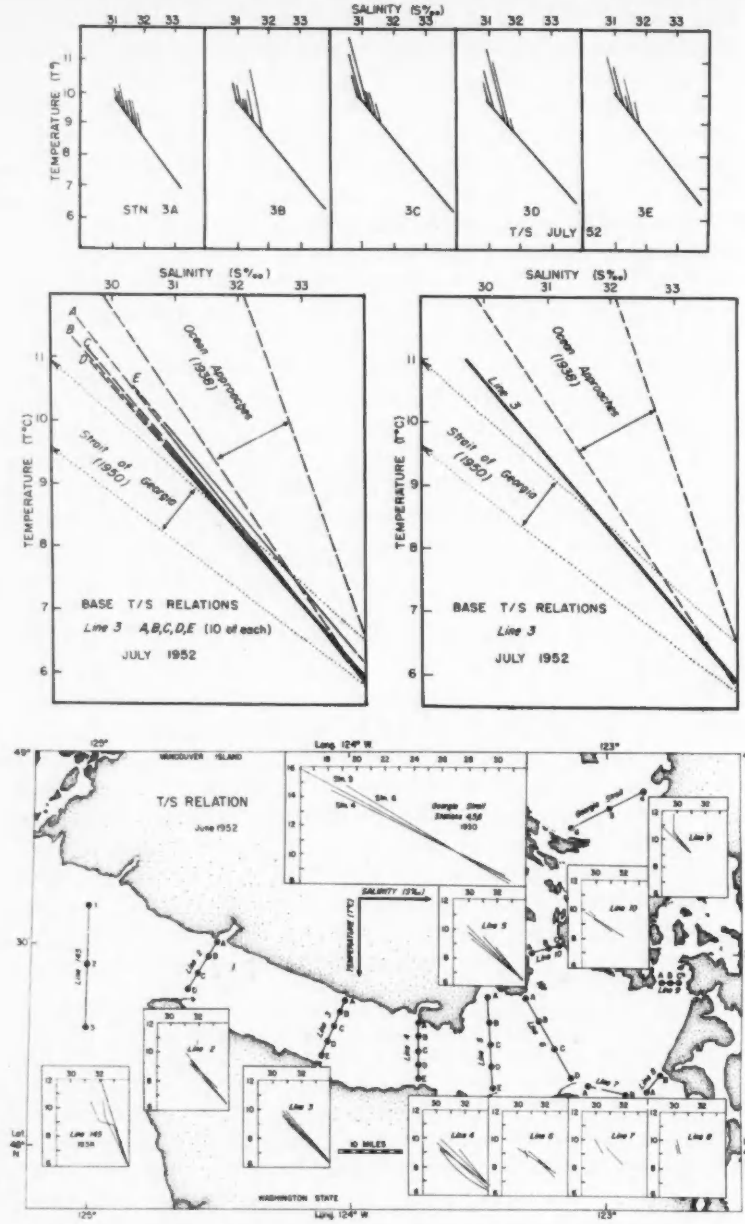

FIG. 30. Temperature–salinity relations at Line 3 in Juan de Fuca Strait, with reference to surrounding areas.

property, similar to salinity. Evidently the linear parts of these curves may be regarded as ***base relations*** at each station at this time.

In the middle diagrams of Fig. 30 these representative curves are brought together, ignoring the surface deviations. They form a tight bundle which can be represented by a single line (right-hand diagram) within 0.2 C°. This may be regarded as the ***base relation for Line 3*** at this time.

The bottom diagram of Fig. 30 shows the base relations for each station observed during the June survey. In general the relations are similar to those shown for Line 3 in July.

In Fig. 31 the base relations for each line of stations are assembled for comparison. It is evident that they form a fan of decreasing slope from the ocean

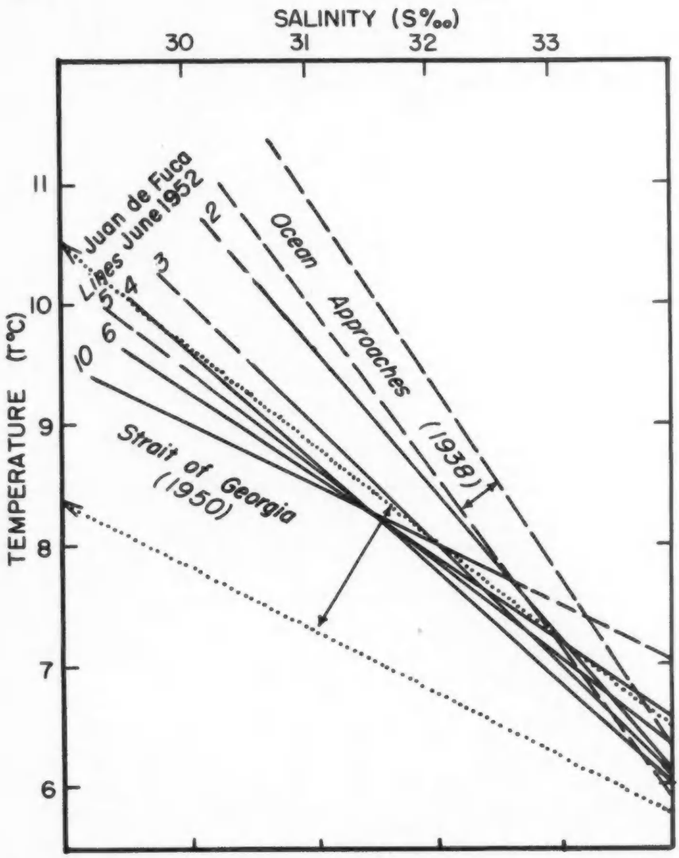

FIG. 31. Base temperature–salinity relations in Juan de Fuca Strait (June 1952) and limits of the relations in the Strait of Georgia (June 1950) and the ocean approaches (June 1938).

approaches at Line 2, to the passages through the San Juan Archipelago at Line 10. The regular sequence is marred only by the position of Lines 7 and 8 in the approaches to Admiralty Inlet, which are not shown.

For purposes of comparison, the envelopes of the data observed in the southern part of the Strait of Georgia in June 1950 (Joint Committee on Oceanography, 1954) and in the ocean approaches to Juan de Fuca Strait in June 1938 (Joint Committee on Oceanography, 1956) were added. There were no corresponding data from these neighbouring regions in June 1952. However, these are consistent with other data from these areas over a period of several years and may be considered representative of the character of these waters in June. The limiting character of the deep water at salinity 33.8‰ is identical throughout the system. At any temperature level above 7.3°C the Strait of Georgia waters are notably less saline than the coastal ocean water. It is at once evident that in Juan de Fuca Strait, the connecting seaway between these two distinct regions, these two water masses are progressively mixed.

In February and March when the upper waters are coldest the distinction between the water masses from the Strait of Georgia and the ocean approaches depends primarily on the salinity characteristics. These are illustrated in Fig. 32. The T–S diagrams at each station in Line 3 forms a tight bundle as before,

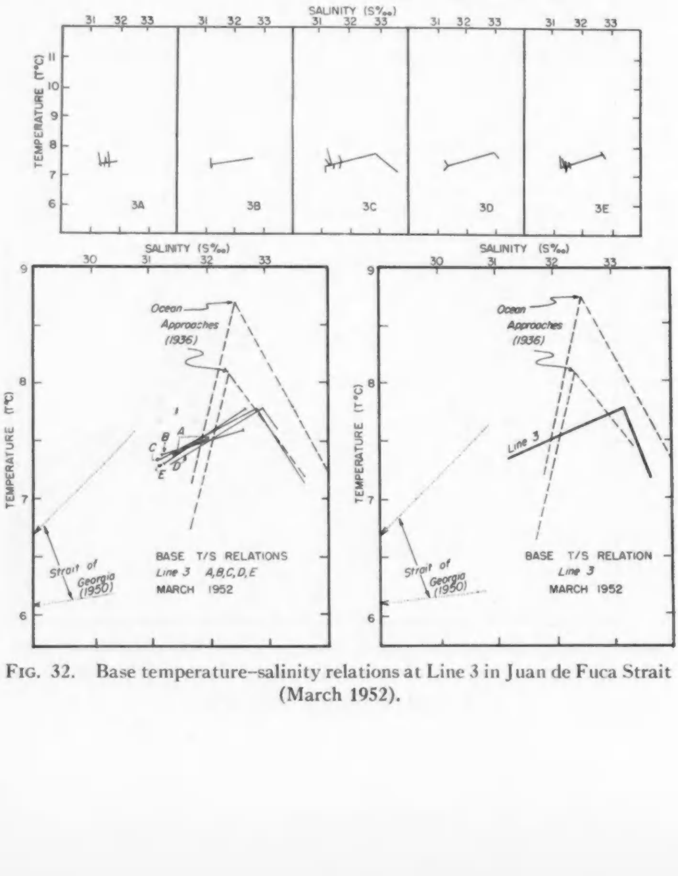

FIG. 32. Base temperature–salinity relations at Line 3 in Juan de Fuca Strait (March 1952).

but the slope is near zero or slightly positive, indicating that the temperature distinction had vanished at this time. Similar data are collected in Fig. 33 to show that the characteristics of the water masses are graded along Juan de Fuca Strait from the Strait of Georgia to the ocean approaches. It is evident that the gradation exists in winter as well as summer. Evidence from the other surveys shows that this gradation exists throughout the year.

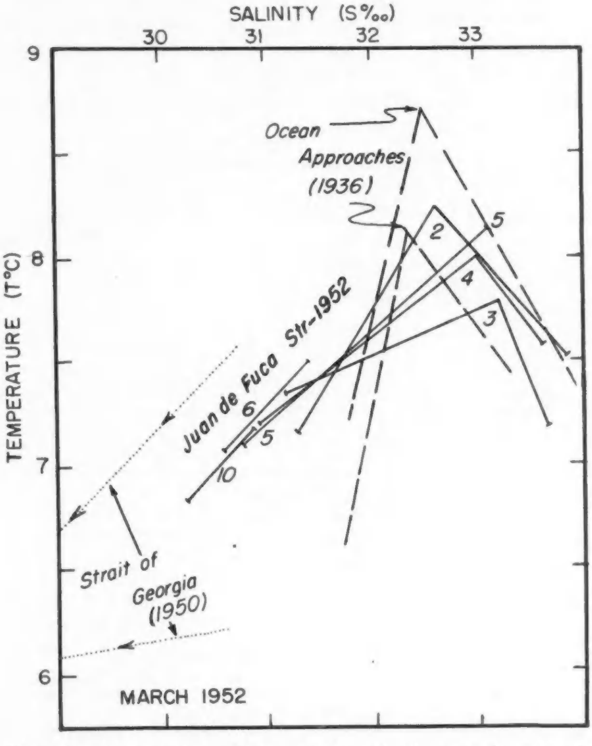

FIG. 33. Temperature–salinity relations in Juan de Fuca Strait (March 1952), the Strait of Georgia (March 1950) and the ocean approaches (March 1936).

The upper diagram of Fig. 34 shows the representative monthly base relations in mid-Outer Strait (Station 3C) compiled from all available data (1934–1952). These form an annual cyclic pattern which is emphasized in the lower diagram, where only the near-surface (2-m) and deep (100-m) data are shown. The configuration of these curves results from the annual cycles of salinity and temperature in the surface and deep waters which have been discussed already.

Recalling the gradient of T–S relations along the strait as shown in Fig. 31, it would be anticipated that the slope of the relation at any fixed position in the

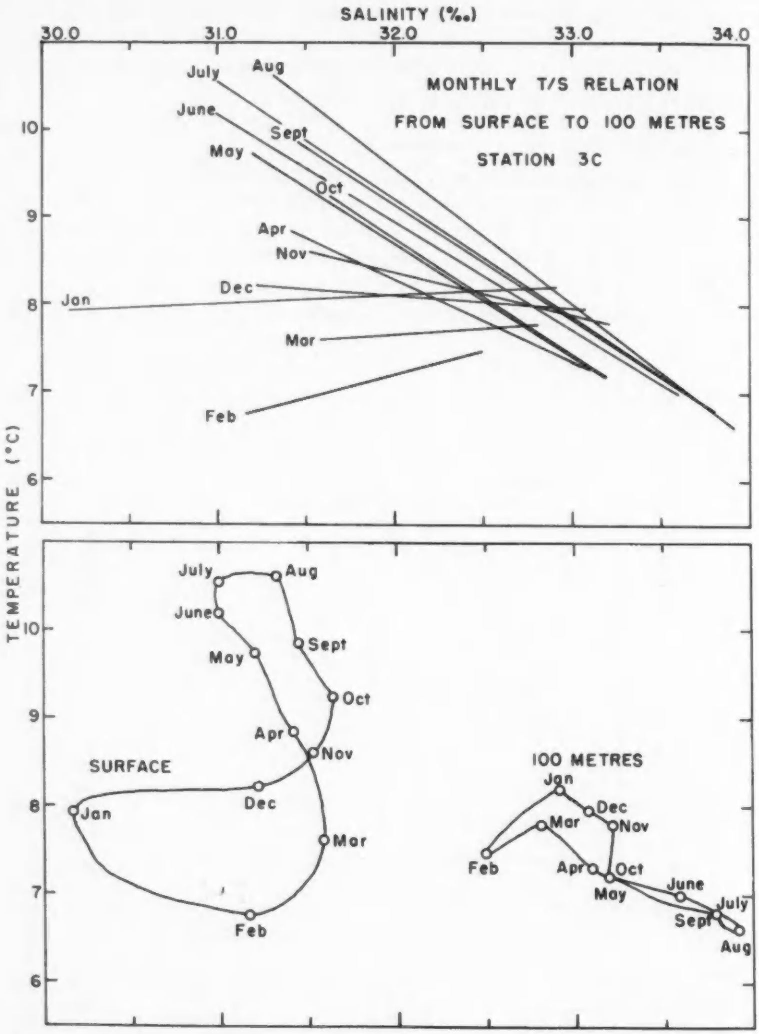

FIG. 34. Representative monthly temperature–salinity relations at Station 3C in Juan de Fuca Strait, and the annual cycle of relations at the surface and 100 metres depth.

strait would alter towards the character of the Strait of Georgia water during the ebb flow, and towards the character of ocean coastal water during the flood flow. The phenomenon is illustrated, with data from Station 3C, in the lower diagram of Fig. 35. In the vicinity of the sill (Line 5) the effect is most marked (as shown in the upper diagram) because the deep coastal water intrudes during the flood, and retreats during the ebb flow. This phenomenon is confirmed in all the data, and accounts for the variation (± 0.1 C°) between the several curves forming the base relation at each station (Fig. 30).

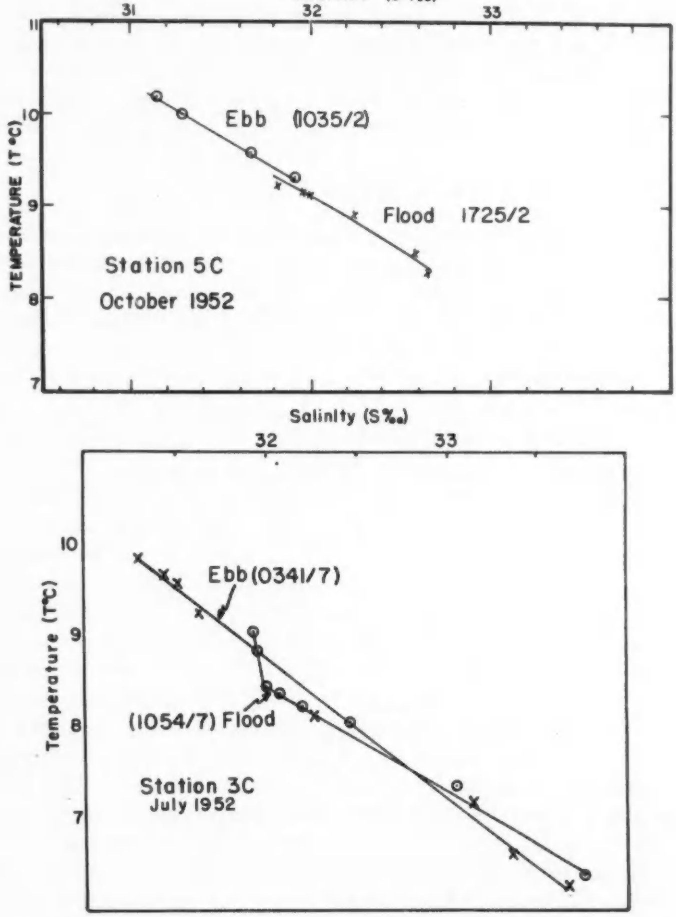

FIG. 35. Temperature–salinity relations at Stations 5C and 3C in Juan de Fuca Strait during the flood and ebb phases of the tide.

At locations of corresponding depth, the curves are longest where stratification is greatest (Fig. 30) in the Outer Strait (Lines 2, 3, and 4) and in Haro Strait (Line 10). The curves are short in the locations of greatest mixing where the waters are most nearly homogeneous, as in the vicinity of the sill (Lines 5 and 6). The curve is short in Rosario Strait (Line 9) because the location is shallow and admits only upper water of the same character as the upper water of Haro Strait (Line 10).

Consideration of these data indicates that the temperatures of the upper waters are seasonal features while the salinity is definitive of locality throughout the year.

If the temperature and salinity are observed at two depths, one near the surface and the other near the bottom, the relation and length of the curve are defined. Intermediate values of salinity may then be interpolated from a bathythermogram with considerable accuracy ($\pm 0.1‰$) through periods of several days. This facilitates routine observations, particularly time series, in the area.

OBSERVED CURRENTS AND STRUCTURES

The tides and tidal currents are major oceanographic features of Juan de Fuca Strait. However, the principal interest in this paper is the relation of the tidal phenomena to the properties and structure of the waters. In this deep seaway the tidal rise is a small fraction of the total depth, and in itself has little effect on the properties or structure of the waters, except in shallow near-shore areas. However, the ebb and flood tidal streams and the residual currents are major considerations.

The tides and tidal streams in Juan de Fuca Strait are of the mixed type with a marked semi-diurnal inequality. Throughout the seaway the tide occurs mainly as a standing oscillation, being high along the ocean coast when it is low in the Strait of Georgia and vice versa. In these circumstances the tidal streams are strongest at half tide, and flow towards the region where the tide is rising. The criteria and features of such situations have been discussed by Doodson and Warburg (1941) and are immediately apparent from an examination of the Tide and Current Tables (Canadian Hydrographic Service, Annual).

Herlinveaux (1957) ,studied these data. The average tidal speeds pass through semi-monthly cycles associated with the moon's phases. He observed that the near-surface temperatures and salinities followed similar cycles. The salinities increased during periods of maximum flow. In summer, the temperature decreased, and in winter it increased during these periods. He concluded that these effects were caused by mixing of the near-surface and deep water, and that the mixing forces were dependent on the speeds of tidal flow.

Herlinveaux (1954) also observed the velocity of flow (tidal streams plus residual currents) at intervals from the surface to near bottom, at three positions (A, B, and C) across Juan de Fuca Strait in the vicinity of Line 3 (Fig. 2) during March, July and October of 1952. From these data he deduced the distribution

of the velocity of flow through the cross-section at hourly intervals through a representative tidal day (Fig. 36). It is evident that the tidal streams flood and ebb at all depths.

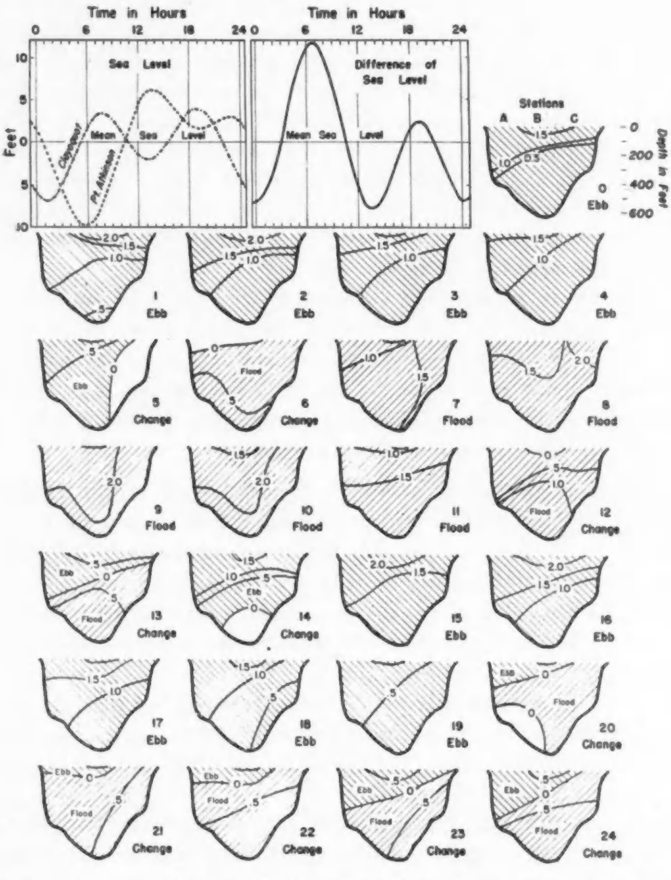

FIG. 36. Flow velocities through a cross-section (Line 3) of Juan de Fuca Strait, at hourly intervals (after Herlinveaux, 1954).

The mean flow velocities in the flood and ebb directions, from surface to near bottom in mid-strait (Station B) are shown in the upper diagram of Fig. 37, along with the net or residual current.

At this location, the residual current sets seaward in the upper 70 m of depth. Below this, the current is inward. This current structure has been discussed in some detail by Tully (1958). He showed that when the fresh water from land drainage enters the sea it moves seaward at the surface, entraining sea

water en route, to form a brackish upper zone. The dimensions of this zone are determined by the rate of mixing of fresh and sea water by the tidal streams and wind. In the upper zone and halocline, the residual current must set persistently seaward, else fresh water would accumulate in the system. In the lower zone ocean water intrudes at a rate sufficient to supply the demand for entrainment into the upper zone. Hence the residual current in the lower zone must be inward, and there must be a depth of no-net-motion between them. These conclusions are confirmed in Herlinveaux's data.

The lower diagram in Fig. 37 shows that the depth of no-net-motion was deepest (110 m) on the northern side of the strait (Station A) and shallowest (40 m) on the southern side, owing to Coriolis force. Hence the seaward transport of light water is greatest on the northern side, and the inward transport of dense water is greatest on the southern side.

It is desirable to consider the features of the transport (residual current) in relation to the tidal flow. However, as this cross-section is the only place where the flow at all depths has been determined, it is necessary to deduce the flow elsewhere in the seaway from the descriptions of surface flow given in the British Columbia Coast Pilot (Canadian Hydrographic Service, 1959), and the knowledge of the properties and structure of the water.

During the flood flow the excursion[3] in all parts of the system is inwards as shown in Fig. 38. Ocean water intrudes the outer part of Juan de Fuca Strait. Being more dense (saline) it under-runs the upper zone, and contributes to the lower zone. From consideration of the properties, it is evident that the deep Juan de Fuca waters, below 100 m depth, are continuous with the ocean waters at 150 to 200 m depth. It is probable that the deep inflow migrates up the canyon through the approaches (Fig. 2).

In the Outer Strait this ocean water intrudes along the bottom, below the level of no-net-motion, carrying the upper zone water backward against its seaward tendency. Consequently the largest currents during the flood are in the lower zone as shown in Fig. 36 and 37.

The channel of the Outer Strait is slightly curved such that both the Coriolis and centrifugal forces act together to influence the flood flow toward the southern side, where it is stronger and flows for a longer period than on the opposite side. Thus the flood flow slackens first on the northern side, as observed by Herlinveaux (1954).

From the Outer Strait the waters move over the sill into the Inner Strait. The flow must be accelerated because of the vertical constriction of the channel. Although it is not visible at the surface, there must be considerable turbulence in the wake of the sill, extending into the Inner Strait during the flood flow. The seawater structures (Fig. 11, 14, 23 and 28) indicate that the ocean water

[3]The excursion of the tide is the distance travelled by a parcel of water during a period of inward (flood) flow, or outward (ebb) flow.

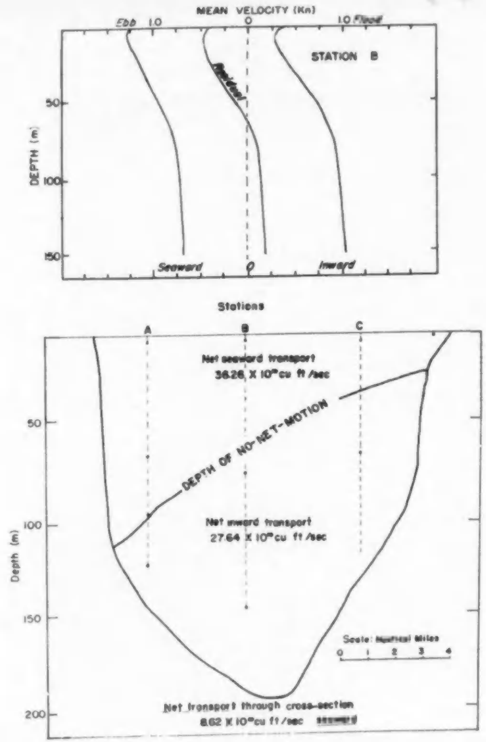

FIG. 37. Features of the mean tidal motion at Line 3 in the Outer Strait of Juan de Fuca Strait (after Herlinveaux, 1954).

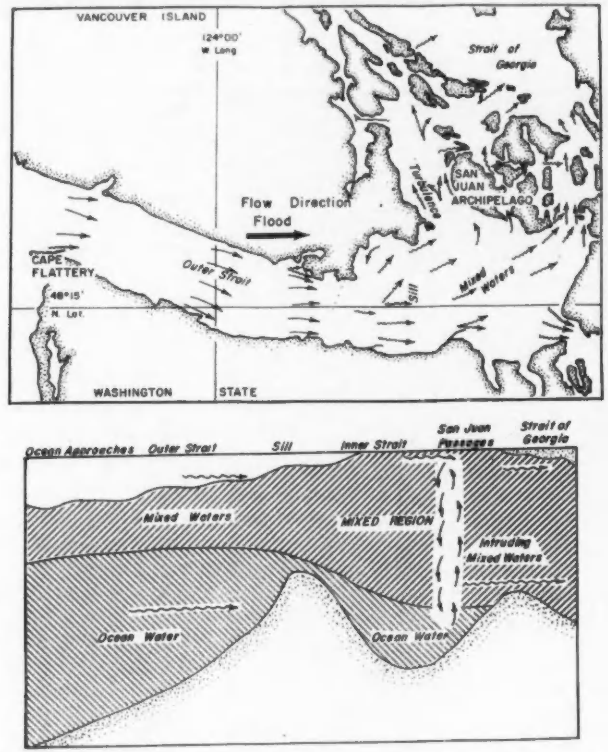

FIG. 38. Features of the flood excursions of the flow in Juan de Fuca Strait and approaches.

rides up the seaward slope of the ridge and cascades into the Inner Strait. The data show that the greater part of this ocean water intrudes over the southern end of the sill where it is deepest (Fig. 2), a lesser part crosses in mid-channel, and little or none crosses the shallow northern end of the sill near Victoria. It is probable that this deep ocean water is carried forward over this obstruction partly by its momentum, and partly by the venturi effect of the stream over the sill.

In this process the halocline that was evident in the Outer Strait (Fig. 13, 14 and 17) is largely destroyed as the upper and deep-zone waters are mixed in the submerged wake stream in the Inner Strait. A small degree of stratification remains, and the salt content of the Inner Strait waters is replenished. It is probable that there is a thin zone of ocean water lying in the bottom of the deep channel through the Inner Strait (Fig. 2) but no observations were made to detect this.

The flood flow is mainly confined to the southern half of the strait and an eddy is formed in the approaches to Victoria. This is a region of strong streams and tide rips, though less violent during the flood than during the ebb.

From the Inner Strait the waters move into the San Juan Passages. The flow is strong (3 to 5 knots at strength) and there is visible turbulence (eddies and boils) particularly near the shores and in the narrower channels. The slight stratification observed in the Inner Strait vanishes and the waters attain virtual homogeneity by the time they reach the northern end of the passages (Tully and Dodimead, 1957).

From the San Juan Passages the flow enters the quiet stratified waters of the Strait of Georgia as jets. The momentum of the flow is quickly dissipated in the spectacular turbulence (Waldichuk, 1957) and internal waves (Shand, 1953) associated with the wake stream (Fig. 39). The mixed waters under-run the upper zone of the Strait of Georgia, and become the lower zone (Waldichuk, 1957).

During the ebb flow (Fig. 40) the excursion in all parts of the system is seaward (5 to 10 miles)[4]. The waters from the Strait of Georgia move into the San Juan Passages. Here the velocities reach 3 to 5 knots on the large tides. Turbulence is apparent in "boils" and "eddies" throughout the area. The upper and lower zone waters are mixed to near homogeneity.

The waters from the San Juan Channels issue as jets, accompanied by violent tide rips in the Inner Strait. As the rate increases to its maximum, the ebb stream must expand across the strait. This conclusion is supported by the observations of a convergence region, marking the shear zone between the opposing streams. The convergence moves from near Victoria towards the southern shore as the seaward flow develops. The flow from Haro Strait tends to cross the Inner Strait and converge with the stream from Rosario Strait, which

[4]Distance is measured in nautical miles (1 minute of latitude = 6080 feet = 1.853 km) in keeping with the use of Mercator charts. Velocities are measured in knots (50.2 cm/sec).

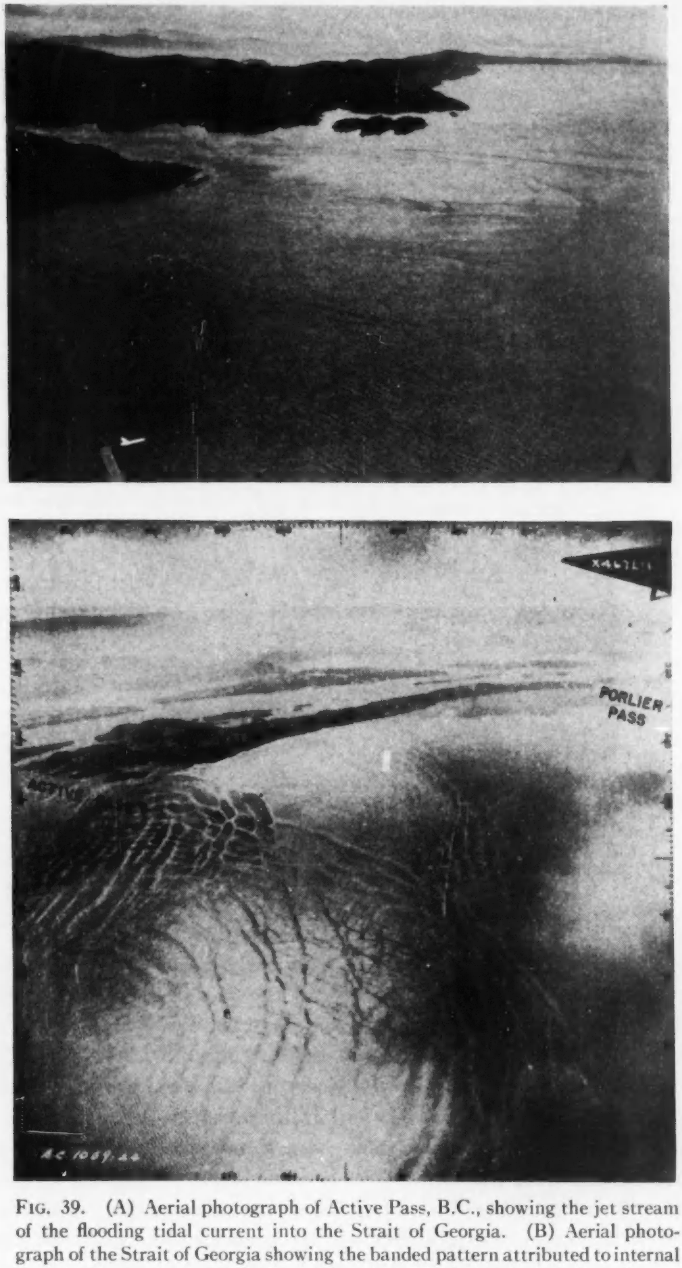

FIG. 39. (A) Aerial photograph of Active Pass, B.C., showing the jet stream of the flooding tidal current into the Strait of Georgia. (B) Aerial photograph of the Strait of Georgia showing the banded pattern attributed to internal waves generated by the flood jet flow from Active and Boundary Passes, (after Shand, 1953).

(Courtesy Pacific Naval Laboratory and Royal Canadian Navy.)

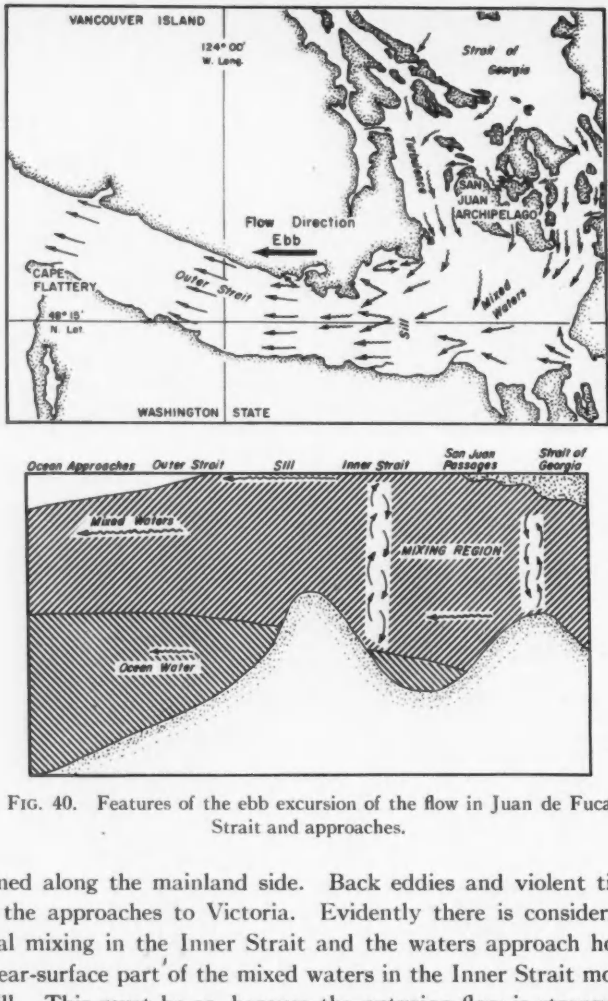

FIG. 40. Features of the ebb excursion of the flow in Juan de Fuca Strait and approaches.

is constrained along the mainland side. Back eddies and violent tide rips are formed in the approaches to Victoria. Evidently there is considerable lateral and vertical mixing in the Inner Strait and the waters approach homogeneity.

The near-surface part of the mixed waters in the Inner Strait move seaward over the sill. This must be so, because the outgoing flow is strongest near the surface, and there is no evidence in the structure that deep water from the Inner Strait crosses the sill (Fig. 11, 14, 23 and 28). However, because of the vertical constriction of the channel, there must be a submerged stream (wake stream) extending seaward from the sill.

In the Outer Strait the flow is reduced to the order of one knot at strength. The zone structure is re-established as the mixed waters over-run the dense ocean water, and are refreshed by the considerable land drainage. In this reach, the upper part of the double halocline (Fig. 15) represents the unaltered waters

from the Inner Strait. The lower part of the halocline is doubtless the result of entrainment of ocean waters in the wake stream at the sill.

The first of the seaward flow is almost entirely confined to the northern side, but as it strengthens it expands across the strait. When the seaward flow is fully developed the velocity distribution is nearly uniform, and the time of change to inward flow is first noticed on the southern side of the strait.

From the Outer Strait, the waters enter the ocean approaches which are, comparatively, a resting body of water. Here the discharge forms a wake stream (Tully, 1941) which veers to the right (Coriolis force) and is dissipated northward along the coast of Vancouver Island. This is illustrated by the calculated stream lines shown in Fig. 41.

This phenomenon occurs at the ocean outlet of each coast drainage system. Together these discharges create a geostrophic current flowing northward, close inshore, along the whole coastline north of the Columbia River (Latitude 46°N).

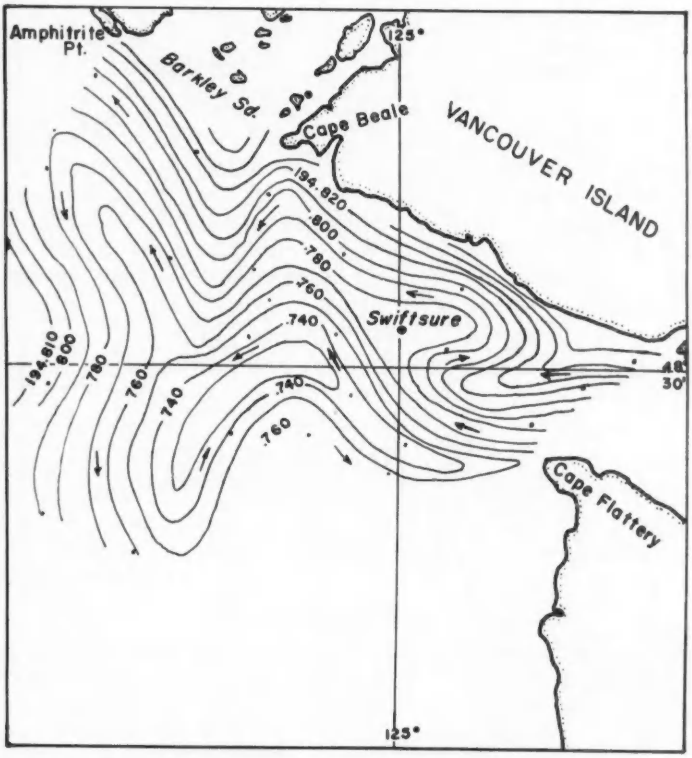

FIG. 41. Calculated stream lines in the approaches to Juan de Fuca Strait (after Tully, 1941).

Excursion

The mean tidal excursions in Herlinveaux's (1954) section (A, B, C) are shown in Fig. 42. These are representative of the Outer Strait.

The excursions of the surface water in Haro and Rosario Straits, determined from analyses of the data in Tidal Current Tables (U.S. Coast and Geodetic Survey, 1959) are shown in Table III.

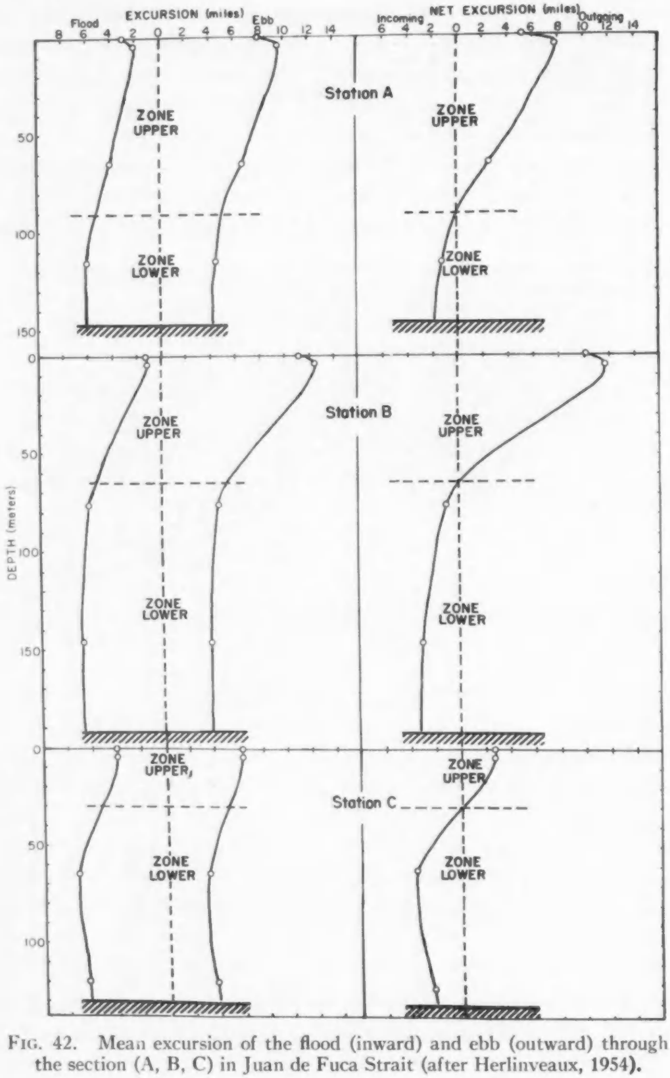

Fig. 42. Mean excursion of the flood (inward) and ebb (outward) through the section (A, B, C) in Juan de Fuca Strait (after Herlinveaux, 1954).

TABLE III. Surface water excursion in Haro and Rosario Straits, September 1960 (30 days = 29 tidal days). Calculated from tidal current data (U.S. Coast and Geodetic Survey, 1959).

	Haro	Rosario
	Flood (mean)	
Duration (minutes)	356.6	396.7
Mean speed (knots)	0.99	1.01
Excursion (nautical miles)	5.87	6.67
	Ebb (mean)	
Duration (minutes)	389.4	349.6
Mean speed (knots)	1.41	1.09
Excursion (nautical miles)	−9.15	−6.33
Net excursion (nautical	Ebb 3.28	
miles)	Flood	0.34

THE TIDAL PUMP

The mechanism in Juan de Fuca Strait (Fig. 38 and 40) is in effect a pump, the sill acting as a valve. During the ingoing flow, ocean water is transferred to the Inner Strait because the deep currents are stronger than those near the surface. This water is conserved near the bottom. It does not escape seaward during the ebb, because then the surface flow is the stronger and the weaker bottom flow is not sufficient to return the deep water seaward over the sill. Thus the intruding ocean water, brought in by the strong ingoing flow, cannot escape seaward and remains to be carried forward towards the Strait of Georgia on the next flood. The Inner Strait is a region of exchange. In effect, the water that reaches the Inner Strait from the Strait of Georgia is mixed to homogeneity and enriched with ocean water; part is returned to the lower zone of the Strait of Georgia, and the remainder escapes seaward. Undoubtedly, as proposed by Waldichuk (1957) this is the important mechanism for limiting the salt budget of the Strait of Georgia.

CONCLUSION

This report provides a factual overall description of the properties of the water, oceanographic structure, the current, and the variations and interrelations of these. It was designed and written to be a primary reference for ready use, and to provide a basis for more sophisticated discussions of particular features, which we trust will follow.

REFERENCES

BOUGHNER, C. C., AND M. K. THOMAS. 1948. Climatic summaries for selected meteorological stations in Canada, Newfoundland, and Labrador. Volume II, Humidity, wind speed and direction. Canada, Dept. of Transport, Meteorological Division, Toronto, Ont., 88 pp.

CANADIAN HYDROGRAPHIC SERVICE. 1959. British Columbia Pilot Volume I. Sixth Edition. Dept. Mines and Tech. Surveys, Ottawa, 480 pp.

Annual. Tide Tables for the Pacific Coast of Canada. Surveys and Mapping Branch, Dept. of Mines and Tech. Surveys, Ottawa.

CANADIAN METEOROLOGICAL SERVICE. 1896–1957. Monthly record, meteorological observations in Canada. Dept. of Transport, Toronto, Ont., 100 pp. (approx.)

CANADIAN WATER RESOURCES BRANCH. (Annual.) Surface water supply of Canada, Pacific Drainage, British Columbia and Yukon Territory. Dept. of Northern Affairs and National Resources, Ottawa, Ont.

DODIMEAD, A. J. MS, 1961. Some features of the upper zone in the sub-Arctic Pacific Ocean. *International North Pacific Fisheries Commission Bull.* No. 3, pp. 11–24.

DOODSON, A. T., AND H. D. WARBURG. 1941. Admiralty manual of tides. Hydrographic Department, Admiralty, London, 270 pp.

FJARLIE, R. L. I. 1953. A seawater sampling bottle. *J. Mar. Res.*, **12**(1): 21–30.

HARRIS, R. G., AND M. RATTRAY, JR. 1954. The surface winds over Puget Sound and the Strait of Juan de Fuca and their oceanographic effects. *University of Washington, Dept. of Oceanography, Tech. Rept.* No. 37, 101 pp.

HELLAND-HANSEN, B. 1916. Nogen hydrografiske metodes. *Skand. Naturforsker möte*, Kristiania (Oslo), pp. 357–359.

HERLINVEAUX, R. H. 1954. Tidal currents in Juan de Fuca Strait. *J. Fish. Res. Bd. Canada*, **11**(6): 799–815.

1957. On tidal currents and properties of the sea water along the British Columbia Coast. *Fish. Res. Bd. Canada, Pac. Prog. Rept.*, No. 108, pp. 7–9.

1962. Oceanography of Saanich Inlet in Vancouver Island, British Columbia. *J. Fish. Res. Bd. Canada*, **19**(1) (in press).

JOINT COMMITTEE ON OCEANOGRAPHY. MS, 1954. Physical and chemical data record. Strait of Georgia 1949–1953, with Appendix I, current measurements, March 1953. Fisheries Research Board of Canada, Pacific Oceanographic Group, Nanaimo, B.C., 437 pp.

MS, 1955. Physical and chemical data record. Juan de Fuca Project, 1951–52, with Appendix I, current measurements. Fisheries Research Board of Canada, Pacific Oceanographic Group, Nanaimo, B.C., 182 pp.

MS, 1956. Physical and chemical data record. Approaches to Juan de Fuca Strait 1936–1938. Fisheries Research Board of Canada, Pacific Oceanographic Group, Nanaimo, B.C., 99 pp.

KENDREW, W. G., AND D. KERR. 1955. The climate of British Columbia and the Yukon Territory. Department of Transport, Ottawa, 222 pp.

MCCRACKEN, L. H. 1955. The salinity of sea water. *Fish. Res. Bd. Canada, Pac. Prog. Rept.*, No. 102, pp. 24–26.

MS, 1956. A simple technique for sealing seawater samples. MS Rept., Fisheries Research Board of Canada, Pacific Oceanographic Group, Nanaimo, B.C., 5 pp.

PRITCHARD, D. W. 1956. The dynamic structure of a coastal plain estuary. *J. Mar. Res.*, **15**(1): 33–42.

REED, T. R. 1931. Gap winds of the Strait of Juan de Fuca. *Monthly Weather Review*, **59**(10): 373–376.

SHAND, J. A. 1953. Internal waves in Georgia Strait. *Trans. Amer. Geophys. Union*, **34**(6): 849–856.

SVERDRUP, H. U., M. W. JOHNSTON AND R. H. FLEMING. 1946. The Oceans. Prentice-Hall Inc., New York, 1087 pp.

TULLY, J. P. 1941. Surface non-tidal currents in the approaches to Juan de Fuca Strait. *J. Fish. Res. Bd. Canada*, **5**(4): 389–409.

1949. Oceanography and prediction of pulpmill pollution in Alberni Inlet. *Fish. Res. Bd. Canada, Bull.* No. 83, 167 pp.

1952. Notes on the behaviour of fresh water entering the sea. *Proc. 7th Pacific Science Congress* (1950), **3**: 376–289.

1958. Structure, entrainment, and transport in estuarine embayments. *J. Mar. Res.*, T. G. Thompson, Seventieth Anniversary Vol., **17**: 523–535.

TULLY, J. P., AND A. J. DODIMEAD. 1957. Properties of the water in the Strait of Georgia, British Columbia, and influencing factors. *J. Fish. Res. Bd. Canada*, **14**(3): 241–319.

UNITED STATES COAST AND GEODETIC SURVEY. 1959. Tidal Current Tables Pacific Coast of North America and Asia for the year 1960. U.S. Dept. of Commerce, Washington, D.C., 238 pp.

UNITED STATES WEATHER BUREAU. 1953. Climatological data, Washington. **56**(13): 186–195. Kansas City.

UNIVERSITY OF WASHINGTON, DEPARTMENT OF OCEANOGRAPHY. 1954. Physical and chemical data for Puget Sound and approaches. *Univ. Washington Dept. of Oceanog., Tech. Rept.* No. 35, 61 pp.

1956. Physical and chemical data for Puget Sound and approaches. *Ibid.* No. 45, 212 pp.

1956. Physical and chemical data for Puget Sound and approaches. *Ibid.* No. 46, 259 pp.

1956. Physical and chemical data for Puget Sound and approaches. *Ibid.* No. 51, 141 pp.

WALDICHUK, M. 1957. Physical oceanography of the Strait of Georgia, B.C. *J. Fish. Res. Bd. Canada*, **14**(3): 321–486.

Temporal Changes of Salinity, Temperature, and Dissolved Oxygen Content of the Water at Station "P" in the Northeast Pacific Ocean, and Some of Their Determining Factors[1]

By Susumu Tabata

Fisheries Research Board of Canada
Pacific Oceanographic Group, Nanaimo, B.C.

ABSTRACT

Oceanographic data collected at Ocean Weather Station "P" (Lat. 50°N, Long. 145°W) during the 2 years between August 1956 and July 1958 are presented to show the principal features of the variations of salinity, temperature, and dissolved oxygen content of the water at the station. Probable factors influencing the water properties are discussed and explanations are given to account for these variations. Only those causing changes in the upper zone are discussed in detail.

There is good agreement between the observed changes of salinity in the upper zone and changes attributable to the effect of precipitation minus evaporation for the period summer through winter, 1956. However there is generally poor agreement for the rest of the period. The main factor influencing temperature in this zone is heat transfer at the air–sea boundary. Changes of dissolved oxygen content in this zone are governed primarily by changes of solubility of oxygen in water.

Horizontal transport of water in the locality influences the properties at the station appreciably. The general increase of salinity, temperature, and dissolved oxygen content that occurred during summer 1957 through summer 1958, is attributed to the northward transport of water. Transport, both from the region of the "dome" located northwest of the station, and from the west, also appears to influence the properties of water at the station during autumn and winter. Intense vertical mixing during autumn and winter affects the structure of water in the upper zone by redistributing the properties.

INTRODUCTION

Since the summer of 1955, the waters of the northeast Pacific Ocean region[2] have been examined by oceanographic surveys in summer and winter. These data have been reported (Fish. Res. Bd. Canada, 1956; 1957a; 1957c; 1958a).

In addition, oceanographic observations have been made regularly through alternate 6-week periods at Ocean Weather Station "P" (Lat. 50°N, Long. 145°W) (Fig. 1) since August 1956. The details of the cruises associated with these observations are shown in Table I. Data collected here have been reported (Fish. Res. Bd. Canada, 1957b; 1958b; 1959) and some aspects of the data discussed (Tabata, 1960). These data reveal many features of the temporal variations of the properties of water at this fixed position. Furthermore, they provide data of sufficient continuity so that it is possible to interpret some of the sequences of oceanographic events that have occurred in the region between the periods of the major surveys.

[1]Received for publication May 23, 1961.

[2]Hereafter, the northeast Pacific Ocean region bounded by Lat. 40°N and Long. 180°W, and the coast of North America will be referred as "the region", unless ambiguity results.

J. Fish. Res. Bd. Canada, 18(6), 1961.
Printed in Canada.

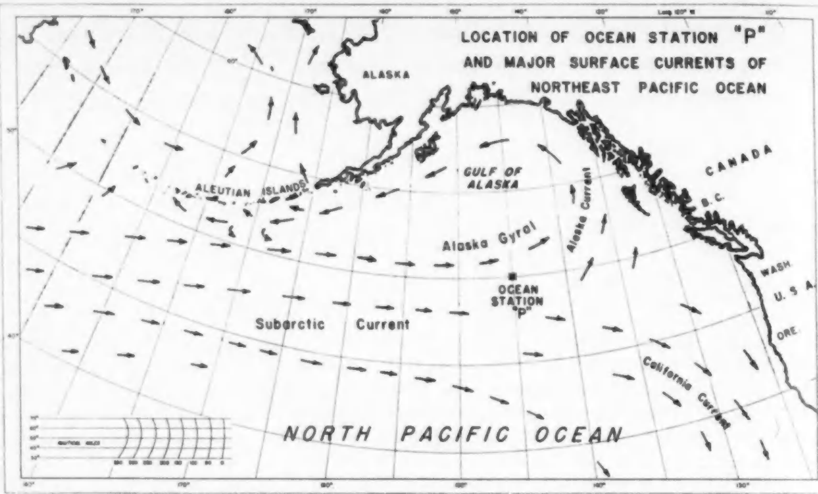

FIG. 1. Chart showing location of Ocean Weather Station "P" and major surface ocean currents of Northeast Pacific Ocean.

TABLE I. Catalogue of cruises during which observations were made.

Cruise number	Dates	Number of hydrographic stations occupied	Number of days between mid-dates of cruises
P-56-1	25 August–26 September 1956	7	–
P-56-2	10 November–7 December 1956	4	74
P-57-1	27 January–2 March 1957	8	83
P-57-2	20 April–29 May 1957	12	86
P-57-3	13 July–21 August 1957	11	84
P-57-4	28 September–29 October 1957	10	73
P-57-5	14 December 1957–22 January 1958	12	81
P-58-1	9 March–16 April 1958	11	84
P-58-2	31 May–8 July 1958	12	84

GENERAL OCEANOGRAPHIC FEATURES OF THE EASTERN SUBARCTIC WATER

The general features of the Eastern Subarctic Water have already been discussed by several authors (Doe, 1955; Tully and Dodimead, 1957; Dodimead, 1958; Bennett, 1959). As some aspects of these have bearing on the fluctuations of oceanographic properties at Station "P", they are briefly reviewed here.

The main feature of the salinity structure of this Water in the region is the presence of an upper zone (0–100 m), a halocline (100–200 m), and a lower zone (> 200 m). As shown in Fig. 2, the upper zone is characterized by a relatively low-salinity water (32.7‰). In winter, the water in this zone is mixed to homogeneity, and hence the salinity in the zone is constant (Fig. 2a). However, in summer, an appreciable vertical salinity gradient is present in the zone as shown in Fig. 2b. The halocline represents a transitional zone between the upper and the lower zone. Here, the salinity increases markedly with depth, by as much as 1.0‰ within an interval of 100 m. The lower zone represents the layer in which the salinity increases gradually with depth. From a value of about 33.8‰ at the

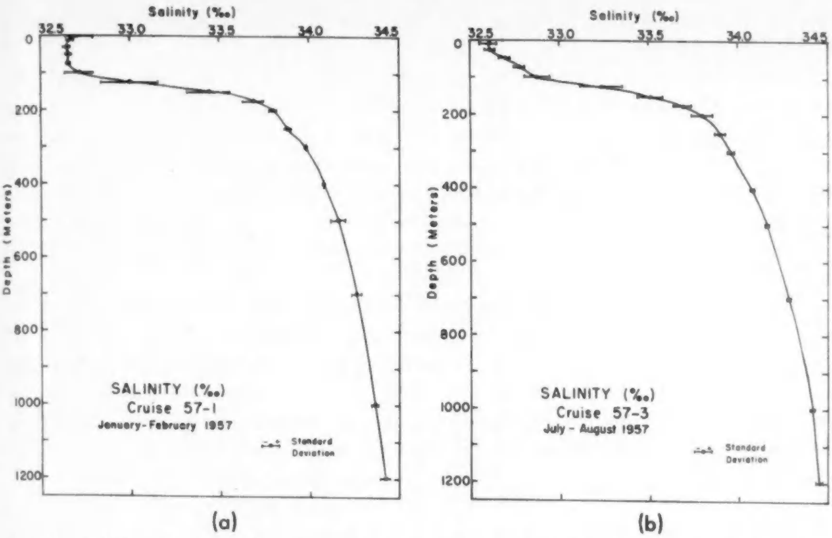

FIG. 2. Salinity–depth profiles for water at Station "P" (mean values for each cruise). (a) Winter. (b) Summer.

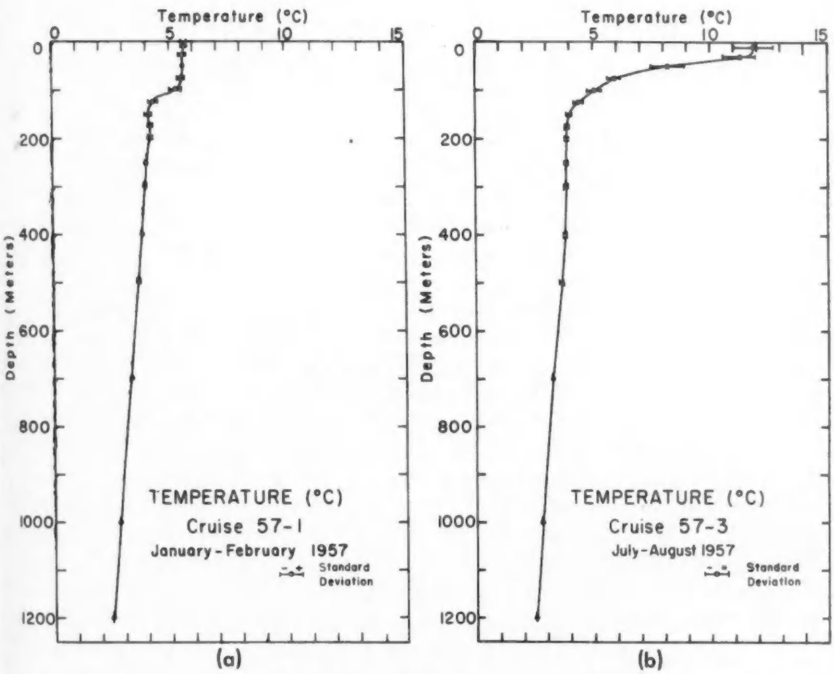

FIG. 3. Temperature–depth profiles for water at Station "P" (mean values for each cruise). (a) Winter. (b) Summer.

bottom of the halocline, the salinity increases to 34.4‰ at a depth of 1000 m, and finally to 34.7‰ near the ocean bottom.

The water in the upper zone is isothermal in winter, as shown in Fig. 3a. However, in summer, a well-defined thermocline occurs in the zone (Fig. 3b) where the temperature may decrease with depth by as much as 8 C° within an interval of 20 m. In the halocline, the temperature generally decreases with depth (Fig. 3b). But occasionally, a temperature inversion (temperature increasing with depth) occurs, as shown in Fig. 3a. In the lower zone, the temperature decreases gradually with depth, reaching 2.8°C at a depth of 1000 m, and finally 1.5°C near the ocean bottom.

These three zones can be identified conveniently by reference to the three segments of the temperature–salinity (T–S) curve shown in Fig. 4.

The dissolved oxygen content (hereafter called the oxygen) in the upper zone is generally constant (0.63 milligram atoms per litre (mg-at/l)) in winter, as shown in Fig. 5a. But in summer (Fig. 5b) the oxygen increases with depth in the zone from a value frequently less than 0.6 mg-at/l at the surface to a maxi-

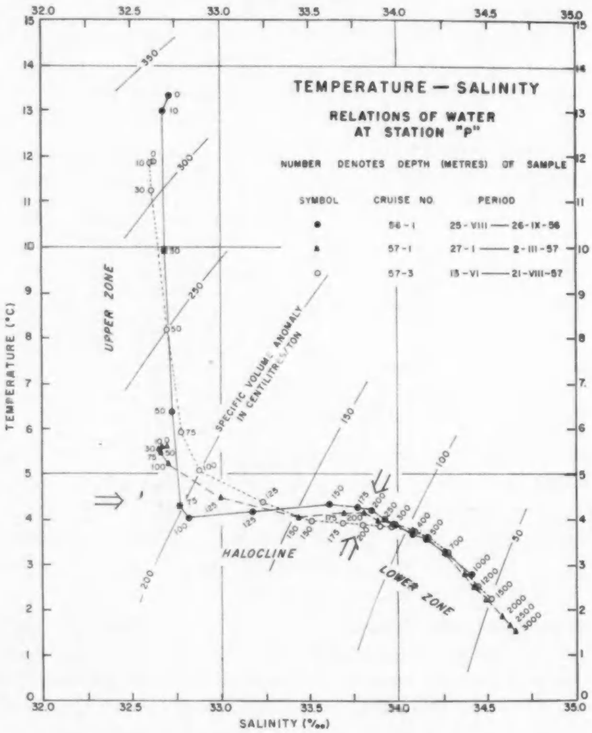

FIG. 4. Temperature–salinity relations of water at Station "P". (Mean values for each depth, for each cruise, have been plotted. Large arrows indicate limit of various zones.)

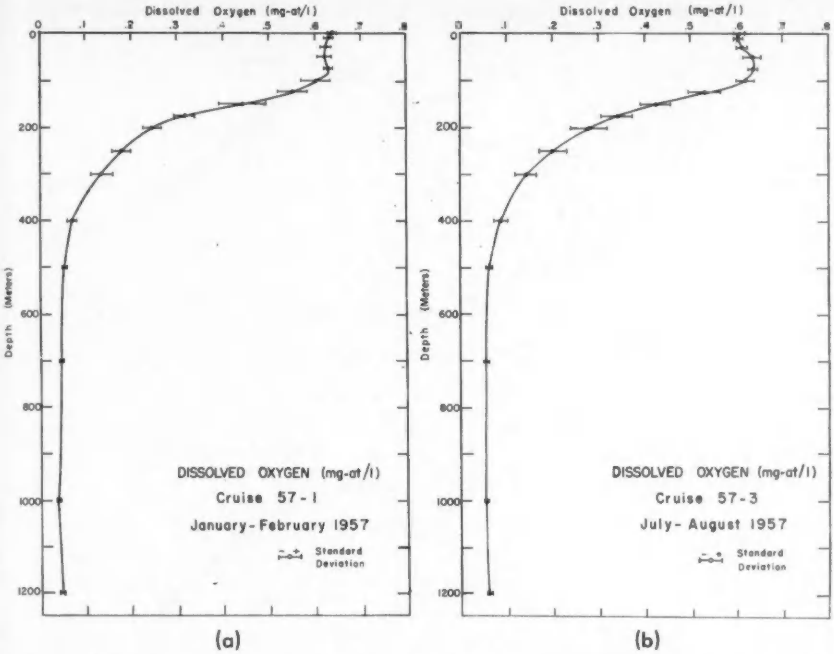

FIG. 5. Dissolved oxygen content–depth profiles for water at Station "P" (mean values for each cruise). (a) Winter. (b) Summer.

mum (0.63 mg-at/l) at depths between 50 and 100 m. It decreases markedly in the halocline, reaching 0.3 mg-at/l at the bottom of the halocline. It then decreases gradually in the lower zone to a minimum of less than 0.05 mg-at/l at depths varying from 200 to 1200 m (between 500 and 1200 m at Station "P"). From this minimum it increases gradually with depths to 0.3 mg-at/l near the ocean bottom.

To the south of the Subarctic Water lies the Subtropic Water. The Subarctic Boundary separates these two water masses. Its location has been determined by Dodimead (1958) and is shown in Fig. 6. At the longitude of Station "P", the boundary lies about 400 miles[3] south of the station. The Subtropic Water is more saline and warmer than the Subarctic Water. It has been shown (Tully and Dodimead, 1957; Dodimead, 1958) that the Subtropic Water lacks the characteristic halocline of the Subarctic Water and possesses a salinity minimum at depths ranging from 200 to 600 m. Furthermore the Subtropic Water has no major temperature inversion. In Fig. 7 are shown the T–S characteristics of these water masses. Being so close to this boundary, the characteristics of this Subtropic Water still have some of the features characteristic of the Subarctic Water. For instance, there is a remnant of a halocline between the depths of 100 and 200 m.

[3]All horizontal sea distances expressed in miles in this paper are nautical miles (1.85 km).

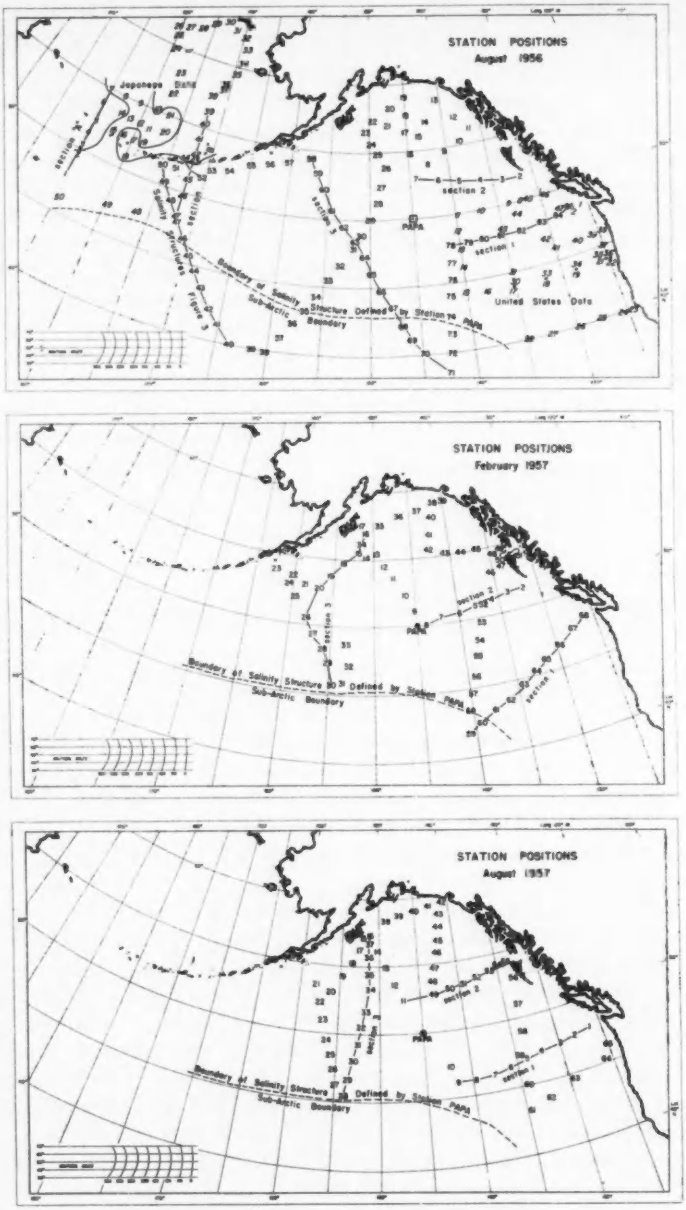

FIG. 6. Chart showing the location of Subarctic Boundary and stations occupied during the major surveys (Dodimead, 1958).

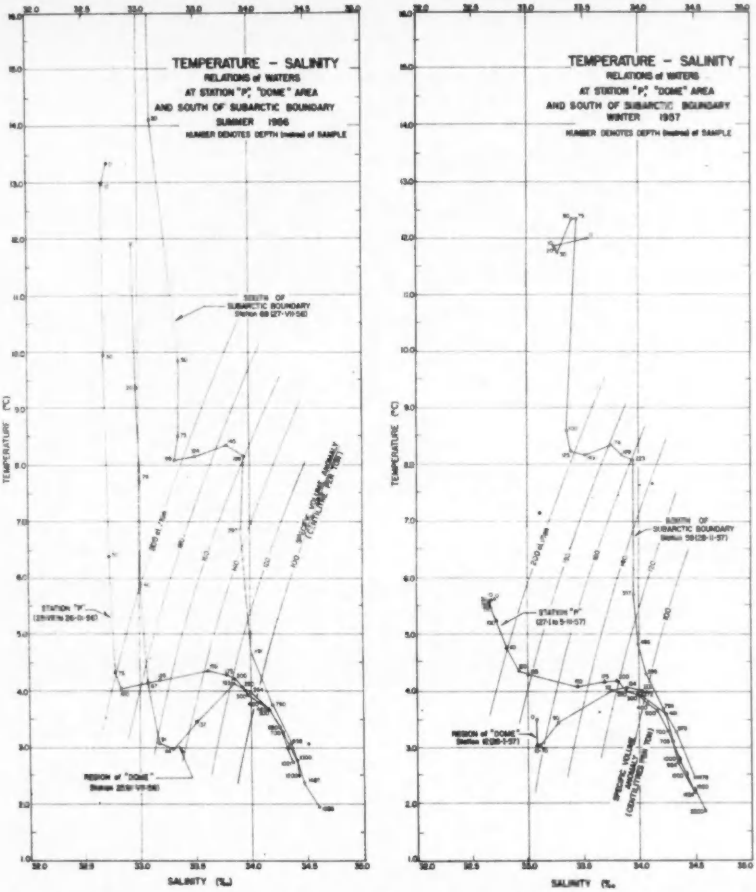

FIG. 7. Temperature–salinity relations of waters near the Subarctic Boundary, in the "dome" area, and at Station "P" (for location of stations, see Fig. 6).

Northwest of Station "P" lies the "dome"[4]. It is characterized by having water of relatively higher salinity (Fig. 8–10), lower temperature (Fig. 11–13) and lower oxygen (Fig. 14–16), than is present in the immediate surroundings. This feature of salinity and temperature of the "dome" water is verified in the T–S curve as shown in Fig. 7.

A comparison of the geopotential topographies which represent the currents (Fig. 17), with the distributions of salinity (Fig. 8–10), temperature (Fig. 11–13), and oxygen (Fig. 14–16), indicates that the "dome" lies in the centre of the counter-clockwise circulation system of the Alaska Gyral (Fig. 1).

[4]The term "dome" is used since the isometers of all properties on sections drawn through the cold centre of the Gulf of Alaska are dome-shaped.

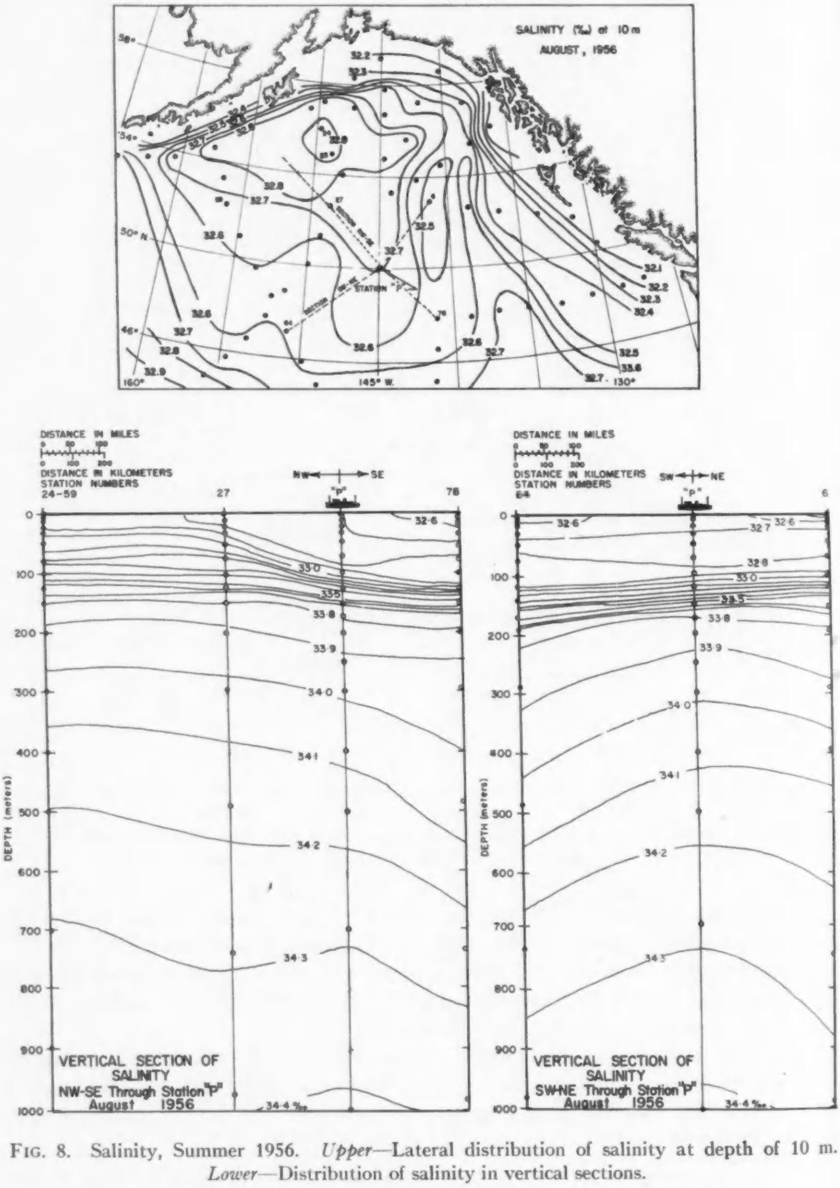

FIG. 8. Salinity, Summer 1956. *Upper*—Lateral distribution of salinity at depth of 10 m. *Lower*—Distribution of salinity in vertical sections.

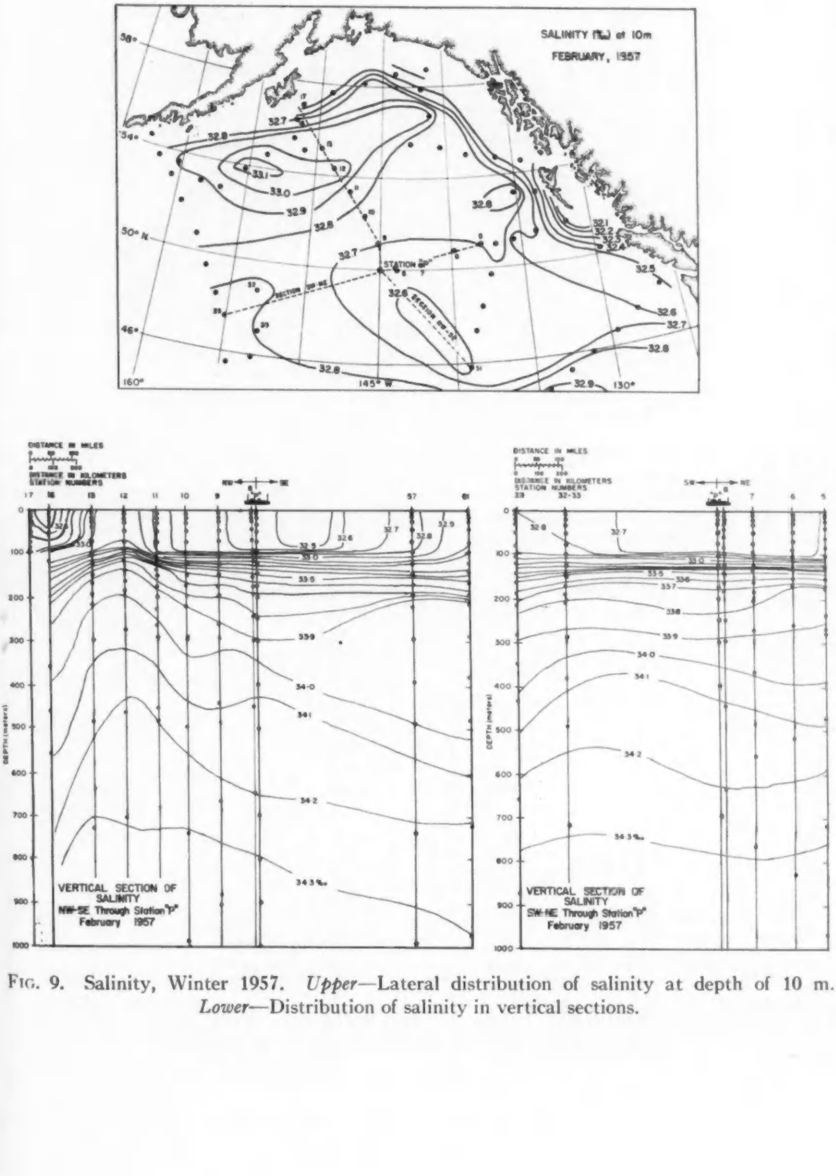

FIG. 9. Salinity, Winter 1957. *Upper*—Lateral distribution of salinity at depth of 10 m. *Lower*—Distribution of salinity in vertical sections.

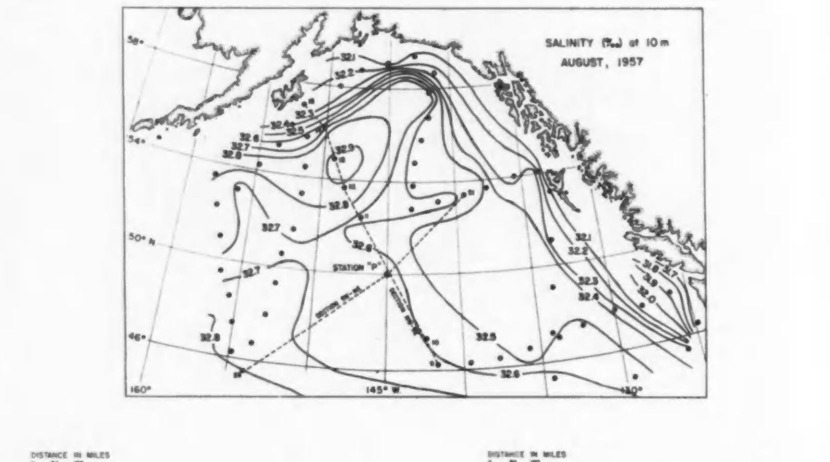

FIG. 10. Salinity, Summer 1957. *Upper*—Lateral distribution of salinity at depth of 10 m. *Lower*—Distribution of salinity in vertical sections.

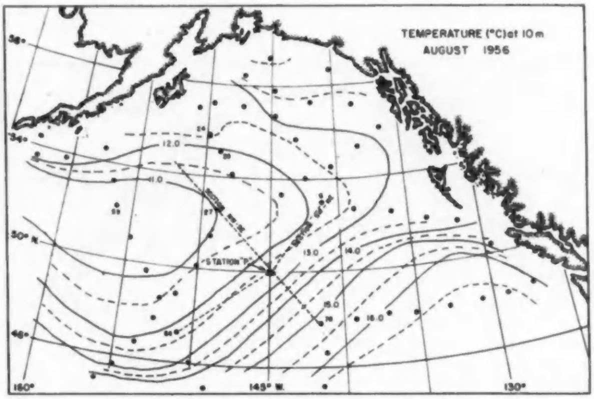

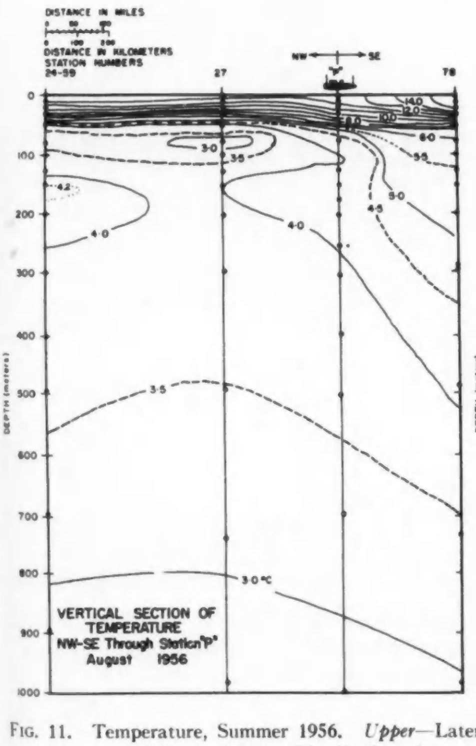

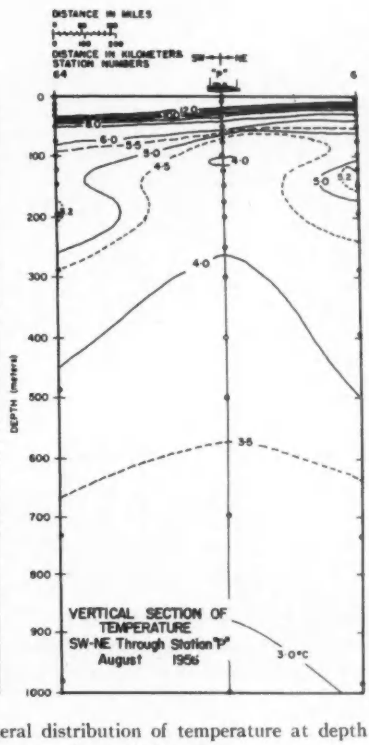

FIG. 11. Temperature, Summer 1956. *Upper*—Lateral distribution of temperature at depth of 10 m. *Lower*—Distribution of temperature in vertical sections.

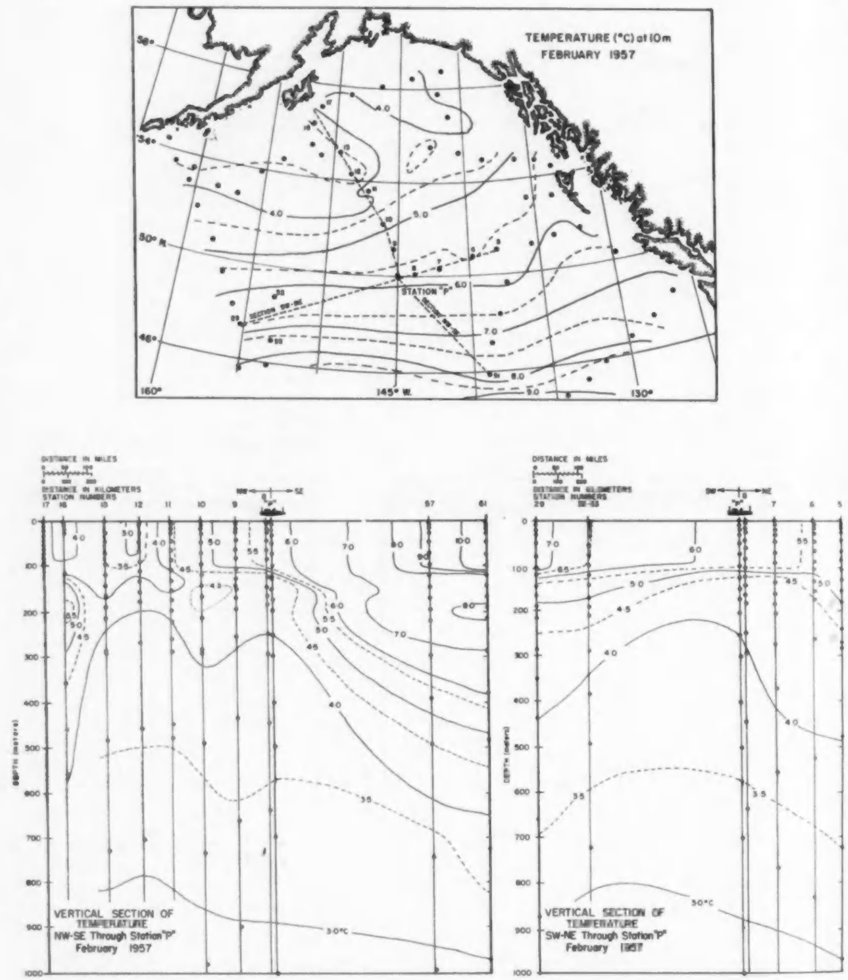

FIG. 12. Temperature, Winter 1957. *Upper*—Lateral distribution of temperature at depth of 10 m. *Lower*—Distribution of temperature in vertical sections.

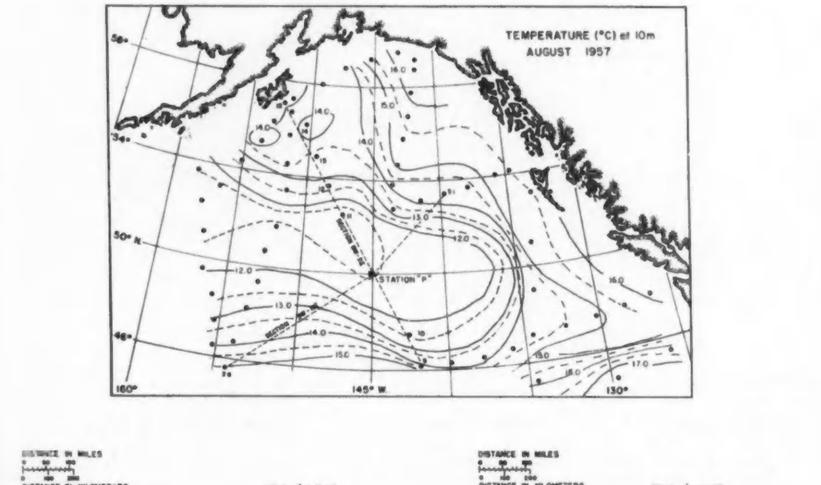

FIG. 13. Temperature, Summer 1957. *Upper*—Lateral distribution of temperature at depth of 10 m. *Lower*—Distribution of temperature in vertical sections.

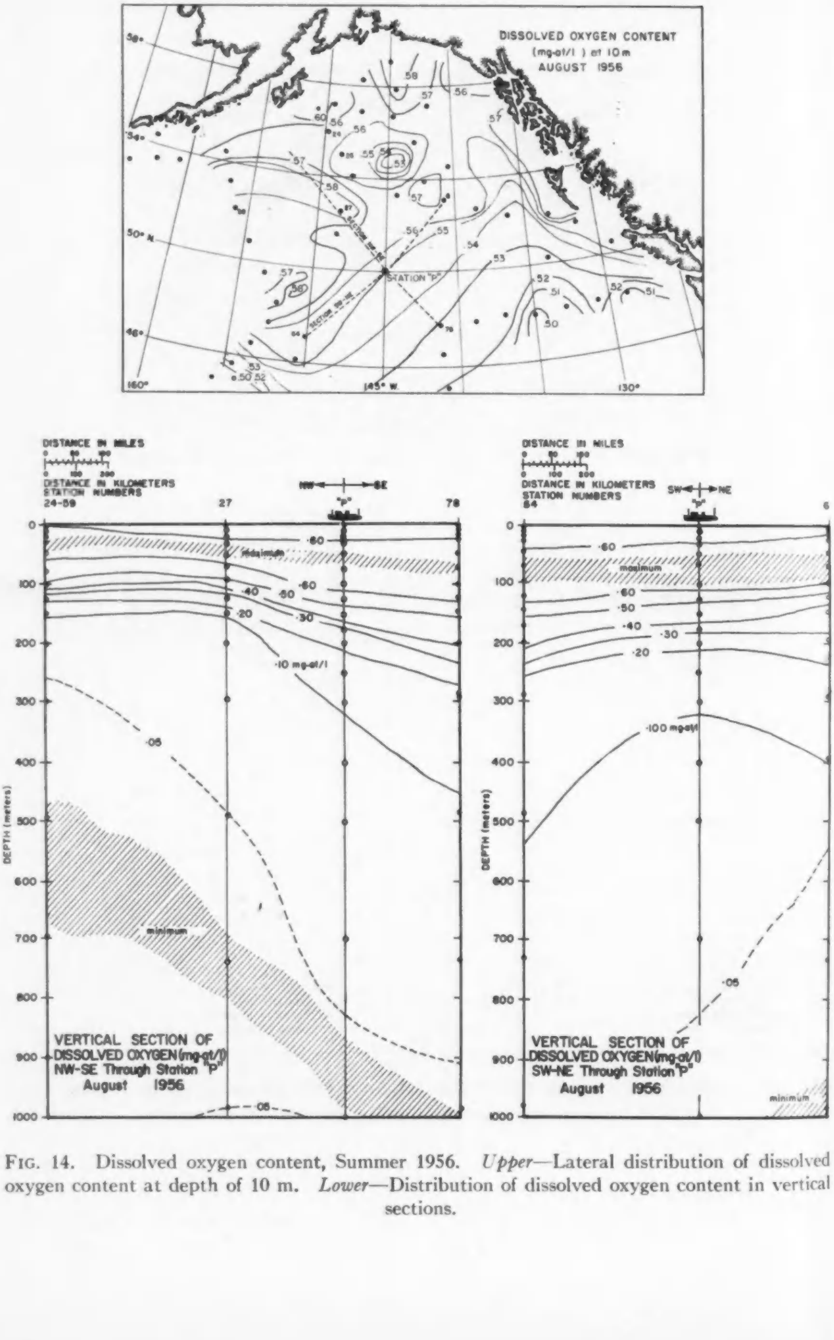

FIG. 14. Dissolved oxygen content, Summer 1956. *Upper*—Lateral distribution of dissolved oxygen content at depth of 10 m. *Lower*—Distribution of dissolved oxygen content in vertical sections.

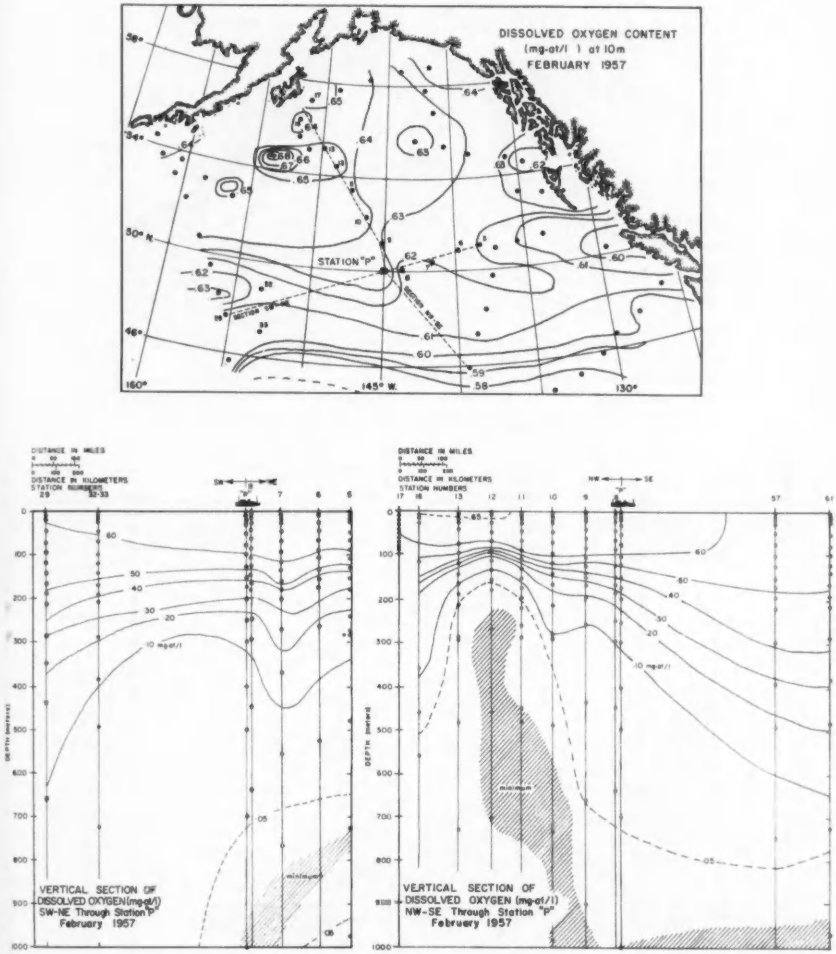

FIG. 15. Dissolved oxygen content, Winter 1957. *Upper*—Lateral distribution of dissolved oxygen content at depth of 10 m. *Lower*—Distribution of dissolved oxygen content in vertical sections.

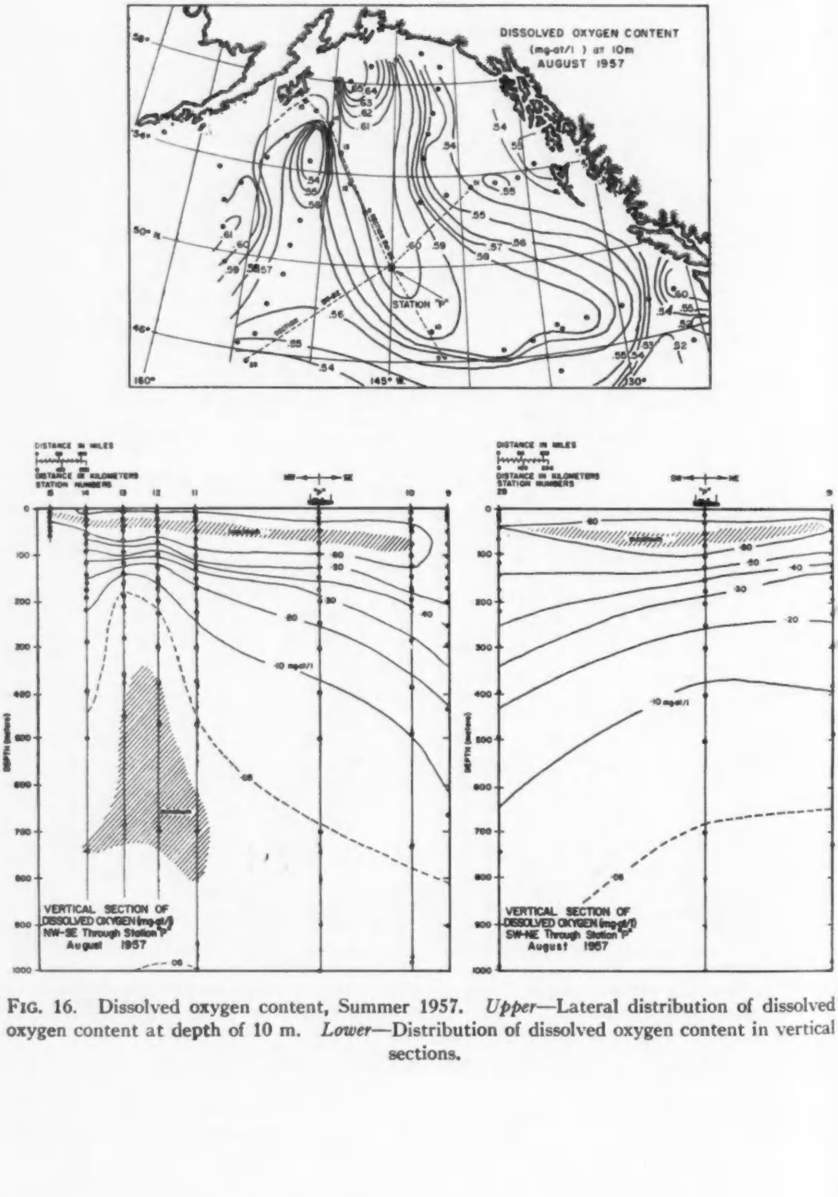

FIG. 16. Dissolved oxygen content, Summer 1957. *Upper*—Lateral distribution of dissolved oxygen content at depth of 10 m. *Lower*—Distribution of dissolved oxygen content in vertical sections.

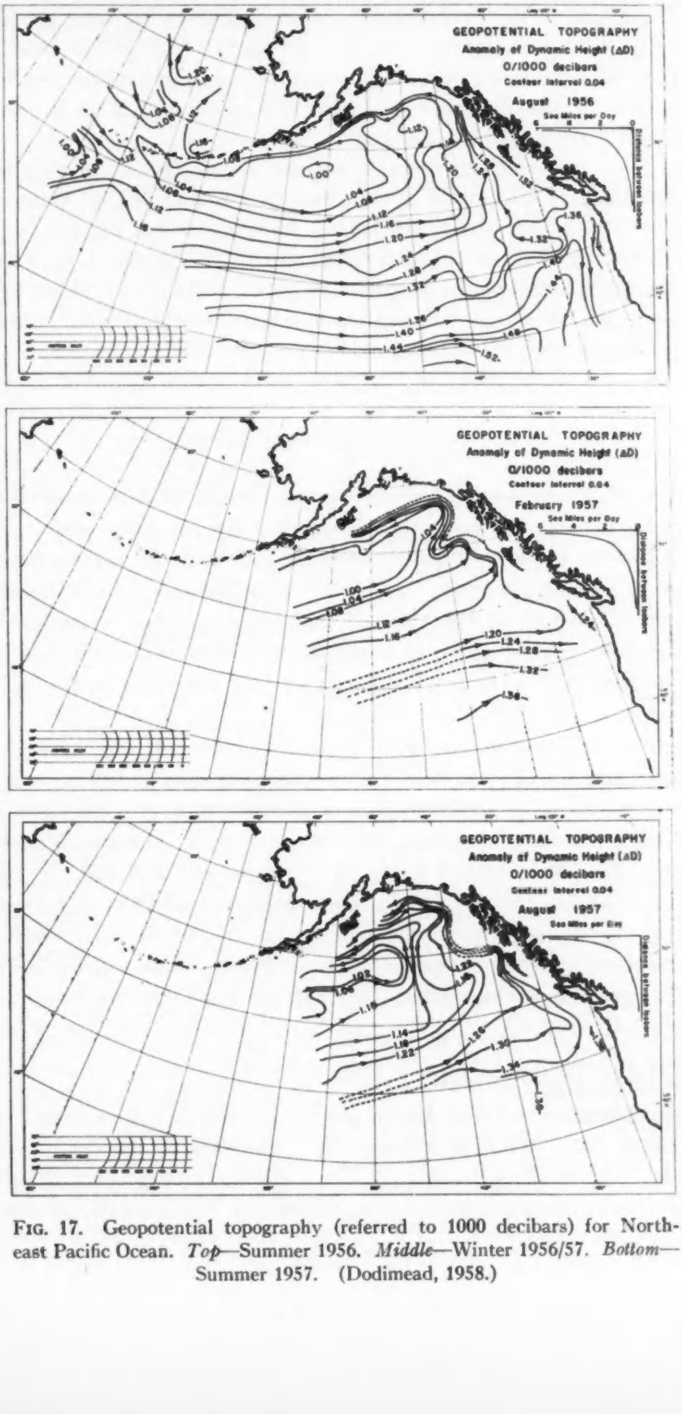

FIG. 17. Geopotential topography (referred to 1000 decibars) for Northeast Pacific Ocean. *Top*—Summer 1956. *Middle*—Winter 1956/57. *Bottom*—Summer 1957. (Dodimead, 1958.)

In order to show the distributions of the properties of water at Station "P" relative to those of the surroundings, vertical sections of these properties are drawn (Fig. 8–16). A comparison of these sections of salinity, temperature, and oxygen through this station indicates that the most pronounced horizontal gradients are in the direction northwest to southeast. This is particularly noticeable with the gradient of oxygen.

The Subarctic Current flows westward across the north Pacific Ocean (Sverdrup *et al.*, 1942) until it approaches the coast of North America. Here it divides to form the northward-flowing Alaska Current and the southward-flowing California Current (Fig. 1). Station "P" lies in the path of this near-zonal Subarctic Current where it changes its course northward. It lies well within the region of the Subarctic Water but is between the well-defined "dome" water to the northwest, and the Subtropic Water to the south.

VARIATIONS OF SALINITY

In Fig. 18 A and B are shown the seasonal values of salinity of the water at Station "P" for the 2 years between August 1956 and July 1958. The same data are plotted in three different ways to facilitate the presentations. The variations of salinity are most marked in the upper zone and in the halocline, and are less marked in the lower zone. Noticeable variations occur at all depths to at least 1000 m (Fig. 18A *upper* and *lower*). However, the annual range of salinity in the lower zone is about an order less than that in the upper zone (Tabata, 1960).

There is little evidence of cyclic annual variations of salinity in the upper zone, except perhaps at a depth of 100 m where the salinity reaches a maximum in autumn and decreases to a minimum in winter. In five of the eight intervals between the cruises, the changes in the halocline are in phase with those in the upper zone (Fig. 18A, *upper*; Table II). During the remainder of the time, they are in opposite phase. Although the magnitudes of the variations in the lower zone are smaller than those in the upper zone and the halocline, there appears to be some phase agreement between them. Moreover, 50% of the time there is a good phase agreement between the variations in all three zones (Table II).

Factors Influencing Salinity

In the discussion to follow, factors associated with air–sea boundary processes are discussed first. This is followed by comments on horizontal transport (advection) and finally on other factors. Similar introductory remarks also apply later to the discussions on factors influencing temperature and oxygen.

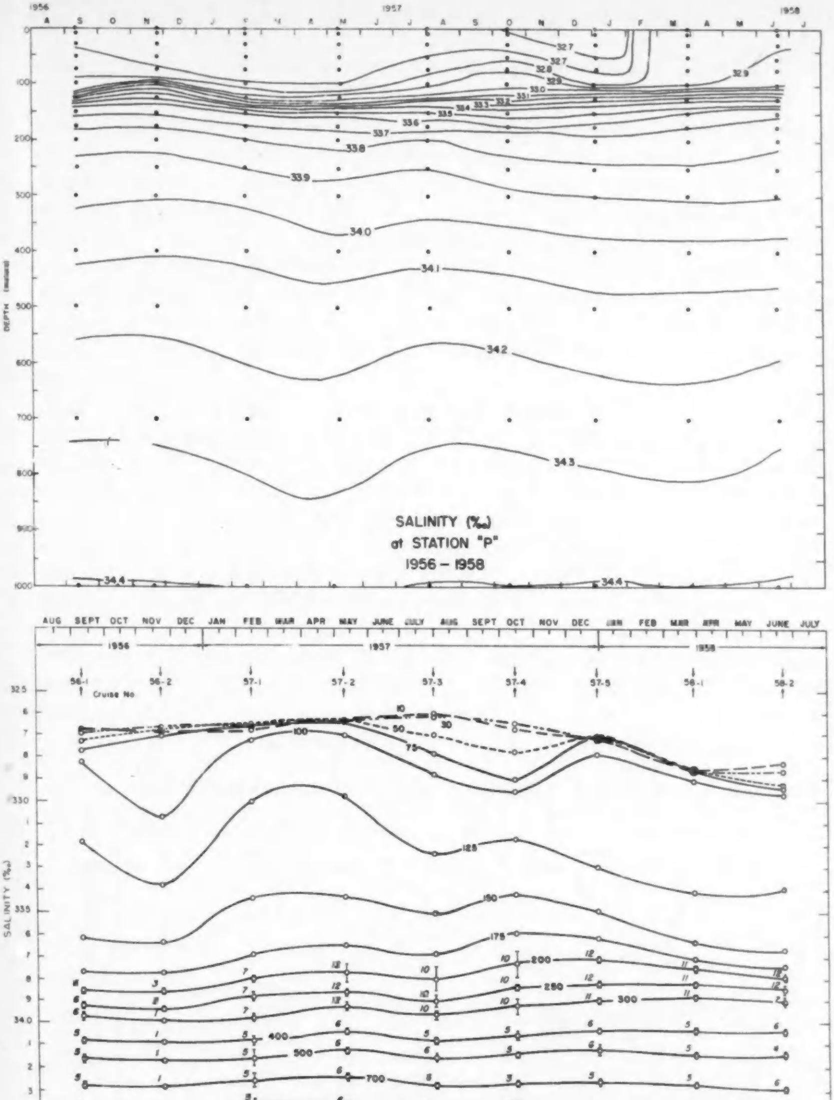

FIG. 18A. Salinity at Station "P", Summer 1956–Summer 1958. (The data over the approximate 6-week period are combined and plotted as a single point. This corresponds to observations at mid-date of the cruise period.) *Upper*—Seasonal distribution of salinity (0–1000 m). *Lower*—Seasonal values of salinity at depths: 0, 10, 30, 50, 75, 100, 125, 150, 175, 200, 250, 300, 400, 500, 700, 1000, 1200, and 1500 m.

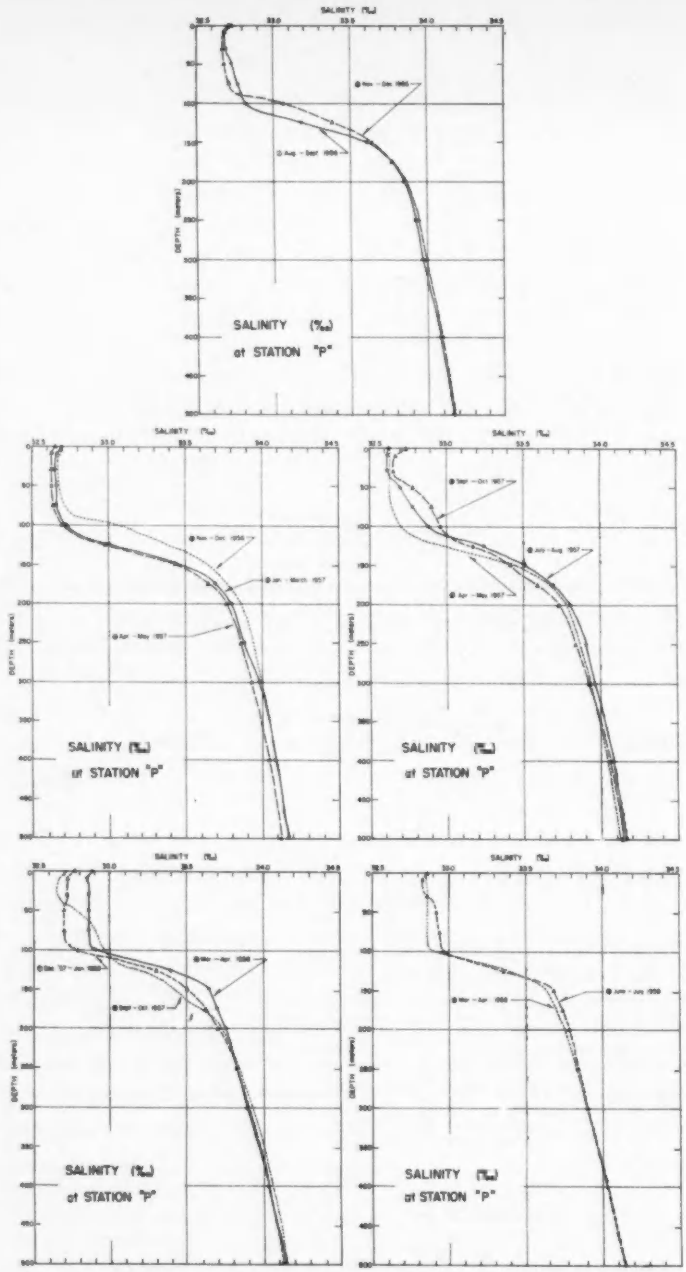

FIG. 18B. Salinity at Station "P", Summer 1956–Summer 1958. Vertical profiles of salinity (0–500 m).

FRESH WATER EXCHANGE ACROSS THE AIR–SEA BOUNDARY: PRECIPITATION AND EVAPORATION

The surface water of the ocean becomes diluted or concentrated, depending on whether or not fresh water is added or taken away. Dilution in the open ocean is accomplished by precipitation in the form of rain, snow, and hail, and to a very small extent by the condensation of water vapour above the sea surface. Concentration, on the other hand, is accomplished by evaporation of fresh water from the sea surface. Therefore, fresh water exchange across the air–sea boundary due to precipitation and evaporation is the most important factor influencing the salinity of the surface water. In the northeast Pacific Ocean, its influence is said to be confined primarily to the water above the halocline (Tully and Barber, 1960).

Jacobs (1951) indicated that in this region there is usually an excess of precipitation (P) over evaporation (E) throughout the year. For instance, in the general vicinity of Station "P", the excess of precipitation over evaporation fluctuates from a maximum (20 cm/season) in autumn to a minimum (10 cm/season) in winter. He further indicated that this excess generally increases to landward from the vicinity of that station to the coast of Alaska, British Columbia, and Washington, and decreases to westward and to southward. However, in the immediate neighborhood of the station, say within a radius of 100 miles, the values of this excess are relatively uniform, according to the charts prepared by him.

The monthly mean values of precipitation (unpublished meteorological record data, 1958, Meteorological Services of the Department of Transport, Canada), evaporation (calculated from Formula (6a) of the present paper), and $P-E$ at Station "P" are shown in Fig. 19. It is evident from this Figure

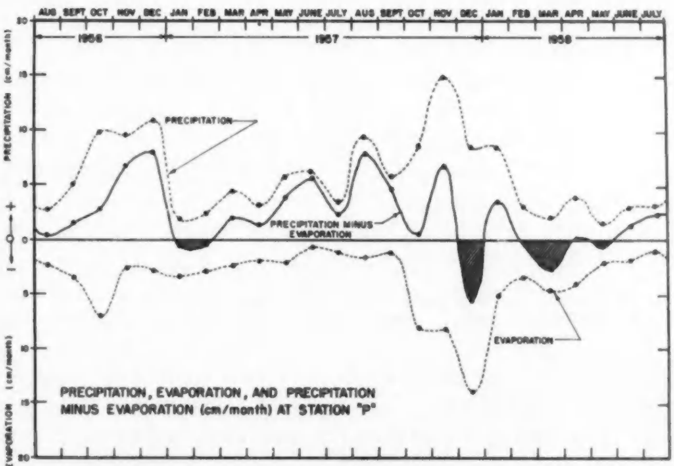

FIG. 19. Monthly mean values of precipitation, evaporation, and precipitation minus evaporation $(P-E)$ at Station "P", Summer 1956–Summer 1958. (By $P-E$ is meant the difference of precipitation and evaporation where precipitation and evaporation have *positive* values.)

that precipitation generally exceeds evaporation during all seasons except in winter.

The change of salinity, ΔS due to $P-E$, during the time interval Δt may be evaluated from the formula:

$$\Delta S = S_f - S_i \simeq -S_i\left(\frac{P-E}{z}\right) \qquad \ldots\ldots (1)$$

where: S_f is the final salinity (‰),

S_i is the initial salinity (‰),

z is the depth (cm) of column considered (upper zone), and

$P-E$ is the difference of precipitation and evaporation in centimetres during the time interval Δt.

At Station "P", the salinity of the upper zone is about 32.7‰. Thus, given a value of $P-E$ of 10 cm, the salinity of the upper zone (0–100 m) would decrease by 0.03‰, a magnitude of change well within the detectable limits. (Precision of salinity determinations at 35‰ level is ±0.004‰ at 0.05 probability level (Strickland and Parsons, 1960) when determinations are made with UW–PNL conductivity bridge (Paquette, 1959).)

The observed seasonal changes of salinity in the upper zone and also those changes that could result from the effect of seasonal variations of $P-E$ are shown in Table II. Comparison of these changes indicates that through summer

TABLE II. Observed seasonal changes of salinity in upper zone (0–100 m), precipitation minus evaporation (P – E), and effect of P – E in changing the salinity in upper zone.

Seasons:	Summer		Autumn		Winter		Spring		Summer		Autumn		Winter		Spring		Summer
Cruise No.:	56-1		56-2		57-1		57-2		57-3		57-4		57-5		58-1		58-2
Increase (+) or decrease (–) of salinity:																	
Upper zone (0–100 m)		–		–		–		+		+		–		+		+	
Halocline (100–200 m)		+		–		–		+		–		+		+		+	
Lower zone (>200 m)		+		–		–		+		–		–		negli-gible		+	
Observed change of salinity (‰/month) in upper zone:																	
		–0.014		–0.019		–0.007		+0.023		+0.032		–0.033		+0.054		+0.020	
Precipitation minus evaporation (cm/month):																	
		+3.71		+4.75		+1.03		+3.94		+4.34		+5.01		–0.081		–1.31	
Salinity change (‰/month) in upper zone that can be accounted for by effect of P – E:																	
		–0.014		–0.016		–0.003		–0.013		–0.013		–0.016		+0.003		–0.011	

and winter of 1956, the decrease of salinity in the upper zone could be almost wholly accounted for by dilution from excess of precipitation. During the first part of 1957, about 50% of the decrease could be accounted for by dilution. But from spring 1957 through summer 1958 (except for the decrease that occurred between autumn and winter 1957), the salinity increased despite the excess precipitation.

Horizontal transport

Transport of water from regions of different properties could cause changes in the properties at any fixed position.

If it can be assumed that vertical currents, vertical and horizontal mixing, and effects of divergence and convergence are negligible compared to horizontal currents (in the present discussion these are assumed to be negligible to the first approximation) then the influence of currents in changing the property of water may be expressed by:

$$\frac{ds}{dt} = v\frac{ds}{dx} \qquad \ldots\ldots (2)$$

where: s is any conservative concentration such as salt or heat,

$\frac{ds}{dt}$ is the change of concentration per day,

v is the current speed in kilometres per day, and

$\frac{ds}{dx}$ is the gradient of concentration parallel to the direction of the current in units of concentration per kilometre.

The effects of transport at certain periods are discussed only at the periods when data from adjacent regions are available.

The general increase of salinity in the upper zone and halocline during spring 1957 through summer 1958 is attributed to the northward transport of water. The water lying to the south of Station "P" is usually more saline than in the vicinity of the station (Tully and Dodimead, 1957; Dodimead, 1958). Hence, a northward transport of this water would tend to increase the salinity at the station. From the consideration of the horizontal salinity gradients (Fig. 10, *upper*) and surface currents (Fig. 17, *bottom*) for August 1957, it is estimated, from Equation (2), that due to this effect, an increase of salinity at the rate of 0.040‰/month occurred. This transport effect, plus that due to $P-E$, gives the observed increase of salinity for summer 1957 (Table II), and it is probable that a similar situation also occurred at other periods, except during autumn to winter, 1957. This northward transport is consistent with the anomalous warming of water in the northeast Pacific Ocean during the corresponding period, a phenomenon attributed to the intrusion of warm southern water into the region (Namias, 1959; Tully *et al.*, 1960; Sette and Issacs, 1960).

The decrease of salinity that occurred in the upper zone during autumn through winter, 1957, is due partly to dilution (Table II). The remainder is attributable to the transport of less-saline water from the west or northwest direction. The manner in which this transport might have occurred could be explained from the shift of winds in the region. In Fig. 21 (*upper*) is shown the usual atmospheric pressure system over the northeast Pacific Ocean. Figure 21

(*lower*) shows the system that occurs occasionally in autumn and winter, as in October 1956 and December 1957. The westerly winds associated with this latter system are indicated in Fig. 20. It is probable that, due to these westerly winds, the less-saline water frequently lying to the west or northwest of Station "P" during the summers (Tully and Dodimead, 1957; Dodimead, 1958) was driven into the vicinity of the station by drift currents associated with these winds.

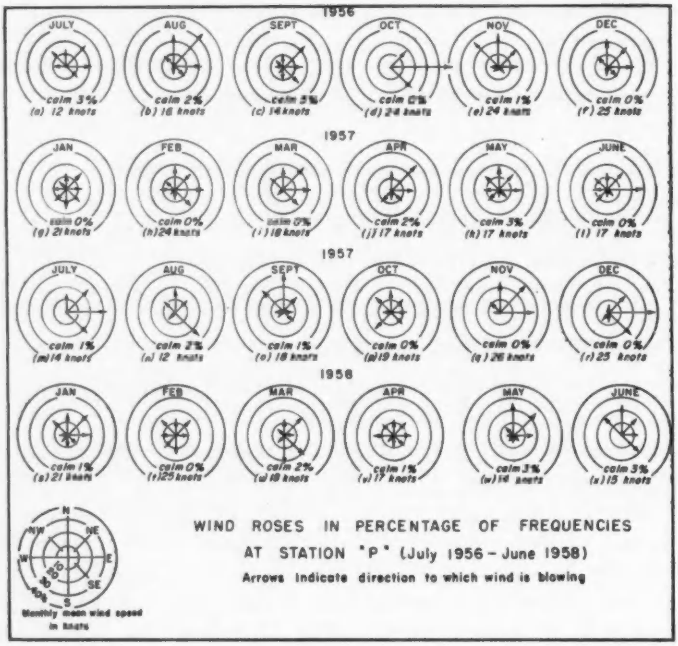

FIG. 20. Wind rose in percentage of frequencies and mean monthly wind speed at Station "P", Summer 1956–Summer 1958.

The increase of salinity in the halocline and lower zone during summer through autumn, 1956, appears to have been due to transport of the relatively saline water from the northwest, particularly from the vicinity of the "dome". It is only in the direction of the "dome" that the water at these levels is more saline than at Station "P" (Fig. 8, *lower left*), and southward transport of the water from this direction could account for the increase.

Conversely, the decrease that occurred at these levels during autumn through winter, 1956, is probably due to the northward transport of water, since it is in the southerly direction that relatively low salinity water presumably occurred, as in summer 1956 (Fig. 8, *lower*).

While the salinity increased in the halocline and the lower zone between summer and autumn, 1956, it decreased at these levels during the corresponding

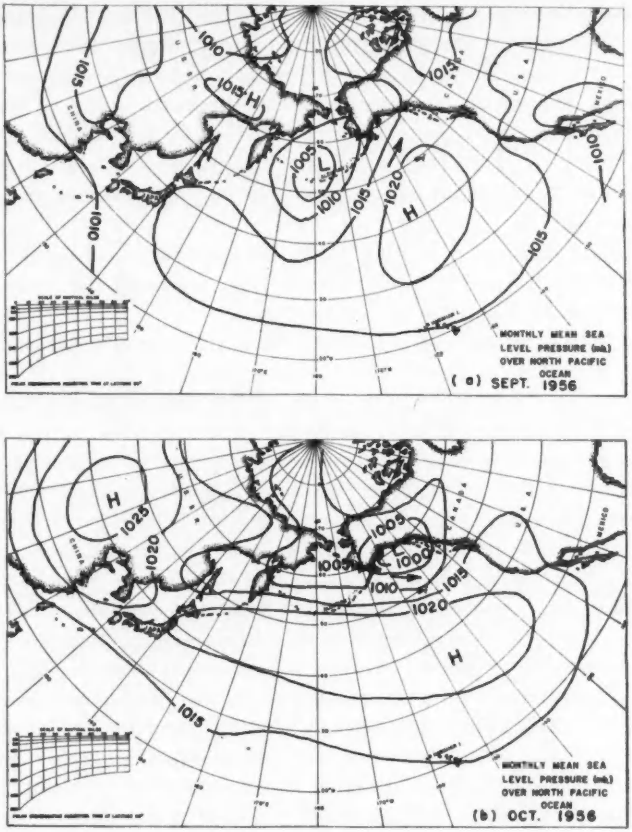

FIG. 21. Monthly mean sea level pressure charts for North Pacific Ocean. *Upper*—September 1956. *Lower*—October 1956. (Extended Forecast Section, U.S. Weather Bureau.) (December 1957 chart is similar to that for October 1956.)

period in the following year, 1957. This decrease is perhaps due to the transport of less-saline water from the south (Fig. 10, *lower*).

Any salinity change that is common to all three zones, as shown in the above example, is associated with transport of the entire column of water in the same general direction. This is consistent with the conclusion made by Bennett (1959), who pointed out that geostrophic currents occur to a depth of at least 1000 m, and that they flow in the same general direction as the surface current.

VERTICAL MIXING

Since the effect of fresh water exchange due to precipitation and evaporation is confined primarily to the immediate surface layer of the ocean, it is necessary

to examine the process of vertical mixing[5] by which this effect is distributed into the deeper layers. To illustrate how this mixing affects the structure of the properties of the water in the upper zone, Fig. 22 depicts the progressive deepening of the mixed-layer depth (bottom of the homogeneous layer). The thickness of the homogeneous layer reflects the extent to which the vertical mixing is effective in redistributing the properties of water. The manner in which mixing alters the structures may be seen in more detail from the comparison of the structures, as shown in Fig. 23.

At present, the exact mechanism of this mixing is not well understood. Presumably it is due to the combination of two processes, one associated with winds and the other associated with evaporation.

Winds may promote mixing by their accompanying effects such as stirring due to wave actions, wind-generated helical currents (Langmuir, 1938), and vertical turbulence associated with shear in the drift current (Ekman, 1905; Rossby and Montgomery, 1935). Comparison between the occurrence of strong winds in autumn and winter (Fig. 20) and the thickening of the homogeneous layer during this period (Fig. 22) suggests that winds are influential in causing mixing.

The effect of evaporation in initiating mixing is perhaps easier to understand than that of the winds. By continuously evaporating fresh water from the sea surface and by cooling, the surface water becomes denser than the water lying immediately below. As a result, the surface water sinks until it encounters water of the same density. The end result is that convection currents are set up and overturning of water occurs. Provided evaporation is large enough, this overturning could penetrate to great depths, as in the Mediterranean Sea where such a process causes convection currents to reach the bottom (Sverdrup *et al.*, 1942). As shown in Fig. 19, the evaporation is large in autumn and winter. Comparison of these periods and those of the deepening of the mixed-layer depth (Fig. 22) suggests that the large evaporation period is associated with period of this mixing.

It is sufficient to state here that there is an apparent relation between the winds and evaporation, and mixing. And as stated earlier, by such mixing redistribution of properties occurs. As is evident from Fig. 23, the salinity of the surface water increases while that immediately below decreases. Similarly, the temperature of the surface water decreases while the temperature of the layer immediately below increases. If $P-E=0$, then the gain of salt in the surface layer should equal the loss of salt in the layer below (i.e. the shaded area should equal the hatched area in Fig. 23).

The increase of salinity in the upper 50 m, and a part of the decrease that occurred below 50 m during autumn through winter, 1957, are both attributed to vertical mixing. Also, the occurrence of minimum annual salinity at a depth of 100 m in winter is believed to be due to this mixing.

[5]The term "vertical mixing" used here is associated with the autumnal breakdown of the structure of properties in the upper zone.

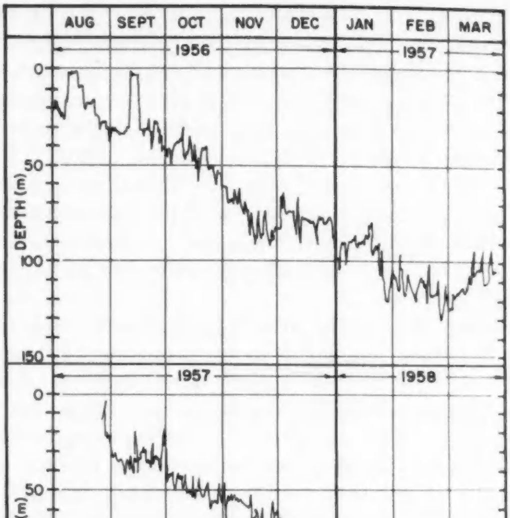

FIG. 22. Progressive deepening of the mixed-layer depth (thickness of homogeneous layer).

FIG. 23. Alteration of structures of properties of water due to vertical mixing.

Other factors

Lateral and vertical eddy diffusion of salt may also affect the salinity at Station "P" if there are large lateral and vertical salinity gradients present in the locality, and if the magnitudes of the eddy coefficients are sufficiently large. Unfortunately, no data are available concerning the magnitudes of these coefficients. However, there are appreciable horizontal gradients of salinity in the vicinity of the station, as shown in the upper panels of Fig. 8, 9 and 10. In the summer of 1956 (Fig. 8, *upper*) the water at the station was almost surrounded by water of salinity less than that at the station. A horizontal eddy system in the vicinity would tend to decrease the salinity at the station under such conditions. There are no data to support this assumption of lateral eddy diffusion, but the possibility remains.

As shown earlier (Fig. 2 and 18A, *upper*), a fairly large salinity gradient occurs between the upper and lower zones throughout the year. As diffusion of salt proceeds from large concentration to lesser concentration, it follows that there must be a continuous upward transfer of salt across the halocline due to vertical eddy diffusion. This would tend to make the upper zone progressively more saline with time. But due presumably to the dilution from excess precipitation, the upper zone is prevented from becoming more saline. In a recent paper, Tully and Barber (1960) postulated the upward transport of salt across the halocline by entrainment, a process which occurs in estuarine waters (Tully, 1949). It is probable that this entrainment (a special type of eddy diffusion process) probably contributes to the upward transport of salt and may increase the salinity of the upper zone. But to what extent this process affects the salinity has not been ascertained.

Wind-induced divergences and convergences of water (Hidaka, 1955; Hidaka and Akiba, 1955) may also affect the structure of properties, the former by upwelling and the latter by "piling-up" of water. Although there is no proof, the atmospheric low-pressure area that prevailed over Station "P" during February 1958 may have resulted in local upwelling. The somewhat large salinity increase that occurred during this period may have been partly due to this effect.

VARIATIONS OF TEMPERATURE

The annual cycles of surface sea temperatures at Station "P" for the years 1956, 1957, 1958, and for the mean period 1950–1958, are shown in Fig. 24. The salient feature of the annual cycle is that the maximum (13–14°C) generally occurs in the late summer, and the minimum (5–6°C) in late winter. From the comparison of the 8-year means with the temperatures for the individual years, it is evident that the temperature in autumn and winter, 1956, is less than the corresponding long-term means, but that for spring 1957 through summer 1958 is consistently higher. This latter period coincides with the period of anomalous warming of water in the northeast Pacific Ocean (Namias, 1959; Tully *et al.*, 1960).

Two annual cycles of air and surface sea temperature are shown in Fig. 25. On comparing these cycles, it is evident that the major features of the two are

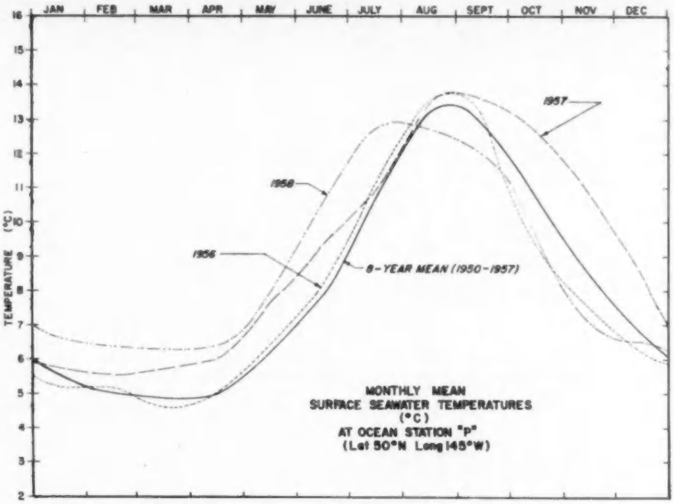

FIG. 24. Monthly mean surface sea temperature at Station "P", January 1956–December 1958, together with grand monthly means (1950–1957).

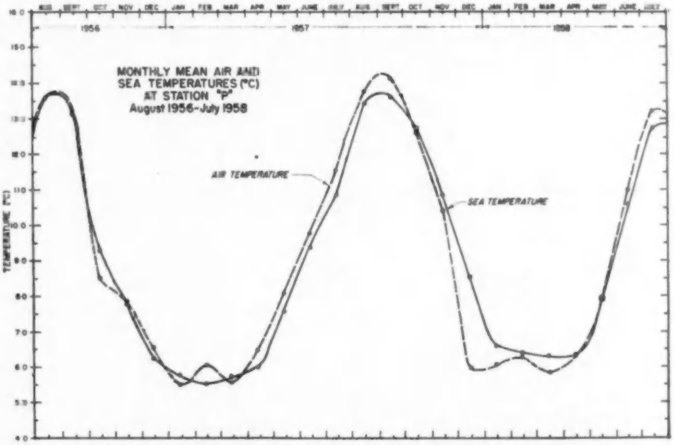

FIG. 25. Monthly mean values of air and sea temperature at Station "P", Summer 1956–1958 Summer.

similar. But in the winter the cycle of air temperature is more irregular than that of the sea temperature. Pickard and MacLeod (1953) showed that the shore water along the Canadian Pacific coast is warmer than the air in autumn and winter. Such a relation does not appear to hold at Station "P". In fact, during autumn and winter, 1956, the air was warmer than the sea.

The temperature of the subsurface water at Station "P" is shown in Fig. 26A and 26B. Marked annual variations occur at the surface and to a depth of

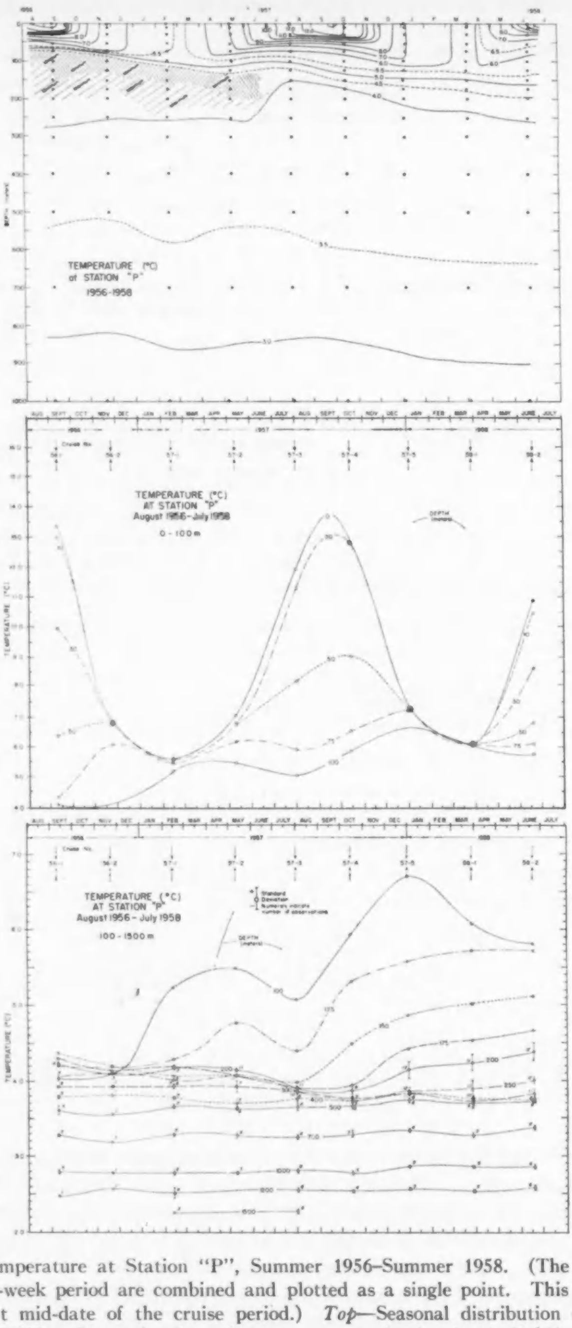

FIG. 26A. Temperature at Station "P", Summer 1956–Summer 1958. (The data over the approximate 6-week period are combined and plotted as a single point. This corresponds to observations at mid-date of the cruise period.) *Top*—Seasonal distribution of temperature (0–1000 m). *Middle*—Seasonal values of temperature at depths: 0, 10, 30, 50, 75, and 100 m. *Bottom*—Seasonal values of temperature at depths: 100, 125, 150, 175, 200, 300, 400, 500, 700, 1000, 1200, and 1500 m.

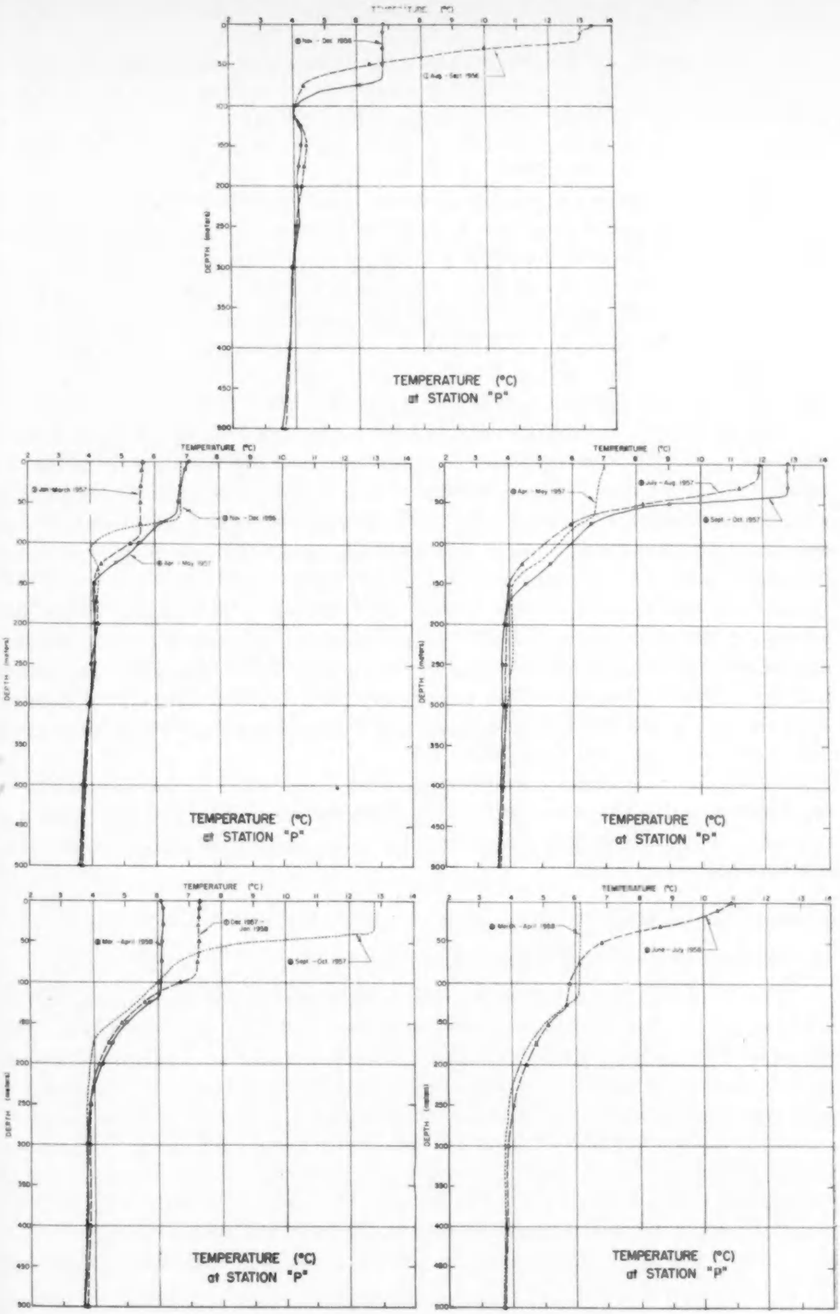

FIG. 26B. Temperature at Station "P", Summer 1956–Summer 1958. Vertical profiles of temperature (0–500 m).

30 m. At a depth of 50 m the annual amplitude is one-half that at the surface. At depths of 75 and 100 m, the annual variations are apparent, but they are even less marked. At a depth of 75 m, there is some indication of semi-annual variations. These have been reported in other parts of the north Pacific Ocean (Robinson, 1957).

A comparison of the annual cycles of air temperature (Fig. 25) and sea temperature between the surface and 100 m depth (Fig. 26A, *middle*) indicates that while the cycle of the surface sea temperature is in phase with that of the air temperature, the cycles of sea temperature below the depth of 30 m are not. In fact, the annual maximum of the sea temperature occurs progressively later with depth. For example, at a depth of 30 m it occurred in early autumn; at 50 m, in late autumn; and at 75 m, in early winter. This phenomenon recurs year after year as Hollister (1956) and Robinson (1957) have already shown.

Appreciable non-seasonal variations of temperature occur in the halocline. At a depth of 150 m for example (Fig. 26A, *bottom*), the temperature varied by about 1 C° during the 2 years. However, there does not seem to be any definite periodicity present in the variations. There was a general increase of temperature during winter 1956 through summer 1958, except during spring to summer, 1957, (Fig. 26A, *bottom*, and Fig. 26B).

In the depths between the top of the halocline (100 m) and the shallow portion of the lower zone (400 m) the variations of temperature are complicated due to the presence of temperature inversion in these levels (Fig. 26A, *top*, *bottom*, and Fig. 26B). These inversions were quite marked and occurred from summer 1956 through spring 1957, but deepened and became imperceptible by summer of 1957 (Fig. 26A, *top*, and Fig. 26B).

Significant variations of temperature occur in the lower zone to a depth of at least 500 m and perhaps to 1000 m (Fig. 26A, *bottom*). The water between the depths of 500 m and 1000 m was about 0.1 C° warmer in 1958 than in 1956 and in the first half-year of 1957.

Factors Influencing Temperature

Heat transfer across the air–sea boundary

The dominant factor influencing the temperature in the upper zone, and to some extent in the halocline, is heat transfer at the air–sea boundary. The flux of heat through the air–sea boundary is due to the combined effects of incident solar radiation, reflected solar radiation, effective back radiation, evaporation (and condensation), and conduction of sensible heat. The heat transfer equation across the air–sea boundary during a time interval Δt is written:

$$Q_t = Q_i - Q_r - Q_b - Q_e - Q_h \quad \text{.....} (3)$$

where: Q_t is the net heat transfer across the air–sea boundary,

Q_i is the short-wave radiation from the sun and sky, both direct and diffuse,

Q_r is the reflected short-wave radiation from the sea,

Q_b is the effective back radiation (long wave radiation from the sea surface minus that from the atmosphere),

Q_e is the heat transfer by evaporation (and condensation), and

Q_h is the conduction of sensible heat between the atmosphere and the sea.

In this paper, all these quantities are expressed in units of gram-calories per square centimetre per day (g-cal/cm²/day).

The concepts and theories of these components of the heat transfer process are discussed briefly in "The Oceans" (Sverdrup *et al.*, 1942) and in more detail in a report by Anderson (1952). A fairly extensive study of these components has recently been made for a near-shore situation at Triple Island in northern British Columbia (Tabata, 1958). Here it was found that the annual cycle of incident solar radiation, and the cycle of the combination of evaporation and conduction, controlled the seasonal fluctuations of the net heat transfer across the air–sea boundary. Although the heat loss by effective back radiation was appreciable, the absence of large seasonal variations prevented it from being influential in contributing to the seasonal fluctuations of net heat transfer. A somewhat analogous study is made at Station "P" in the mid-ocean.

The magnitudes of solar radiation for cloudless days are based on values for the coast of British Columbia at Lat. 50°N, interpolated from monthly charts prepared by Mateer (1955). The formula:

$$Q_s = Q_0\ (1 - 0.071C) \qquad \ldots\ldots (4)$$

where: Q_s is the solar radiation reaching the sea surface after the effect of cloud has been taken into consideration,

Q_0 is the total incoming solar radiation under clear sky, and

C is the amount of clouds in scale 0 to 10,

is used to correct for absorption of solar radiation by clouds (Sverdrup *et al.*, 1942).

The values of reflection of solar radiation (Q_r) from the sea surface were obtained from charts prepared by Anderson (1952).

The formula:

$$Q_b = 1.141\left\{\theta_s^4 - \theta_a^4(a + be_a)\right\}10^{-7} \qquad \ldots\ldots (5)$$

where: θ_s is the absolute temperature of the sea surface,

θ_a is the absolute temperature of the air above the sea surface, and

e_a is the vapour pressure (millibars) of the atmosphere where the air temperature is measured, and the constants a and b are related to both the cloud amount and height and were obtained from charts prepared by Anderson (1952),

is used to compute effective back radiation (Q_b) (Tabata, 1958).

For computing evaporation (E in mm/cm^2/day and Q_e in g-cal/cm^2/day), these formulae are used:

$$E = 0.105(e_s - e_a)u_a \qquad \text{.....} (6a)$$

$$Q_e = LE = 6.13(e_s - e_a)u_a \qquad \text{.....} (6b)$$

where: e_s is the vapour pressure (mb) of the saturated air at the sea surface,

e_a is the vapour pressure (mb) of the air at a height of 6 m above the sea surface, and

u_a is the wind speed (metres per second) at a height of 6 m above the sea surface[6],

L is the latent heat of vaporization and is equal to 585 g-cal/g.

These formulae are based on the evaporation formula derived by Sverdrup (1937), with the modification proposed by Marciano and Harbeck (1952).

The conduction of sensible heat (Q_h) is computed from values of evaporation multiplied by the Bowen Ratio (Bowen, 1926). The Bowen Ratio is:

$$\frac{Q_h}{Q_e} = \frac{0.61(T_s - T_a)P}{(e_s - e_a)1013} \qquad \text{.....} (7)$$

where: T_s is the surface sea temperature (°C),

T_a is the air temperature (°C), and

P is the sea level barometric pressure (mb). (For all practical purposes, P may be considered as having standard pressure of 1013 mb.)

The data resulting from the computations are shown in Fig. 27. As mentioned in an earlier paper (Tabata, 1958) the accuracy obtainable depends on validity of theories. Lacking direct measurements, the evaluation of such errors are difficult. Errors as large as 20% cannot be considered unreasonable.

As is common in other localities, there is a marked annual cycle of solar radiation. But the magnitude of the absorbed solar radiation (Q_s) is reduced to almost one-third of that which is potentially avaiiable (Fig. 27a) because of cloud cover. The annual amplitude of effective back radiation (Q_b) is small compared to that of solar radiation (compare Fig. 27a with Fig. 27b). However, the amount of the heat lost by this process is appreciable. The annual cycle of heat loss by evaporation (Q_e) is marked, with the maximum occurring in winter and the minimum in summer (Fig. 27c). The annual cycle of conduction of sensible heat (Q_h) from the sea to air is generally in phase with that of evaporation but the magnitudes involved are smaller (compare Fig. 27c with Fig. 27d). The main feature of the annual cycle of the net heat transfer (Q_t) across the air–

[6]While air temperatures were observed at a height of about 6 m above the sea surface, wind velocities were observed at a height of about 20 m. Wind speeds at a height of 20 m have been reduced to those at a height of 6 m by subtracting 1.8 m/sec from the observed winds speeds at that height according to data reported by Wagner (1958). This constant reduction of wind speeds may not be correct in detail for various strengths of winds and various stability conditions of air above the sea, but they are assumed to be approximately correct.

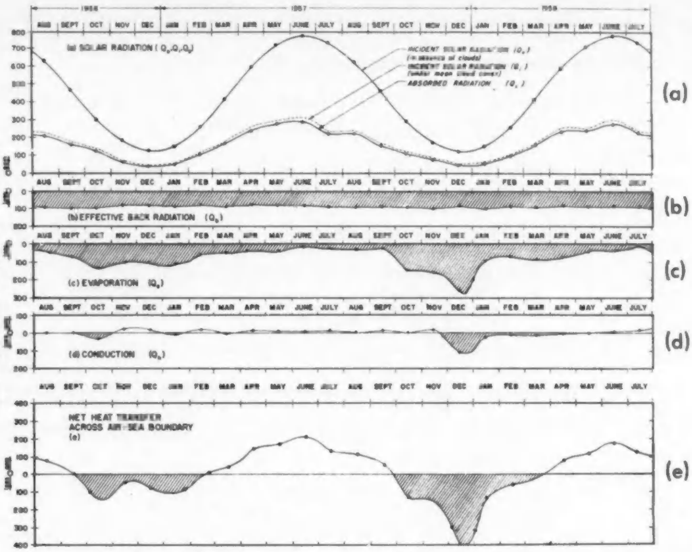

FIG. 27. Monthly mean values of heat transfer process at Station "P", Summer 1956–Summer 1958. (a) Solar radiation (Q_o, Q_i, Q_s). (b) Effective back radiation (Q_b). (c) Evaporation (Q_e). (d) Conduction of sensible heat (Q_h). (e) Net heat transfer across air–sea boundary (Q_t).

sea boundary is that the greatest heat gain occurs in summer (200 g-cal/cm²/day) and the greatest loss (400 g-cal/cm²/day) in winter. The transitional periods during which there is no net heat transfer occur in early spring and in early autumn (Fig. 27e).

During the summer, the main factor contributing to heat gain by the sea is solar radiation. The large loss of heat in winter is attributed mainly to the increase of evaporation and conduction, the former being dominant. Thus the annual cycle of net heat transfer is dependent primarily on these three components of the process. Similar conclusions were reached for heat transfer in the coastal waters (Tabata, 1958).

The sea warms or cools depending on whether or not the net heat transfer is directed into or out of the sea. The rate of change of heat content in a column of water of unit cross sectional area and z cm deep may be calculated as:

$$Q_\theta = \frac{\partial}{\partial t}\int_0^z \rho c_p T \mathrm{d}z$$

$$\simeq \frac{\overline{\rho c_p}\int_0^z \triangle T \mathrm{d}z}{\triangle t} \quad \ldots\ldots (8)$$

where: Q_θ is the change of heat content (g-cal/cm²/day),

ρ is the density of sea water (g/cm³),

c_p is the specific heat of sea water (g-cal/g/°C) obtained from recent determinations by Cox and Smith (1959),

z is the depth (cm) of the column of water, above which major changes of heat content occur,

$\bar{\rho}$ is the mean density of sea water (g/cm³),

$\bar{c_p}$ is the mean specific heat of sea water (g-cal/g/°C),

$\triangle t$ is the time interval in days, and

$\triangle T dz$ is the element of area bounded by two temperature–depth curves.

The mean density of sea water in the water column at Station "P" is about 1.0265 g/cm³ and its specific heat 0.954 g-cal/g/°C. Thus the above Formula (8) becomes:

$$Q_\theta = \frac{0.980 \int_0^z \triangle T dz}{\triangle t} \quad \ldots . (9)$$

From the consideration of net heat transfer at the air–sea boundary at Station "P", the surface water should begin to cool in September, since from this time on, the sea begins to lose heat to the atmosphere, principally from the increase in evaporation. Warming of surface water should commence in March, as from this time on, the sea begins to gain heat, principally from solar radiation (Fig. 27). These two periods, when the net heat transfer changes from being afferent to efferent and vice versa, are confirmed in the annual cycle of surface sea temperatures as shown in Fig. 28. Therefore, the seasonal variations of temperature of the surface water are mainly due to the seasonal variations of net heat transfer at the air–sea boundary.

In order to show the relation between the seasonal variations of net heat transfer and the variations of sea temperature in more detail, the changes of heat content estimated by the heat transfer formulae (Fig. 27e) and the observed changes of heat (Formula (9)) are shown in Table III. It is evident, from the comparison of values shown in that Table, that in most cases more than 50% of the changes of heat content in the upper zone can be attributed to heat transfer, and that most of the seasonal changes of heat content are confined to the upper zone. But during summer through autumn, 1956, only 30% of the change could be accounted for by heat transfer. Evidently, during this period some other process was more influential in changing the temperature.

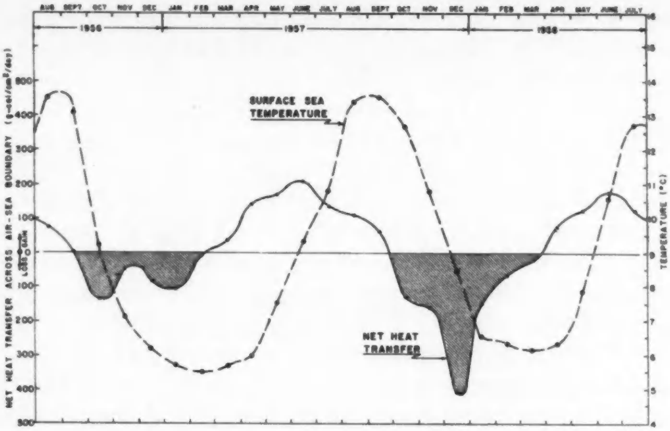

FIG. 28. Relation between surface sea temperature and net heat transfer at Station "P".

TABLE III. Observed seasonal change of heat content in upper zone (0–100 m) and halocline (100–200 m) and changes brought about by heat transfer at air–sea boundary.

Seasons:	Summer		Autumn		Winter		Spring		Summer		Autumn		Winter		Spring		Summer
Cruise No.:	56-1		56-2		57-1		57-2		57-3		57-4		57-5		58-1		58-2
Increase (+) or decrease (-) of heat content:																	
Upper zone (0–100 m)		-		-		+		+		+		-		-		+	
Halocline (100–200 m)		-		0		+		-		+		+		+		+	
Lower zone (> 200 m)		-		+		negligible		negligible		negligible		+		negligible		-	
Observed change of heat content (g-cal/cm²/day) (mainly in upper zone):		-197		-79		+126		+194		+138		-473		-130		+198	
Depth interval:		0–120		0–130		0–150		0–150		0–100		0–100		0–110		0–130	
Change of heat content (g-cal/cm²/day) from heat transfer at air–sea boundary:		-74		-80		+87		+170		+69		-309		-111		+109	
Percent of change accounted for by heat transfer at air–sea boundary:		32		101		69		88		50		65		85		55	

HORIZONTAL TRANSPORT

The water lying to the south is generally warmer, and that lying to the west and northwest generally colder, than the water at Station "P" (Fig. 11, 12, 13). Hence any current that flows from the south would transport warm water, and any current from the west or northwest would transport cold water into the vicinity.

A transport of relatively warm water from the south, and perhaps southwest, appeared to have caused an additional increase of temperature at the station during summer through autumn 1957 and spring through summer, 1958. During these two periods, heat transfer at the air–sea boundary accounted for only 50% of the increase in temperature.

During the summer of 1957, a temperature increase at the rate of 0.40 C°/month occurred. Heat transfer at the air–sea boundary accounted for 50% (0.20 C°/month) of the observed increase. From the consideration of horizontal temperature gradients (Fig. 13, *upper*) and surface currents (Fig. 17) for August 1957, and by the use of Formula (2), it is estimated that in the upper zone a temperature increase at the rate of 0.23 C°/month could occur. Therefore, the combined effect of heat transfer at the air–sea boundary and advection accounts for the right observed increase. It is probable that the large temperature increase during spring through summer, 1958, and to a lesser degree during winter through spring, 1957, was also due to horizontal transport. This transport is consistent with that causing the change of salinity during the corresponding periods and is attributed to the intrusion of southern water, as mentioned earlier.

The increase of temperature in the halocline from summer 1957 through summer 1958 (Fig. 26A, *bottom*) is also attributed to the transport of warm water from the south (Fig. 13, *lower*). However, a decrease occurred in the halocline during spring through summer, 1957 (Fig. 26A, *bottom*, and third panel of Fig. 26B). A decrease also occurred both above (75 m) and below the halocline (200–300 m) during the same period. The decrease that occurred just below the halocline may be explained by assuming a transport of colder water from the southwest (*lower right* panels of Fig. 12 and 13). Attention is drawn to the positions of the 4°C isotherms for February 1957 (Fig. 12, *lower right*) and for August 1957 (Fig. 13, *lower right*) which indicate that the colder water had, by August 1957, moved to the northeast. It is further evident, from the temporal distribution of the isotherms as shown in Fig. 26A, *top*, that a noticeable movement of the water occurred between spring and summer 1957. However, the temperature decrease in and just above the halocline must have been due to the transport of cold water from the northwest which was the only source of cold water at these depths (*lower left* panels of Fig. 12 and 13).

The manner in which the intrusion of warm water affected the water at Station "P" may also be illustrated by comparing the T–S characteristics of the water at various periods, as shown in Fig. 29. Attention is drawn to the curves for 1957 and 1958. The gradual shift of the T–S characteristics, corresponding to the progressive increase of temperature and salinity above the lower zone, is quite evident. Comparison of these with the T–S classification of water masses in the region (Fig. 30—Tully and Dodimead, 1957) indicates that the water at the station has undergone a gradual change towards a more southern type. A comparison with the water lying south of the Subarctic Boundary (Fig. 7) suggests that the intruding water had characteristics intermediate between the Subarctic and Subtropic Waters.

A transport of relatively cold water from the northwest during summer through autumn, 1956, and autumn through winter, 1957, appears to have caused

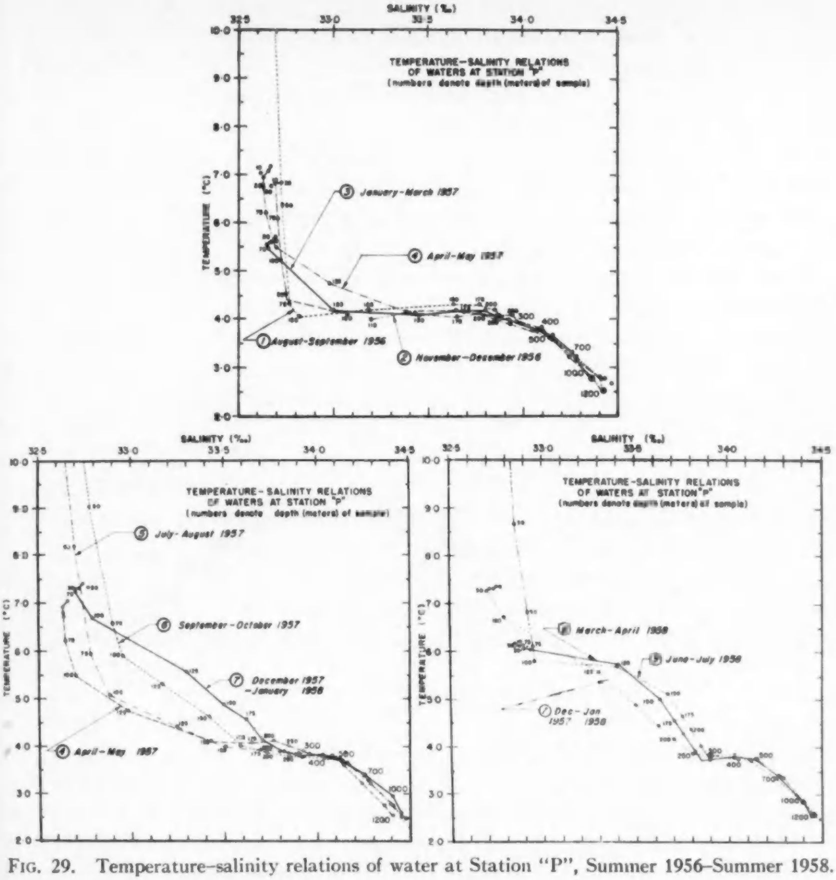

FIG. 29. Temperature–salinity relations of water at Station "P", Summer 1956–Summer 1958.

a decrease of temperature, as in both cases heat transfer at the air–sea boundary could account for only a portion of the decrease (Table III).

During summer 1956, the isotherms in the vicinity of Station "P" lay almost parallel to the direction of the surface geostrophic current (Fig. 11, *upper*, and Fig. 17). Thus the transport of water due to this current could not alter the temperature at the station. However, a transport of colder water from the west or northwest could cause a decrease. This seems likely, as during summer 1956 colder water lay in these directions (Fig. 11, *upper*). Also, during October 1956 the winds were generally from these directions (Fig. 20d and 21, *lower*). If the distribution of surface temperature observed in summer (Fig. 11, *upper*) can be assumed to have continued through the autumn, then it may be concluded that the transport of cold water associated with these winds were the main

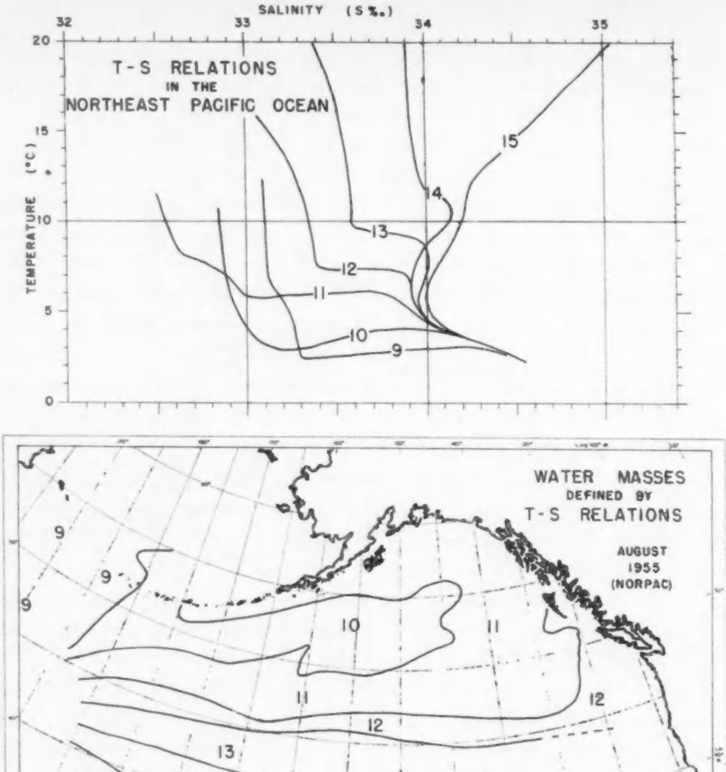

FIG. 30. Temperature–salinity classification of water masses of northeast Pacific Ocean region (Tully and Dodimead, 1957).

cause for the decrease of temperature that occurred between summer and autumn of 1956. The corresponding increase of salinity in the halocline (Fig. 18B) lends support to the concept of transport from these directions.

There is one temperature feature in the halocline (100–200 m depth) for summer and autumn, 1956 (Fig. 11, *lower*, and first panel of Fig. 26B), that is of particular interest. During the summer, Station "P" appeared to lie in the axis of a tongue of cold water which originated in the "dome" area. The tongue, characterized by the 4°C isotherm (Fig. 11, *lower*) continued past the station until it finally lost its identity about 200 miles to the southeast. From consideration of the vertical temperature gradients (first panel of Fig. 26B) it is reasonable to anticipate a progressive increase of temperature in the minimum temperature layer, due to eddy diffusion of heat. But the temperatures of this layer in summer and in autumn were exactly the same. It is speculated that the rate of horizontal movement of this tongue, presumably to southeastward, was just sufficient to neutralize the increase of temperature that may have resulted from vertical eddy diffusion of heat.

Only 65% of the decrease of temperature (Table III) during autumn through winter, 1957, is due to heat transfer at the air–sea boundary. The remainder is attributed to wind transport of colder water from the west and northwest since winds were generally from these directions in December 1957. This is consistent with the explanation given earlier for the change of salinity at the station during the same period.

Vertical mixing

As shown earlier, the homogeneous layer thickened progressively from autumn through winter due to vertical mixing (Fig. 22). This process brings about the redistribution of heat, as well as salt, in the homogeneous layer. By doing so, it transports the warmer water downward and the colder water upward (Fig. 23, *right*). The net result is that warming of water at some depths in the upper zone may occur, even when the sea is actually losing heat to the atmosphere. It is this mixing that causes the maximum annual temperature to occur progressively later with depth, in the upper zone (Fig. 26A, *middle*).

Other factors

It is possible that both lateral and vertical eddy diffusion of heat could also affect the temperature of the water at Station "P". It is assumed that their effects are small compared to those of heat transfer at the air–sea boundary and horizontal transport.

However in summer 1957, lateral eddy diffusion may have had some effect. As shown in Fig. 13, *upper*, the water at the station was almost surrounded by warmer water. And although it is difficult to prove, it is possible that a temperature increase at the station may have resulted from lateral eddy diffusion.

VARIATIONS OF DISSOLVED OXYGEN CONTENT

The dissolved oxygen, together with the oxygen solubility and the degree of saturation, of the surface water at Station "P" are shown in Fig. 31 (*upper part*). In Fig. 32 are shown the oxygen in the surface and subsurface waters. It is evident from the comparison of the annual cycle of the oxygen, and of the solubility

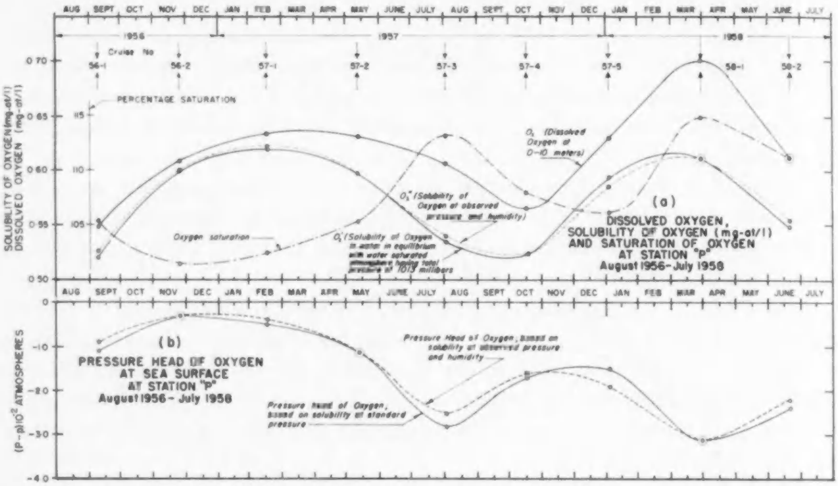

FIG. 31. *Upper part*—Seasonal values of dissolved oxygen content, solubility of oxygen in water, and degree of saturation, of the surface water at Station "P", Summer 1956–Summer 1958. *Lower part*—Pressure head of oxygen at the sea surface at Station "P", Summer 1956–Summer 1958. (The data over the approximate 6-week period are combined and plotted as a single point. This corresponds to observations at mid-date of the cruise period.)

(Fig. 31 (*upper part*) and middle panel of Fig. 32A), that marked annual variations of oxygen which are in general phase agreement with those of solubility occur at the surface and to a depth of 30 m. The oxygen in the surface water reaches a maximum in early spring and a minimum in early autumn. The surface water remains supersaturated throughout the year. It reached maximum supersaturation in summer 1957, and again in spring 1958, and minimum in the two winters.

Appreciable annual variations of oxygen occur at depths of 50 and 75 m (Fig. 32 A and B) and they appear almost in phase with those at the surface. However, in some periods, as during autumn through winter 1956, they were in opposite phase to those at the surface.

The oxygen in the depths above 75 m decreases from spring through autumn (Fig. 32 A and B). But it does not seem to decrease at the same rate at all depths. In fact, the rate decreases with depth, being largest at the surface, and becomes progressively smaller with depth. Because of this decrease and

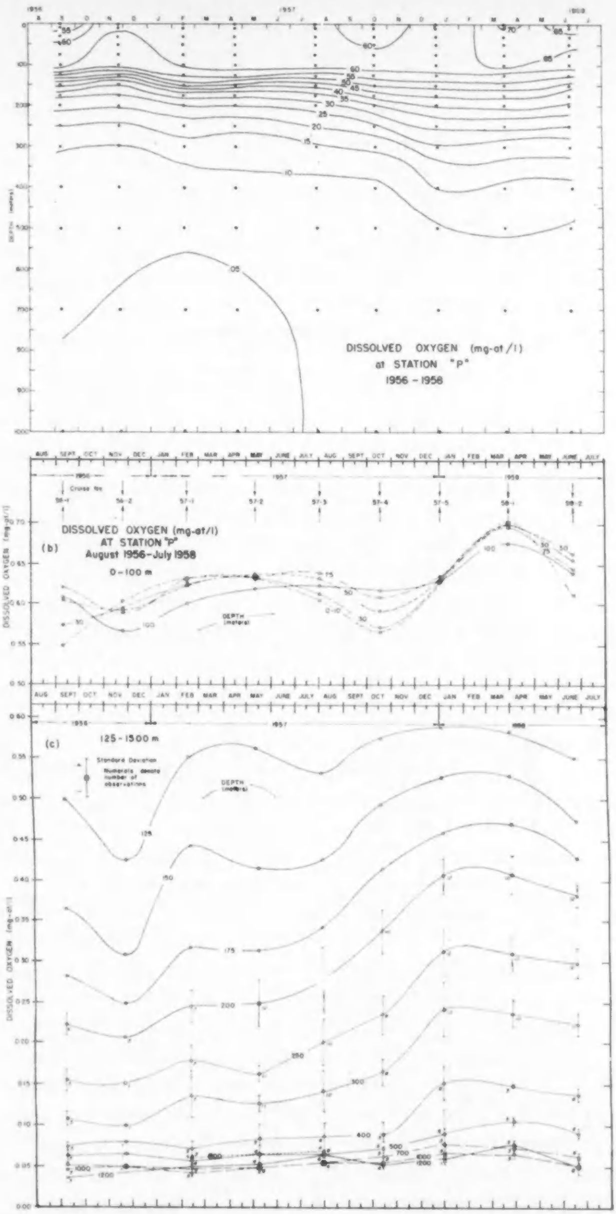

FIG. 32A. Dissolved oxygen content at Station "P", Summer 1956–Summer 1958. (The data over the approximate 6-week period are combined and plotted as a single point. This corresponds to observations at mid-dates of the cruise period.) *Top*—Seasonal distribution of dissolved oxygen content (0–1000 m). *Middle*—Seasonal values of dissolved oxygen content at depths: 0, 10, 30, 50, 75, and 100 m. *Bottom*—Seasonal values of dissolved oxygen content at depths: 125, 150, 175, 200, 300, 400, 500, 700, 1000, 1200, and 1500 m.

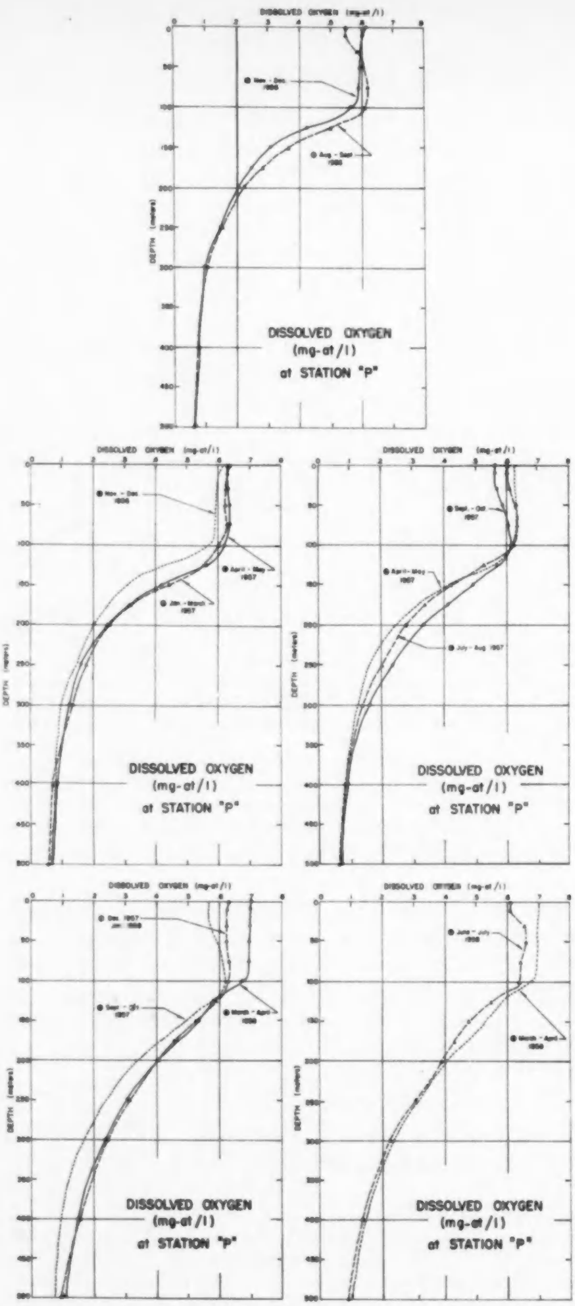

FIG. 32B. Dissolved oxygen content at Station "P", Summer 1956–Summer 1958. Vertical profiles of dissolved oxygen content (0–500 m).

because the oxygen decreases with depth from 100 m downward, it follows that in the summer and early autumn a maximum oxygen layer occurs between 50 and 100 m depth.

There is little evidence of definite annual variations of the oxygen at the depths below 100 m. However, there are conspicuous non-annual variations in both the halocline and the lower zone. For instance, at depths between 150 and 500 m, the oxygen doubled from autumn 1956 to spring 1958 (Fig. 31, lower part). The trend in the lower zone at depths between 400 and 1000 m was generally similar to that in the halocline. The minimum occurred in winter 1956, and the maximum in winter 1957. The variations at 1200 m depth were more irregular however, than at depths less than 1000 m (Fig. 31, lower part).

Factors Influencing Dissolved Oxygen Content

Oxygen exchange at the air–sea boundary: solubility of oxygen in sea water

Oxygen exchange at the air–sea boundary would occur if there is a difference of partial pressure of oxygen across the sea surface. In areas of large production of oxygen (by photosynthesis) the excess oxygen produced would result in excess partial pressure of oxygen in the sea, hence oxygen would tend to escape to the atmosphere. On the other hand, in areas of high organic consumption, or in areas of upwelling where unsaturated water is brought to the surface, oxygen would tend to be absorbed, because the partial pressure of oxygen in the sea would probably be less than in the atmosphere. The surface water in contact with the atmosphere would tend to reach equilibrium by releasing or absorbing oxygen until the water is saturated. In fact, large areas of the ocean are essentially in equilibrium with the atmosphere (Richards and Corwin, 1956).

The solubility of oxygen in sea water decreases with increasing temperature and salinity. The values of solubility have long been based on the data obtained by Fox (1909). However, Truesdale *et al.*, (1955) obtained values that were generally 4% lower than those obtained by Fox. Recent work by Steen (1958) provides values that are in agreement with those of Fox. Controversy continues regarding the correct values of solubility.

At Station "P" the temperature varies annually by more than 8 C°, and the salinity by 0.05‰. The variation due to the salinity change is less than 2% of that due to the temperature change. Consequently, temperature is the dominant factor controlling the solubility of oxygen at the station.

The values of solubility of oxygen of the water at Station "P" were determined from a nomograph prepared by Richards and Corwin (1956), based on measurements of Truesdale *et al.* Their values were chosen because they seemed to give reasonable values for saturation of the surface waters in the ocean.

The solubility values of Truesdale *et al.* were obtained for equilibrium conditions established under a standard atmosphere (1013 millibars) saturated with water vapour, at the temperature in question. For detailed work, consideration of the atmospheric pressure and humidity of the air is necessary.

Carritt (1954) has pointed out that the seasonal changes in atmospheric pressure that occur over the ocean are sufficient to impart measurable change in the solubility, by as much as 0.03 mg-at/l. Richards and Corwin (1956) have shown that the humidity effect can cause a change of 1% in the saturation values.

The solubility values obtained under standard conditions may be corrected for pressure and humidity effects from the Richards and Corwin formula:

$$\frac{O_2''}{O_2'} = \frac{P - e_s(h/100)}{1013 - e_s} \qquad \ldots\ldots (10)$$

where: O_2'' is the solubility of oxygen (mg-at/l) in water in equilibrium with an atmosphere having a pressure of P (mb) and a relative humidity of h%,

O_2' is the solubility of oxygen (mg-at/l) in water in equilibrium with a water-saturated atmosphere with a standard pressure of 1013 mb (solubility data of Truesdale *et al.*, 1955),

e_s is the vapour pressure (mb) of water at the observed temperature.

In the upper part of Fig. 31 are shown the two sets of values: those under standard conditions (continuous curve), and those under observed atmospheric conditions (dashed curve). Comparison indicates that the differences are small.

Redfield (1948) examined the problem of oxygen exchange at the air–sea boundary in the Gulf of Maine. He evaluated the pressure head of oxygen at the sea surface as:

$$P - p = p\left(\frac{O_2' - O_2}{O_2'}\right) \qquad \ldots\ldots (11)$$

where: P is the partial pressure of oxygen in water-saturated atmosphere and is equal to $0.21(1 - e_s)$, e_s being the vapour pressure of water at the sea surface,

p is the partial pressure of oxygen in sea water (oxygen tension) and is equal to $p\left(\frac{O_2}{O_2'}\right)$,

O_2' has the same meaning as in Formula (10), and

O_2 is the dissolved oxygen content of water.

The positive values of $(P - p)$ indicate that oxygen is directed from the atmosphere to the sea.

From his study, Redfield concluded that during the winter the pressure head was positive, favouring the movement of oxygen from the atmosphere into the sea, and *vice versa* in summer. Richards and Corwin recomputed the values of pressure heads, employing the solubility values of Truesdale *et al.* and concluded that the conditions favouring the escape of oxygen from the sea to atmosphere are more pronounced, and prevailed during a larger part of the year than Redfield has estimated.

Computations of differences of the pressure heads were made for the water at Station "P", and from the results, as shown in the lower part of Fig. 31, it is

evident that the conditions favouring the escape of oxygen from the sea to atmosphere prevail throughout the year, being most pronounced in spring and summer. In winter of 1956–1957 the partial pressures of oxygen in the sea and atmosphere were almost in equilibrium. The continuous curve in the Figure represents values of pressure head difference under standard conditions, and the dashed curve represents values under observed atmospheric conditions. Comparison indicates that an error as large as 20% may be introduced by using standard rather than actual conditions.

The apparent correlation between the oxygen and the solubility in the surface water (upper part of Fig. 31) suggests that the seasonal variations of the oxygen are governed by the seasonal variations of solubility. It can also be seen from the comparison of temperature–depth profiles (Fig. 26B) and the oxygen–depth profiles (Fig. 32A, *bottom*) that the changes of oxygen in the depths between 0 and 75 m are correlated with the changes of temperature at corresponding depths; that is, in and above the thermocline. It follows that the structure of oxygen during the summer, with a maximum occurring at depth of about 75 m, is a consequence of the decrease of solubility above the thermocline.

Production and utilization of dissolved oxygen by marine organisms

In the euphotic zone of the ocean, which is controlled by the depth of the penetration of light, oxygen is produced by photosynthesis by the phytoplankton. Oxygen is utilized principally by respiration of the zooplankton and fish (Sverdrup *et al.*, 1942). However, little study, if any, has been made to estimate the production and utilization of oxygen in the waters of the northeast Pacific Ocean.

Large values of supersaturation of the surface water frequently denote extensive photosynthetic activity (Sverdrup *et al.*). The relatively large values observed during summer 1957 and spring 1958 may possibly be due to high production by phytoplankton. Moreover, the fact that the surface water was supersaturated throughout the year suggests that even in winter some production must have taken place.

There is an appreciable population of zooplankton at Station "P", particularly during the summer (McAllister, 1960) and these animals might affect the distribution of oxygen. But there does not appear to be any apparent correlation between the size of zooplankton population and the oxygen in the upper zone. It is likely that the effect of solubility masks changes of oxygen brought about by respiration of these animals.

Horizontal transport

As in the case with the discussions of salinity and temperature, horizontal transport of water is likely to influence the oxygen at Station "P". But it appears that changes associated with transport are also masked by the effect of solubility. However, in the halocline and in the lower zone, where the effect of change of solubility is small, there is evidence that horizontal transport is effective in changing the oxygen.

The progressive increase of oxygen in the halocline and in the lower zone during summer 1957 through spring 1958 (Fig. 32A, *middle* and *bottom*) is attributed to the northward transport of the water. As shown in Fig. 14, 15, 16, the oxygen at these levels is greater to the south and less to the north. Hence the "oxygen-deficient" water is removed from the vicinity of the station by transport to the north and is replaced by water of a higher oxygen content from the south. This is consistent with the intrusion of warm, saline water into the region, as discussed earlier.

The decrease that occurred between summer and autumn, 1956, is in all likelihood due to the intrusion of the "oxygen-deficient" water from the northwest (Fig. 14, *lower left*). This is consistent with the argument presented earlier in which such intrusion was inferred from the changes of salinity and temperature.

The decrease that occurred below the depth of 500 m during spring through summer, 1958, suggests that perhaps a retreat southward of the relatively "oxygen-rich" water occurred.

Other factors

Redistribution of oxygen by vertical mixing occurs at the same period when the salinity and temperature are affected. The increase of oxygen in the upper 50 m depth that occurred during summer through autumn, 1956 (Fig. 32B, *first panel*), is mainly the result of such mixing.

Lateral eddy diffusion may have tended to decrease the oxygen at Station "P" during summer 1957, when the oxygen at the station was greater than in any of the surrounding area except to the north (Fig. 16, *upper*).

SUMMARY AND CONCLUSIONS

The principal feature of the annual variations of salinity of the water at Station "P" is that they are most marked in the upper zone and in the halocline, and are less marked in the lower zone. Noticeable variations occur at all depths to at least 1000 m. There is little evidence of definite cyclic annual variations in the upper zone, except at a depth of 100 m. During 50% of the time, the trend of variations in the upper zone, halocline, and lower zones is similar.

The annual cycle of surface sea temperature is in phase with that of the air temperature. Moreover the annual amplitude of the variations of surface sea temperature is similar to that of the air temperature. Marked annual variations of temperature occur to depth of 30 m, and to lesser extent to depth of 100 m. Appreciable non-seasonal variations of temperature occur in the halocline and also in the shallow portion of the lower zone. There was a progressive increase of temperature at these levels during spring 1957 through summer 1958. A minimum and a maximum temperature layer occurred during the latter half of 1956 and continued to the spring of the following year but became imperceptible by the summer.

Marked annual variations of dissolved oxygen content occur in the upper zone, especially in the upper 30 m depth, the values reaching maximum in winter

or spring, and dropping to minimum in summer or autumn. The variations of oxygen, and those of solubility of oxygen, in the surface water are similar in both the phase and amplitude. The surface water is supersaturated throughout the year, this condition being more pronounced in summer 1957 and spring 1958 and less so in the winters. There is little evidence of the annual variations below the depth of 100 m. However, in both the halocline and the lower zone appreciable variations with a period greater than one year are evident.

Dilution of water in the upper zone, due to excess precipitation over evaporation, was mainly responsible for the decrease of salinity during summer through winter, 1956. But during winter through spring, and autumn through winter, 1957, only 50% of the decrease could be accounted for by this excess. From spring 1957 through summer 1958, the salinity generally increased (except between autumn and winter, 1957), despite the tendency to decrease from excess precipitation.

The principal factor influencing the temperature in the upper zone is heat transfer at the air–sea boundary. It accounted for more than 80% of the temperature changes during autumn through winter, 1956, spring through summer, 1957, and winter through spring, 1958. It accounted for 50 to 75% of the changes during winter through spring, 1957, summer through winter, 1957, and spring through summer, 1958. During summer through autumn, 1956, it accounted for only 30%.

The close correlation between the oxygen and the solubility of oxygen in the surface water indicates that the variation of the oxygen is determined primarily by the solubility, and hence oxygen exchange across the air–sea boundary. The decrease of oxygen in the upper zone during spring through summer is related to the increase of temperature above the thermocline. The occurrence of maximum-oxygen layer at a depth between 50 and 100 m in summer and autumn is attributed to this effect. Hence the temperature, which affects the solubility, appears to be the dominant factor influencing the oxygen above the thermocline. The persistent supersaturation of the surface water, and the persistent higher values of partial pressure of oxygen in the water, indicate that a condition favouring the escape of oxygen from the sea to atmosphere prevails throughout the year. This was most pronounced in summer 1957 and spring 1958. During such periods when supersaturation was relatively high, it is possible that oxygen may have been produced in large quantity by high photosynthetic activity.

Horizontal transport seems to exercise appreciable influence on the properties of water at Station "P". The general increase of salinity, temperature, and oxygen that occurred during spring 1957 through summer 1958 was due to the northward transport of water into the region. Transport of water from the general vicinity of the "dome" lying northwest of the station appears to have caused an increase of salinity, decrease of temperature, and decrease of oxygen in the halocline and lower zone during summer through autumn, 1956. The large decrease of temperature in the upper zone during this period was due mainly to this transport. The occurrence of winds from the west and northwest during this period, leads one to suspect that the transport in the upper zone may

be due to winds. The large decrease of salinity in the upper zone during autumn through winter, 1957, was also partly due to such winds.

Vertical mixing causes the homogeneous layer to thicken during autumn through winter. This mixing results in the redistribution of properties of water in the vertical column. The increase of salinity in the shallow portion of the upper zone, and the decrease in the deeper portion in winter, are attributed to this effect. It also accounts for the occurrence of an annual salinity minimum at a depth of 100 m in winter. The progressive lag with depth at which the maximum annual temperature is reached is also due to this effect. This also contributes partly to the increase of oxygen in the upper 50 m depth during the late autumn.

Effects of lateral and vertical eddy diffusion have not been treated quantitatively owing to the uncertainty in the values of eddy coefficients. However, lateral eddy diffusion may affect the properties of water at the station especially when it is surrounded with water having different properties.

ACKNOWLEDGMENTS

Grateful acknowledgment is made to Captain J. A. Sleight and the officers and men of C.M.S. *St. Catharines* who ably assisted in the observations; to the Director of the Meteorological Services of the Canada Department of Transport for providing the meteorological data; to the Extended Forecast Section of the United States Weather Bureau for making available the monthly mean sea level pressure charts; and to the staff of this Board's Pacific Oceanographic Group, especially Mr C. D. McAllister, who made observations and assisted in the processing of the data and particularly to Dr N. P. Fofonoff and Dr J. P. Tully for their interest, suggestions, and criticisms in the work. Acknowledgment is also made to Mrs M. Robinson of Scripps Institution of Oceanography and Mr J. F. T. Saur, Jr. of the United States Fish and Wildlife Service, who made critical reviews of the paper.

REFERENCES

ANDERSON, E. R. 1952. Energy-budget studies. Water loss investigations, Vol. I, Geological Survey, Circular 229. Geological Survey, U.S. Dept. of the Interior, Washington, D.C., pp. 71–117.

BENNETT, E. B. 1959. Some oceanographic features of the northeast Pacific Ocean during August 1955. *J. Fish. Res. Bd. Canada*, **16**(5): 565–633.

BOWEN, I. S. 1926. The ratio of heat losses by conduction and by evaporation from any water surface. *Physical Review*, Ser. 2, **27**: 779–787.

CARRITT, DAYTON E. 1954. Atmospheric pressure changes and gas solubility. *Deep Sea Res.*, **2**(2): 59–62.

COX, R. A., AND N. D. SMITH. 1959. The specific heat of sea water. *Proc. Roy. Soc. Lond.*, A. **252** (1268): 51–62.

DODIMEAD, A. J. MS 1958. Report on oceanographic investigations in the northeast Pacific Ocean during August 1956, February 1957, and August 1957. *Fish. Res. Bd. Canada MS Rept. Series (Oceanogr. and Limnol.)* No. 20, 14 pp., 35 fig.

DOE, L. A. E. 1955. Offshore waters of the Canadian Pacific coast. *J. Fish. Res. Bd. Canada*, **12**(1): 1–34.

EKMAN, WALFRID V. 1905. On the influence of the earth's rotation on ocean currents. *Kongliga Svenska Venlenskaps Akademien Arkiv for Matematik, Aston och fysik*. **2**(11).

FISHERIES RESEARCH BOARD OF CANADA PACIFIC OCEANOGRAPHIC GROUP. MS 1956. Physical, chemical, and plankton data record, Project NORPAC, July 26 to September 1955. MS Rept. Joint Committee on Oceanography, 202 pp. (Unpubl.)

MS 1957a. Physical, chemical and plankton data record, North Pacific survey, January 23 to March 4, 1957. MS Rept. Joint Committee on Oceanography, 110 pp. (Unpubl.)

MS 1957b. Data record, 1956, Ocean Weather Station "Papa" (Latitude 50°00′ N, Longitude 145°00′ W). MS Rept. Joint Committee on Oceanography, 122 pp. (Unpubl.)

MS 1957c. Physical, chemical and plankton data record, North Pacific Survey, July 23 to August 30, 1957. *Fish. Res. Bd. Canada MS Rept. Series (Oceanogr. and Limnol.)*, No. 4, 103 pp.

MS 1958a. Physical, chemical and plankton data record, North Pacific Survey, March 11 to April 10, 1958. *Ibid.*, No. 16, 220 pp.

MS 1958b. Data record, Ocean Weather Station "P" (Latitude 50°00′ N, Longitude 145°00′ W) January 1, 1957–January 24, 1958. *Ibid.*, No. 14, 261 pp.

MS 1959. Data record, Ocean Weather Station "P" (Latitude 50°00′ N, Longitude 145°00′ W) January 22–July 11, 1958. *Ibid.*, No. 31, 112 pp.

FOX, C. J. J. 1909. On the coefficients of absorption of nitrogen and oxygen in distilled water and sea water and of atmospheric carbonic acid in sea water. *Trans. Faraday Soc.*, **5**: 68–87.

HIDAKA, K. 1955. Divergence of surface drift currents in terms of wind stresses, with special application to the location of upwelling and sinking. *Japan. Jour. of Geophysics*, **1**(2): 47–56.

HIDAKA, KOJI, AND YOSHIO AKIBA. 1955. Upwelling induced by circular wind system. *Records of Oceanogr. Works in Japan*, **2**(1): 7-18.

HOLLISTER, H. J. MS 1956. The program of bathythermograph observations at the Canadian Ocean Weather Station "Papa" (50°00′ N, 145°00′ W). [Fish. Res. Bd. Canada] MS Rept., Joint Committee on Oceanography. 17 pp., 15 fig. (Unpubl.)

JACOBS, W. C. 1951. The energy exchange between sea and atmosphere and some of its consequences. *Bull. Scripps Inst. Oceanogr.*, **6**(2): 27–67.

LANGMUIR, I. 1938. Surface motion of water induced by wind. *Science*, **87** (2250): 119–123.

MCALLISTER, C. D. 1961. Zooplankton studies at Ocean Weather Station "P" in the northeast Pacific Ocean. *J. Fish. Res. Bd. Canada*, **18**(1): 1–29.

MARCIANO, J. J., AND G. E. HARBECK, Jr. 1952. Mass-transfer studies. Water Loss Investigations, Vol. I, Geological Survey, Circular 229. Geological Survey, U.S. Dept. of the Interior, Washington, D.C., pp. 46–70.

MATEER, C. L. 1955. Average insolation in Canada during cloudless days. *Canadian J. Technol.*, **33**: 12–32.

NAMIAS, JEROME. 1959. Recent seasonal interactions between North Pacific waters and the overlying atmospheric circulation. *Jour. of Geophys. Res.*, **64**(6): 631–646.

PAQUETTE, ROBERT G. 1959. Salinometers. Conference on physical and chemical properties of sea water. Publ. 600, Nat. Acad. of Science–Nat. Res. Council, pp. 128–145.

Pickard, G. L., and D. C. McLeod. 1953. Seasonal variation of temperature and salinity of surface waters of the British Columbia Coast. *J. Fish. Res. Bd. Canada*, **10**(3): 125–145.

Redfield, A. C. 1948. The exchange of oxygen across the sea surface. *J. Mar. Res.*, **7**(3): 347–361.

Richards, F. R., and N. Corwin. 1956. Some oceanographic applications of recent determinations of the solubility of oxygen of sea water. *Limnol. and Oceanogr.*, **1**(4): 263–267.

Robinson, M. K. 1957. Sea temperature in the Gulf of Alaska and in the Northeast Pacific Ocean. 1941–1952. *Bull. Scripps Inst. Oceanogr.*, **7**(1), 98 pp.

Rossby, C-G., and R. B. Montgomery. 1935. The layer of frictional influence in wind and ocean currents. Papers in physical oceanography and meteorology. Massachusetts Institute of Technology and Woods Hole Oceanographic Institution. Vol. III, No. 3, 101 pp.

Sette, Oscar E., and John D. Issacs (editors). MS 1960. Symposium on "The changing Pacific Ocean in 1957 and 1958". California Cooperative Oceanic Fisheries Investigation Reports. Vol. VII, 1 January 1958 to 30 June 1959. 217 pp. State of California Department of Fish and Game, Marine Research Committee.

Steen, H. 1958. Determinations of the solubility of oxygen in pure water. *Limnol. and Oceanogr.* **3**(4): 423–426.

Strickland, J. D. H., and T. R. Parsons. 1960. A manual of sea water analysis. *Bull. Fish. Res. Bd. Canada*, No. 125, 185 pp.

Sverdrup, H. U. 1937. On the evaporation from the oceans. *J. Mar. Res.*, **1**(1): 3–14.

Sverdrup, H. U., R. H. Fleming and M. W. Johnson. 1942. The oceans. Their physics, chemistry, and general biology. Prentice-Hall, Inc., New York, 1087 pp.

Tabata, Susumu. 1958. Heat budget of the water in the vicinity of Triple Island, British Columbia. *J. Fish. Res. Bd. Canada*, **15**(3): 429–451.

1960. Characteristics of water and variations of salinity, temperature, and dissolved oxygen content of the water at Ocean Weather Station "P" in the northeast Pacific Ocean. *Ibid.*, **17**(3): 353–370.

Truesdale, G. A., A. L. Downing and G. F. Lowden. 1955. The solubility of oxygen in pure water and sea water. *J. Appl. Chem.*, **5**(2): 53–62.

Tully, J. P. 1949. Oceanography and prediction of pulp mill pollution in Alberni Inlet. *Bull. Fish. Res. Bd. Canada*, No. 88, 169 pp.

Tully, J. P., and F. G. Barber. 1960. An estuarine analogy of the sub-Arctic Pacific Ocean. *J. Fish. Res. Bd. Canada*, **17**(1): 91–112.

Tully, J. P., and Allen J. Dodimead. MS 1957. Canadian oceanographic research in the Northeast Pacific Ocean. MS Rept., Fish. Res. Bd. Canada Pacific Oceanographic Group, 11 pp., 18 fig. (Unpubl.)

Tully, J. P., A. J. Dodimead, and S. Tabata. 1960. An anomalous increase of temperature in the ocean off the Pacific Coast of Canada through 1957 to 1958. *J. Fish. Res. Bd. Canada*, **17**(1): 61–80.

Wagner, N. K. 1958. An analysis of some over-water wind profile measurements. *Trans. Amer. Geophy. Union*, **39**(5): 845–852.

Order of Succession of Different Types of Infraoral Lamina in Landlocked Sea Lamprey (*Petromyzon marinus*)[1]

BY V. D. VLADYKOV AND G. N. MUKERJI

Department of Biology, University of Ottawa
Ottawa, Ontario

ABSTRACT

Infraoral lamina were studied of 630 lampreys from Lake Erie, Ontario, Lake Seneca, New York, and the Père Marquette River, Michigan. The number of cusps on the first set of the lamina is always repeated in consecutive new sets, but the size of the cusps and their orientation vary. The width of the lamina increases slowly from 4.5 to 16.5 mm, with successive replacements of the corneous sheath. The main types of lamina are: ***normal*** (teeth large, evenly spaced, their points nearly parallel), ***inclined*** (teeth large, evenly spaced, their tips inclined mesad), and ***rosebud*** (teeth very small and clustered near the middle of the lamina; concentric lines on the basal portion). There is also the type ***intermediate*** between inclined and normal. Newly transformed lampreys and others less than 180 mm long have normal laminae. The rosebud lamina is characteristic of half-grown specimens, being most frequent among lampreys 250–400 mm long. In adults, feeding in lakes, the predominant type is the inclined lamina. In spawning specimens the normal lamina is most characteristic. Thus the usual succession throughout life is: normal, rosebud, inclined, and finally normal again. In spawning specimens there are two new sheaths underneath the old one, one below the other.

INTRODUCTION

WHILE EXAMINING the "tongue" (lingual lamina) in several hundreds of spawning sea lampreys from the St. Lawrence River, Great Lakes, and Finger Lakes of New York, the senior author observed closely the peculiarities in the development of other teeth. Lampreys from these different localities exhibited close similarity in the type of the cusps on the infraoral lamina. Typically their cusps were strong, sharp, and parallel to each other. Then two years ago, Mr W. J. Christie kindly sent us some half-grown *Petromyzon marinus* from the Bay of Quinte, Lake Ontario. Several of them exhibited a rather unusual type of infraoral lamina, which we called "rosebud" (Table II, Fig. 1, 3). Later we secured more half-grown specimens of sea lamprey from other localities, such as Lake Erie, Lake Seneca and the Père Marquette River, in some of which the "rosebud" type of infraoral lamina was present also.

To find out why some specimens have normally developed infraoral laminae, while others have the "rosebud" type, the present investigation was undertaken. Altogether, 630 transformed specimens of landlocked sea lampreys from five different localities have been studied in detail (Table I).

[1]Received for publication May 15, 1961.

J. FISH. RES. BD. CANADA, 18(6), 1961.
Printed in Canada.

The material from Lake Erie consisted of newly-transformed, half-grown and adult lampreys, all of which were feeding. A sample from Big Creek, a main spawning stream in Lake Erie, was composed of lampreys which would have spawned in 2 or 3 weeks. From the Lake Seneca area we had a sample of immature specimens feeding in the lake, and a sample of spawning lampreys caught in Catherine Creek. Lampreys from the Père Marquette River represented an early spawning run; they would have spawned in about 3 or 4 weeks.

METHODS OF MEASUREMENTS

Measurements listed below were made with dividers on the left side of the specimen and expressed in millimetres.

Length of the lamprey: The total length, measured from the anterior-most tip of the oral fimbriae to the end of the caudal fin.

Branchial region: From the front of the first gill opening to the posterior edge of the last (7th) gill opening.

Distance between dorsal fins: This distance was measured along the horizontal line of the back, from the hind end of the first dorsal fin base to the origin of the second dorsal fin. The origin of the second dorsal fin was considered the anterior point where the profile of this fin starts to rise from the horizontal line. In young and half-grown specimens the distance between the two dorsal fins is very distinct. In mature specimens this distance diminishes greatly and sometimes, in spawning lampreys, both fins can touch each other. Also in spawning specimens, the skin along the back swells considerably and thus obstructs from view the true origin of the second dorsal fin. For this reason the measurements of the distance between the two dorsal fins in younger specimens is more accurate than in spawning ones. Nevertheless, the difference in the distance between two dorsal fins of lampreys of different ages is very pronounced and amply compensates for the occasional inaccuracy of this measurement. The distance between the two dorsal fins in spawning specimens usually varies from 12 to 30%, average 22% of the length of the branchial region; in young or half-grown lampreys this distance varies from 40 to 70%.

Width of intestine: The exterior diameter of the intestine, empty or with food, was measured immediately behind the hind end of the liver. In spawning specimens the width varies from 1.5 to 3 mm, while in half-grown specimens, actively feeding, it may be as much as 27 mm.

Infraoral lamina: Maximum width of the infraoral lamina was measured, with fine dividers, along the anterior surface of its base between the two most distant points. In young specimens these measurements were made under a binocular microscope. By the same method the distances along the anterior surface between the exterior bases of the extreme cusps was measured; this is called a "cusp-row" in this paper. In Table II this distance is expressed as a percentage of the maximum width of the lamina.

COLOUR PHOTOGRAPHS

Due to the smallness of lamprey teeth and their yellow or orange colour, it is not easy to show their exact shape in black-and-white photographs. Hence colour photographs were taken, some of which are reproduced in Fig. 4. After several trials, the following procedures were adopted. We employed the Linhof Super Technica camera, with triple extension and 60 or 90 mm lenses. The construction of this camera permits the final critical focusing to be made on the ground glass of the swinging back, and hence avoids a distortion in the shape of the infraoral lamina cusps. The camera was fixed on a solid tripod. As a source of illumination several 6-volt spotlights were used. We used 4 × 5 inch cut films for 3200° K light. The exposure time varied from 1 to 10 seconds at *f*16–32.

The discs of lampreys were photographed while submerged in water and held in position by pins stuck to a cork sheet. The corneous sheaths and the infraoral laminae with their cartilaginous bases were photographed in dry condition. To hold them in a proper position, they were embedded into modelling clay ("plasticine") of different colours. The empty corneous sheaths retained the normal position very well; however the cartilaginous bases of the laminae, owing to desiccation, were bent inward and thus somewhat distorted the natural shape of the infraoral laminae.

The series of old and new sets of the infraoral lamina from any one lamprey were embedded into a putty of a particular colour, thus helping to identify the individuals. The infraoral laminae and their corneous sheaths were photographed from the front, that is, the anterior surface.

STAGES OF MATURITY

To determine accurately the stages of maturity in lampreys, histological slides should be made and sex cells properly measured. However, for the purpose of the present paper, only general characteristics, applicable to both sexes, are required.

For a convenient comparison of the degrees of gonad development we use a numerical system, based not only on the degree of development of the sex cells, but also on the degree of degeneration of the intestinal tract and on the decrease of the space between the two dorsal fins at the onset of sexual ripening caused by shrinkage in the body length (Vladykov and Follett, 1958).

STAGE 0: IMMATURE CONDITION. At least × 60 magnification required to distinguish sex cells, gonads like narrow cords; intestine functional; dorsal fins widely separated, the distance between them averaging 50% of the branchial region; lampreys usually smaller than 250 mm in length.

STAGES 1 AND 2: EARLY DEVELOPMENT OF GONADS. Sex cells distinguishable at lower magnification; although gonads are a little larger in Stage 2 than in Stage 1 they are very narrow; lampreys feed greedily and their intestine is very large, up to 27 mm in external diameter; dorsal fins widely separated, distance between them varies from 40 to 70% of the branchial region; size typically larger than 250 mm.

STAGE 3: MID-POINT OF DEVELOPMENT OF GONADS. Gonads of each sex can often be distinguished with the naked eye by their characteristic appearance, and they occupy more than half of the body cavity; colour of the liver in this and preceding stages is yellow; intestine still large but beginning to diminish in diameter (Table XII); distance between dorsal fins as wide as in the preceding stages. Lampreys reach their maximum size.

STAGE 4: PRE-SPAWNING. Gonads are easily distinguishable by the naked eye and occupy nearly the whole of the body cavity; intestine no longer functional, and greatly reduced, its diameter less than 6 mm (Table XII); space between dorsal fins has begun to decrease, this distance averaging about 40% of the branchial region; in males a "rope-like" ridge along the back begins to appear; colour of liver greenish rather than yellow.

STAGE 5: SPAWNING. Gonads occupy entire body cavity; intestine at its maximum degeneration, its diameter 3 mm or less (Table XII); liver green; pronounced shrinkage in body length, the distance between the dorsal fins 12 to 30% of the branchial region; an "anal fin-like fold" present in females and a "rope-like" ridge along the back in males.

STAGE 6: POST-SPAWNING. Body cavity practically empty of sex cells; general appearance similar to Stage 5; specimens dying.

Lampreys in Stages 0 to 2 live in lakes and can be called *immature* specimens. Lampreys in Stage 3 are *adults of the early spawning run* (Tables VIII, XV), as they approach their respective spawning streams early in spring. Lampreys in Stages 4–6, can be called *mature* specimens; they are present in spawning streams.

Several authors who have studied *Petromyzon marinus* have observed a pronounced shrinkage of the body in spawning specimens. Lennon (1954, p. 275) reported a shrinkage in length from 1 to 3 inches in Lake Huron lampreys. Wigley (1959, p. 593) observed in Cayuga Lake that spawning lampreys lose 11% of their length in males and 18% in females. Cotronei (1926) found even greater shrinkage in anadromous specimens of sea lamprey from Italy, up to 20%.

INFRAORAL LAMINA

On the sucking disc of the lamprey, among the numerous yellow or orange corneous teeth the infraoral lamina is the largest structure (Fig. 1). It is arch-like in shape, with a convex anterior surface, and bears several strong cusps on its upper edge. Very little attention has been given to this lamina in papers dealing with *Petromyzon marinus*.

The number of cusps on the infraoral lamina varies from 6 to 10 both in anadromous specimens (Vladykov, 1949, p. 22) and in landlocked specimens from Lakes Cayuga and Seneca in New York (Wigley, 1959, p. 574). During the present study we found a single male, 419 mm long, from Père Marquette River with only 5 cusps on the infraoral lamina.

In the sea lamprey, as in other parasitic species, there is a periodic replacement of all old teeth by new ones. Bridge (1932, pp. 247–248), quoting Warren (1902, p. 632), stated that in lampreys "each tooth consists of an axial papilla of the dermis, sometimes enclosing a pulp-cavity, and invested by the epidermis, and also by a stratified horny cone which forms the projecting hard part of tooth... The old teeth are vertically replaced by new teeth developed beneath the functional teeth".

Similar periodic changes are observed in the infraoral lamina as well. It is unfortunate that these periodic replacements of the lamina sheath with its cusps have never been followed through during the life span of a lamprey in captivity[2]. Thus there is no exact information as to how many times replacement of the external corneous covering of the infraoral lamina occurs.

In the spring of 1960 we tried to keep newly transformed *P. marinus* in captivity. Unfortunately, due to an inadequate water supply, we lost our experimental animals. Thus, to continue our studies we were limited to observations on formalin-preserved lampreys. The main points of interest were: (1) observation on growth, i.e., the increase in size of the infraoral lamina with the growth of the lampreys; (2) establishing the different types of the lamina; and (3) studying the order of succession of different types of lamina.

GROWTH OF THE INFRAORAL LAMINA

Our specimens show clearly that the width of the infraoral lamina, irrespective of its type, increases directly with the size of the lamprey.

Lake Erie Area

During 1957–1959 lampreys from Lake Erie proper were collected principally off Port Maitland and Port Burwell (Table I). From the 130–149 to the 550–599 mm length class the average increase in size of the infraoral lamina was from 4.8 to 13.8 mm (Table XIII). There was some overlap in width of the lamina among individuals from neighbouring length classes. The extreme range of sizes was from 4.5 mm in several newly transformed lampreys up to 16.5 mm in a female 525 mm long, i.e., about a 4-fold increase. However, the largest lampreys do not necessarily possess the largest laminae. In our largest specimen from Lake Erie, a female 635 mm long, the width of the lamina was only 15 mm.

Samples from Lake Erie collected during 1957–59 differ greatly from lampreys obtained in 1960 from Big Creek, a principal lamprey spawning stream of that lake (Table XIII). The average width of the lamina in immature specimens was always less than in spawning individuals of corresponding lengths. This doubtless results from the shrinkage of the body of the mature lampreys, so that their lamina widths correspond to those of immature individuals of larger size.

Lake Seneca Area

Two samples were obtained from this area. One consisted of spawning lampreys from the Catherine Creek, and the other of immature specimens taken in the lake proper. This material shows results similar to those described for Lake Erie (Table XIV). In both localities spawning lampreys have wider infraoral lamina than immature specimens of corresponding sizes.

[2]The natural life-span of transformed anadromous *P. marinus* is about two years (Vladykov, 1949). Very similar longevity has been observed in landlocked specimens (Applegate, 1950).

Catherine Creek lampreys have on the average larger laminae than Big Creek specimens of corresponding sizes. This difference may be attributed to local conditions or, what is more likely, to a differing degree of maturity of each group of lampreys. Those from Big Creek (Tables XII, XIII) were pre-spawning specimens, while lampreys from Catherine Creek (Table XIV) were actually spawning and some were even spent. So the shrinkage in the body length of the Catherine Creek specimens had reached its maximum. The following schedule illustrates the importance of length shrinkage (sexes combined):

Length class	Average width of infraoral lamina, mm	
mm	Big Creek	Catherine Creek
250–99	9.0	9.8
300–49	9.8	10.9
350–99	10.8	12.4
400–49	12.0	13.2
450–99	13.5	—

In Catherine Creek lampreys the width of the infraoral lamina of any length-class corresponds almost exactly to that of Big Creek specimens in the next higher length class.

Variation with Sex

Lampreys from the Lake Erie area (Table XIII) do not show any difference between sexes in respect to the width of infraoral lamina. This might result from the fact that our material was obtained throughout four different years and probably represented several distinct populations, each spawning in different brooks.

In Lake Seneca apparently there is only one spawning area (Catherine Creek), where all our mature lampreys were collected. The immature specimens caught during the same year in the lake proper probably belong to the same population. This explains the uniformity of the Seneca material. In the Seneca lampreys males have on the average, larger infraoral laminae than females, both when immature and when spawning.

THE "ROSEBUD" INFRAORAL LAMINA

The rosebud lamina (*r*) is the most striking type. Its cusps are very small, and the cusp-row, practically of the same size as in newly-transformed specimens, represents only about 50% of the laminar width, while in other types the cusp-row is at least 72% of laminar width (Table II). Below the cusps on the horny (or corneous) part of the lamina several horizontal lines are present which do not occur on other types of infraoral lamina. These horizontal lines represent stratification of the horny sheath. We believe that during the growth of the animal the original horny sheath of the infraoral lamina of the newly-transformed

lamprey is not sloughed off and replaced by a new larger one (as in the case of other types of the infraoral lamina), but rather is retained for some time. This original lamina (or rather its exterior sheath) grows in width and height by adding extra rings around its lower edge. The pronounced growth of the lower section of the infraoral lamina, while the original cusps remain unaltered, results in a formation of the rosebud type (Fig. 4e, 4g). Histological studies have been undertaken to find out the exact method of rosebud lamina formation, whose results will be published in a subsequent paper.

Frequency According to Size of Lamprey

Among 288 Erie lampreys, irrespective of sex, rosebud laminae were found only in half-grown specimens ranging in length from 182 to 551 mm. The highest frequencies were in length classes 250–99 mm (94%), 300–49 mm (80%), and 350–99 mm (69%) (Table III). In 58 young specimens 130–180 mm in length no rosebuds were present. Similarly, among 113 large lampreys 400–635 mm in length, only 11 cases (about 10%) of rosebuds were observed. A comparable situation existed in the Seneca lampreys (Table VI).

Frequency According to Stage of Maturity

By arranging the Erie specimens according to stages of maturity, we find that 15% rosebuds are present in Stage 0 immature lampreys, 48% in Stage 1, and 24% in Stage 2. Other details are found in Table VIII.

Among the Seneca specimens rosebud laminae were confined to the immature group, and involved 12 lampreys out of 26 (Table IX). No rosebuds were present in 122 spawning individuals.

The occurrence of different types of infraoral lamina in *Petromyzon marinus* from the five localities studied is summarized in Table X. Among Père Marquette lampreys, which represented an early spawning run, only one specimen had the rosebud type while the remaining 86 had other types of infraoral lamina. Rosebuds were completely absent among lampreys in advanced spawning conditions from Big Creek and Catherine Creek.

Altogether 92 specimens with rosebuds were observed during the present study. Grouping them by lamprey length classes irrespective of localities (Table XI), almost 73% fall within the range 250–400 mm. Among specimens longer than 500 mm, only 2 individuals carried rosebuds (about 2%). Rosebuds were equally rare (about 3%) among specimens smaller than 200 mm. Thus, rosebud laminae were characteristic of the half-grown lampreys only, while the young and adults possessed other types.

OTHER TYPES OF LAMINA

The other types of infraoral lamina, *inclined* (*i*), *normal* (*n*) and *intermediate* (*i-n*), differ only in the direction of the cusps, being quite similar otherwise. The cusp-row in these types occupies 86–90% of the laminar width (Table II). Their cusps are much stronger and sharper than in the rosebud type (Fig. 1).

YOUNG LAMPREYS. Among the Erie material there were 13 newly transformed lampreys 130–149 mm in length, all of which possessed a normal infraoral lamina. In the 150–199 mm class also the normal type was most common (73%).

HALF-GROWN LAMPREYS. As already mentioned, rosebud is the characteristic type of infraoral lamina in half-grown lampreys (Tables III-XI).

ADULT LAMPREYS. Among 123 large Erie lampreys 400 to 635 mm long, 101 specimens (82%) had inclined laminae. Many of these were still immature individuals (Tables III, VIII). Equally high incidence (84%) of the inclined type of lamina was observed in Père Marquette lampreys caught in April (Tables VII, X). Among lampreys from Big Creek, many of which were almost ready to spawn (Stage 4), the incidence of the inclined type was much lower, only 56% (Table X).

SPAWNING LAMPREYS. About half of the sample from Big Creek consisted of lampreys in an advanced stage of maturity (Table XII); thus many of these specimens have replaced the inclined type of lamina by other types: 28% had the intermediate type, 16% the normal type. On the other hand, spawning Catherine Creek lampreys had over 80% normal laminae (Table X) and none of the inclined type at all.

ORDER OF SUCCESSION OF TYPES OF INFRAORAL LAMINA

In addition to direct observation on types of infraoral lamina present in lampreys of different sizes, we tried to remove the existing outer sheath of the lamina to study the underlying cusps. The existing sheath is called in this paper the "old set", and the underlying one the "new set" (Table XV). In many preserved specimens, especially of spawning lampreys, the old set of infraoral lamina was ready to be sloughed off. In nature, spawning specimens regularly replace the old sets by new ones.

Among half-grown specimens, where the old set is of the rosebud type, it also was easily detachable. However, a forcible removal of the old set of other types of lamina in half-grown specimens, and especially in newly-transformed lampreys, presented difficulty, with the result that the old set was often damaged. The use of a dissecting needle and a binocular microscope was helpful.

There is little published information regarding the manner and sequence of tooth replacement in lampreys. For the genus *Ichthyomyzon*, Hubbs and Trautman (1937, p. 29) state that "each new tooth, formed as the core of its predecessor, is the image of the former tooth which is sloughed off as a hollow corneous structure". Ivanova-Berg (1933, p. 27) observed that in spawning *Lampetra fluviatilis* the infraoral cusps were blunt, while those in half-grown specimens were sharp.

In our spawning *Petromyzon marinus*, the old set of infraoral lamina was very often worn out, while the new set always carried sharp cusps. On several

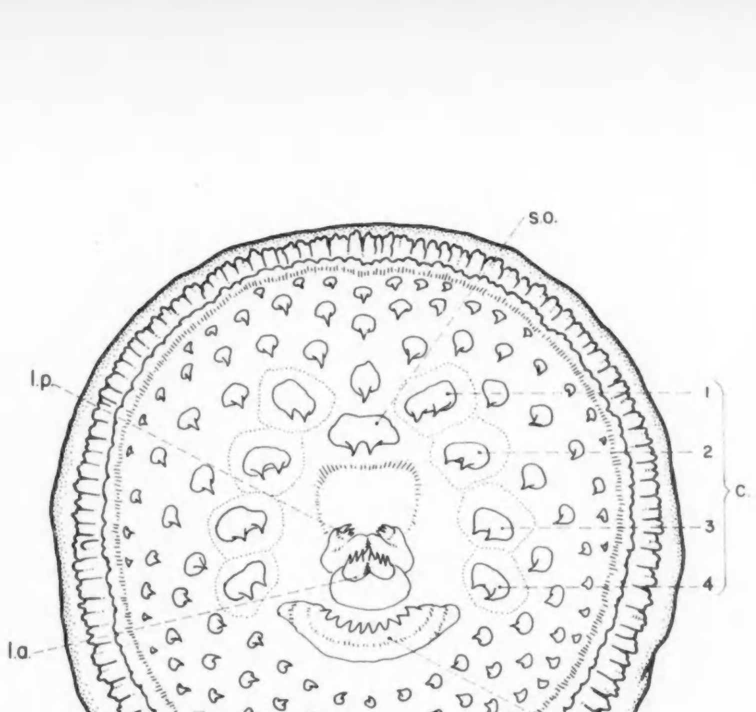

FIG. 1. Schematic drawing of the disc and dentition in the landlocked sea lamprey, *Petromyzon marinus*. The significance of the abbreviations used in this drawing is as follows:

c.—Four circumorals or enlarged laterals.
i.o.—Infraoral lamina or infraoral cusps.
l.a.—Transverse, or anterior, lingual lamina.
l.p.—Longitudinal, or posterior, lingual laminae.
s.o.—Supraoral lamina or supraoral cusps.

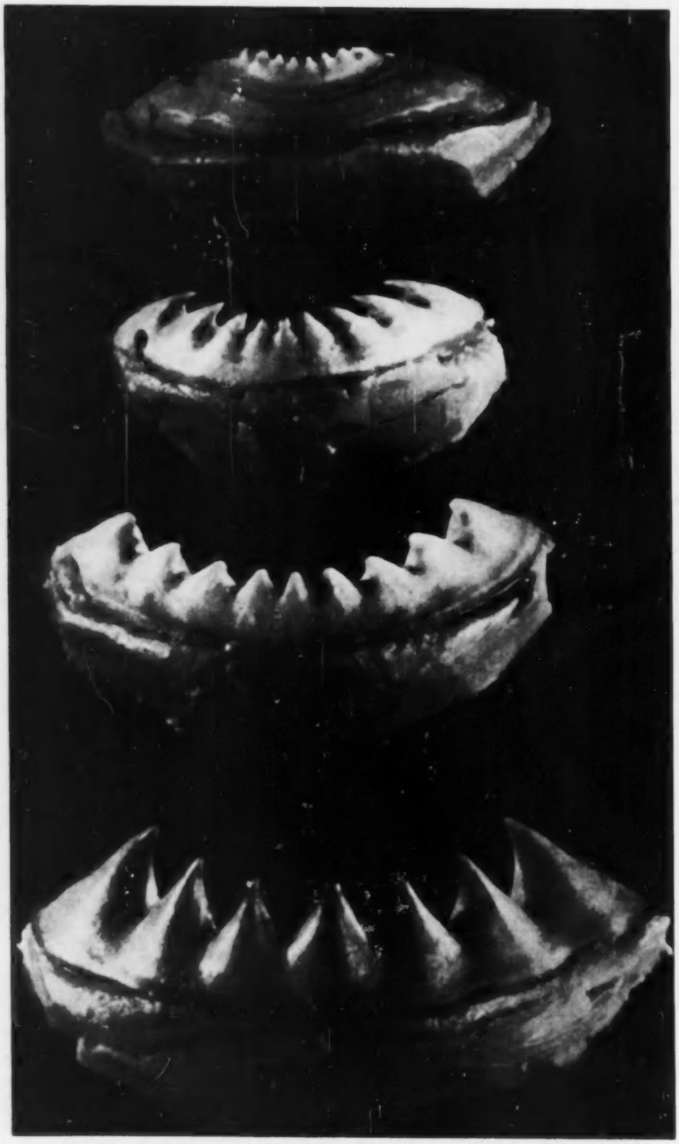

FIG. 2. Examples of the 4 types of infraoral lamina (×5.4). From top downward:

Rosebud—♀, 551 mm, Lake Erie, 1960.
Inclined—♀, 450 mm, Big Creek, 1960.
Intermediate—♀, 525 mm, Lake Erie, 1959.
Normal—♂, 695 mm, Minho River, Portugal, 1959.

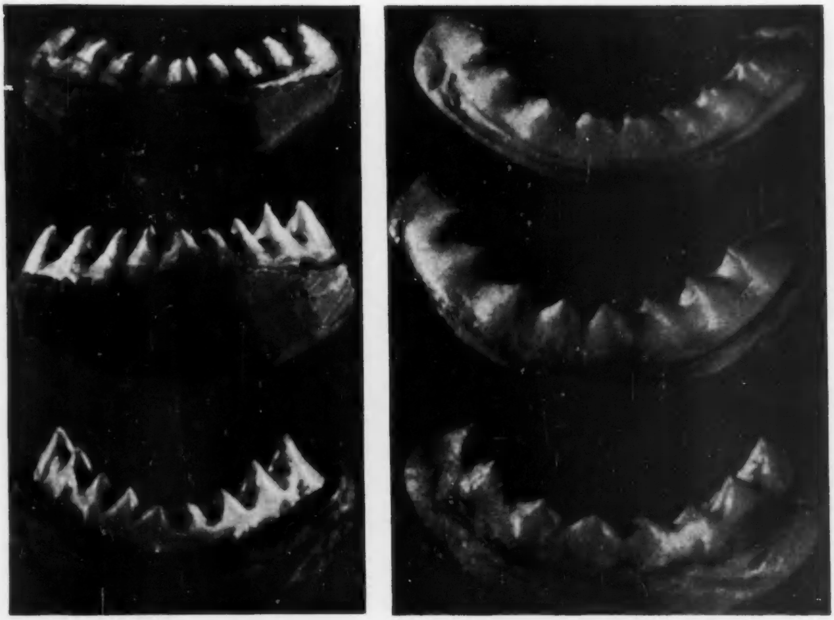

FIG. 3. Successive sets of sheaths taken from the same lamprey (×4.4), the oldest (functional) set at the top.

Left: ♀, 475 mm, Big Creek, 1960. *Top*—inclined; *middle*—inclined; *bottom*—normal.
Right: ♀, 497 mm, Lake Erie, 1959; *Top*—normal; *middle*—normal; *bottom*—normal.

Fig. 4. (colour plate opposite). Double sets of infraoral laminae (×2). Functional set *above*, new set *below*, except in (a) where positions are reversed.

(a) Inclined (old set) and intermediate (new set): ♂, 380 mm, Big Creek, 1960.
(b) Both normal; ♂, 548 mm, Lake Erie, 1957.
(c) Both normal: ♂, 465 mm, Lake Erie, 1958.
(d) Both inclined: ♂, 365 mm, Catherine Creek, 1959.
(e) Rosebud above, inclined below: ♂, 458 mm, Père Marquette River, 1958.
(f) Inclined above, intermediate below: ♀, 399 mm, Père Marquette River, 1958.
(g) Rosebud above, inclined below: ♂, 380 mm, Lake Erie, 1959.
(h) Inclined above, intermediate below: ♂, 411 mm, Chocolay River, Lake Superior, 1958.

(a) (b) (c) (d)

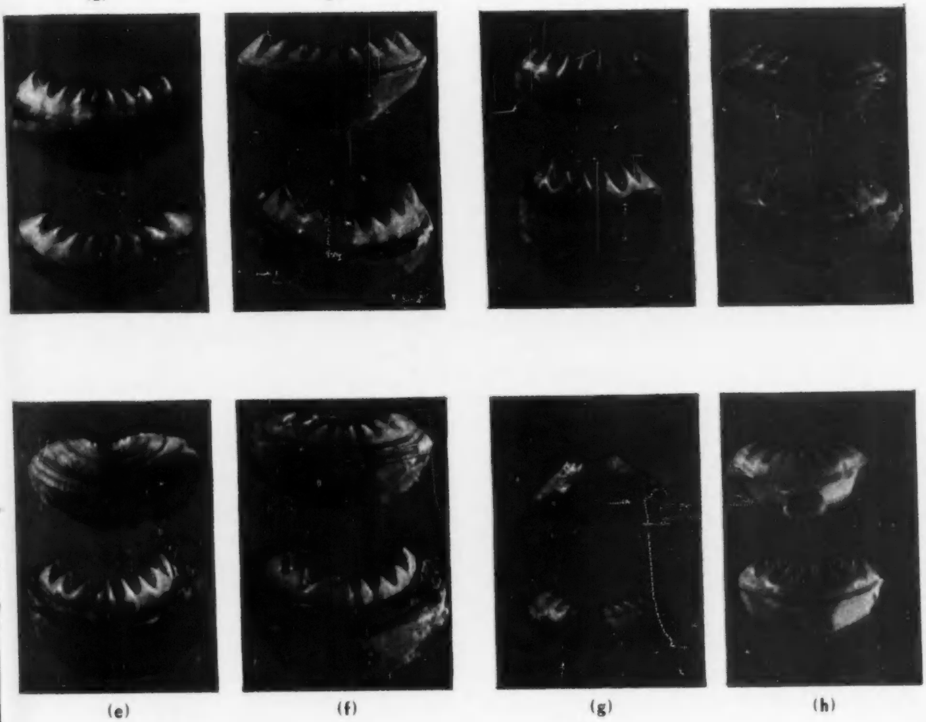

(e) (f) (g) (h)

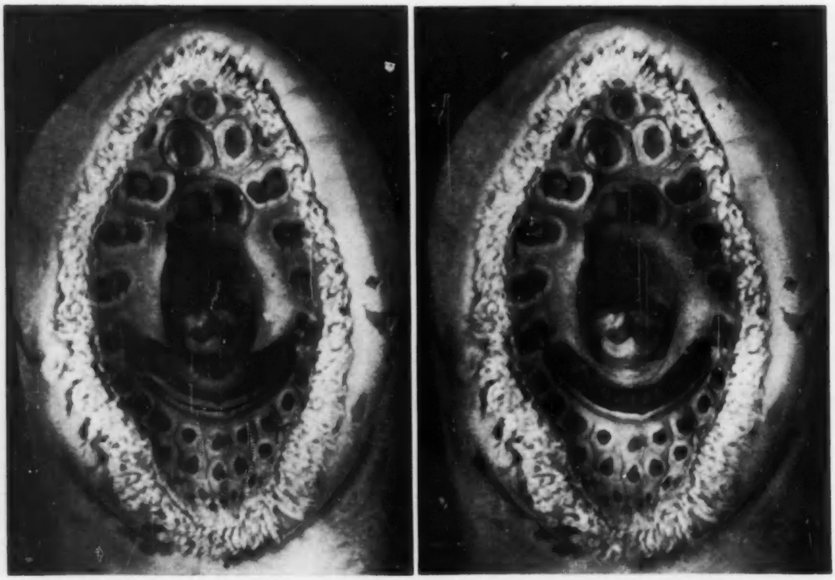

FIG. 5. Oral disc (×2) of ♀ lamprey No. 2157, 389 mm, Lake Erie, 1957.
Left: as captured, with rosebud lamina.
Right: inclined lamina exposed by removal of the rosebud.

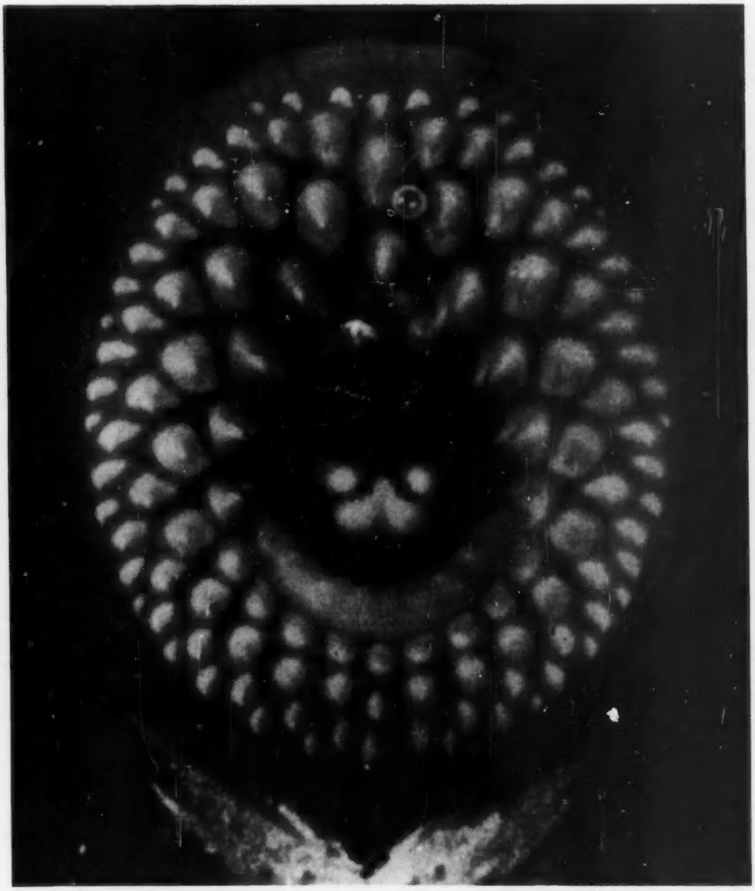

FIG. 6. Oral disc (×10) of a newly transformed lamprey, 139 mm long, Carp Lake River, Michigan, February 1960. Infraoral lamina of the normal type.

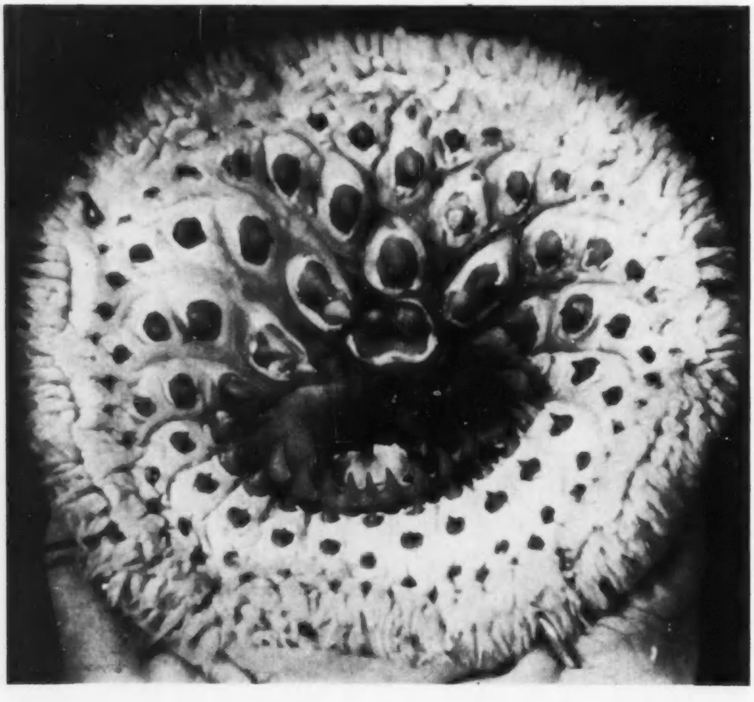

FIG. 7. Oral disc (×3) of a spawning ♂ lamprey, 389 mm long, Catherine Creek, Seneca Lake, N.Y., May 1959. Infraoral lamina of the normal type.

occasions, when collected specimens were properly handled previous to preservation in formalin, we observed that beneath the first new set, a second new set was present with equally sharp cusps (Fig. 3). We are convinced that in nature all spawning sea lampreys have two new sets of the infraoral lamina. Apparently a similar situation, in the case of other teeth, was observed in spawning anadromous *P. marinus* in France by Fontaine (1958, p. 73), who wrote that "nous avons fréquemment constaté, chez la Lamproie marine, la présence sur les grosses dents de 3 coiffes cornées emboîtées".

FREQUENCY OF REPLACEMENT OF CORNEOUS SHEATHS

There is no definite information available as to the frequency of replacement of corneous sheaths of the infraoral lamina. A new sheath is always somewhat larger than the preceding old sheath. This can help us to evaluate, at least approximately, the number of sheath changes throughout the life-span.

We were able to measure with fine dividers the old and new laminar sheaths of 76 Big Creek lampreys. The differences in width are summarized below:

Difference, *mm*	0–0.4	0.5–0.9	1.0+
Occurrence, %	48.7	47.4	3.9

Table XIII shows that the width of the infraoral lamina increases from 4.5 mm in the newly-transformed lamprey to about 14 mm in grown-up individuals. Thus, the difference between these extremes is about 10 mm. If the absolute increase in the size of the lamina with each new replacement of the corneous sheath is uniform, then we can speculate as to how often a lamprey replaces its corneous sheaths. If at each replacement the width of the lamina increases by 0.5 mm on the average, the number of replacements should be about 20. If the increase is only 0.25 mm, the number of replacements is 40. The true figure must lie between these two—possibly close to 30.

ORDER OF SUCCESSION

In order to understand better the succession of different types of infraoral lamina, we studied in detail the old and new sets in 210 specimens of *Petromyzon marinus* from several localities and in different stages of maturity (Table XV).

YOUNG LAMPREYS. In 10 specimens with the normal type of lamina in the old sets, the new sets were represented mainly (90%) by normal and intermediate types. However these new sets consisted of only a soft core, the outside sheathing of which was not corneous as yet. Thus, a future new set could be different from the one in the process of formation, as mentioned in Table XV.

HALF-GROWN LAMPREYS. Among 28 semi-adult specimens with old sets of the rosebud type, the new sets were invariably of the inclined type.

ADULT LAMPREYS. Among grown-up lampreys with old sets of the inclined type, the kind of new set underneath varies with stage of maturity. Among 47 Erie specimens, nearly 92% of the new sets were inclined again. Père Marquette lampreys, more advanced in maturity, had less than 15% of inclined sets, while intermediate and normal types were represented by 43% each. Among

Big Creek lampreys, many of which were ready to spawn, the inclined type among the new sets was only about 7%, and the normal type was most frequent (52%) in the sample. The spawning Catherine Creek lampreys did not have an inclined type among the new sets, and the normal type was present in over 83% of specimens.

SPAWNING LAMPREYS. The small number of available specimens shows that the intermediate type of lamina is replaced mainly (83%) by the normal type. The normal type is replaced invariably by a normal type again (Table XV). It should be added that in spawning lampreys the cusps of the normal infraoral lamina are usually narrow, hence farther apart, and their tips are often bent. In feeding adult landlocked sea lampreys, the cusps of the normal lamina are rather broad and wedge-like. The latter type of cusp is particularly characteristic of anadromous *P. marinus* (Fig. 2, bottom).

SUMMARY

1. Detailed study was made of 630 landlocked *Petromyzon marinus* from three lake areas: Erie, Superior, and Seneca.

2. The three main types of infraoral lamina were: *rosebud* (*r*), *inclined* (*i*), and *normal* (*n*), the latter including an intermediate type (*i-n*).

3. Newly-transformed and young lampreys, smaller than 180 mm, have the normal type of lamina. The rosebud lamina is a characteristic of half-grown specimens, being found most frequently among lampreys 250–400 mm in length (Table III). In adults, feeding in lakes, the predominant type is the inclined lamina. In spawning specimens the normal lamina is most characteristic.

4. The old corneous sheaths of inclined, intermediate, or normal infraoral laminae can be succeeded not only by different types, but also by a new one of the same type (Table XV). On the other hand, we have never seen a lamprey in which the old lamina sheath of the rosebud type was succeeded by a new set of rosebud.

5. Inclined infraoral laminae can appear successively several times before they are finally replaced by intermediate or normal type.

6. In some mature lampreys the intermediate type of lamina can be succeeded again by the same type, instead of the normal type. These two types are very similar in appearance, and are found concurrently (Fig. 4f, 4h).

7. Irrespective of the type, the size (width) of the infraoral lamina increases slowly with successive replacements of the previous corneous sheaths, the extreme range observed being from 4.5 to 16.5 mm (Table XIII).

8. It is not definitely known how often a sea lamprey, during its life-span, replaces the corneous sheaths of its teeth, but the average increase in width between successive laminae suggests that there are about 30 changes.

9. The number of cusps on the first set of the infraoral lamina is always repeated in the consecutive new sheaths.

10. There is a tendency for successive types of infraoral lamina to have a pattern of replacement which permits the tips of the cusps to spread further apart with each new corneous sheath. Beneath the small parallel cusps of the rosebud are found larger cusps of the inclined lamina, the tips of which are still cramped and directed towards the centre. In an intermediate type, the cusps are spread farther apart and are almost parallel to one another; in the normal type they are even more so (Fig. 4b).

11. Landlocked *Petromyzon marinus* exhibit the following changes in the infraoral lamina. The first set is normal followed only once by a rosebud, which is then succeeded several times by inclined; during the spawning period the inclined type is replaced at least twice by the intermediate type or, more frequently, by normal lamina. The first and the last sets are typically normal.

12. In gently handled spawning specimens (most probably in all of them), in addition to an old corneous sheath, two new sets of corneous sheaths were found, one beneath the other. It seems a "very extravagant luxury" for a mature lamprey to have even one extra corneous sheath, as this animal does not feed during spawning and dies very soon after.

ACKNOWLEDGMENTS

Much of this work was done during the senior author's seasonal employment by the Fisheries Research Board of Canada. Dr W. A. Kennedy, Director of the Board's London Biological Station, encouraged this investigation. Mr R. W. McCauley of the same Biological Station helped to obtain specimens from Big Creek. Mr W. J. Christie and Dr R. G. Ferguson, Biologists, Ontario Department of Lands and Forests, provided numerous specimens of sea lampreys from Lakes Ontario and Erie. Mr W. A. McGregor, Biologist, New York Conservation Department at Scottsville, N.Y., obtained very valuable material from the Lake Seneca area. Dr Mario Ruivo, Institute de Biologia Maritima, Lisbon, Portugal, kindly provided anadromous specimens of sea lamprey from northern Portugal. Mr S. U. Quadri, graduate student of our Department, helped in measuring of specimens. Mr G. A. Ben-Tchavtchavadze of the Univerity of Ottawa expertly took the colour and black-and-white photographs. The drawing (Fig. 1) for this paper was done by Mr Paul I. Voevodine, artist of the Department of Fisheries, Quebec. To all these persons, the authors wish to express their most sincere thanks.

REFERENCES

APPLEGATE, V. C. 1950. Natural history of the sea lamprey (*Petromyzon marinus*) in Michigan. *U.S. Fish and Wildlife Service, Spec. Sci. Rept.—Fisheries*, No. 55, 237 pp.

BRIDGE, T. W. 1932. Fishes. *Cambridge Nat. History*, **8**: 141–537. London.

COTRONEI, G. 1926. Sulla biologia dei Petromizonti. III. Il fenomeno dell'accorciamenta nella maturita sessuale del *Petromyzon marinus*. *Atti Reale Accad. Naz. Lincei*, **3**: 37–40. Roma.

FONTAINE, M. 1958. Anatomie. Formes actuelles. Super-ordres des Petromyzonoidea et des Mixinoidea. *Traité de Zoologie* par P.-P. Grassé. **13**: 13–144. Paris.

HUBBS, C. L., AND M. B. TRAUTMAN. 1937. A revision of the lamprey genus *Ichthyomyzon*. *Misc. Publ. Mus. Zool. Univ. Michigan*, No. 35, 109 pp.

IVANOVA-BERG, M. M. 1933. Zur Biologie des Flussneunauges (*Lampetra fluviatilis* L.) *Archiv für Hydrobiologie*, **25**: 22–37.

LENNON, R. E. 1954. Feeding mechanism of the sea lamprey and its effect on host fishes. *U.S. Fish and Wildlife Service. Fish. Bull.*, **56**(98): 247–293.

VLADYKOV, V. D. 1949. Quebec lampreys (Petromyzonidae). I. List of species and their economical importance. *Quebec Dept. of Fish., Contrib.*, No. 26, 67 pp. Quebec, P.Q.

VLADYKOV, V. D., AND W. I. FOLLETT. 1958. Redescription of *Lampetra ayresii* (Günther) of Western North America, a species of lamprey (Petromyzontidae) distinct from *Lampetra fluviatilis* (Linnaeus) of Europe. *J. Fish. Res. Bd. Canada*, **15**: 47–77.

WARREN, E. 1902. On the teeth of *Petromyzon* and *Myxine*. *Quart. Journal Micr. Sci.*, **45**: 631–636.

WIGLEY, R. L. 1959. Life history of the sea lamprey of Cayuga Lake, New York. *U.S. Fish and Wildlife Service, Fish Bull.*, **59**(154): 561–617.

TABLE I. Number and range of lengths of samples of landlocked sea lampreys.

Locality	Date	Collector	Lamprey samples			
			Males		Females	
			no.	*mm*	*no.*	*mm*
Lake Erie, Ontario	Summer-fall, 1957–59	R. G. Ferguson	84	143–548	153	130–635
Lake Erie, Ontario	Fall, 1960	R. G. Ferguson	19	295–572	32	342–551
Big Creek, Lake Erie, Ont.	May-June, 1960	Douglas Morris	60	276–546	47	292–523
Catherine Creek, Lake Seneca, N.Y.	May 20–29, 1959	W. A. MacGregor	71	275–430	51	266–401
Lake Seneca, New York	Fall, 1959	W. A. MacGregor	9	328–453	17	337–429
Père Marquette R., Michigan	April 10–24, 1958	W. E. Gaylord	60	322–512	27	354–531
Total	1957–1960		303	143–572	327	130–635

TABLE II. Definition of the different types of infraoral lamina in landlocked sea lampreys. "Width of the cusp row" is expressed as a percentage of the total laminar width.

Type	Specimens	Width of cusp row		Cusps	
		Range	Average	Size	Direction
	no.	%	%		
Rosebud	25	31.6–65.0	50.5	Small	Straight
Inclined	75	72.6–95.5	86.1	Large	Inclined toward the centre of the lamina.
Normal	35	83.3–95.7	90.2	Large	Straight and parallel to one another
Intermediate	23	79.5–96.0	88.6	Large	Outermost inclined toward centre of lamina, remainder straight

TABLE III. Frequency of different types of infraoral lamina according to lamprey length for *Petromyzon marinus* from Lake Erie, collected during 1957–59 and 1960 (sexes combined). Symbols for lamina types are as follows: *r*—rosebud; *i*—inclined; *i-n*—intermediate; *n*—normal.

Length	Specimens	Types of lamina			
		r	*i*	*i-n*	*n*
mm	*no.*	*no.*	*no.*	*no.*	*no.*
130–49	13	—	—	—	13
150–99	59	3	4	8	44
200–49	20	8	5	2	5
250–99	16	15	1	...	...
300–49	25	20	4	...	1
350–99	32	22	10	...	...
400–49	38	5	33	...	...
450–99	39	4	31	...	4
500–49	40	1	33	...	6
550–99	5	1	3	...	1
635	1	...	1	...	...
Total	288	79	125	10	74

TABLE IV. Frequency of different types of infraoral lamina according to lamprey length, from Big Creek, 1960 (sexes combined). Symbols as in Table III.

Length	Specimens	Types of lamina		
		i	*i-n*	*n*
mm	*no.*	*no.*	*no.*	*no.*
250–99	5	4	...	1
300–49	25	16	6	3
350–99	27	19	5	3
400–49	15	7	4	4
450–99	30	13	14	3
500–49	5	1	1	3
Total	107	60	30	17

TABLE V. Frequency of different types of infraoral lamina according to lamprey length, from Catherine Creek, Lake Seneca, 1959 (sexes combined). Symbols as in Table III.

Length	Specimens	Types of lamina		
		i	*i-n*	*n*
mm	*no.*	*no.*	*no.*	*no.*
250–99	10	...	1	9
300–49	57	6	3	48
350–99	47	...	9	38
400–49	8	4	1	3
Total	122	10	14	98

TABLE VI. Frequency of different types of infraoral lamina according lamprey length in immature *P. marinus* from Lake Seneca, 1959 (sexes combined). Symbols as in Table III.

Length	Specimens	Types of lamina	
		r	*i*
mm	*no.*	*no.*	*no.*
300–49	3	2	1
350–99	17	8	9
400–49	5	2	3
450–99	1	...	1
Total	26	12	14

TABLE VII. Frequency of different types of infraoral lamina according to lamprey length in specimens from Père Marquette River, 1958 (sexes combined). Symbols as in Table III.

Length	Specimens	Types of lamina			
		r	*i*	*i-n*	*n*
mm	*no.*	*no.*	*no.*	*no.*	*no.*
300–49	4	...	4	...	...
350–99	48	...	42	3	3
400–49	26	...	19	7	...
450–99	7	1	6	...	...
500–49	2	...	2	...	...
Total	87	1	73	10	3

TABLE VIII. Frequency of rosebud (*r*) and other types (*o*) of infraoral lamina in *P. marinus* from Lake Erie, collected in 1957–59 and 1960, grouped according to stage of maturity.

Length	Specimens	Stages of maturity (sexes combined)									
		0		1		2		3		Total	
		r	*o*	*r*	*o*	*r*	*o*	*r*	*o*	*r*	*o*
mm											
130–49	13	...	13	...	...	...	...	...	...	...	13
150–99	59	3	56	–	–	–	–	–	–	3	56
200–49	20	8	12	–	–	–	–	–	–	8	12
250–99	16	3	1	12	–	–	–	–	–	15	1
300–49	25	–	–	17	4	3	1	–	–	20	5
350–99	32	–	–	13	4	9	6	–	–	22	10
400–49	38	–	–	3	20	2	13	–	–	5	33
450–99	39	–	–	3	17	–	11	1	7	4	35
500–49	40	–	–	–	5	–	16	1	18	1	39
550–99	5	–	–	–	2	1	–	–	2	1	4
635	1	–	–	–	–	–	–	–	1	–	1
Total	288	14	82	48	52	15	47	2	28	79	209

TABLE IX. Frequency of different types of infraoral lamina in *Petromyzon marinus* from the Lake Seneca area, 1959. I = immature, taken in Lake Seneca in autumn, 1959; S = spawning specimens collected in Catherine Creek, spring, 1959.

Length	Infraoral lamina types									
	Rosebud		Inclined		Intermediate		Normal		Total	
	I	S	I	S	I	S	I	S	I	S
mm										
250–99	–	–	–	–	–	1	–	9	–	10
300–49	2	–	1	6	–	3	–	48	3	57
350–99	8	–	9	–	–	9	–	38	17	47
400–49	2	–	3	4	–	1	–	3	5	8
450–99	–	–	1	–	–	–	–	–	1	–
Total, *no.*	12	–	14	10	–	14	–	98	26	122
Total, %	46.0	–	54.0	8.2	–	11.5	–	80.3	100	100

TABLE X. Frequency of the different types of infraoral lamina from five localities (sexes combined). Based on Tables III–VII; symbols as in Table III.

Locality	Date	Length	Maturity	Specimens	Types of lamina			
					r	*i*	*i-n*	*n*
		mm		*no.*	%	%	%	%
Lake Erie	Summer–Fall 1957–60	130–635	Immature (Stages 0–3)	288	27.4	43.5	3.5	25.6
Lake Seneca	Fall, 1959	328–453	Immature (Stages 0–2)	26	46.1	53.9	0	0
Père Marquette River	April, 1958	322–531	Early spawning run (Stage 3)	87	1.2	84.0	11.5	3.3
Big Creek, Lake Erie	May–June, 1960	276–546	Pre-spawning (Stage 4)	107	0	56.0	28.0	16.0
Catherine Creek, Lake Seneca	May, 1959	266–430	Spawning (Stages 5–6)	122	0	8.1	11.4	80.5

TABLE XI. Frequency of the rosebud type of infraoral lamina according to size of lamprey. Specimens of both sexes from three different localities are combined, data from Tables III–VII.

Length	Frequency	
mm	*no.*	%
150–99	3	3.3
200–49	8	8.7
250–99	15	16.3
300–49	22	23.9
350–99	30	32.6
400–49	7	7.6
450–99	5	5.4
502	1	1.1
551	1	1.1
Total:	92	100.0

TABLE XII. Frequency of the different widths of intestine in *Petromyzon marinus* from three spawning areas (sexes combined).

Locality	Date	Speci-mens	Width of intestine (*mm*)							
			1.5-3	4–6	7–9	10–12	13–15	16–18	27	Av.
			%	%	%	%	%	%	%	*mm*
Père Marquette River, Lake Michigan	April, 1958	87	0	19.5	42.5	25.3	10.3	1.2	1.2	9.0
Big Creek, Lake Erie	May–June, 1960	107	33.7	62.6	3.7	0	0	0	0	3.9
Catherine Creek, Lake Seneca	May, 1959	122	97.6	1.6	0.8	0	0	0	0	2.4

TABLE XIII. Increase in the width of infraoral lamina with size and stage of maturity of *Petromyzon marinus* from Lake Erie area, 1957–1960.

Length	Sex	Immature, Lake Erie, 1957–59			Spawning, Big Creek, 1960		
		Specimens	Width of lamina		Specimens	Width of lamina	
			Range	Av.		Range	Av.
mm		*no.*	*mm*	*mm*	*no.*	*mm*	*mm*
130–49	♂	4	4.5–5.5	4.8			
	♀	9	4.5–5.5	4.8			
150–99	♂	20	5.0–5.5	5.2			
	♀	39	4.5–6.5	5.4			
200–49	♂	6	5.5–9.0	7.1			
	♀	14	5.0–7.5	6.3			
250–99	♂	6	7.0–9.0	7.7	4	8.5–9.0	8.9
	♀	9	7.0–9.5	8.1	1	9.5	9.5
300–49	♂	10	7.5–10.0	9.1	16	8.5–11.0	9.7
	♀	11	8.0–10.0	9.0	9	8.5–11.0	9.9
350–99	♂	10	9.0–11.5	10.1	14	9.0–12.0	10.8
	♀	16	8.0–12.0	10.1	13	9.5–12.0	10.7
400–49	♂	9	9.0–14.0	11.2	5	11.0–13.0	12.3
	♀	13	9.5–12.0	10.9	10	11.0–13.0	11.9
450–99	♂	6	10.0–13.5	11.9	19	11.5–15.0	13.6
	♀	15	10.0–15.0	12.7	11	12.0–14.5	13.4
500–49	♂	12	13.0–16.0	14.7	2	13.0–13.5	13.3
	♀	20	11.5–16.5	13.3	3	13.0–16.0	14.5
550–99	♀	2	13.0–13.5	13.3			

TABLE XIV. Increase in the width of infraoral lamina with size and stage of maturity, Lake Seneca area, 1959.

Length	Sex	Immature (L. Seneca)			Spawning (St. Catherine Creek)		
		Specimens	Width		Specimens	Width	
			Range	Av.		Range	Av.
mm		*no.*	*mm*	*mm*	*no.*	*mm*	*mm*
250–99	♂	0	. . .	. . .	2	9.5–11.0	10.3
	♀	0	. . .	. . .	8	8.0–11.0	9.7
300–49	♂	2	9.0–11.0	10.0	18	10.5–13.0	11.8
	♀	1	. . .	8.0	28	8.5–12.0	10.3
350–99	♂	5	8.0–11.0	10.9	35	11.5–14.0	12.6
	♀	12	7.5–11.0	9.5	7	11.0–11.5	11.2
400–49	♂	2	10.5–12.0	11.3	5	12.5–14.0	13.2
	♀	4	9.0–11.0	10.0	. . .	. . .	. . .

TABLE XV. Order of succession of different types of infraoral lamina, according to size and sexual maturity, in specimens of *Petromyzon marinus* from different localities (sexes combined). Symbols as in Table III.

Locality[a]	Maturity[b]	Length	Specimens	Succession of lamina types				
				Old set	New set			
					r	*i*	*i-n*	*n*
		mm	*no.*		%	%	%	%
L. Erie	Young[c]	164–193	10	*n*	0	10.0	40.0	50.0
L. Erie	Semi-adult	227–551	28	*r*	0	100.0	0	0
L. Erie	Adult	346–572	47	*i*	0	91.5	8.5	0
Père Marquette R.	Pre-spawning	322–531	63	*i*	0	14.4	42.8	42.8
Big Creek	Pre-spawning	276–548	54	*i*	0	7.4	40.7	51.9
L. Erie	Adult	404–548	6	*i-n*	0	0	83.4	16.6
Catherine Ck.	Spawning	275–383	6	*i-n*	0	0	16.6	83.4
Catherine Ck.	Spawning	291–338	6	*n*	0	0	0	100.0

[a]Localities and dates of collection are as in Table I.

[b]Degrees of maturity on this table correspond approximately to the following stages of the numerical system: young (0–1), semi-adult (1–2), adult (2–3), pre-spawning (3–4), spawning (5–6).

[c]In young specimens, sheaths of new sets of infraoral laminae were not corneous as yet.

oc
Fi
an
be
Ca
ho
58
of
wh
58
su
50'
la
fa

F
an
fis
te
by
su

ea
19
ha
su
su
o
(
d
H

in
a

S

J
F

Ocean Temperatures and Their Relation to Albacore Tuna (*Thunnus germo*) Distribution in Waters off the Coast of Oregon, Washington and British Columbia[1]

By Dayton L. Alverson[2]

ABSTRACT

Commercial albacore fishing offshore from Oregon, Washington and British Columbia, occurs during summer months when offshore surface water temperatures exceed 58°F (14.4°C). Fishermen have established 58°F (14.4°C) surface temperature as an indicator of "tuna water", and this rule-of-thumb relationship for surface water temperatures and albacore has generally been substantiated by total catch versus temperature records made during albacore investigations. Catch-per-hour data are also in accord with this general thesis. Catch-per-unit-effort data, however, do not indicate as marked a decline in availability at temperatures between 54 and 58°F (12.2–14.4°C) as might be interpreted from qualitative observations. With the exception of one albacore caught by a gillnet in 1956, all albacore have been taken in Bureau investigations where surface temperatures exceeded 54°F (12.2°C) and highest catch rates were obtained between 58 and 61°F (14.4–16.1°C). As the thermocline depth averages about 60 feet (18.3 m) in the summer months offshore from the Pacific Northwest states and temperatures are all well below 50°F (10°C) at the bottom of the thermocline, albacore probably inhabit only the overlying (mixed layer) lens of warm oceanic water. Concentrations of albacore appear to occur along the interface of the warm oceanic waters and the cooler waters adjacent to the coast.

Following the inception of albacore fishing contiguous to the States of Oregon and Washington and the Province of British Columbia (about 1937), northwest fishermen quickly established an empirical relationship between surface water temperature and the occurrence of albacore. The expression "tuna water" used by northwest fishermen refers to the typical deep blue oceanic water having surface temperatures equal to or greater than 58°F (14.4°C).

Observations made during numerous albacore investigations in the northeastern Pacific Ocean (Powell and Hildebrand, 1950; Powell *et al.*, 1952; Partlo, 1950) generally substantiate this relationship, and concentrations of albacore have seldom been observed or harvested during research cruises in areas where surface temperatures fall much below 58°F (14.4°C). Powell *et al.* (1952) report surface water temperature as one of the limiting factors governing the occurrence of albacore adjacent to the continent of North America. The depth of the lens (mixed layer) of warmer water, >57°F (>13.9°C) is also regarded as an important determinant of the occurrence of albacore (Powell *et al.*, 1952; Powell and Hildebrand, 1950).

Although 58°F (14.4°C) surface water temperature has proved a reliable indicator of the lower limit for occurrence of commercial quantities of this species, albacore have been captured in areas where surface temperatures were as low as

[1]Received for publication June 24, 1961.

[2]Director, Exploratory Fishing and Gear Research Base, U.S. Bureau of Commercial Fisheries, Seattle, Washington.

J. Fish. Res. Bd. Canada, **18**(6), 1961.
Printed in Canada.

54°F (12.2°C) (Powell *et al.*, 1952; Neave and Hanavan, 1960). In a few instances relatively good fishing has been reported at temperatures to 56° (13.3°C).

Water colour has also been used by fishermen as a general guide to "tuna water" and it has been reported by various investigators to bear some relationship to successful albacore fishing, i.e., albacore are not normally taken adjacent to the Pacific Northwest coast in the greenish inshore waters which overlie the continental shelf and slope (Powell and Hildebrand, 1950).

It is the objective here to review and summarize observations which appear pertinent to the occurrence and distribution of albacore in waters adjacent to the States of Oregon, Washington, and the Province of British Columbia, and to evaluate quantitatively, by measure of catch per unit of effort, fishing success at various surface water temperatures.

BACKGROUND

The albacore fishery in the Pacific Northwest normally begins in mid-July, peaks in August and September, and tapers off during late October. In some years fishing has continued into early November. Fishing operations are geared to get under way in mid-summer and the fishermen constantly check offshore water temperatures. Following reports of warm or "tuna water" scouting for tuna quickly commences.[3] In a typical year the fishery will first begin in the area between Newport and Astoria, Oregon, and gradually extend northward to areas off Washington and southern Vancouver Island. The northern extent of reported commercial operations has been offshore from the northern Queen Charlotte Islands. Commercial fishing generally occurs in waters within 50 to 200 miles (81–322 km) off the coast.

REVIEW OF PAST EXPLORATIONS

Since 1949 the U.S. Bureau of Commercial Fisheries has conducted 5 exploratory fishing cruises to determine the general distribution patterns of albacore in waters contiguous to Washington, Oregon, British Columbia, and Alaska (Fig. 1). During the explorations water temperature, thermocline depth, and water colour and availability of albacore were recorded. A summary of these observations is shown in Table I.

Surface water temperatures in areas where albacore were caught ranged from 54 to 63°F (12.2–17.2°C). These temperature ranges for albacore distribution in the northeastern Pacific area are in accord with observations made by Neave and Hanavan (1960), and the range 58 to 60°F (14.4–15.6°C) given by Partlo (1950) for the best catches of albacore taken off Vancouver Island. The depth of the thermocline in areas where good catches were taken ranged between 50 and 75 feet (15.2–22.9 m) with an average of about 60 feet (18.3 m).

[3]Temperature data are provided to the fishing fleet by offshore fishing craft engaged in other fisheries. Surface temperature charts issued by U.S. Bureau of Commercial Fisheries Biological Laboratory at San Diego, California are now in use.

The blue colour of water which has been associated with good albacore fishing by various authors is another empirical relationship established by fishermen exploiting tunas from Pacific Northwest ports. The decrease in availability of albacore in green waters is well documented (Powell *et al.*, 1952; Powell and Hildebrand, 1950). Fair catches have, however, been reported in blue-green water, although the blue oceanic waters have constantly yielded best catches. Water colour itself is probably unimportant. The transition from blue oceanic water to coastal green water generally demarks the inshore limit of water having surface temperatures greater than 57°F (13.9°C). The temperature gradient is normally relatively sharp at the boundary (blue to green) between oceanic and coastal waters.

It should be noted that this rule-of-thumb relationship (58°F or 14.4°C = tuna water) is one of negative rather than positive association, i.e., waters with surface temperatures less than 58°F are not likely to yield commercial quantities of albacore, but on the other hand, 58°F surface temperatures or greater do not necessarily insure successful albacore fishing.

It has been suggested by Powell *et al.* (1952) and Radovich (1960) that distribution of albacore within the temperature regime that the species normally inhabits in the Pacific Northwest area is probably associated with feeding or other biological determinants rather than being temperature dependent. Appraisal of the surface water temperature-albacore relationship for past explorations has been based on the availability of the species to troll or gillnet gear fished in waters of different temperature ranges. Published data for these investigations as well as other investigations (Partlo, 1950; Craig and Graham, 1961) have shown either percentage catch or absolute catch in numbers of albacore for specified

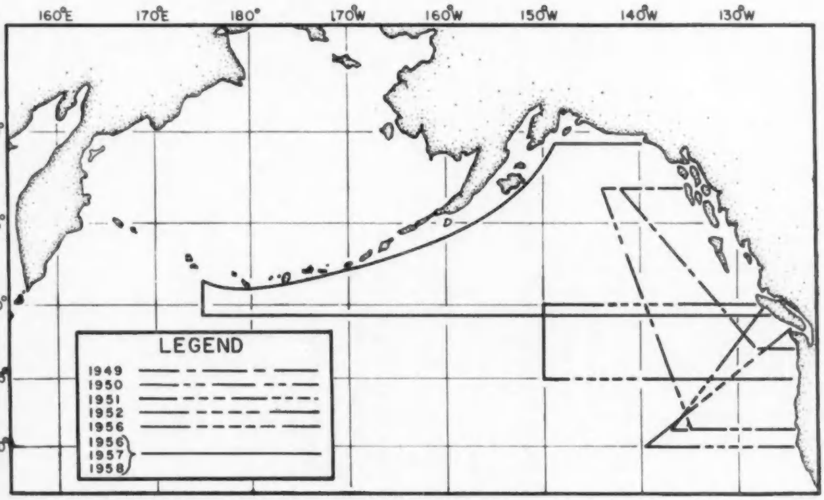

FIG. 1. Areas surveyed by years.

TABLE I. Surface water temperatures for albacore catches, best fishing temperatures, and water colour reported in areas of best fishing for five exploratory cruises in the northeastern Pacific Ocean.

Authors	Year	Temperature ranges				Thermocline depth, best catches		Water colour, best catches
		Occurrence		Good catches				
		°*F*	°*C*	°*F*	°*C*	*feet*	*meters*	
Powell and Hildebrand (1950)	1949	56.8–61	13.8–16.1	58–61	14.4–16.1	50	15.21	blue
Powell *et al.* (1952)	1950	54–62	12.2–16.7	57–61	13.9–16.1	60	18.29	blue
Schaefers (1952)	1951	58–62	14.4–16.7	58–61	14.4–16.1	. . .	. . .	. . .
Schaefers (1953)	1952	54–61	12.2–16.1	58–62	14.4–16.7	. . .	. . .	. . .
Powell (1957)	1956	55–63	12.8–17.2	58	14.4	50–75	15.21–22.86	. . .

temperatures. These indices have not accounted for expenditure of varying amounts of fishing effort.

To evaluate availability changes of albacore, data from the five exploratory operations conducted by the Bureau along with data from albacore catches taken during North Pacific salmon studies in the years 1956, 1957, and 1958, were analyzed to yield information on the catch-per-hour fishing by 2-degree F (1.1-degree C) temperature intervals of surface water. Units used were catch-per-lure-hour and catch-per-shackle-hour, where a lure-hour equalled one hour's fishing with a single trolling lure and a shackle-hour equalled one hour's fishing with a 50-fathom (91-meter) shackle of gillnet.

RESULTS

Hours fished and catch-per-hour fishing by gear are shown for each cruise in Tables II through IV. These data are summarized in Table V which gives the mean value of catch-per-hour for the five exploratory cruises plus albacore gillnet catches taken during high seas salmon studies for the years 1956, 1957 and 1958. Catch rates for trolling were highest when temperatures ranged between 58 and 61°F (14.4-16.1°C) and in all years, with the exception of 1956, the catch rates fell rapidly at temperatures below 58°F. These data generally support catch-temperature data tabulated without regards to fishing effort,

TABLE II. Trolling catch per unit of fishing effort by year and surface temperature ranges. (Original data were recorded in degrees Fahrenheit.)

Temperature		1950		1951		1952		1956	
°F	°C	Fish per 100 lure hours	Lure hours	Fish per 100 lure hours	Lure hours	Fish per 100 lure hours	Lure hours	Fish per 100 lure hours	Lure hours
<52	<11.10	0	15	...	...	...	...	...	...
52–53	11.10–11.95	0	2235	0	266	0	320	0	153
54–55	11.96–13.05	5.45	550	0	140	0.08	1181	1.39	216
56–57	13.06–14.15	11.94	1617	0	847	1.09	1282	2.14	794
58–59	14.16–15.30	22.74	2164	1.13	2114	8.99	2057	0.89	1127
60–61	15.31–16.40	11.97	1011	6.12	1535	0	367	3.10	226
>61	>16.40	0	159	0	278	...	...	1.04	96

TABLE III. Total gillnetting effort (shackle hours) by year and surface temperature ranges.

Temperature		Total shackle hours fished						
°F	°C	1949	1950	1951	1952	1956	1957	1958
<52	<11.10	...	...	...	...	15,005	24,728	33,977
52–53	11.10–11.95	...	...	...	...	7,787	3,083	1,258
54–55	11.96–13.05	84	21	...	...	5,081	1,947	...
56–57	13.06–14.15	419	246	93	...	2,543	600	319
58–59	12.16–15.30	331	238	125	786	1,531	384	276
60–61	15.31–16.40	158	96	270	757	1,224	396	...
>61	>16.40	...	...	222	...	674	...	...

TABLE IV. Albacore gillnet catch per unit of fishing effort by year and surface temperature ranges.

Temperature		Number of fish per 100 shackle hours						
°F	°C	1949	1950	1951	1952	1956	1957	1958
<52	<11.10	...	...	...	...	0.01	0	0
52–53	11.10–11.95	...	...	...	...	0	0	0
54–55	11.96–13.05	0	0	...	...	0.18	0	...
56–57	13.06–14.15	9.78	67.07	0	...	0.43	1.50	0
58–59	14.16–15.30	18.43	19.75	2.40	0.25	0.91	0	0
60–61	15.31–16.40	39.24	33.33	5.92	0	0.16	0	...
>61	>16.40	...	...	4.05	...	0.44	...	...

TABLE V. Gillnet and trolling catch-per-unit-of-fishing effort (all years combined) by surface temperature ranges.

Temperature (°F)	Trolling		Gillnetting	
	Total lure hours fished	Fish × 10^2 per lure hour	Total shackle hours fished	Fish × 10^2 per shackle hour
<52	15	0	73,710	
52–53	2,974	0	12,128	0
54–55	2,171	1.57	7,049	0.13
56–57	4,959	5.34	3,801	4.87
58–59	7,793	9.91	3,340	1.98
60–61	3,291	8.63	2,743	1.82
61+	533	.19	896	1.34

but it is interesting to note that the indicated decline in availability at temperatures below 58°F is not nearly as sharp as that suggested by qualitative observations. For example, Powell *et al.* (1952) show that about 55% of the total catch was caught at temperatures from 58 to 59°F (14.4–15.0°C) and less than 10% of the total catch was taken at temperatures ranging from 56 to 57°F (13.3–13.9°C). Catch-per-hour fishing of trolling lures for 1950 shows a decline in availability for the 56–57°F (13.3–13.9°C) temperature range of about one-half that of the 58–59°F (14.4–15.0°C) temperature zone. Availability also appears higher in the next lower temperature zone of 54–55°F (12.2–12.8°C) than is evident from catch-temperature data alone.

The data for all years of gillnetting are strongly weighted by one excellent catch made in the Queen Charlotte Sound area in 1950 when surface temperatures were recorded at 57°F (13.9°C). For individual years best catches were normally made at temperatures of 58°F (14.4°C) or higher. In 1956 a single albacore was reported caught in a gillnet when the surface temperature was only 51°F (10.6°C).

DISCUSSION

The data reviewed generally substantiate the relationship suggested by other authors for surface water temperature and albacore occurrence in the Pacific Northwest. It is not surprising that the catch-per-effort data by temperature

increments does not indicate as rapid a decline in availability as might be interpreted from catch data alone. By concentrating in areas where albacore are most available the catches of commercial fishermen are strongly weighted to the temperature interval existing in areas of high availability.

Some evidence exists which suggests that albacore within the geographic area under discussion probably inhabit only those waters above the thermocline. This thesis, however, still lacks good supporting data. Powell *et al.* (1952) showed the majority of gillnet-caught albacore was taken in the upper portion of the nets and Powell and Hildebrand (1950) reported no albacore were captured by troll lines set to fish subsurface depths. Longline gear fished during Bureau explorations have also failed to take albacore in waters off the Pacific Northwest coast.[4] If temperature limits the geographic distribution of albacore, then it may also be assumed a factor controlling bathymetric distribution. The limiting surface temperature appears to be about 54°F (12.2°C). As this temperature is well above that which is normally observed (about 46°F or 7.8°C) at the bottom of the summer thermocline structure in the Pacific Northwest, it is doubtful that the species sounds to depths greater than that of the thermocline.

It has been shown that the location of first catches of albacore off the Oregon coast accord well with the geographic position of the 57–58°F (13.9–14.4°C) isotherms. During late spring (June) the 27.5°F (14.2°C) isotherm generally parallels the Pacific coast of North America between San Diego and San Francisco, and then bends sharply to the west between San Francisco and Cape Blanco, Oregon. In mid-June this isotherm generally lies about 350 to 400 miles (564–644 km) west of Cape Blanco, Oregon. From July through September the 57°F (13.9°C) isotherm is found progressively northward. During mid- and late summer a pouch of warm water will normally develop adjacent to the coast of British Columbia with colder water lying both to the east and west of the pouch. Albacore catches are confined to the warmer water areas. Schaefers (1952) reports albacore can be taken with troll gear off Oregon prior to commercial fishing season by running west to the area of warm water. In three successive years (1950 through 1952) albacore were taken in Bureau explorations about 30 days prior to the start of the normal fishing season (mid-July). The albacore were caught shortly after exploratory fishing commenced in water where surface temperatures were greater than 57°F (13.9°C) at distances from 280 to 370 miles (451–569 km) offshore.

Throughout the fishing season commercial operations take place at distances from about 50 to 200 miles (81–322 km) seaward of the coast. It appears that albacore concentrate along the inter-face of the warmer oceanic waters and the cooler waters overlying the continental shelf and terraces. Exploratory fishing activities conducted at distances greater than 200 miles (322 km) seaward of the

[4]Acceptance of this evidence assumes that trolling and longline methods are effective methods of sampling albacore in subsurface waters and all areas of the gillnets are equally effective for capture of albacore. The use of longlines for capture of albacore is well documented in commercial and experimental fishing. Evidence of the vertical distribution of albacore, however, might be better defined by surface and subsurface gillnets, set above and below the thermocline.

coast during August and September have failed to take commercial concentrations of albacore, although surface temperatures were within the favorable range of 58–61°F (14.4–16.1°C). This is also substantiated by reports of albacore catches made by United States picket vessels (Johnson, 1961).

ACKNOWLEDGMENT

The author extends thanks to Gerald V. Howard, James H. Johnson, and Felix Favorite, U.S. Bureau of Commercial Fisheries, for review and suggestions for improvement of this manuscript. I am also indebted to the Seattle Biological Laboratory of the U.S. Bureau of Commercial Fisheries for making available data on albacore catches taken during offshore salmon gillnetting.

REFERENCES

CRAIG, W. L., AND J. J. GRAHAM. 1961. Report on a co-operative, preseason survey of the fishing grounds for albacore (*Thunnus germo*) in the eastern North Pacific, 1959. *California Fish and Game*, **47**(1): 73–85.

JOHNSON, J. H. 1961. Navy vessels catch 447 albacore in 1961. *California Fishery Market News Monthly Summary, Part II–Fishing Information*, February, 1961. (U.S. Department of the Interior, Bureau of Commercial Fisheries.)

NEAVE, F., AND M. G. HANAVAN. 1960. Seasonal distribution of some epipelagic fishes in the Gulf of Alaska region. *J. Fish. Res. Bd. Canada*, **17**(2): 221–233.

PARTLO, J. M. 1950. A report on the 1949 albacore fishery. *Fisheries Research Board of Canada, Nanaimo Biological Station Circular*, No. 20, 37 pp.

POWELL, D. E. 1957. North Pacific albacore tuna explorations by the M/V *John N. Cobb*, 1956. *Commercial Fisheries Review*, **19**(6): 1–9.

POWELL, D. E., D. L. ALVERSON AND R. LIVINGSTON JR. 1952. North Pacific albacore tuna explorations, 1950. *U.S. Fish and Wildlife Service, Fishery Leaflet*, No. 402, pp. 1–56.

POWELL, D. E., AND H. A. HILDEBRAND. 1950. Albacore tuna explorations in Alaskan and adjacent waters, 1949. *U.S. Fish and Wildlife Service, Fishery Leaflet*, No. 376, pp. 1–33.

RADOVICH, J. 1960. Redistribution of fishes in the eastern North Pacific Ocean in 1957 and 1958. *Rept. California Cooperative Oceanic Fisheries Investigations*, No. 7, pp. 163–171.

SCHAEFERS, E. A. 1952. North Pacific albacore tuna explorations, 1951. *Commercial Fisheries Review*, **14**(5): 1–12.

1953. North Pacific albacore tuna explorations, 1952. *Ibid.*, **15**(9): 1–6.

Seasonal Fishing Quality Provided by the Natural Reproduction of Speckled Trout in Three Ontario Ponds[1]

By Hugh R. McCrimmon

Department of Zoology, Ontario Agricultural College, Guelph, Ontario

ABSTRACT

A study was made of semi-monthly speckled trout catches from three similar ponds during the 5 fishing seasons for the 1956 to 1960 period. A catch totalling 15,088 trout and taken by 3,696 rod-hours was analyzed. Above-average catches of 2.9 undersized and 3.3 keeper trout per rod-hour occurred during the May 1–15 interval when the trout were particularly susceptible to angling. After this time, semi-monthly catches, composed of approximately equal numbers of undersized and keeper trout, averaged 3.8 trout per rod-hour. Except for the May 1–15 interval, variations in the levels of semi-monthly catches were found to result from differences in fishing intensity rather than from significant changes in the availability of trout. Annual natural reproduction and the continuous recruitment of young fish into the size group vulnerable to angling, therefore, maintained a standing population of trout at a level adequate to provide stability in the quality of angling throughout the fishing season.

INTRODUCTION

Fishing records provided by the Glen Major Fishing Club afford the opportunity to study the relationship of the size of trout catches to the time of year, fishing intensity, and the availability of trout in three ponds fished exclusively by its members. An analysis has been made of the daily angling and catch statistics kept by members for the 5 year period extending from 1956 to 1960. The method of angling was restricted to fly casting only. For the purpose of this paper, the the May 1st to September 15th open trout season has been divided into 9 semi-monthly intervals.

The ponds, located in agricultural southern Ontario at Lat. 44°N and Long. 79°W are very similar in limnological features. Each is slightly less than 2 acres (0.6–0.8 ha) in surface area with a maximum depth of about 9 feet (3 m), and is abundantly supplied with cold water and beds of *Chara*. Each of the ponds is fed by a spring creek providing excellent conditions for the natural reproduction of speckled trout, *Salvelinus fontinalis*, on which angling was dependent. The reader is referred to Ricker (1932) and McCrimmon and Berst (1961) for detailed descriptions of the ponds and their fisheries dating back to 1895.

The cooperation of A. M. Wilson, President, and members of the Glen Major Fishing Club in providing data necessary for the study is gratefully acknowledged.

[1]Received for publication June 12, 1961.

J. Fish. Res. Bd. Canada, 18(6), 1961.
Printed in Canada.

TABLE I. Total catch of trout for the 1956–1960 fishing seasons.

Period	Catch of trout											
	Pond A			Pond B			Pond C			Composite, 3 ponds		
	Rod-hours of fishing	No. less than 7″	No. 7″ and over	Rod-hours of fishing	No. less than 7″	No. 7″ and over	Rod-hours of fishing	No. less than 7″	No. 7″ and over	Rod-hours of fishing	No. less than 7″	No. 7″ and over
May 1–15	164	359	544	128	348	459	133	519	402	425	1226	1405
May 16–31	176	371	292	119	323	219	117	344	242	412	1038	753
June 1–15	212	351	388	119	236	210	160	432	234	491	1019	832
June 16–30	161	273	279	95	186	168	109	310	158	365	769	605
July 1–15	142	249	295	98	113	125	133	271	199	373	633	619
July 16–31	136	275	335	128	252	278	116	256	193	380	783	806
Aug. 1–15	128	221	350	82	102	125	107	139	141	317	462	616
Aug. 16–31	198	310	421	135	255	282	150	266	253	483	831	956
Sept. 1–15	180	325	404	111	206	233	159	313	254	450	844	891
May 1–Sept. 15	1497	2734	3308	1015	2021	2099	1184	2850	2076	3696	7605	7483

FISHING INTENSITY

During the 5 year period from 1956 to 1960, the 3 ponds provided a total of 3,696 rod-hours of angling (Table I). Each of the ponds was fished for an average of 71–75 days each season at a level averaging 3.3 rod-hours per day. The maximum daily fishing pressure exerted on any of the ponds was 21 rod-hours, and daily angling rarely exceeded 10 rod-hours per pond.

Each of the ponds was subjected to similar total fishing intensities over the 5 year period, ranging from 1,015 rod-hours in Pond B to 1,497 rod-hours in Pond A. Fishing was distributed uniformly over the season when analyzed on a semi-monthly basis, reaching a low of 22.9% of the semi-monthly seasonal average of 411 rod-hours during the first half of August.

CATCH STATISTICS

A total catch of 15,088 trout was reported for the ponds during the 5 year period. This included 7,483 trout 7 inches (178 mm) or more in total length (to the tip of the tail when squeezed to maximum extension) which were mostly retained, and 7,605 trout of less than 7 inches which were returned to the water (Table I). The 7-inch length limit on keeper trout was a Provincial regulation discontinued after the 1959 season but retained by the Club for the purpose of this study. Keeper trout ranged upward from 7 inches and seldom exceeded 12 inches (305 mm) in length. Undersized trout in the catch were normally from 5 to 7 inches (127–178 mm) in length and the catch statistics include an unknown number of recaptures in this length range. On account of the selectivity of the angling gear, few trout less than 5 inches in length were caught.

Keeper Trout

Total catches of keeper trout from each of the ponds ranged from 2,076 and 2,099 fish for ponds C and B, respectively, to 3,307 fish for Pond A (Table I). However, fishing intensity was highest also in Pond A and fishing success there, when expressed as catch per unit effort, and was only 10% higher than the average of 2.0 trout per rod-hour for the three ponds. A total annual harvest of 294 trout per acre (726 per hectare) from the 3 ponds was realized.

A comparison of the composite catch by semi-monthly intervals (Fig. 1) shows a substantially higher catch for the first interval (May 1–15) than for any subsequent interval. Semi-monthly angling success was 3.3 trout per rod-hour during the first interval, which was 65% above the season average. During the remaining 8 semi-monthly intervals, fishing success was remarkably stable, varying no more than 20% from the seasonal average of 2.0 trout per rod-hour. Fishing quality for keeper trout was consistently higher in each pond on opening day of the season, averaging 4.4 trout per rod-hour.

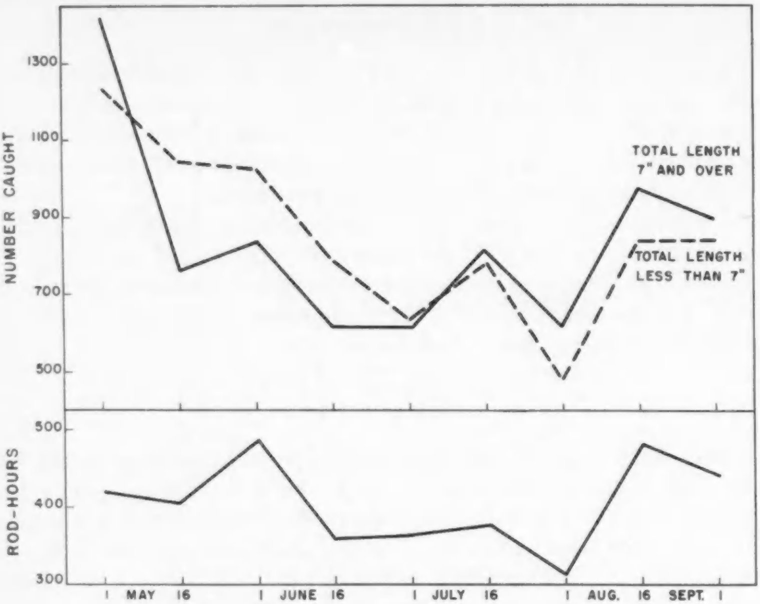

FIG. 1. Composite angling and catch statistics of the 3 ponds for the 1956–1960 fishing seasons.

UNDERSIZED TROUT

All trout measuring less than 7 inches and a few over 7 inches in total length were returned to the water and hence statistics include some recaptures. However, many of these undersized fish grew to become keeper trout during the angling season. Likewise, there was a continuous recruitment of smaller trout into that length range of undersized fish susceptible to the angler's hook.

Total catches of undersized trout from each of the ponds over the 5 year period (Table I) ranged from 2,021 fish from Pond B to 2,734 and 2,850 fish from Ponds A and C, respectively. In spite of these differences in total catches, fishing success for small trout was actually very similar at 1.8, 2.0, and 2.1 trout per rod-hour for Ponds A, B, and C, respectively.

A comparison of combined catches from the 3 ponds on a semi-monthly basis during the fishing season (Fig. 1) shows the highest catch of undersized trout to have occurred within the period extending form May 1 to June 15 when 43.2% of the total catch was handled. The lowest catch was reported during the first half of August but was followed by higher catches in the latter half of August and September than had been realized since June.

A review of semi-monthly catches of undersized trout when expressed in relation to unit fishing effort reveals that the highest catches occurred during

May, after which time semi-monthly catches averaged about 1.9 fish per rod-hour over the remainder of the season. The optimum catch of undersized trout at 3.6 fish per rod-hour occurred on opening day of the fishing season.

Seasonal Fishing Quality

From the semi-monthly composite catch per unit effort data plotted in Fig. 2, it is apparent that the quality of angling was highest at the beginning of the fishing season but dropped off by late May to a level of approximately 3.8 trout per rod-hour which was maintained for the remainder of the season. The shape of the curve approximates that for either undersized or keeper trout except that the actual curve for undersized trout is less steep in the semi-monthly intervals beginning on May 16 and June 1.

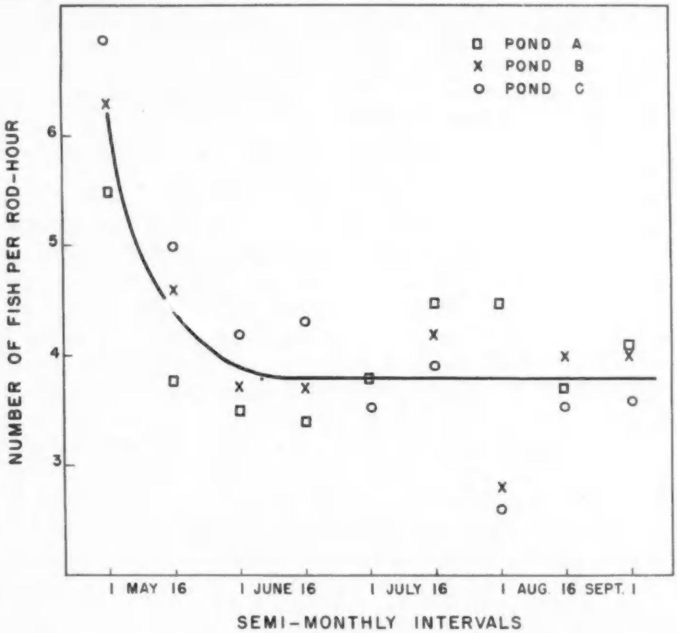

Fig. 2. Semi-monthly angling quality for the 3 ponds during the 1956–1960 fishing seasons.

The higher quality of angling at the beginning of the fishing season may be attributed to a build-up of trout in the length range susceptible to angling during the previous closed season and to the voracious appetite of the trout at that time of the year. The stability of angling quality through the summer months attests to the continuous recruitment of keeper trout from fish in the sub-keeper length range.

CONCLUSION

From the analysis of the 5 year fishing statistics for the 3 ponds, it may be concluded that natural reproduction and the continuous recruitment of smaller fish into the size group susceptible to angling was at least adequate to maintain the standing population of catchable trout at a level necessary to provide a consistent quality of angling throughout the fishing season. The correlation of fishing intensity with catch size through the season after mid-May is evidence of the availability of ample trout for angling of this intensity at all times.

Except for the above-average catches of trout during the May 1–15 interval when the fish are the most vulnerable to angling, variations recorded in the size of the catches for each of the semi-monthly intervals of the fishing season are a result of differences in fishing intensity rather than of significant changes in the availability of trout.

REFERENCES

McCrimmon, H. R., and A. H. Berst. 1961. An analysis of sixty-five years of fishing in a trout pond unit. *J. Wildlife Management*, **25**(2): 168–178.

Ricker, W. E. 1932. Studies of trout producing lakes and ponds. *Univ. Toronto Stud., Biol. Ser.*, No. 36; *Pub. Ontario Fish. Res. Lab.*, No. 45, pp. 111–167.

Diving and Photographic Techniques for Observing and Recording Salmon Activities[1,2]

BY D. V. ELLIS

Fisheries Research Board of Canada
Biological Station, Nanaimo, B.C.

ABSTRACT

Techniques have been developed for underwater observation and photographic recording of salmon activities that are useful in various kinds of behaviour studies. Scuba divers can approach salmon sufficiently closely under some conditions to permit clear observation. From tests made both above the surface and under water, an exposure chart has been prepared for salmon photography in rivers. Two examples are demonstrated. Colour film can be used, with appropriate filters, to render underwater objects in the colours they would have in air, or to give them untrue colours that assist in differentiating them from their background.

INTRODUCTION

FIELD STUDIES of salmon ecology and behaviour in rivers have long been hindered by two technical problems: how to observe salmon clearly and how to record their activities. The first problem can be partly solved by observing at the occasional favourable locality with calm, clear water, but a major breakthrough has recently come with the development of amateur scuba diving. In 1958 three of the Nanaimo Biological Station personnel, part of a group investigating the physiology and behaviour of salmon, were trained to dive, and since then have observed salmon in many previously inaccessible habitats (Fig. 1). The second problem has been tackled in part by developing photography as a recording technique. Most of the technical difficulties concerned have been overcome during two years' testing, 1959 and 1960. As a result the photography of salmon, both from above surface and under water, has taken its place as an effective research tool in the group's investigations. This paper describes the tests undertaken during the development of the photographic recording techniques, in particular those involving diving.

METHODS

Photographic equipment included a 6×6 Rolleiflex in Rolleimarin housing for underwater tests, a 35 mm Exakta for above surface photography, and a 16 mm Bell and Howell cine-camera in Sampson-Hall underwater housing. A Multiblitz Press electronic flash unit was used for above-surface recording at night. Little use was made of an underwater exposure meter, as surface turbulence prevented accurate and reliable readings.

[1]Received for publication. May 16, 1961.
[2]Paper No. 4 concerning the physiology and behaviour of salmonid fishes from the Fisheries Research Board of Canada, Biological Station, Nanaimo. B.C.

J. FISH. RES. BD. CANADA, 18(6), 1961.
Printed in Canada.

Testing was mainly carried out at the Stamp and Sproat Rivers on Vancouver Island while based at the Fisheries Research Board field camp near Alberni.

The first tests in 1959 showed the necessity for reducing processing variation of film to a minimum. Consequently facilities were established to process black and white film at the field camp and the Biological Station, and arrangements were made with custom photofinishers to process colour and cine-film.

Two processing techniques were adopted for black and white roll film. The first was a field technique using Unibath 2 (Cormac Mfg. Co.) in a daylight loading tank. Fixed negatives were obtainable 8 minutes after shooting the final exposure. The second processing technique relied on Promicrol (May and Baker Ltd) as a one-shot developer using standard equipment and timing. Promicrol was selected as the single developer to be used throughout the tests with a variety of films, in view of its versatility and comprehensive instruction sheet. Developed film was cut into strips, contact printed (1 roll to an 8 × 10 sheet) and stored.

The following method was finally adopted for determining exposures in completely new situations. A roll of intermediate speed film (Kodak Plus X) was exposed with a range of 2 exposure values on either side of an estimate of the exposure. This film was developed (on the spot in Unibath if speed was essential) and the negatives examined to check correct exposure. If the particular photographic objective required a change of film emulsion, e.g., to colour, finer grain, faster speed, etc., appropriate exposure was calculated from the test roll, and the selected film then used.

Colour correction tests were undertaken to find means of restoring colours differentially absorbed by water. Three standard scenes in the Stamp River at depths of 2, 8 and 15 feet were selected and a series of 16 exposures taken at each depth using 5 densities of Kodak red, yellow and magenta filters plus a 0 filter control.

Tests with artificial light sources under water have so far been limited to still photography with No. 5 bulbs in Rolleimarin flash-holder. Series of bracketed exposures have been made of several scenes, with four emulsions at exposures calculated from manufacturer's guide numbers divided by the underwater light path (= twice focusing distance). Electronic flash has been used to obtain prints of nocturnal, surface-migrating fry and smolts. In these tests camera and flash were held, or mounted, vertically above the water surface.

During the tests little difficulty was found for scuba divers to approach salmon sufficiently closely for clear observation and for photography. Approach was easiest when many salmon were crowded together in small pools and subjected to strong currents. Under such conditions, salmon tended to ignore divers, particularly if they were approached stealthily from down-river and close to the bottom. However, it was almost impossible to approach adult salmon in open water, i.e., large pools and lakes. Sockeye were easier to approach than coho. Fry would come so close to quiet divers that the problem was to keep them sufficiently far away for focusing.

During the course of two summers a student assistant was trained to dive, and handle both the photography and processing whenever necessary.

The concept of "underwater light path" is important in calculating exposures for underwater photography, due to the rapid rate of absorption of light and underwater scattering (Schenck and Kendall, 1954). The underwater light path in natural light photography is the depth of the object plus the focusing distance. These are not completely interchangeable, however, in calculating exposures as scattering also limits the focusing distance by reducing definition. The maximum focusing distance for effective photography in the tested areas was 10 feet, even though salmon were usually visible at a distance of 20 to 30 feet in the clear river water.

For underwater exposure calculation, it is a considerable help to use the recently adopted A.S.A. Additive Speed Value system of film rating, and the Exposure Value (EV) system for light measurement, shutter speeds and apertures. However, the cameras used in these tests were calibrated in the traditional manner, as most photographic equipment still is, and so exposure data are presented in both systems. A conversion table is provided (Table I).

TABLE I. Conversion of Exposure Value (EV) system into terms of shutter speeds, apertures, film speeds and scene brightness.

Basic formula:

$$\text{Exposure value} = \text{Time value} + \text{Aperture value} = \text{Speed value} + \text{Brightness value}$$

Time value	Shutter speed	Aperture value	f/ stop	Speed value	ASA rating	Brightness value	Scene brightness[a]
	sec						*candles per sq. ft.*
0	1	0	f/1	0	3	0	0.352
1	1/2	1	f/1.4	1	6	1	0.704
2	1/4	2	f/2	2	12	2	1.41
3	1/8	3	f/2.8	3	25	3	2.82
4	1/15	4	f/4	4	50	4	5.63
5	1/30	5	f/5.6	5	100	5	11.3
6	1/60	6	f/8	6	200	6	22.5
7	1/125	7	f/11	7	400	7	45.1
8	1/250	8	f/16	8	800	8	90.1
9	1/500	9	f/22	9	1600	9	180
10	1/1000	10	f/32	10	3200	10	360
						11	721
						12	1442
						13	2884

[a] Reflected light exposure meter reading off 18% reflectance card. Can also be measured as a light value in foot-candles by an incident light-meter.

RESULTS

Table II gives selected exposures for some scenes intensively photographed during the tests (Fig. 2–4). Fast shutter speeds and hence wide apertures were preferred in order to stop the normally rapid movements of salmon and water.

Such shutter speeds were usually possible in the tested area using medium speed black and white film to a maximum underwater light path of about 20 feet. The use of colour film was limited to very short underwater light paths of 12 feet or less, due to the need for colour correction by filters.

TABLE II. Effective underwater exposures in bright sun between 09:00 and 15:00 hours for the scenes most intensively photographed. *Film A:* Plus X. *Film B:* Superanscochrome daylight. *Film C:* HS Ektachrome daylight.

Scene	Underwater light path	Film	Filter	Exposure value	Shutter speed	Aperture
Fig. 2					*sec*	
Into water from above surface, with rock or gravel background	8 ft (=2× depth)	A	Polaroid	9.5	1/50	f/3.5
		B	Polaroid & CC30R	8.5	1/25	f/3.5
		C	Polaroid & CC30R	9	1/25	f/4.5
Fig. 3						
Under water, with plain background of water, rock, gravel or plants	5 ft	A	None	12.3	1/250	f/4.5
		B	CC30R	11	1/125	f/4.0
		C	CC30R	11.6	1/250	f/3.5
	12 ft	A	None	11.3	1/125	f/4.5
		B	CC50R	9.6	1/60	f/3.5
		C	CC50R	10.3	1/60	f/4.5
	20 ft	A	None	10.6	1/125	f/3.5
Fig. 4						
Under water, with white water background or surface	10 ft	A	None	13	1/500	f/4.0
		B	CC40R	12	1/250	f/4.0
		C	CC40R	12.6	1/500	f/3.5

Effective photography of salmon from above surface is limited by the need for polarising filters to eliminate surface glare (Fig. 2).

Table III shows colour correction filters selected for two underwater light paths using Superanscochrome daylight film. Even the usual minimum path, with object 3 feet from camera and both situated immediately below the surface, required a fairly strong filter (CC30R, or possibly CC20R) for satisfactory colour rendition. Interpolating into the table suggests a CC40R filter for an 8-foot underwater light path. Colour correction became almost impossible with an 18-foot underwater light path. Exposures with other colour films, Kodak

TABLE III. Colour correction filters required in Stamp River area.

Underwater light path	Correction filter
5 ft	CC30R
12 ft	CC50R
18 ft	Correction not practical

High-Speed Ektachrome and Anscochrome, both in daylight emulsions, suggested that different filter corrections might be necessary.

Correction for above-surface colour photography gave quite unnatural effects due to surface reflections, and hence would only be advisable if the reflections could be completely eliminated by polarising filters.

Results of test exposures of colour cine-film underwater showed that exposure calculations and colour correction established for 120 rolls of Superanscochrome daylight film could be applied without change to the same product in 16 mm cine-film. The test footage obtained has been made into a short movie demonstrating wandering movements of salmon schools in a turbulent pool, holding in a waterfall eddy, and deliberate selection of a narrow limited path through a calm and placid stretch of river.

Table IV shows effective underwater guide numbers for 4 films. These apply to shutter speeds of 1/500th sec and No. 5 clear bulbs. In general, flash photography is more suitable for recording young salmon (Fig. 5) than for adults, which are too large for even illumination at the short focusing distances imposed. The results showed little constancy in ratio between manufacturers' guide numbers and the effective underwater guide number. Hence, the latter cannot be accurately predicted, and need to be derived by the photographer for each film-flashbulb combination.

TABLE IV. Guide numbers for No. 5 clear flashbulbs at 1/500 sec in Rolleimarin 7-inch polished reflector.

Film	Manufacturers' Guide No.[a]	Underwater Guide No.
Black and white film		
Kodak Panatomic X	70	50
Adox R14	50	20
Colour film		
Anscochrome daylight	65	20
Kodacolor	65	15

[a]Based on extrapolation from data supplied with flashbulbs.

Colour tests were made using clear bulbs and daylight film, which gave reasonable colour rendition without filtering through red adsorption by the water. However, colours could undoubtedly be improved. The use of blue bulbs was not satisfactory, as filtering was necessary for correct colour rendition, and they produced considerably less light than clear bulbs.

Nocturnal surface migrants can be photographed from above surface (Fig. 6) using electronic flash and normal guide numbers. By the use of high contrast, fine grain film in 35 mm camera, series of enlarged prints can be obtained demonstrating the direction of orientation of these migrants in relation to current direction.

CALCULATION OF EXPOSURE UNDER RIVER CONDITIONS

From these various tests a chart has been devised for calculating exposures within the testing rivers (Tables V, VI). Table V gives a basic above-surface Exposure Value taken from a Kodak, 18% reflectance, gray card. Table VI is a series of corrections to be made for weather, underwater light path, nature of background and filters. The basic exposure value depends in part on the processing techniques used. The factor "depth corrections" depends on turbidity, and consequently may vary from place to place and time to time. It should be checked frequently. The other factors should be constant within the period May-September, 09:00–15:00 hours.

TABLE V. Basic exposure values for three films, from light-meter reading of Kodak 18% reflectance gray card in bright sun 09:00–15:00 hours.

Film	Film speed	Exposure value	Shutter speed	Aperture
Plus X	5.5°	15	1/500	f/8
Superanscochrome daylight	5°	14.5	1/500	f/6.3
HS Ektachrome daylight	5.5°	15	1/500	f/8

TABLE VI. Chart for calculating underwater exposures in Stamp and Sproat Rivers. The "primary underwater correction" is for approximately 5 ft underwater light path. The "secondary correction" is minus 1 EV for each 7 ft of additional underwater light path.

Weather corrections	
Bright sun	Basic exposure value (Table V)
Cloudy bright	minus 1 EV
Cloudy dull	minus 2 EV
Heavy cloud	minus 3 EV
Primary underwater correction	minus 2.5 EV
Secondary underwater corrections	
12 ft underwater light path	minus 1 EV
20 ft underwater light path	minus 2 EV
Background corrections	
Much white water	plus 2 EV
Some white water	plus 1 EV
Open water	No correction
Unshaded background	No correction
Light shade	minus 1 EV
Much shade	minus 2 EV
Filter corrections	
CC20R	minus 0.5 EV
CC30R	minus 0.8 EV
CC40R	minus 1.1 EV
CC50R	minus 1.5 EV
Polaroid	minus 1.5 EV

FIG. 1. Scuba diver (D. V. Ellis) making cine-photographic recordings of the activities of a group of sockeye salmon holding in a waterfall eddy. Plus X film, bright sun, depth 3 feet, focusing distance 5 ft, some white water, turbulent surface, rock background with shadows, Exposure Value 13, 1/500 sec, f/4.0. Photograph by R. J. F. Smith.

FIG. 2. A group of sockeye salmon picking their way slowly upriver. Photographed from above the surface. Plus X film, bright sun, depth 4 feet (underwater light path 8 feet = 2 × depth), water surface calm, rock background, polaroid filter, Exposure Value 9.5, 1/50 sec, f/3.5.

FIG. 3. School of sockeye salmon wandering in a turbulent pool. Improved Tri-X film, bright sun, depth 6 feet, focusing distance 5 feet, surface slightly turbulent, rock background, Exposure Value 13.5, 1/500 sec, f/4.5.

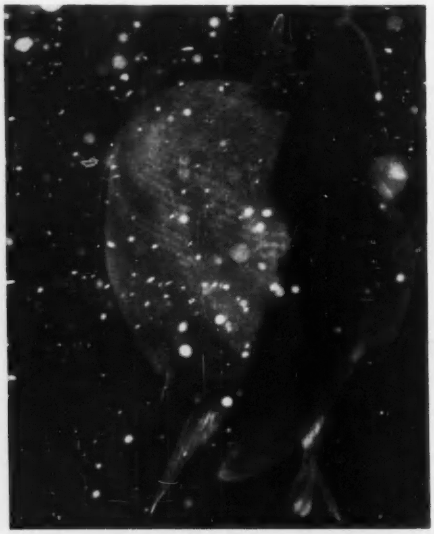

FIG. 4. Sockeye salmon amongst air bubbles from falling water. Plus X film, cloudy dull weather, depth 3 feet, focusing distance 4 feet, much white water, turbulent surface, rock background, Exposure Value 12.5, 1/500 sec, f/3.5.

FIG. 5. Part of a loose school of mixed 6-month-old coho fingerlings and young trout. Adox R14 film, No. 5 flashbulb, GN 20, focusing distance 4 feet, Exposure 1/500 sec, f/5.0.

FIG. 6. Sockeye smolts migrating downriver close to surface at night, over about 6 feet water depth. Camera held pointing vertically downward over side of anchored boat. Plus X film, Multiblitz Press flash unit, GN 50, focusing distance 6 feet, exposure 1/50 sec, f/8.

FIG. 7. Mixed group of young trout and coho fingerlings feeding in a waterfall eddy at the edge of the white water. Plus X film, bright sun, depth 3 feet, focusing distance 3 feet, white water background, turbulent surface, yellow filter (factor = minus 1 EV), Exposure Value 13.5, 1/500 sec, f/4.5.

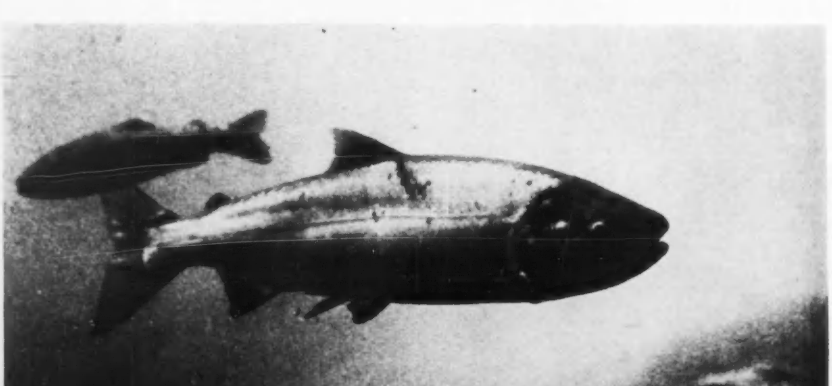

FIG. 8. Adult sockeye holding at the edge of white water. The streamlined shape and clear, silvery scales demonstrate the appearance of early-run sockeye before change to spawning form. Black and white print from Superanscochrome (daylight) colour transparency, bright sun, depth 5 feet, focusing distance 5 feet, turbulent surface, white water background, CC40R filter, Exposure Value 12.5, 1/500 sec, f/3.5.

Exposures calculated from this chart agree to within 0.5 EV of data given in Table II. The chart has been used to check exposures for each photographic project in the better known situations, and as a guide to exposing a test roll of 120 black and white film in new situations. Two examples will be given to demonstrate its use.

Figure 2 illustrates a common problem in photographing salmon; that of recording them from above surface as they swim through calm, shallow water. For the sake of demonstrating exposure calculation the basic data will be changed from that quoted with the photograph. Given cloudy dull weather, maximum depth of 5 feet (= 10 feet underwater light path), and use Royal X Pan film at 9° film speed and a Polaroid filter, the exposure calculation is as follows:

Basic exposure in bright sun	EV 19
Corrections	
Weather (cloudy dull)	Minus 2
Primary underwater	Minus 2.5
Depth (10 ft ULP)	Minus 1
Background (unshaded bottom)	No correction
Filter (Polaroid)	Minus 1.5
Total corrections	Minus 7 EV
Calculated exposure	EV 19–7 = EV 12, 1/250 sec, $f/4.0$

Figure 1 represents a far more difficult problem, due to surface turbulence causing great light fluctuations. Given basic data of 4 feet focusing distance and 3 feet depth, cloudy bright weather, and use of Superanscochrome daylight film for 16 mm cine-recording, then exposure calculation is as follows:

Basic exposure in bright sun	EV 14.5
Corrections	
Weather	Minus 1
Primary underwater	Minus 2.5
Depth (7 ft ULP)	Minus 0.5
Background (some white water)	Plus 1
Filter (7 ft ULP = CC30R)	Minus 0.8
Total corrections	Minus 3.8 EV
Calculated exposure at 24 f.p.s.	EV 14.5–3.8 = EV 10.7, 1/50 sec, $f/5.6$

SIGNIFICANCE OF COLOUR FILM IN RECORDING

In general, colour photographic records are more easily interpreted than black and white, due to the low tonal range of the underwater world. However, below about 20 feet depth, colours become a monochromatic green (or blue). As a result, in deep water and using natural light, colour film loses its special advantages over black and white for research work. It still has legitimate uses, of course, for documentation and illustration.

Nevertheless, colour film can be used to show colours which exist underwater but are not visible to a diver due to the differential absorption of light. The standard ways of doing this at present are by the various techniques of artificial

lighting devised by Rebikoff, Cousteau, Hass, etc. Such artificial lighting introduces seriously disturbing factors, and at present seems of little use for cine-recording any range of animal behaviour, although it has its functions in still photography for ecological or morphological studies.

There are, fortunately, ways of correcting natural light in shallow water by means of filters differentially absorbing colours complementary to those absorbed by water. It is for this reason that colour correction tests have been undertaken here. The technique can be used to produce colours on film equivalent to those we would see were the fish swimming in air, for instance. Such added colour is a great aid to perception of the film image, and hence of considerable value as a tool for increasing the ease of analysing photographic records. As the correction filters remove much of the light, the technique can only be used effectively in shallow water—about 12 feet depth in the Somass system. It should not be forgotten though that the use of this technique produces colours on film which may have no visual significance to the species concerned. Indeed, it is even possible by the manipulation of filters to produce completely unnatural but vividly contrasting colours, which are of value through increasing the visibility of the photographed object against its background.

SUMMARY OF THE USES OF PHOTOGRAPHY AS A RECORDING MEDIUM

It is now possible to utilize photographic recording methods in field studies of salmon ecology and behaviour. In particular, cine-photography has value in recording salmon movements under turbulent or restricted conditions where note-writing by divers is impossible. Cine-photography is also useful for slow-motion recording of rapid movements such as jumping, attacking, etc., thus permitting detailed analysis of the sequence of events, and for sequence recording of simultaneous movements of schooling migrants.

Still photography permits obtaining enlarged prints on which to base descriptions of underwater environments, particular habitats selected by salmon and also trout (Fig. 7), the orientation of salmon and their seasonal morphological changes (Fig. 8). Photographs also provide means of illustrating these aspects of salmon biology as well as many others, e.g., social behaviour, feeding, etc.

ACKNOWLEDGMENTS

I am grateful to student assistant Mr R. J. F. Smith for his help with diving, photography and processing, to Messrs C. Shoop and C. Groot for occasionally acting as companion divers, and to the latter also for advice on photography.

REFERENCES

Schenck, H., and H. Kendall. 1954. Underwater photography. Cornell Maritime Press, 110 pp.

NOTES

Additional Records of the Argentinid Fish, *Leuroglossus stilbius* Gilbert, from British Columbia, with Remarks on its Taxonomy

Leuroglossus stilbius is a representative of the family Argentinidae, commonly referred to as deep-sea smelts. In describing the synonymy and distribution of this species from the North Pacific, Cohen (1956) examined many specimens from localities to the north and south of British Columbia. Only a single specimen, from off Five Finger Island, Strait of Georgia, was listed and this constituted the first record of the species from British Columbia.

Recently 12 additional specimens were caught in bottom trawls having fine mesh codends, during experimental shrimp fishing conducted aboard the Fisheries Research Board's vessel *Investigator No. I.* Three were collected from a depth of 139 fathoms between Bowen and Gambier Islands in Howe Sound on November 17, 1960. Eight more specimens were taken from the same locality on June 8, 1961. A single fish was caught off the Middle Arm of the Fraser River at a depth of 90 fathoms on March 23, 1961[1].

Table I shows the fin ray counts and body measurements of these 11 specimens. Following Cohen's procedure, the last 3 lines of the Table show head length and body depth as percentages of standard length, and length of snout as percentage of head length. The values supplement Cohen's data, which deal with the entire known range of *L. stilbius* from the Okhotsk and Bering Seas to Central America.

Rass (1955, p. 329) divided *L. stilbius* into two subspecies. He considered the population inhabiting northern waters a distinct form, *L. stilbius schmidti*, because there was no overlapping in the range of measurements of the 3 characters above with specimens from southern waters. However, data presented by Cohen showed that southern specimens had a wider variation than previously recorded. In the comparison below our calculated percentages (from Table I) fall within the ranges found by Cohen and appear to support his contention that there is little reason to recognize subspecies in *L. stilbius*.

Source	Body depth	Head length	Snout length
	%	%	%
Howe Sound, B.C.	15.8–18.7	28.1–34.1	24.0–31.0
Rass, 1955	13.3–16.5	25.4–31.0	28.4–33.8
Cohen, 1956	15.2–20.6	27.9–33.7	24.0–30.4

[1]More specimens were caught in Howe Sound, at the above locality on August 24, 1961, and north of Woodfibre at 97 to 107 fathoms a day later; and off Crofton in Stuart Channel, east coast of Vancouver Island, at 110 fathoms on November 6, 1961.

J. Fish. Res. Bd. Canada, 18(6), 1961.
Printed in Canada.

TABLE I. Meristic counts and measurements of *Leuroglossus stilbius* from British Columbia.

	Howe Sound											Off Fraser R.
	November 17, 1960			June 8, 1961								Mar. 23, 1961
Specimen No.	1	2	3	4	5	6	7	8	9	10	11	12
Dorsal rays	10	10	10	9	10	9	10	10	10	10	10	10
Anal rays	13	12	12	12	13	12	13	13	12	13	13	. . .
Pectoral rays	8	9	9	9, 8	9	9	8	9	9	9	[illegible], 9	9
Ventral rays	9	9	9	9	9	9	9	9	8, 9	9	9	9
Standard length, *mm*	48.0	50.0	62.0	38.0	41.0	41.0	41.5	44.0	59.0	72.0	89.0	. . .
Head length, *mm*	16.0	16.0	19.5	12.5	14.0	14.0	14.0	14.5	18.5	20.5	25.0	20.5
Snout length, *mm*	4.0	4.6	5.5	3.0	3.5	3.7	4.0	4.5	5.0	5.5	7.0	6.0
Eye diameter, *mm*	5.0	5.0	5.5	3.5	4.5	4.5	4.5	4.5	5.5	6.5	7.0	6.5
Predorsal length, *mm*	27.0	28.0	35.0	22.5	24.5	24.5	25.0	26.5	34.5	38.5	51.0	39.0
Preanal length, *mm*	37.0	38.0	47.0	29.5	32.5	31.0	33.0	35.0	46.0	56.0	72.0	. . .
Body depth, *mm*	9.0	9.0	10.5	6.0	7.5	7.5	7.5	7.5	10.5	12.0	15.0	12.0
Head ÷ st. length, %	33.0	32.0	31.5	32.9	34.1	34.1	33.8	33.0	31.4	28.5	28.1	. . .
Body depth ÷ st. length, %	18.7	18.0	16.9	15.8	18.3	18.3	18.1	17.0	17.8	16.7	16.9	. . .
Snout ÷ head length, %	25.0	25.3	28.2	24.0	25.0	26.4	28.6	31.0	27.0	26.9	28.0	29.3

Specimens are deposited in the National Museum, Ottawa, and the museum of the Institute of Fisheries at the University of British Columbia.

Fisheries Research Board of Canada
Biological Station, Nanaimo, B.C.

W. E. Barraclough
T. H. Butler

Received for publication July 6, 1961.

REFERENCES

Cohen, D. M. 1956. The synonymy and distribution of *Leuroglossus stilbius* Gilbert, a north Pacific bathypelagic fish. *Stanford Ichthylogical Bull.*, **7**(2): 19–23.

Rass, T. S. 1955. Glubokovodnye ryby Kurilo-Kamchatskoy vpadiny. *Trudy Instituta Okeanologii*, **12**: 328–339.

INDEX TO VOLUME 18 OF THE JOURNAL OF THE FISHERIES RESEARCH BOARD OF CANADA

T